

Cruise Speed Reduction for Air Traffic Flow Management

LUIS DELGADO MUÑOZ

*Aeronautical Engineer
Computer Science Engineer*

Advisor

DR. XAVIER PRATS I MENENDEZ

Doctorate program in Aerospace Science and Technology
Technical School of Telecommunications and Aerospace of Castelldefels
Technical University of Catalonia – BarcelonaTech

Programa de doctorat en Ciència i Tecnologia Aeroespacial
Escola d'Enginyeria de Telecomunicacions i Aeronau espacial de Castelldefels (EETAC)
Universitat Politècnica de Catalunya (UPC)

*A dissertation submitted for the degree of
International Doctor of Philosophy*

February 2013

Cruise Speed Reduction for Air Traffic Flow Management

Author

Luis Delgado Muñoz

Advisor

Dr. Xavier Prats i Menendez

Reviewers

Dr. Hartmut Fricke

Dr. David Lovell

Thesis committee

Dr. Hartmut Fricke

Dr. David Lovell

Dr. Miquel Àngel Piera

Doctorate program in Aerospace Science and Technology

Technical University of Catalonia – BarcelonaTech

February 2013

This dissertation is available on-line at the *Theses and Dissertations On-line (TDX)* repository, which is managed by the Consortium of University Libraries of Catalonia (CBUC) and the Supercomputing Centre of Catalonia (CESCA), and sponsored by the Generalitat (government) of Catalonia. The TDX repository is a member of the Networked Digital Library of Theses and Dissertations (NDLTD) which is an international organisation dedicated to promoting the adoption, creation, use, dissemination and preservation of electronic analogues to the traditional paper-based theses and dissertations

<http://www.tdx.cat>

This is an electronic version of the original document and has been re-edited in order to fit an A4 paper.

PhD. Thesis made in:

Technical School of Telecommunications and Aerospace of Castelldefels

Esteve Terradas, 5.

08860 Castelldefels

Catalonia (Spain)



This work is licensed under the Creative Commons Attribution-Non-commercial-No Derivative Work 3.0 Spain License. To view a copy of this license, visit http://creativecommons.org/licenses/by-nc-nd/3.0/es/deed.en_GB or send a letter to Creative Commons, 171 Second Street, Suite 300, San Francisco, California, 94105, USA.

*To my parents
Luis and Antonia*

Contents

List of Figures	vii
List of Tables	xi
List of Publications	xiii
Acknowledgements	xv
Abstract	xvii
Resumen	xix
Resum	xxi
Notation	xxiii
List of Acronyms	xxvii
CHAPTER I Introduction	1
I.1 Reaching the system capacity	2
I.2 Motivation of this PhD thesis	4
I.3 ATFM delay management by speed reduction	5
I.4 Objectives of this PhD thesis	7
I.5 Scope and limitations of this PhD thesis	8
I.6 Outline of this PhD thesis	9
CHAPTER II Background and progress beyond the state of the art	11
II.1 Airspace Organisation & Management	13
II.2 Airport capacity	13
II.3 Airspace capacity and air traffic control	15
II.4 Air traffic flow management strategies	16
II.5 SESAR and NextGen	20
II.6 State of the art in speed variation techniques	22

CHAPTER III	Fuel and time trade-off	25
III.1	Aircraft operations	25
III.2	The specific range	30
III.3	Effect of speed variations on fuel consumption	31
III.4	The equivalent speed: Air delay with the same fuel consumption	34
III.5	Parameters influencing the specific range curve and the equivalent speed	36
III.6	Discussion	42
CHAPTER IV	Airborne Delay by Cruise Speed Reduction	45
IV.1	Airborne delay at the equivalent speed: Calm wind situation	45
IV.2	Airborne delay at the equivalent speed: Wind situation	61
IV.3	Airborne delay with extra fuel consumption	73
IV.4	Discussion of the results	77
CHAPTER V	Application of Cruise Speed Reduction to ATFM initiatives	81
V.1	Speed reduction and ATFM initiatives	82
V.2	Study and clustering of ground delay programs	82
V.3	Assumptions for the study and simulation set up	85
V.4	Assessment without radius of exemption	86
V.5	Assessment with radius of exemption	97
V.6	Ration policies for speed reduction in GDPs	106
V.7	Impact on the air traffic management	113
V.8	Discussion of the results	115
CHAPTER VI	Concluding Remarks	117
VI.1	Summary of contributions	117
VI.2	Future Research	120
APPENDIX A	Ground Delay Program	123
APPENDIX B	Airbus and BADA Performance	131
APPENDIX C	Quality of the simulations	135
APPENDIX D	Application of the GDP in the analysed scenarios	141
References		149

List of Figures

I-1	Delay distribution in Europe and North American ground delay programs statistics	3
I-2	Relationship between delay, demand and system capacity	3
I-3	Schematic representation of ATFM delays in the baseline and speed reduction scenarios and the delay recovery in case of early ATFM initiative cancellation	6
I-4	Comparison between the realisation of delay in current and proposed operations in a 4D trajectories scenario	6
II-1	Typical relationship between airport arrival and departure capacity for a single runway	14
II-2	Aggregate arrival demand and delay in a ground delay program	17
II-3	CFMU network operations unit operational structure	18
II-4	Stakeholders interaction under SESAR concept of operations	20
II-5	Trajectory development under SESAR concept of operations	21
III-1	Aircraft operating costs as a function of the cruise speed	26
III-2	Scheme of the current flight optimisation ($J = Fuel + CI \cdot Time$) realised by aircraft operators	27
III-3	Typical ascent and descent profiles as a function the cost index	28
III-4	Characteristics of nominal flights with A320 in no wind conditions and considering great circle distances	28
III-5	Thrust required and available curve	29
III-6	Typical relationship of fuel flow as a function of the true air speed	30
III-7	Typical specific range (SR) as a function of cruise speed curve and equivalent speed (V_{eq}) definition	32
III-8	Fuel consumption variation as a function of the true air speed variation	33
III-9	Percentage of fuel consumption variation with respect to the initially planned as a function of percentage of true air speed variation	33
III-10	Aerodynamic characteristics of the N.A.C.A. 009-93 airfoil	35
III-11	Specific range as a function of speed, flight level and aircraft mass for an A320	37
III-12	Specific Range as a function of cruise speed and flight level for an A320 with constant weight	38
III-13	Airborne delay and extra fuel burned for different Flight Levels in 100 NM	38

III-14	Distance needed to absorb 10 minutes of delay without extra fuel burned	39
III-15	Relationship between V_0 and V_{eq} for an Orlando International to Chicago O'hare flight at FL360	39
III-16	Typical SR curve with different winds	40
III-17	Effects of wind on the optimal flight level and in the margins between V_0 and V_{eq} speeds	41
III-18	Margin between V_0 and V_{eq} as function of CI in calm wind scenario	42
IV-1	Example of FACET simulation: inbound traffic to San Francisco International Airport	49
IV-2	Example of different routes in FACET for flights from Denver to Chicago O'Hare	50
IV-3	Diagram of the steps to generate the nominal traffic	50
IV-4	Diagram of the demand and delayed demand generation	51
IV-5	Diagram of the flight simulation in FACET	52
IV-6	Histogram of traffic arrivals as a function of flight plan distance to SFO, EWR and ORD	53
IV-7	Airborne delay as a function of the flight plan distance for flights with destination EWR, ORD and SFO	54
IV-8	Difference in flight time (airborne delay) between the simulated nominal flight and the speed reduction flight	55
IV-9	Potential delay recovered as a function of flight time and the length of the flight plan for flights with destination EWR, ORD and SFO	56
IV-10	Airborne delay and optimal flight level as a function of flight plan distance for A320 and A321 aircraft types	57
IV-11	Airborne delay as a function of flight plan distance for Airbus aircraft with fitting lines	58
IV-12	Recovery delay as a function of cruise time when aircraft speeds up to V_0 for an A320 with a flight plan of 1,600 NM	59
IV-13	Recovery delay as a function of cruise time when aircraft speeds up to V_0 for an A320 with flight plans up to 2,500 NM	60
IV-14	Maximum airborne delay as a function of flight level and wind (constant wind during the cruise)	62
IV-15	Example of FACET screen-shot simulation with RUC wind loaded	64
IV-16	Optimal flight level, cost and maximum airborne delay as a function of route for Orlando International to Chicago O'Hare flights	65
IV-17	Optimal flight level, cost and maximum airborne delay as a function of route for Austin-Bergstrom International to Chicago O'Hare flight	65
IV-18	Optimal flight level, cost and maximum airborne delay as a function of route for Washington Dulles International to Chicago O'Hare flight	66
IV-19	Normalised trip time difference as a function of the normalised values of wind forecast and its error	68
IV-20	ΔT if speed is maintained as initially planned if wind is not as forecast for Orlando International to Chicago O'Hare flight	70
IV-21	Differences in fuel consumption if the CTA is respected and the wind is different than forecast as a function of wind forecast error	71
IV-22	Cumulative probability distribution of fog clearance time at SFO	73
IV-23	Airborne delay and speed reduction for the Dublin to London Heathrow route as a function of the extra fuel allowance	74
IV-24	Airborne delay and speed reduction for the Rome Fiumicino to Paris–Charles de Gaulle route as a function of the extra fuel allowance	75

IV-25	Airborne delay and speed reduction for the Frankfurt to Madrid route as a function of the extra fuel allowance	75
IV-26	Airborne delay and speed reduction for the Lisbon to Helsinki route as a function of the extra fuel allowance	76
IV-27	Airborne delay, speed reduction and flight level for the Dublin to London Heathrow route as a function of the extra fuel allowance	76
IV-28	Airborne delay, speed reduction and flight level for the Rome Fiumicino to Paris–Charles de Gaulle route as a function of the extra fuel allowance	77
IV-29	Airborne delay, speed reduction and flight level for the Frankfurt to Madrid route as function of the extra fuel allowance	77
IV-30	Airborne delay, speed reduction and flight level for the Lisbon to Helsinki route as a function of the extra fuel allowance	78
V-1	Clustering of GDPs implemented in San Francisco International Airport during 2006	84
V-2	Diagram of the computation of the ground and airborne delay	86
V-3	Delay accrued and saved for the baseline and speed reduction scenarios for SFO airport	91
V-4	Delay accrued and saved for the baseline and speed reduction scenarios for EWR airport	92
V-5	Delay accrued and saved for the baseline and speed reduction scenarios for ORD airport	93
V-6	Extra delay recovered, aircraft flying at V_{eq} and extra take-offs	94
V-7	Hour when delay accrued is the same in baseline and speed reduction scenarios for SFO airport	96
V-8	Equidistant radius around SFO, EWR and ORD airports with 400 NM, 800 NM and 1,200 NM lengths	99
V-9	Delay division by GDP	100
V-10	Aircraft affected by GDP	101
V-11	Delay assigned, ground delay and airborne delay realised as a function of the flight plan distance	102
V-12	Extra delay recovered as a function of cancellation time and radius of exemption	103
V-13	Delay recovered at cancellation time with radius of exemption	105
V-14	Airborne delay realised and un-realised with RBS policy	107
V-15	Delay distribution histogram with different ration policies for Chicago O’Hare’s <i>Afternoon</i> GDPs	108
V-16	Delay division by ration policy for GDPs without radius of exemption	109
V-17	Airborne delay realised and un-realised by ration policy for GDPs without radius of exemption	110
V-18	Delay recovered at cancellation time with ration policy for GDPs without radius of exemption	111
V-19	Delay recovered at cancellation time comparing RBS and RBD for GDPs without radius of exemption	112
V-20	Difference in trajectory position flying at V_{eq} or only doing ground delay	114

Figures in Appendices

A-1	Projected demand and capacity	124
A-2	Example of a regulated area with 5 slots every five minutes	124

A-3	Ground delay program implementation phases	125
A-4	Ground delay program parameters	127
A-5	Demand and capacity at San Francisco International Airport with a GDP implemented	128
A-6	Ground delay program statistics	129
B-1	Medium size twin jet engine Airbus model. BADA and PEP performances comparison as a function of cruise speed	132
B-2	BADA B757-200 performances as a function of the cruise speed	133
B-3	Specific range as a function of altitude for typical twin engine aircraft at M0.78	134
C-1	Difference in total fuel burnt between Airbus PEP computation and simulation	136
C-2	Difference in total fuel burnt between Airbus PEP computation and simulation in percentage with respect Airbus fuel	137
C-3	Difference in total flight time between Airbus PEP computation and simulation	138
C-4	Difference in cruise fuel between simulated nominal flight and speed reduction flight in percentage with respect nominal flight	139
C-5	Difference in cruise fuel between simulated nominal flight and speed reduction flight	140
D-1	Aggregated arrival demand and regulated traffic San Francisco International	142
D-2	Histogram demand and regulated traffic San Francisco International	143
D-3	Aggregated arrival demand and regulated traffic Newark Liberty International	144
D-4	Histogram demand regulated traffic Newark Liberty International	145
D-5	Aggregated arrival demand and regulated traffic Chicago O'Hare International	146
D-6	Histogram demand regulated traffic Chicago O'Hare International	147

List of Tables

I-1	Average ground delay program statistics for SFO GDPs (2005-2007)	4
II-1	Acceptance rate per hour for San Francisco International Airport	14
III-1	Analysed flights to study the effect of cruise speed variations on fuel consumption	32
IV-1	Maximum airborne delay without incurring extra fuel consumption in calm wind situation	47
IV-2	Aircraft grouping according to equivalent Airbus types with nominal cost index .	49
IV-3	Origin–Destination pairs with highest volume of traffic in the airborne delay and recovery study	52
IV-4	Parameters of fitting air delay as a function of flight plan distance	58
IV-5	Parameters fitting air delay recovered as a function of flight plan distance and cruise time when speeding up to V_0	60
IV-6	Flights to Chicago O’Hare performed by A320 aircraft types originated within a 1,200 NM radius	63
IV-7	Average wind, optimal flight level and airborne delay for characteristic analysed flights	65
IV-8	Optimal flight level, route, average wind and maximum airborne delay for flights inbound to Chicago O’Hare International within a 1,200 radius	67
IV-9	Slopes of the linear approximations of the controlled time of arrival error and fuel burnt difference for flights maintaining the cruise speeds computed with the forecast winds	70
IV-10	Differences in fuel burnt for flights adapting the cruise airspeed in order to fulfil the CTA	72
V-1	Statistics of the 10 airports with the most GDPs in 2006	83
V-2	Cluster centroids for the 2006 GDPs of SFO, EWR and ORD	84
V-3	Number of aircraft inbound to SFO, EWR and ORD on the August 24th-25th 2005 and their grouping according to equivalent Airbus types	87
V-4	Results of the delay assigned for the simulated GDPs	88
V-5	Division between ground and airborne delay for the simulated GDPs	89

V-6	Maximum number of aircraft flying and doing airborne delay at the same time, number of extra take-offs and extra delay recovered	95
V-7	Results of the simulated GDPs at the actual cancellation time	95
V-8	Amount of delay recovered at aggregate level by GDP cluster	97
V-9	Aggregated extra delay saved for all GDPs during one year per airport and radius of exemption	105

Tables in Appendices

A-1	Example of application of a GDP with substitution, cancellation and compression phases	126
A-2	Direct cost of air transportation delay in 2007 in the NAS	129

List of Publications

The list of publications resulting from this PhD. work is given in inverse chronological order as follows:

Journal Papers

- DELGADO, LUIS, PRATS, XAVIER & SRIDHAR, BANAVAR. 2013. Cruise Speed Reduction for Ground Delay Programs: A Case Study for San Francisco International Airport Arrivals. *Submitted*.
- DELGADO, LUIS & PRATS, XAVIER. 2013. Effects of wind on operating cost based cruise speed reduction for delay absorption. *Transactions on Intelligent Transportation Systems*. *In Press*.
- DELGADO, LUIS & PRATS, XAVIER. 2012. En route speed reduction concept for absorbing air traffic flow management delays. *Journal of Aircraft*, ISSN 0021-8669 **49**(1), 214–224.

Conference Proceedings

- DELGADO, LUIS & PRATS, XAVIER. 2012 (May). ATFM airborne delays without extra fuel consumption in wind conditions. *In: Proceedings of 5th International Conference on Research in Air Transportation (ICRAT)*. Berkeley, California (USA).
- DELGADO, LUIS & PRATS, XAVIER. 2011 (Nov.). Simulation of airborne ATFM delay and recovery by cruise speed reduction. *In: Proceedings of 1st SESAR Innovation days*. Toulouse, France.
- DELGADO, LUIS & PRATS, XAVIER. 2010 (Jun.). An optimisation framework for aircraft operators dealing with capacity-demand imbalances in SESAR. *In: Proceedings of 4th International Conference on Research in Air Transportation (ICRAT)*. 339-346, Budapest, Hungary.
- DELGADO, LUIS & PRATS, XAVIER. 2009 (Sept.). Fuel consumption assessment for speed variation solutions during the cruise phase. *In: Proceedings of the Conference on Air Traffic Management (ATM) Economics*. German Aviation Research Society and University of Belgrade, Belgrade, Serbia.

- DELGADO, LUIS & PRATS, XAVIER. 2009 (Sept.). En-route speed reduction for the management of ATFM delays. *In: Proceedings of 9th AIAA Aviation Technology Integration and Operations Conference (ATIO)*. AIAA, Hilton Head, South Carolina (USA).

Acknowledgements

Firstly, I would like to acknowledge Dr. Hartmut Fricke and Dr. David Lovell for agreeing to do the review of this dissertation and being members of the committee. Their comments have helped to improve the quality of the final version of this document. Dr. Miquel Àngel Piera should also be acknowledged for agreeing to be part of the committee.

This thesis is the result of my work at the Technical University of Catalonia (UPC), which started in 2007, and has been a long journey that began even earlier. I decided to study engineering, and, specifically, computer science and aeronautics, partially thanks to the advise of Dr. Maria Ribera, whom I would like to thank. From my undergraduate studies, I should also acknowledge Dr. Xavier Franch and Dr. Dolors Costal for giving me the first opportunity to work as a computer science engineer. Later, Dr. Michel Taix and Dr. Jean-Paul Laumond introduced me to the world of research at the Laboratory of Analysis of Architectures of Systems (LAAS) in Toulouse, from which I thank them.

Car sharing between Barcelona and Toulouse, I had the good luck of meeting Xavier Prats. He encouraged me to submit my application to teach at the Technical School of Castelldefels (EETAC), part of the UPC, where he was still a PhD. candidate, little did we know that he would become my advisor. Thanks to his advice, I started my work at the UPC. I should acknowledge Dr. Ricard Gonzalez and Dr. Miguel Valero for giving me that opportunity.

At that time, Dr. Daniel Crespo was responsible for the doctoral program, so I would also like to acknowledge him for his help making in contact with the Development of Air Navigation System Division of the Air Navigation Service Provider of Spain (AENA) at the beginning of my PhD.

At the EETAC I joined the Icarus research group. I acknowledge their help and support during all the work undertaken in this thesis: Dr. Enric Pastor, Dr. Cristina Barrado, Jorge Ramirez, Dr. Pablo Royo, Marc Pérez, Raul Cuadrado and Juan Manuel Lema. Dr. Enric Pastor should be specially acknowledged, as, acting as head of the research group, he encouraged Xavier Prats and myself to start a new line of research focused on Air Traffic Management. Dr. Xavier Prats is the advisor of this PhD. I thank him for deciding to take the risk with me and allowing me to be his first graduate student. I know I will be the first of many, but I hope this work will always remain something special. We have had to learn many things together, and we have shared many hours of work and enjoyment. His perfectionism has helped greatly to improve the quality of the thesis and the publications obtained from this work. Dr. Xavier Prats has become my advisor and one of

my dear friends. I would also like to acknowledge my students, especially Marc Melgosa.

Dr. Banavar Sridhar helped me to obtain a licence of FACET simulator, which has been used extensively in this work. I thank him also for giving me the opportunity to go to live in the Bay Area and do a research stay at NASA Ames Research Centre. From that research stay I acknowledge Dr. Hok Kwan Ng, Dr. Avijit Mukherjee and Mr. Alex Morando for helping me with FACET and their useful comments; Riana Delossantos for letting me share her office and helping me feel comfortable working there; and Deborah Murchison, who was a great help in dealing with the required paperwork. The visiting period was sponsored by the Catalan government under the research mobility grant program: *Beques BE del departament d'Economia i Coneixement de la Generalitat de Catalunya*. Thanks to this research stay in NASA I met Dr. David Miller, whom I acknowledge for the bibliography style used in this thesis and remember for the nice talks we had in Redwood City.

Airbus is acknowledged for the use of the Airbus Performance Engineer's Programs (PEP) suite which allowed me to undertake realistic aircraft performance simulations. This has been possible thanks to Mr. Ferran Pous.

From Castelldefels I should also acknowledge my colleagues and friends from the aeronautical group: Xevi, Jorge, Dago, Pep, Adeline and Santi. They have been a great support. Dr. Adeline de Villardi has been a great doctorate program coordinator and very helpful in validating the quality of some graphs. She has also taught me how to be a good, productive and international researcher and friend. Dr. Santiago Arias has helped with some of the flight mechanics and he should be specially acknowledged for becoming one of my best friends. Thanks for all the coffees, trips, late nights and priceless support.

Penelope Slocombe has undertaken the tedious work of correcting the English of this dissertation. To her goes the merit of an understandable English. She has also been one of the most important people in my life, giving me the support and help needed, especially during this last and never ending year, and during the final part of this PhD. I hope I will be able to support her with her projects as much as she has supported me. Thanks for keeping me sane.

Finally, I want to specially thank my family, none of this would have been possible without their unconditional support: my brother, Alberto, the person I love the most and who is responsible of the cover of this dissertation; my mum, Antonia, who has shown me how to love and work; and finally my dad, Luis, who taught me how to live and die.

Castelldefels, February 2013
Luis Delgado Muñoz

Abstract

Nowadays, many air transport infrastructures suffer from congestion. This situation is worsened by a continuous increase in traffic, and, traffic density due to hub and spoke systems. Weather is one of the main causes which leads to punctual capacity reduction. To mitigate these imbalances, air traffic flow management (ATFM) initiatives are usually undertaken, ground delay at the origin airport being one of the main ones used. By assigning delay on ground at the departure airport, the arrival traffic is spread out and the arrivals are metered at the congested infrastructure. However, forecasting when these capacity drops will be solved is usually a difficult task. This leads to unnecessarily long regulations, and therefore to the realisation of unnecessary delay and an underuse of the capacity of the infrastructures.

The implementation of precise four dimension trajectories, envisaged in the near future, presents new opportunities for dealing with these capacity demand imbalances. In this context, a promising technique is the use of speed variation during the cruise. Generally, it is considered that flying slower than the maximum range speed (MRC) is neither efficient nor desirable. In this dissertation a new approach is presented. When airlines plan their flights, they consider the cost of time along with the cost of fuel. It is therefore common practice to select speeds that are faster than MRC. Thus, it is possible to fly slower than MRC while maintaining fuel consumption as initially planned. This airborne delay can be considered at a pre-tactical phase to divide the assigned air traffic flow management delay between ground and airborne delay. With this strategy, the delay is absorbed gradually during the flight using the same fuel as initially planned, but with the advantage that, if the regulation is cancelled before planned, the flights which are already airborne are in a better position to recover part of their assigned delay.

This dissertation focuses on the study of this concept. Firstly, a study of the trade-off existing between fuel consumption and flight time, when modifying the nominal cruise speed, is presented. Secondly, the airborne delay that can be realised without incurring extra fuel consumption is defined and assessed in the absence and presence of wind. The influence of selecting a different flight level than initially planned, and the use of extra fuel consumption to obtain higher delay are also considered and analysed. Results show that for short and mid-range flights around 5 minutes of airborne delay can be realised, while for longer flights this value increases up to around 25 minutes. The flight level is identified as one of the main parameters which affect the amount of airborne delay realisable.

Then, the application of the suggested cruise speed reduction on realistic ATFM initiatives,

and, in particular, on ground delay programs (GDP) in the United States, is presented. In order to obtain significant results, the GDPs implemented in North American airspace during 2006 are analysed. Scenarios for San Francisco International, Newark Liberty International and Chicago O'Hare International are studied in detail, as these airports were the ones where the most GDPs were implemented in 2006. In addition, due to their location, they present different traffic behaviours. In order to consider the traffic, Federal Aviation Administration data and the aerodynamics and fuel consumption characteristic form Airbus are used.

Finally, the use of a radius of exemption in the GDPs and the use of ration policies different from the operative ration-by-schedule, are also analysed. To conclude, a brief discussion of the impact of this speed reduction strategy on the air traffic management is presented.

Resumen

Hoy en día un número considerable de infraestructuras del transporte aéreo tienen problemas de congestión. Esta situación se ve empeorada por el incremento de tráfico existente y por su densidad producida por el sistema de *hub y spoke* utilizado por las compañías aéreas. Esta congestión se ve agravada puntualmente por disminuciones de capacidad debidas a causas como la meteorología. Para mitigar estos desequilibrios, normalmente se implementan medidas de gestión del tráfico aéreo (ATFM), siendo el retraso en el aeropuerto de origen una de las más utilizadas. Asignando retraso en tierra previo al despegue, el tráfico de llegada se distribuye durante un intervalo mayor de tiempo y se controlan las llegadas. Pese a esto, la predicción de cuando estas reducciones de capacidad se solventarán es generalmente una tarea compleja. Por esto, se suelen definir regulaciones durante un periodo de tiempo superior al necesario, comportando la asignación y realización de retraso innecesario y el desaprovechamiento de las infraestructuras.

La definición de trayectorias precisas permite nuevas oportunidades para gestionar estos desequilibrios. Una técnica prometedora es el uso de variaciones de velocidad durante el crucero. Suele considerarse que volar más lento que la velocidad de máximo alcance (MRC) no es eficiente. En esta tesis se presenta una nueva aproximación. Cuando las aerolíneas planifican sus vuelos consideran el coste del tiempo junto con el del combustible. Por consiguiente, es una práctica habitual seleccionar velocidades más rápidas que MRC. Así es posible volar más lento que la velocidad de MRC manteniendo el mismo consumo que el inicialmente planificado. Este retraso realizable en el aire puede ser considerado en la fase pre-táctica para dividir el retraso asignado entre retraso en tierra y retraso durante el crucero. Con esta estrategia, el retraso es absorbido de manera gradual durante todo el vuelo utilizando el mismo combustible que el planificado inicialmente por la compañía. Esta estrategia presenta la ventaja de que los vuelos que están en el aire se encuentran en una situación más favorable para recuperar parte del retraso que tenían asignado si la regulación se cancela.

En primer lugar se ha realizado un estudio de la relación existente entre el combustible usado y el tiempo de vuelo cuando la velocidad de crucero es modificada. A continuación, se ha definido y analizado el retraso que se puede realizar sin repercutir en el consumo en la ausencia y en la presencia de viento. También se ha considerado la influencia de elegir un nivel de vuelo diferente al planificado y el uso de combustible extra para incrementar el retraso. Los resultados muestran que para vuelos de corto y medio alcance, la cantidad de retraso es de en torno a 5 minutos, esta cantidad aumenta a unos 25 minutos para vuelos de largo recorrido. El nivel de vuelo se ha identificado como uno de los parámetros principales que afectan a la cantidad de retraso que

puede ser absorbido.

Seguidamente se presenta la aplicación de esta técnica en regulaciones de ATFM realistas, y en particular de *ground delay programs* (GDP). Con el objetivo de mostrar resultados significativos, los GDPs definidos en 2006 en el espacio aéreo norteamericano han sido analizados. Han sido estudiados en detalle escenarios en los aeropuertos de San Francisco, Newark y Chicago. Estos tres aeropuertos fueron los aeropuertos que implementaron más GDPs en 2006 y por su situación geográfica presentan tráficos con diferentes características. Para considerar el tráfico se han utilizado datos de la Federal Aviation Administration y características aerodinámicas y de consumo provenientes de Airbus.

Finalmente, se presenta el efecto de usar radios de exención en los GDPs y el uso de políticas de priorización de vuelos diferentes a la utilizada actualmente (*ration-by-schedule*). Para concluir se ha realizado una breve discusión sobre el impacto de esta estrategia en la gestión del tráfico aéreo.

Resum

Avui dia un considerable nombre d'infraestructures del transport aeri tenen problemes de congestió. Aquesta situació es veu empitjorada amb l'increment de trànsit existent i amb la seva densitat deguda al sistema de *hub i spoke* utilitzat per les companyies aèries. Aquesta congestió es veu agreujada puntualment per disminucions de capacitat per causes com la meteorologia. Per mitigar aquests desequilibris, normalment són implementades mesures de gestió del flux de trànsit aeri (ATFM), sent el retard a l'aeroport d'origen una de les més utilitzades. Assignant retard previ a l'enlairament, el trànsit d'arribada és repartit durant un interval de temps superior i les arribades es distribueixen. Malgrat això, la predicció de quan aquestes reduccions de capacitat es solucionaran una tasca difícil. Això comporta que es defineixin regulacions que són més llargues del necessari i per tant, porta a la realització de retard innecessari i al desaprofitament de capacitat.

La definició de trajectòries precises ofereix noves oportunitats per gestionar aquests desequilibris. Una tècnica prometedora és la utilització de variacions de velocitat durant el creuer. Generalment, es considera que volar més lent que la velocitat de màxim abast (MRC) no és eficient. En aquesta tesis es presenta una nova aproximació. Quan les aerolínies planifiquen els seus vols, consideren el cost del temps junt amb el del combustible. Per tant, és habitual seleccionar velocitats més ràpides que MRC. Així és possible volar més lent de la velocitat de MRC tot mantenint el mateix consum inicialment planificat. Aquest retard realitzat a l'aire pot ser considerat a la fase pre-tàctica per dividir el retard assignat a un vol en retard a terra i retard a l'aire durant el creuer. Amb aquesta estratègia, el retard és absorbit de manera gradual durant el vol fent servir el mateix combustible que inicialment planificat. Si la regulació es cancel·la abans del que estava planificat inicialment, els vols que estan a l'aire es troben en una situació més favorable per tal de recuperar part del retard.

La present tesis es centra en l'estudi d'aquest concepte. En primer lloc, s'ha realitzat un estudi de la relació entre el combustible utilitzat i el temps de vol quan es modifica la velocitat nominal de creuer. A continuació, s'ha definit i analitzat el retard que pot ser realitzat sense incorre en un consum extra de combustible en l'absència i en la presència de vent. També s'ha considerat i analitza la influència de triar un nivell de vol diferent del planificat inicialment i la utilització de combustible extra per tal d'obtenir major quantitat de retard. Els resultats mostren que per vols de curt i mitja distància, la quantitat de retard realitzable és d'entorn a 5 minuts, aquesta quantitat augmenta a uns 25 minuts per vols de llarg recorregut. El nivell de vol s'ha identificat com un dels paràmetres principals que afecten a la quantitat de retard que pot ser absorbit a l'aire.

A continuació es presenta l'aplicació de la tècnica a regulacions d'ATFM realistes, i particularment a *ground delay programs* (GDP). Per tal de mostrar resultats que siguin significatius, els GDPs implementats en 2006 en el espai aeri nord-americà han sigut analitzats. Han sigut detalladament estudiats escenaris als aeroports de San Francisco, Newark i Chicago. Aquests tres aeroports van ser els que van declarar més GDPs durant el 2006 i per la seva situació geogràfica presenten trànsits amb diferents característiques. Per tal de considerar el trànsit s'ha utilitzat dades de la Federal Aviation Administration i característiques aerodinàmiques i de consum realistes provinents d'Airbus.

Finalment, la tesis presenta l'efecte d'utilitzar radis d'exempció en els programes de regulació de trànsit i l'ús de polítiques de prioritització de vols diferents a l'utilitzada actualment (*ration-by-schedule*). Per concloure, s'ha realitzat una breu discussió sobre l'impacte d'aquesta estratègia en la gestió del trànsit aeri.

Notation

$A_{CD0,1}$	first coefficient of $C_{D,0}$ fitting with respect the TAS expressed in Mach
$A_{CL0,i}$	i -th coefficient of $C_{L,0}$ fitting with respect the TAS expressed in Mach
AD	airborne delay
AD_0	airborne delay coefficient for the fitting of airborne delay as a function of the flight plan distance for zero distance flight plan
AD_{0f}	airborne delay with no extra fuel consumption
$A_{kj,1}$	j -th coefficient of k_i fitting with respect the TAS expressed in Mach
a	speed of sound
C_D	total drag coefficient
$C_{D,0}$	parasitic drag coefficient
$C_{D,i}$	lift induced drag coefficient
$C_{D,min}$	minimum parasitic drag coefficient independent of the TAS
C_L	total lift coefficient
$C_{L,0}$	zero lift coefficient
C_{min}	minimum zero lift coefficient independent of the TAS
D	total assigned delay
σ_D	standard error deviation of airborne delay
D_c	total cruise distance
d_c	cruise distance flown
d_f	distance of the flight plan
d_i	delay realised at waypoint i
EF	amount of extra fuel consumption with respect nominal flight plan
e	efficiency factor
η	thrust specific fuel consumption
F	fuel burnt
ΔF	difference on fuel used
F_D	total drag force
F_L	lift force
FL_0	nominal flight level according to the optimised flight plan
GD	ground delay
GS	ground speed
g	gravitational acceleration

h	altitude
K_e	variation of equivalent speed as a function of cruise distance flown coefficient
K_D	variation of the amount of airborne delay as a function of the flight plan distance
K_{Df}	variation of the percentage of airborne delay as a function of the percentage of extra fuel consumed
K_{Sf}	variation of the percentage of speed reduction as a function of the percentage of extra fuel consumed
K_t	variation of the amount of airborne delay as a function of the cruise flight time
k	Boltzmann constant
k_i	coefficient to consider compressibility effects in the drag coefficient
Λ	aspect ratio
M	Mach
M_0	nominal speed according to the nominal flight plan expressed in Mach
M_{eq}	equivalent speed expressed in Mach
m	mass of the aircraft
\dot{m}_{fuel}	fuel flow
RD	delay recovered
RD_0	airborne delay recovered coefficient for the fitting of airborne delay recovered as a function of the flight plan distance for zero distance flight plan
R_s	molar gas constant
ρ	air density
S	surface of the wing of the aircraft
SR_0	nominal specific range at the nominal cruise speed
SR_{eq}	nominal specific range at the equivalent speed
SR_{ground}	specific range with respect the ground
SRD	speed reduction value in true air speed
SRD_{0f}	speed reduction with no extra fuel consumption
T	static air temperature
T'	normalised value of the trip time over the total trip time
ΔT	trip time difference
$\Delta T'$	normalised value of the trip time difference over the total trip time
T_r	required thrust
T_{V_0}	flight time if aircraft cruising at V_0 speed
ΔT_{V_0}	flight time error if aircraft cruising at V_0 speed
$T_{V_{eq}}$	flight time if aircraft cruising at V_{eq} speed
$\Delta T_{V_{eq}}$	flight time error if aircraft cruising at V_{eq} speed
$T_{V_{red}}$	flight time if aircraft cruising at V_{red} speed
t	time
t_c	time elapsed since the aircraft started flying its cruise
V	aircraft true air speed
V_0	nominal speed according to the nominal flight plan. ECON speed
V_{eq}	equivalent speed
\bar{V}_{eq}	average equivalent speed during the cruise
V_{eq0}	equivalent speed at the beginning of the cruise
V_{mdrag}	minimum drag speed
V_{min}	minimum available cruising speed
V_{MR}	maximum range speed
V_{red}	reduced cruising speed
W	weight of the aircraft
w	wind component in the direction of the flight
\bar{w}	average wind in the direction of the flight for the cruise length

\bar{w}'	normalised value of the wind over the true air speed
$\Delta\bar{w}$	average wind forecast error
$\Delta\bar{w}'$	normalised value of the wind forecast error over the true air speed
x	distance flown

List of Acronyms

AAR	Airport Acceptance Rate
AD	Airborne Delay
ADP	Air Traffic Flow Capacity Management Daily Plan
AFP	Airspace Flow Program
AIP	Aeronautical Information Publication
ANSP	Air Navigation Service Provider
API	Application Programming Interface
ATC	Air Traffic Control
ATCO	Air Traffic Control Officer
ATCSCC	Air Traffic Control System Command Center
ATM	Air Traffic Management
ATFCM	Air Traffic Flow and Capacity Management
ATFM	Air Traffic and Flow Management
BADA	Base of Aircraft Data
BDT	Business Development Trajectory
CATS	Contract-Based Air Transportation System
CDA	Continuous Descend Approach
CDM	Collaborative Decision Making
CNS	Communication Navigation and Surveillance
CI	Cost Index
CTA	Controlled Time of Arrival
CTD	Controlled Time of Departure
CFMU	Central Flow Management Unit
ECAC	European Civil Aviation Conference
ESRA	Eurocontrol Statistical Reference Area
ETA	Estimated Time of Arrival
ETD	Estimated Time of Departure
ETO	Estimated Time of Overfly
ETMS	Enhanced Traffic Management System
FAA	Federal Aviation Administration
FACET	Future ATM Concepts Evaluation Tool
FL	Flight Level

FMS	Flight Management System
FMC	Flight Management Computer
FMP	Flow Management Positions
FF	Fuel Flow
FUA	Flexible Use of Airspace
GCD	Great Circle Distance
GDP	Ground Delay Program
GHP	Ground Holding Problem
GS	Ground Speed
IFATS	Innovative Future Air Transport System
IFR	Instrument Flight Rules
ILS	Instrumental Landing System
LAHSO	Land and Hold Short Operations
MRC	Maximum Range Cruise
MTCD	Medium Term Collision Detection
NAS	National Airspace System
NASA	National Aeronautics and Space Administration
NM	Nautical Miles
NOAA	National Oceanic & Atmospheric Administration
NOP	Network Operations Plan
PAAR	Program Airport Acceptance Rate
PEP	Airbus Performance Engineer's Programs
RBT	Reference Business Trajectory
RTA	Requested Time of Arrival
RUC	Rapid Update Cycle
SBT	Shared Business Trajectory
SESAR	Single European Sky ATM Research
SID	Standard Terminal Arrival Route
SOIA	Simultaneous Close Parallel ILS Approaches
SR	Specific Range
STAR	Standard Instrumental Arrival
TAS	True Air Speed
TC-SA	Trajectory Control by Speed Adjustment
TOC	Top Of Climb
TOD	Top Of Descend
TSFC	Thrust Specific Fuel Consumption
TTA	Target Time of Arrival
VAPP	Visual Approaches
VFR	Visual Flight Rules



— Das Rheingold - Richard Wagner



Introduction

Air transport is a fast, efficient and safe means of transport, which contributes significantly to the world's development and economy. According to ([Air Transport Action Group \(ATAG\), 2012](#)), aviation transports 2.8 billion passenger and over 48 million tones of freight annually. 51% of international tourists and 35% of interregional exports of goods (by value) are transported by air. The air transport industry supports 56.6 million jobs globally including direct, indirect and induced jobs; in the European Union, air transport contributes to 2.6% of the gross domestic product ([Britton *et al.*, 2005](#)). Every year, there are more than 26.7 million commercial aircraft movements, in over 3,800 airports with scheduled commercial flights. In Europe alone, the air traffic management (ATM) network includes more than 100 main airport nodes, linked by around 600 airspace sectors, operated by more than 36 air navigation service providers (ANSP) ([Britton *et al.*, 2005](#)).

In the last 50 years aviation has experienced a rapid expansion: since 1960 passenger traffic has grown at nearly 9% per year, although the rate of growth fell to about 5% in 1997 ([Intergovernmental Panel on Climate Change, 1999](#)). In the period 2003–2025, the average annual growth of air transport is expected to be, at worst, around 2.3% and about 4.9% in the most optimistic scenario according to ([Britton *et al.*, 2005](#)) for the Eurocontrol Statistical Reference Area (ESRA). The forecast of flight movements for the ESRA, in the medium term, indicate that by 2018 there will be around 16% more traffic than in 2011 ([Eurocontrol - STATFOR, 2012](#)). The long term forecasts for the same region indicates that by 2030, in the most likely scenario, there will be 16.9 million IFR movements per year. This represents about 1.8 times more traffic than in 2009 and an annual growth of 2.8% ([Eurocontrol - STATFOR, 2010](#)).

Air transport also has an impact on the environment. In 2012, 261 billion litres of fuel were burned by aircraft, this represents around 2% of man-made carbon dioxide emissions ([Air Transport Action Group \(ATAG\), 2012](#)). During 2008, most airlines reported fuel costs that varied from

between 30 to 40 percent of their total expenses.

The continuous system growth means that, in many cases, the demand exceeds the available capacity, indeed some airports and portions of airspace are already suffering from these congestion problems (SESAR Consortium, 2006). In the ESRA, between 0.7 and 5.0 million flights, which represents between 5% and 19% of the forecast demand, will not be able to be accommodated by 2030. This over demand and limited airport capacity creates pressure on the flow of operations, and is starting to exacerbate delays (Eurocontrol - STATFOR, 2010).

The current situation and the forecast growth, imply that the handling of capacity-demand imbalance situations is, and will continue to be, one of the main ATM problems.

1.1 Reaching the system capacity

In order to deal with this excess of demand, in the majority of European airports, a finite number of administrative slots¹ are given to airlines to schedule flights. With very few exceptions, administrative slots are not imposed in the United States. However, those slots are not enough to adjust the demand as unforeseen situations, such as severe weather affecting a particular airport, might reduce the nominal capacity. If lack of capacity of the system is not managed, the over demand will generate air delay at the destination airport in the form of holding or path stretching in terminal manoeuvring areas (TMA) or during the cruise by re-routing. However, in the air traffic flow management (ATFM) community, it is widely accepted that ground delays at origin airports are preferable to airborne delays near the congested sector/airport. In general, the operating costs and the environmental impact of airborne delays are higher compared to ground delays (Carlier *et al.*, 2007).

Air traffic flow management aims to anticipate capacity shortfalls and/or demand peaks, either at an airport or in the air traffic control (ATC) sector; and imposes traffic management initiatives that delay aircraft on ground in such a manner that airborne traffic do not exceed the capacity. The problem of delaying aircraft at the origin airport, to deal with capacity issues, is generally known as the *ground holding problem* (GHP). According to (Carlier *et al.*, 2007), in 2004 alone, the Eurocontrol area saved around 80 million euros by the effective implementation of ground holding programs (60 million in fuel cost savings and 20 million in emissions) compared to the cost of doing the delay airborne.

Since March 1996, in Europe, the central flow management unit (CFMU) (Eurocontrol, 2012) has implemented a ground delay based tool. A similar initiative exists in the United States of America: the airspace flow program (AFP) (Metron Aviation, 2012) and the ground delay programs (GDP), which have been applied since 1998. The principal difference between the GDP and AFP's (or CFMU's) tools is that in GDP, delays are applied only to a set of flights destined for a single airport, while the AFP's tools can apply delays to a subset of flights predicted to fly through a designated flow constrained area (including one or several sectors).

The ATFM delays cannot be neglected when analysing the performances of the air traffic management system, as an example, in the European civil aviation conference (ECAC) area, during summer 2008, 14.1% of the traffic in Europe was delayed with an average delay of almost 20 minutes (Eurocontrol, 2008b). In December 2008, 2,470 flights per day were regulated, from which 1,443 were delayed, resulting in a total of 28,690 minutes of delay per day (Eurocontrol,

¹The administrative slots are a permission to use the airport infrastructure necessary to operate an air service at an airport on a specific date and time for the purpose of landing or take-off. These slots are defined at airports with high levels of congestion where demand exceeds capacity during the relevant period. Airport slot capacity available for allocation is determined twice a year by the competent authorities, according to the two programming seasons (winter and summer) in place in international aviation. (European Council, 2009).

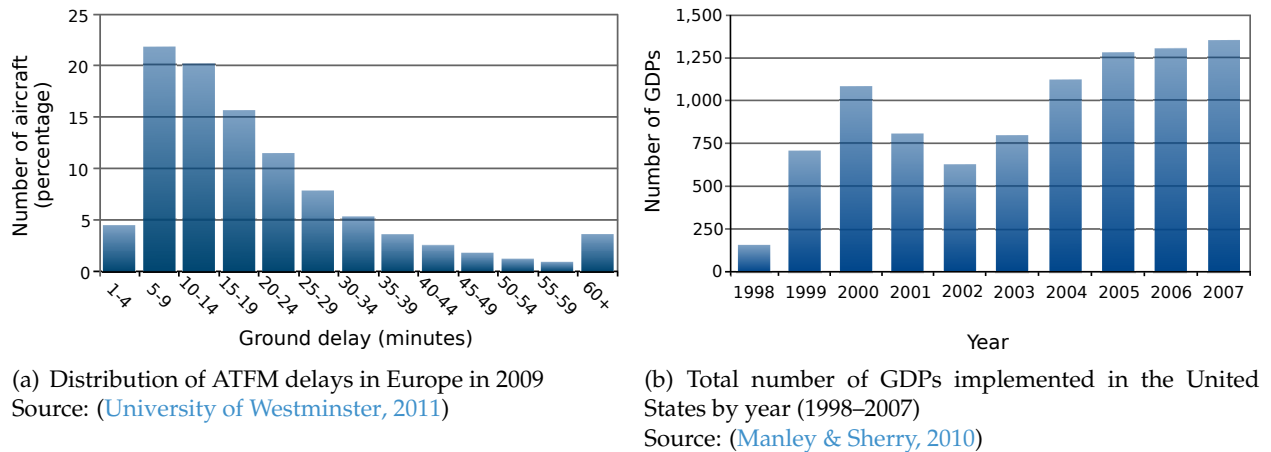
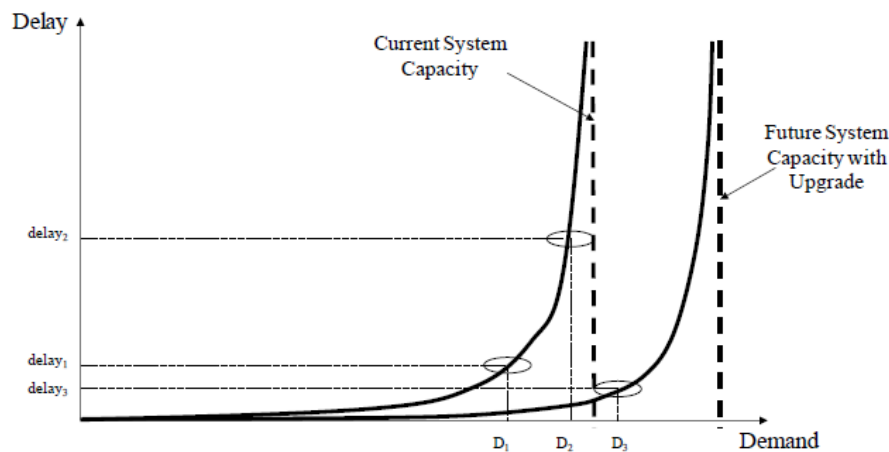


Figure I-1: Delay distribution in Europe and North American ground delay programs statistics



2009a). This represents an average of 19.9 minutes of ground delay per affected flight (see figure I-1(a)). From 2003 to 2008, when the European traffic increased by 19.9% (average of 27,818 flights per day in 2008), the total delay increased by 60.7% (65,138 minutes per day) and the total delay per flight due to capacity-demand imbalance increased by 34% (2.3 minutes on average for every flight) (Eurocontrol, 2008a). As expressed in (Performance Review Unit (PRU), 2012), in 2010, the effort made to reduce the ATM/CNS costs were cancelled due to a sharp increase in ATFM delays.

In the United States the system congestion is an ongoing problem as it is not an exceptional situation to have a ground delay program implemented in the national airspace system (NAS). As can be seen in figure I-1(b), the number of GDPs defined every year keeps an increasing tendency. During the period from 2000 to 2006, there was an 87% chance of having at least one GDP per day (Manley & Sherry, 2010). In 2005, for instance, there were over 1,350 GDPs implemented in the United States, which represents more than 16.8 million minutes of delay (Ball et al., 2010a).

The costs related to air traffic management are high, representing around € 7 billion annually in the European region (around twice as much as in the United States) (SESAR Consortium, 2006). ATM network inefficiencies are estimated to be € 2 billion due to cost effectiveness (route-fragmentation and low productivity), around € 1.4 billion associated with flight inefficiencies and about € 1 billion associated with ground ATM delays.

Table I-1: Average statistics for SFO GDPs (2005–2007) †. Source: (Cook & Wood, 2010)

Initial average affected flights	79
Initial average total delay (min)	3,642
Initial average maximum delay (min)	98
Initial average delay (min)	44
Planned average overall duration	4h51
Actual average duration (Cancellation time minus start time)	2h52
Early average cancellation time (Planned end time minus actual GDP duration)	1h59

† The values are average value, as they are the statistics of the GDPs implemented in the period 2005-2007

These tendencies show that the capacity of the system is becoming overloaded. As is presented in (Ball *et al.*, 2010b), and depicted in figure I-2, when the demand approaches the capacity of the system, a little increment of demand leads to a high augmentation of delay. As the current system is reaching its limits, and new challenges that go further from demand-capacity management are arising, like fuel consumption or the environmental impact of aviation, both in Europe and in the United States, it has been recognised that an update of the air traffic management system is needed. For this reason, the single European sky and ATM research program (SESAR (SESAR Consortium, 2012)) and the next generation program (NextGen (Federal Aviation Administration, 2012f)) are under development in Europe and in the United States respectively. These new concept of operation open the possibility of new forms of managing the ATFM initiatives. According to the objectives defined by SESAR and NextGen, the ATM system will be re-engineered towards a more efficient, better integrated, more cost-efficient and safer network.

I.2 Motivation of this PhD thesis

In the majority of the situations, ATFM regulations are issued due to weather related capacity reduction. For instance, in San Francisco International Airport (SFO), in California, when low ceiling clouds are present, landing capacity can drop from sixty planes per hour to only thirty, due to restrictions on independent parallel runway configurations under instrumental meteorological conditions (IMC) (Janić, 2008). In these cases, it might be difficult to predict the weather conditions and when capacity will increase again (Mukherjee *et al.*, 2012; Inniss & Ball, 2002). Airspace managers are typically conservative with these weather reduction capacity scenarios, preventing costly airborne holdings and maximising safety. Thus, regulations are usually planned to last longer than actually needed. Essentially, it is preferable to have planes waiting on ground, even if it is unnecessary, and cancel the GDP earlier rather than having too many flights arriving at the concerned TMA, when the available capacity cannot yet accommodate all of them.

Table I-1 presents few statistics compiled over the GDPs issued during 2005, 2006 and 2007 in SFO. On average at SFO the GDPs are cancelled almost two hours before the initial planned duration, with the result that, in general, some ground delay is realised when it was not actually needed (Cook & Wood, 2010). If the imposed delay has been completed solely on the ground, the recovery of this unnecessary delay is expensive, since it would involve flying at higher speeds than initially planned, consuming more fuel. Conversely, if reduced capacity conditions last longer than expected, the regulation will have to be extended and/or inefficient air holdings will be necessary near the destination airport. However, due to the conservative nature of the airspace managers, an extension of a GDP in SFO is only issued in 15% of the cases (Cook & Wood, 2010).

Nowadays, ground holding is preferred to airborne delay because airborne delay is realised

by holding stacks and path stretching, leading inevitably to more fuel consumption. However, if cruise speed is reduced, it is possible to realise airborne delay without incurring extra fuel consumption, the aircraft being in a better position when trying to recover part of their assigned delay if the regulation is cancelled beforehand. In that situation, the cruising speed can be increased and in this way part of the delay can be recovered even without incurring higher fuel consumption than originally planned for the flight. This technique would also increase the available capacity used at the arrival airport that is currently underused. The idea is to realise a **linear holding instead of ground or stack holding**. According to (CANSO, 2011), it is believed that the fuel savings for arrivals at congested airports by speed adjustment, potentially represents the most significant near-term opportunity for improvement.

Such speed reduction strategy is difficult to implement with the current concept of operations since controlled time of arrivals (CTAs) are not enforced. Thus, some companies may decide to accelerate their aircraft once airborne, trying to recover part of the delay previously performed on ground (incurring higher fuel costs) and not meeting the assigned arrival slot (Knorr *et al.*, 2011). The situation where aircraft speed up to be the first at the holding stack is incentivised. Nevertheless, 4D trajectories², which will be the base of SESAR and NextGen, will enable the effective enforcement of the control time of arrivals on aircraft, preventing these negative behaviours.

I.3 ATFM delay management by speed reduction

For each controlled flight in an ATFM initiative, a controlled time of arrival or arrival *slot* is assigned at the regulated area or arrival airport. Based on filed flight plans and weather forecasts, trip times can be estimated with reasonable accuracy and consequently, the CTA is translated to a controlled time of departure (CTD) at the origin airport. Thus, the CTD is the CTA minus the trip time, and the total delay assigned (D) is the CTD minus the estimated (scheduled) time of departure (ETD), as is presented in figure I-3(a).

However, cruise speed management provides aircraft operators with an additional option to tackle delays and their associated costs. The main objective of this thesis is the study of cruising speed reduction (V_{red}) in order to realise airborne delay. By flying at this reduced speed, the airline is able to absorb part of the assigned delay in the air, and as a function of the new reduced speed, it is possible to do it even without incurring extra fuel consumption with respect to the initially planned flight at the nominal speed (V_0). As will be presented in this thesis, the airborne delay that can be realised with this technique is typically lower than the total assigned delay due to an ATFM regulation, such as GDP. Thus, the total assigned delay will generally be divided between some ground delay, at the origin airport, plus airborne delay (AD) accrued by flying slower, as shown in figure I-3(b). With the en-route speed reduction strategy, the aircraft incurs a ground delay of GD minutes (with $GD \leq D$), takes off at a new departure time (CTD') and flies slower than initially planned. In this way, it will take $T_{V_{red}}$ minutes to reach the destination airport, being $AD = T_{V_{red}} - T_{V_0}$ and, as $GD + T_{V_{red}} = D + T_{V_0}$, the aircraft arrives at the destination airport at the same CTA as in the baseline scenario. Note that $GD \leq D$, $AD \leq D$ and $D = GD + AD$.

With this strategy, the aircraft will still experience the imposed delay at the arrival airport, only a division on where the delay is realised is made. Therefore, the fairness aspect due to the assignment of the delay, regarding different aircraft of different companies, is not affected by this speed reduction strategy. Reactionary delays are not incremented by using the speed reduction technique as the CTA has been imposed on the airline.

If the GDP is cancelled while the aircraft is still flying, some benefits with respect to the delay

²A precise description of the flight path of an aircraft as a 4 dimensional continuum where every point is precisely associated with a time or a time window (Wilson, 2007).

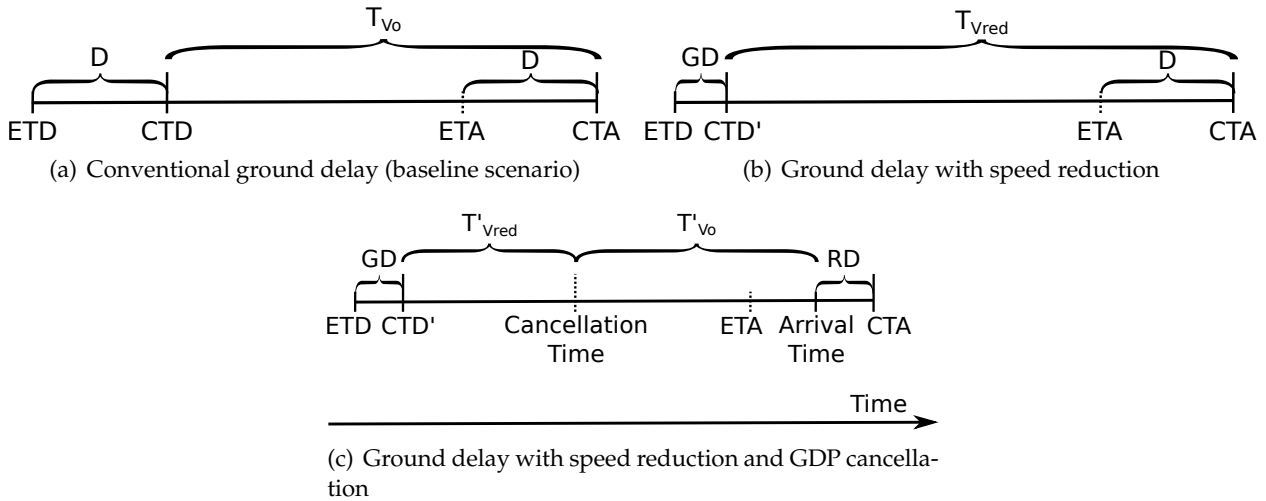


Figure I-3: Schematic representation of ATFM delays in the baseline and speed reduction scenarios and the delay recovery in case of early ATFM initiative cancellation

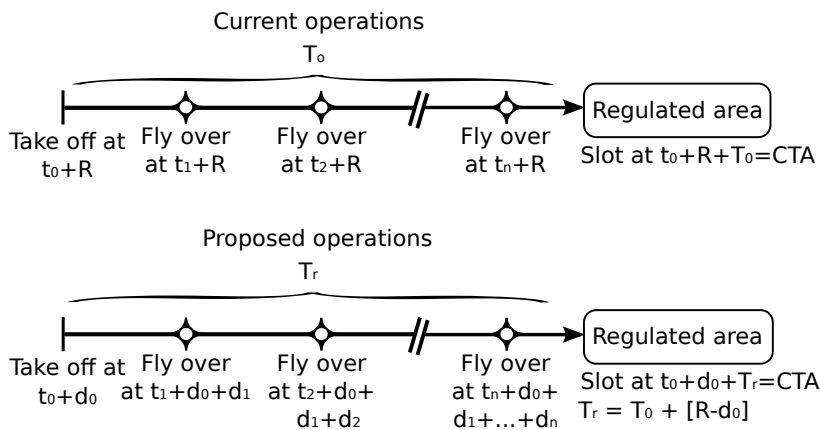


Figure I-4: Comparison between the realisation of delay in current and proposed operations in a 4D trajectories scenario

accrued arise. It could be possible for aircraft crew to increase the cruise speed above the nominal speed in order to maximise the delay recovered, but at the expense of more fuel consumption than initially planned, as has been studied, for instance in (Cook *et al.*, 2009). However, the work presented in this thesis focuses on the case where delay recovery is performed by speeding up to the originally intended nominal speed (V_0) recovering part of the delay, see figure I-3(c). This delay recovered (RD) can even be achieved without incurring extra fuel costs over the initially planned fuel cost. Note that in this case $RD \leq AD$.

This concept, which can be applied to any ATFM regulation which imposes ground delay, is possible if 4D trajectories are used, meaning that fly-over time windows can be attached to the navigation way-points as depicted in figure I-4. The imposed delay will be absorbed along the nominal route, by arriving d_i minutes late at each waypoint i ($D = \sum_{i=0}^n d_i$), where waypoint n is at the entrance of the regulated area or congested airport. Therefore, the moment when the regulation is cancelled is paramount to assessing the amount of delay that can be recovered, as the delay is accrued as the aircraft flies.

In order to fully introduce this strategy ATM technologies such as data link communications between pilots and controllers would be needed. The collaboration between ANSP, airlines and airports is also required.

I.4 Objectives of this PhD thesis

Realising airborne delay by speed reduction opens the possibility of new strategies for dealing with capacity-demand imbalances, as was presented in the previous section. This thesis focuses on the **use of speed variation without incurring extra fuel consumption in order to realise part of the assigned ATFM delay while airborne**, in the context of SESAR and NextGen, where CTAs will be effectively enforced on aircraft and 4D trajectories will be a reality.

To assess this technique, the maximum airborne that can be realised without incurring extra fuel consumption and the parameters that affect this value will be analysed. An assessment needs to be made as to whether the airborne delay that can be realised is interesting from an operational point of view, what the result will be of applying this strategy to realistic scenarios. Finally, some of the potential drawbacks of this technique, such as its impact on the ATC due to the increment of aircraft in the air will be analysed.

By studying the maximum airborne delay that can be achieved, the relationship between speed variation during the cruise and fuel in a general manner is analysed. Speed variation techniques are envisaged for new air transportation management at a tactical level, such as the design of noise abatement procedures or conflict resolution manoeuvres. For instance, the ERASMUS project tries to reduce conflicts by minor speed adjustments or by changes in the required time of arrival (RTA) over waypoints ([ERASMUS Consortium, 2007](#)). However, in general, the effect on fuel consumption of speed variations during the cruise phase is hardly assessed in these types of projects that are focused on the potential of speed variation for conflict resolution. For information about the relationship between speed and fuel regarding the flight planning that airlines realise, the reader is referred to section [III.1](#).

Finally, in SESAR and NextGen, airlines will be owners of their trajectories and collaborative decision making (CDM) will be extended. Therefore, it will be critical for airlines to know the associated cost of solving capacity-demand imbalances in the air transportation network. If a negotiation process is established with concurrent airlines, those with more options, and with better information of the associated costs for each option, will be better placed ([Ross, 2009](#)). As stated in ([Cook & Tanner, 2009](#)): *“A major opportunity, and challenge, facing the airline industry is the integration of disruption management techniques into flight planning. Costs [...] could be used to inform improved decision-making in delay [management], superior to “rules of thumb” currently employed by many airlines”*. In this context, the effect of speed variation during the cruise on the fuel consumption is paramount for airlines.

The main objectives of this research can be summarised as follows:

- to analyse the impact of changes in cruise speed on fuel consumption. In some cases, the airline might be willing to burn more fuel than initially planned in order to realise more airborne delay, or once the regulation is cancelled and the CTA is not longer requested, the crew might increase the speed over the nominal one to increase the recovery.
- to define the speed which allows the airborne delay to be maximised without incurring extra fuel consumption and study the parameters which affect this reduced speed.
- to study the effect of wind and wind forecast accuracy on the flying time and fuel consumption if the cruise speed is maintained as planned or if it is changed to meet the CTA.
- to assess the amount of airborne delay that can be realised with this technique and the amount of delay that could potentially be recovered if this technique is used and the regulation is cancelled before planned without using extra fuel.
- to compute the effect of the speed reduction technique applied to realistic air traffic flow management initiatives.

- to assess how the air traffic management and the air traffic control is affected by the aircraft flying at a reduced speed during their cruise.

1.5 Scope and limitations of this PhD thesis

In the research undertaken in this thesis it is considered that the speed reduction strategy will be used at a pre-tactical phase once the initial flight plan has already been computed. Therefore, the fuel which is used as baseline is the fuel that the airline is going to consume as was planned before the regulation (the nominal fuel block). The suggested strategy tries to realise the airborne delay and recover as much delay as possible, if the regulation is cancelled before planned, without using more fuel than was initially planned. Therefore, it is out of the scope of this dissertation to study the possibility of trade fuel in order to recover extra delay once the regulation is cancelled as suggested in (Cook *et al.*, 2009). The technique used in this thesis allows the fuel cost to be maintained as initially planned, however, the total operating cost is not necessarily constant. There are some costs that might be incremented due to longer block times, such as maintenance or crew costs. For example, most crews on the United States get paid starting when the flight pushes back from the gate.

The application of the speed reduction strategy proposed in this thesis to absorb part of the assigned ATFM delay has been applied to ground delay programs in North America. In order to apply this technique to the ground delay programs, it is assumed that when a ground delay program is defined there are two different airport acceptance rates (AAR): the program airport acceptance rate (PAAR) and the nominal airport acceptance rate. Therefore, the possibility of having a gradual variation of the AAR is not considered. In this thesis there is no a distinction between the technical and practical capacity of the airport and only the AAR is assumed, in reality the capacity of the airport would be affected by dynamic parameters such as fleet mix or dynamic weather changes. When the ground delay program is cancelled, it is assumed that there is no longer any limitation on the airport capacity and that, therefore, all the aircraft that are being held on the ground are allowed to depart without any further delay and that airborne aircraft, realising delay by flying slower, are notified, for instance by data-link, and allowed to speed up as the regulation is no longer needed. Furthermore, it is assumed that when the aircraft arrive at their destination they can be handled and landed without any further additional delay. This assumption is similar to one of the cancellation policies defined in (Ball *et al.*, 2010a), and even if it seems to assume that after the GDP cancellation, the arrival capacity is unlimited, the natural spread of flight times and schedules seems to allow traffic management to use this criterion quite extensively in practice. According to (Ball *et al.*, 2010a), in San Francisco International Airport, around 77% of the GDPs were cancelled under this criteria during the first quarter of 2009. Cooperation between ANSP, airports and airlines is assumed to be implemented.

The climb and descend phases are out of the scope of this research too, and therefore are considered to be flown as in the nominal situation. However, the author acknowledges that in some flights those phases can represent a high part of the total flight. The use of different flight levels rather than those initially computed by the airline is only considered in order to study its effect on the airborne delay that can be achieved without extra fuel consumption, but it is not used when computing its application on a ground delay program. In that case, it is considered that only the cruise speed can be managed.

Safety margins are considered when computing the minimum operational speed, which might limit the reduced speed used. A typical minimum margin against buffeting of 1.3g is generally considered when computing the minimum operational (V_{min}) speed for a given weight and

altitude³. Note that the minimum speed is not limited by the speed stability of the aircraft.

It is worth noting that the tactical level, involving conflict resolution, is not considered and it is assumed to have the same effect on time and fuel as flying at nominal conditions.

Finally, Airbus Performance Engineer's Programs (PEP) suite is used to obtain accurate performance data and to compute the nominal flight plans. Therefore, only Airbus aircraft are able to be simulated. A mapping between non-Airbus aircraft and Airbus ones is applied when necessary.

I.6 Outline of this PhD thesis

The material in the present document is organised in six chapters and four appendices which are summarised as follows:

- **Chapter II** presents the basic concepts related to air traffic management. Special focus is given to the air traffic flow management strategies currently implemented in Europe and in the United States. The new concept of operations defined for SESAR and NextGen is also explained. In this chapter the required background and the state of the art in speed reduction initiatives is also presented.
- **Chapter III** is devoted to the study of the effect of cruise speed variation on the fuel consumption and the flight time. The minimum cruising speed which has the same fuel consumption as initially planned is defined and the parameters which influence the consumption are analysed in detail.
- **Chapter IV** contains the assessment of the maximum airborne delay that can be realised without incurring extra fuel consumption in calm and wind situations. The effect of the wind on the airborne delay is analysed in detail. Finally, the relationship between the use of extra fuel in order to perform extra airborne delay is presented.
- **Chapter V** analyses the use of the speed reduction strategy on realistic air traffic flow management initiatives, in particular ground delay programs. The implication of this technique on the air traffic management is presented. First, an analysis of the ground delay programs is presented, followed by the application of this technique in three representative airports: San Francisco International Airport, Newark Liberty International Airport (EWR) and Chicago O'Hare International Airport (ORD).
- **Chapter VI** gives the conclusions that are drawn from this work and suggests some future work that could be done in the direction of the presented research.
- **Appendix A** explains in detail the implementation of ground delay programs in the United States.
- **Appendix B** shows the principal differences found between the use of Base of Aircraft Data (BADA) database ([Eurocontrol Experimental Centre, 2011b](#)) and the Airbus Performance Engineer's Programs in the context of this dissertation.
- **Appendix C** tackles the analysis of the quality of some of the simulations performed in chapter IV and of the simulations of chapter V. The comparison on fuel consumption between the Airbus software and the simulated flights, and the comparison of the flight times and fuel consumption in the nominal and speed reduction flights are shown.

³In order to ensure good aircraft manoeuvrability, while preventing the aircraft from stalling, the minimum operational speed is set to the stall speed at a given load factor. This load factor is typically chosen at 1.3g. ([European Aviation Safety Agency, 2011](#)).

- **Appendix D** shows the results of application of the GDPs of chapter **V** on the studied demand.

II

Background and progress beyond the state of the art

Air traffic management has been defined by the International Civil Aviation Organisation (ICAO) as the dynamic and integrated management of air traffic and airspace safely, economically and efficiently through the provision of facilities and services. Therefore, when ATM is referred to, it includes the infrastructure of the systems, the people and procedures that enable air transport and other aerial movements to operate in a safe and efficient manner (SESAR Consortium, 2006).

Air traffic management is a continuous process that, for any given flight starts years before the day of operations and ends when the flight is completed. Usually, the ATM process is divided into several phases that can be classified as:

- Medium-term: from between 7 and 5 years to approximately 1 year before the day of operation.
- Strategic: from approximately 12 months to 1 week before the day of operation.
- Pre-tactical: 7 days before the day of operations.
- Tactical: from two hours before push-back until the aircraft is parked at the destination airport.

The ATM system, from an operational viewpoint, is characterised by a number of ATM elements (SESAR Consortium, 2006; Nagle, 2009) :

- Airspace organisation & management (ASM)

Airspace organisations define the airspace structures to accommodate the expected air traffic demand. This process is done in a strategic and medium-term level. Airspace management is defined as the process used by the airspace organisation to apply the airspace options to meet the demand. For more information about the airspace organisation, the reader is referred to section II.1

- Airport operations

Airport operations are an integral part of the ATM system as they provide and manage the ground infrastructure. Airports are one of the bottlenecks of the current system. Their capacity is limited and the extended hub and spoke system favour the congestion (Elhedhli & Hu, 2005; Grove & O’Kelly, 2005; Eurocontrol - STATFOR, 2008). In section II.2 the parameters affecting the airport capacity are detailed.

- Air traffic control (including separation and synchronisation)

The main objective of the air traffic control service is to tactically ensure the separation between aircraft whilst keeping an efficient flow of air traffic. The objective is to reduce the risk of collision to acceptable levels. As expressed in (SESAR Consortium, 2006), aircraft must be separated from other aircraft, terrain, bad weather, wake turbulence, incompatible airspace activities and, when the aircraft is on the ground, surface vehicles and other obstructions on aprons and other manoeuvring areas. As is presented in section II.3, air traffic control will also affect the ATM system capacity.

- Air traffic flow and capacity management (ATFCM)

In the pre-tactical phase the capacity and demand imbalance is analysed. If needed, actions are taken to avoid the overuse of the airspace in order to help the ATC to have a safe and efficient flow of aircraft. Nowadays, this process is conducted in Europe by the central flow management unit, and in the United States by the Federal Aviation Administration (FAA). See section II.4 for details.

- Information management & services

Information management is the basis for the development of collaborative decision making processes. When dealing with highly constrained problems with opposite objectives CDM helps in the achievement of an acceptable solution, taking into consideration the needs of the involved stakeholders. Collaborative decision making requires a spirit of cooperation and, as stated in (Nagle, 2009), is primarily invoked to resolve competing demands for an ATM resource and to organise a safe sharing of that resource among airspace users.

- Airspace user

Airspace users (i.e. airlines) are one of the key stakeholders. They need to plan their flights in advance, in different planning horizons, from seasonal scheduling to prior to flight dispatching. In section III.1, these processes are detailed. ATM accommodates diverse types of vehicles with different characteristics, from civil commercial flights to military aircraft or, in the near future, unmanned aerial systems.

As is indicated in (SESAR Consortium, 2006), the ATC, ASM and ATFCM services that are part of the ATM are provided by national ANSPs, typically, one per state. In some particular cases, it has been delegated to a supranational organisation such as Eurocontrol. It is also possible to provide the above-mentioned services by the military or even by private companies.

For the purpose of this thesis, it is important to understand the underlying concepts related to capacity and capacity-demand imbalance management. Therefore these points are described with more details in the next subsections.

II.1 Airspace Organisation & Management

Airspace organisation consists in the structuring, division and categorisation of the airspace and the definition of the air routes. These activities are developed mainly in a strategic and medium-term basis by studying the expected traffic flows, as well as other aerial activities such as the military. The flexible use of airspace (FUA) has become a main issue of this phase (Eurocontrol, 2009b). The goal being to coordinate the military and civil traffic in order to close some parts of the airspace to the civil aircraft only when military activities are undertaken. In this way, it is possible to increment the capacity of the airspace while being more efficient, flying more direct routes.

At a strategic level, airspace design is reviewed for each season to ensure the best accommodation of expected demand. Research efforts have been made to help, on one hand in determining the best configuration of the aerial routes (Gianazza & Durand, 2005) and on the other hand, in determining the best sectorisation for a given airspace, given the airway configuration, see for instance the work developed in (Bichot, 2006; Bichot & Durand, 2007; Gianazza, 2007; Conker *et al.*, 2007; Tang *et al.*, 2012).

II.2 Airport capacity

As stated in (Gilbo, 1993), airport capacity is defined as the maximum number of operations (arrivals and departures) that can be performed during a fixed time interval (i.e. 15 minutes or one hour) at a given airport under given conditions, such as runway configuration and meteorological conditions. The determination of the capacity of an airport is a complex task as many factors should be considered. Some parameters are related to the airport layout and characteristics, such as number of runways and distance between them, or the presence of fast exit taxi-ways (Federal Aviation Administration, 1983; Fan, 1992). Other parameters depend on the intended use of the infrastructure as arrival/departure ratio, runway configuration or aircraft type mix (Tošić & Horonjeff, 1976; Venkatakrishnan *et al.*, 1993; Butler & Poole Jr., 2008). Furthermore, the practical capacity might be affected by human factors (controllers workload) or even airspace capacity factors (Ball *et al.*, 2007).

In general, the capacity of the arrival fixes exceed the runway capacity, but at some airports and at some times of the day, they can be overloaded (Gilbo, 1993; Gilbo, 1997; Butler & Poole Jr., 2008). Capacity might also be limited by the spacing needed at runway thresholds between inbound aircraft to prevent the effects of wake vortices. This represents a longitudinal wake turbulence separation constraint used by the air traffic control (Hinton & O'Connor, 2000; Butler & Poole Jr., 2008). In this context, the sequencing of arriving aircraft is paramount to determining the acceptance rate of a given airport (Dear & Sherif, 1991). It has been demonstrated that it is necessary to do the sequencing optimisation to reduce the separation required at the beginning of the common path of the inbound traffic, and that little is gained by reducing only the time separation at the runway threshold (Blumstein, 1959). For instance, With algorithms such as the one developed in (Beasley *et al.*, 2001), it is possible to reduce between 2-5% of the time span required to land a set of considered aircraft as a function of the sequencing used.

Airport capacity is comprised of two interdependent capacities, the arrival capacity and the departure capacity. The relationship between them can be shown on an arrival/departure capacity plane as depicted in figure II-1 (Fernandes & Pacheco, 2002). This graph represents a set of capacity values that reflects the operational capabilities of the infrastructure in certain conditions. In order to particularise the relationship for a specific airport, a mathematical approximation of experimental data validated by traffic managers and controllers or simulations are needed (Newell, 1979; Barrer *et al.*, 2005). Both capacities should be considered when optimising the throughput of an airport (Gilbo, 1993). Actual airport capacities are subject to substantial uncertainty as they de-

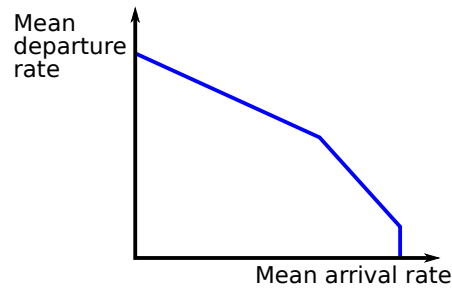


Figure II-1: Typical relationship between airport arrival and departure capacity for a single runway

Based on: (Ball et al., 2007)

Table II-1: Airport acceptance rate per hour for San Francisco International Airport. Source: (Federal Aviation Administration, 2012g)

Arrival	Departure	VMC	LOW VMC	IMC	LOW IMC
28L 28R †	01L 01R	60	45	30	27
28L 28R ‡	28L 28R	45	45	30	27
28L	28L	27	27	25	N/A
28R	28R	27	27	25	25
PRM 28R 28L *	01L 01R	36	36	N/A	N/A
19L 19R ‡	19L 19R	35	25	25	N/A
19L	19L	25	25	25	N/A
19R	19R	25	25	25	N/A
19L 19R ◊	10L 10R	40	27	27	N/A
01R	01L	30	25	N/A	N/A
10L 10R	10L 10R	33	27	27	N/A
10L	10L	27	27	25	N/A
10R	10R	27	27	25	N/A

† Side by procedures. Minimum Ceiling for VAPS 3000-3500 ft

◊ Side by procedures. Minimum Ceiling for VAPS 4000-4500 ft

‡ Stagger by procedures

* SOIA rate for runways 28R—28L with minimum ceiling 1,600 ft and visibility 4 NM

pend on stochastic weather conditions (Inniss & Ball, 2002). Weather conditions determine which runway configuration and landing procedures are used. The combination of the runway configurations and the landing procedures in turn determines an AAR or operational capacity (Liu et al., 2008).

There are two major types of landing procedures, under instrument flight rules (IFR) and under visual flight rules (VFR). For example in San Francisco International Airport, in nominal conditions, the visual approach (VAPP)'s AAR is 60 aircraft per hour, while in IMC the capacity is reduced to 30 aircraft per hour; as the two parallel arrival runways of SFO cannot be independently operated when the visibility is reduced (Janić, 2008). Table II-1 presents the AAR per hour at SFO for different runway configurations and weather conditions as declared by the FAA. It is possible to observe how, as a function of the airport configuration and weather situation, the landing capacity changes from 60 aircraft per hour to only 25 aircraft per hour.

There are differences between Europe and the United States in the use of the airport infrastructures, for example in the United States it is common to perform land and hold short operations

(LAHSO) which are not permitted in Europe (Federal Aviation Administration, 2012a). This leads to the situation where, in the United States, the utilisation of the runway infrastructure can reach up to 30 aircraft per hour when in Europe this value is lower than 20 aircraft per hour. However, if in the United States a higher investment has been made in the construction of runways, while the gates and terminal are starting to become a limitation, in the United States, the ratio of runways to gates is 1:26 while in Europe it is 1:42 (Donohue & Laska, 2000).

II.3 Airspace capacity and air traffic control

For each sector a group of two air traffic controllers (ATCO) are in charge of ensuring the smooth flow of air traffic and the separation of the aircraft from any hazardous situation. The ATCOs have to do demanding mental work to ensure the correct execution of their tasks. The executive controllers are responsible for the separation and sequencing of the flights in their area of responsibility (sector). They have to monitor the aircraft and predict their trajectories. When a conflict is detected, clearances and orders have to be given to aircraft involved in the situation. The executive controllers will use changes in heading and in flight level, as well as changes in speed, to keep the aircraft separated. Once a solution has been implemented, it has to be monitored to ensure its correctness and execution. This mental process is repeated in every control working position. The executive controllers also need to coordinate with the executive controllers of the surrounding sectors and with the planning controller of their own position. The planning controllers check the intended flight plan and help the executive controllers with the coordination with other sectors and with the detection of future conflicts. Some automatism has been introduced to improve the safety and the efficiency of the airspace. For instance, medium term collision detection algorithms (MTCDD) help the controller in the detection of conflicts (Harvey & Costello, 2000).

The ANSPs tactically configure the airspace by combining or dividing sectors in order to adapt the demand to the capacity that the controllers can handle. To do so, they use the information of the foreseen flights and pre-computed sectorisation open schemes that have been developed in the strategic phase of the airspace organisation and management (see section II.1). Projects such as e-TLM (Cano *et al.*, 2007) try to use simulation results of the real forthcoming traffic to help in the selection of the best sectorisation to use from the sectorisation scheme, in order to adapt as much as possible the available capacity to the real expected traffic. In (Gianazza *et al.*, 2009; Gianazza, 2010), neural network and tree search algorithms are suggested to predict the forthcoming workload of the ATCOs and the best airspace configuration.

The maximum capacity for a given sector is defined as the number of aircraft that can enter the sector per hour without overloading the controllers. It is important to have an estimation of this value. However, as the number of aircraft that are in a given sector does not determine directly the workload of the controllers, the estimation of the available capacity is a complex task (Gianazza & Guittet, 2006; Kopardekar *et al.*, 2008). It has been determined that the type of traffic and operations have a direct influence on the maximum number of aircraft that can be handled safely at the same time (Cavcar & Cavcar, 2004; Lee *et al.*, 2007; Song *et al.*, 2007). Therefore, the capacity depends on the structural complexity of the airspace and the complexity of the involved traffic (Sridhar *et al.*, 1998; Delahaye *et al.*, 2004). This is one of the reasons why the capacity of a given airspace is computed from controller workload models (Janić, 1997; Welch *et al.*, 2007; Martín *et al.*, 2008; Lopez-Delgado & Barbas-Gonzalez, 2008), using models of the behaviour of the ATCOs (Bayen *et al.*, 2005) or even with real-time simulation and interviews. Moreover, it has to be considered that the maximum capacity of a sector is a dynamic parameter as it is affected by changing conditions, such as, for example, meteorological hazards (Song *et al.*, 2007; Lee *et al.*, 2008; Lee *et al.*, 2009; Prandini *et al.*, 2010).

The conflict detection and resolution problem has also been tackled from a centralised and

a decentralised perspective in the literature. The first approaches considered centralised geometrical solutions (Chiang *et al.*, 1997), while more recently, the use of mixed-integer linear programming (Pallottino *et al.*, 2002; Vela *et al.*, 2009) to find a quick and efficient solution has been suggested. Other centralised approaches include the use of genetic algorithm techniques (Durand & Alliot, 1995), or even ant colony optimisation (Durand & Alliot, 2009). Other authors consider that in the context of free flights, where the aircraft's crew are able to choose their path freely and assuring self separation, without ATC, the use of distributed conflict detection and resolution techniques is more appropriated (Košecká *et al.*, 1997; Tomlin *et al.*, 1998; Eby & Kelly, 1999; Archambault & Durand, 2004; Devasia *et al.*, 2011). The main problem of all these automatic techniques is that it is very difficult to guarantee that the algorithm will always generate a conflict free trajectory without the supervision of an air traffic controller. Thus, some efforts have also been made to consider the system uncertainties (Granger *et al.*, 2001; Jardin, 2004; Lecchini Visintini *et al.*, 2006). If the reader is interested in a review of conflict detection and resolution method see (Kuchar & Yang, 2000), where 68 techniques are analysed and classified.

II.4 Air traffic flow management strategies

Once the airspace has been configured, it must be ensured that the controllers and the airport infrastructure will be able to handle the real traffic that operates. The ATFM is a ground-based service that, in the pre-tactical phase, evaluates traffic flows in order to balance capacity according to a demand baseline. The goal is to avoid an overload of the air traffic control services and minimise the penalty imposed on the aircraft operators due to congestion (SESAR Consortium, 2006). Nowadays, the principal ATFM measures consist in imposing delayed departure times or proposing alternative routes over non-congested areas. Other alternatives such as holding stacks or speed variations are used only by ATCOs at a tactical level (Eurocontrol, 2009a). Generally, rerouting and air holdings are less desired because of higher operating costs, mainly due to fuel consumption, if compared with ground delays (Carlier *et al.*, 2007).

However, the realisation of ground delay may cause congestion at the departure airports (Carlier *et al.*, 2007), and the actual implementation of the delay assignment algorithm suffers from the discrepancies between planned and actual flights due to the system uncertainty. This leads to a misuse and/or overuse of airspace resources (Gwiggner *et al.*, 2008). These discrepancies are mainly due to the fact that controlled times of arrival are not enforced, since 4D trajectories have not yet been implemented by all operators. As only controlled times of departure are imposed, some aircraft might increase their cruise speed in an attempt to recover some of the time lost on the ground and compete for arrival runway use on a first come first served basis, aggravating the congestion situation at the arrival airport (Knorr *et al.*, 2011).

In Europe, this ground delay strategy is implemented by the central flow management unit (CFMU). While in the United States, the ground delay program and the airspace flow program (AFP) are implemented when capacity-demand mismatches are foreseen at arrival airports and airspace sectors respectively.

II.4.1 Ground holding problem

As stated in (Ball & Lulli, 2004), when an imbalance between demand and capacity takes place, the total amount of delay required to balance demand and capacity, (the sum of holding delay and ground delay), is constant. For a reduced capacity at an arrival airport, this amount of delay depends only on the airport acceptance rates and the flight demand at the airport, as depicted in figure II-2. The ground holding problem, consists in deciding how to assign this delay in order to realise it on ground prior to departure to minimise the expensive holdings. This is true if it is

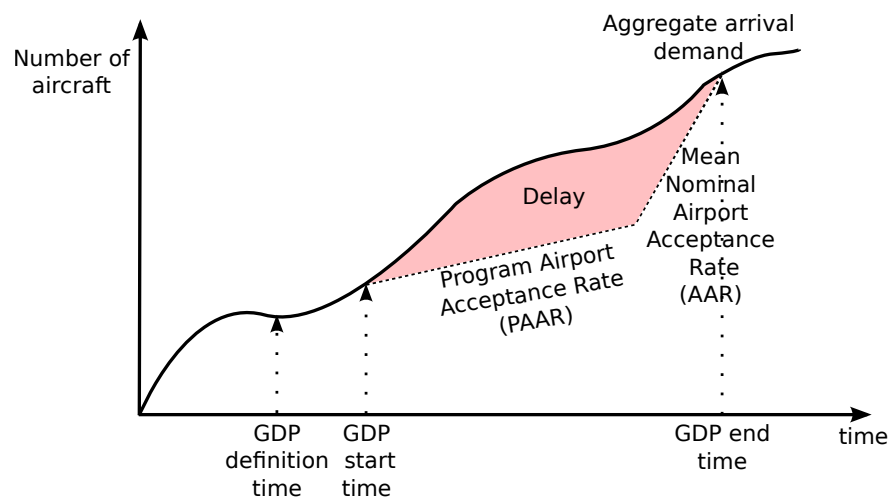


Figure II-2: Aggregate arrival demand and delay in a ground delay program

not considered the traffic mix at the arrivals which would affect the real airport capacity, as it was assumed in section I.5.

Deciding which aircraft to delay and for how long in order to not exceed ATM resources is a complex optimisation problem which has been thoroughly addressed in all its forms: as a deterministic (Odoni, 1987) or stochastic process (Richetta & Odoni, 1993; Terrab & Odoni, 1993; Ball *et al.*, 2003; Mukherjee & Hansen, 2007; Glover & Ball, 2012), and for a single (Odoni, 1987; Mukherjee & Hansen, 2007) or a multi-airport scenario (Vranas *et al.*, 1994b; Navazio & Romanin-Jacur, 1998; Brunetta *et al.*, 1998). The stochastic approach allows weather uncertainty to be considered and the use of dynamic policies, as there is more certainty about the actual airport capacity as time passes. For example, in (Vranas *et al.*, 1994a), the problem is considered in a dynamic environment with weather and fleet availability changes. Some techniques to solve the ground delay problem even consider operational restrictions, such as banking constraints to accommodate hubbing operations (Hoffman & Ball, 2000). Others, as the one described in (Peterson *et al.*, 1995), the propagation of delay on a network of more than one airport to be analysed. However, in general, all these models need accurate information about the flights, and in particular, the costs associated with delay.

These techniques that were originally focused at an airport level have been extended in order to deal with all the network constraints, including airspace capacity restrictions. In this manner, without considering the detailed performances and fuel consumption of the flights, the whole air traffic flow management problem, with ground delay, speed control during cruise and rerouting, can be solved, see for instance (Bertsimas & Patterson, 1998), (Bertsimas & Patterson, 2000) or (Bertsimas *et al.*, 2008). For a wider and excellent literature review of modelling and optimisation in traffic flow management, the reader is referred to (Sridhar *et al.*, 2008).

II.4.2 Europe: Central flow management unit (CFMU)

In Europe, en-route airspace sector congestion is as important, or even more important, than airport congestion (Filar *et al.*, 2002). The central flow management unit is in charge of the ATFCM activities. Acting as a network manager, the CFMU has the responsibility of balancing capacity and demand in order to keep the demand below the capacity for each airport and sector.

Pre-tactically, the European air navigation service providers submit the capacity of their airspace sectors and airports to the CFMU, which analyses how to manage the available capacity resources and coordinates with the national flow management positions (FMP) the required reg-

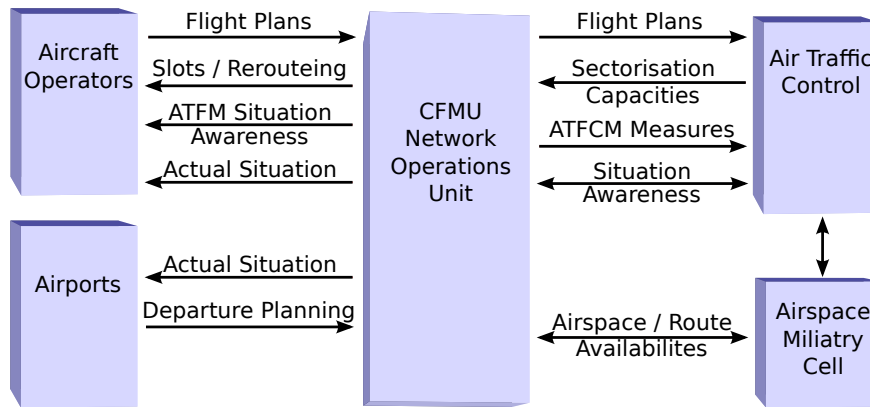


Figure II-3: CFMU network operations unit operational structure.

Based on: (Eurocontrol Central Flow Management Unit, 2011).

ulations, identifying possible re-routing solutions. The result of this process is the air traffic flow capacity management daily plan (ADP). On the other hand, airspace users submit their intended flight plans to the CFMU and, as can be seen in figure II-3, the CFMU regulates the demand by imposing on ground delays when necessary.

The ATFM delay is defined as the time which elapses between the last take off time requested by the aircraft operator and the take off time given by the CFMU (Eurocontrol, 2009a) (see figure I-3(a)). The controlled times of departure are 15 minute time windows around the actual requested time of departure (-5,+10 minutes). The reason for this margin is that there are uncertainties that are intrinsic to the system, and that take off windows give margins to the controllers to deal with taxi and take off sequencing. Nevertheless, by delaying the aircraft, it is ensured that the peaks of demand are smoothed and, therefore, the controller will be able to handle the forecast traffic safely.

The implementation of the algorithm in assigning the slots and the resulting delay is known as the computer assisted slot allocation tool (CASA) (Eurocontrol Central Flow Management Unit, 2011). The assignment is done following a ration-by-schedule policy (RBS). CASA with RBS is a greedy algorithm which is considered to be fair and equitable by definition with respect to the airlines and which achieves the minimisation of the total assigned delay when there is one constrained resource involved (Vossen & Ball, 2006a; Ranieri & Castelli, 2009; Castelli *et al.*, 2011). However, it does not consider the cost for the operators and the repercussion of the imposed delay on that cost. Therefore an optimal solution from an economical point of view is not guaranteed (Barnier & Allignol, 2008). The same amount of delay can indeed be more expensive for one given operator than for another depending on the actual cost structures of the aircraft operator, and the characteristics of each particular flight (i.e. passenger and crew connections) (Ranieri & Castelli, 2009; Cook *et al.*, 2009). The fairness of RBS fails in cases of multiple resources. CASA algorithm uses the most constrained penalising resource policy when dealing with more than one constraint. Some research is undertaken in order to consider the effects of the RBS when dealing with multiple resources, such as (Barnhart *et al.*, 2012; Bertsimas *et al.*, 2011).

One main advantage of CASA is that it is able to consider operational constraints and updates to the flight plans. Airlines can respond to the assigned delay by realising it, submitting updates to their flight plans, cancelling them or requesting a re-routing.

Some effort has been made in order to try to improve the CASA algorithm using new techniques as constraint programming, see for instance (Barnier *et al.*, 2001), or extending the ground delay to deal with conflict resolution and not only with capacity-demand imbalances at an airspace sector level (Barnier & Allignol, 2009). Nevertheless, these modifications of CASA's

algorithm present some issues that stop their practical implementation, such as the difficulties of dealing with real time modifications and cancellations of the flight plans.

II.4.3 USA: Ground delay program

In the United States of America, a similar principle as in Europe is used in order to deal with capacity–demand imbalances, but with some particularities. A ground delay program is implemented when an airport is expected to have insufficient arrival capacity to accommodate forecast arrival demand. The Federal Aviation Administration, acting in its role as traffic flow manager and through the Air Traffic Control System Command Center (ATCSCC), activates a program where aircraft are assigned to available slots following a RBS principle (Richetta, 1994). After this assignment, airlines are given an opportunity to reassign and cancel flights based on updated flight status information and their internal business objectives. This is achieved in a CDM process motivated by a need to combine information sources (Wambsganss, 1997; Ball *et al.*, 2000; Vossen & Ball, 2006b).

As was stated previously, assuming that no holding delay is assigned, the total ground delay is approximately constant. However, and in order to deal with uncertainty, a particularity of the North American ground delay program is that some flights are exempted from the FAA assigned delay, and therefore a trade-off between which aircraft receive the delay exists. A first set of exempted flights are those airborne at the time the GDP is implemented and international non-Canadian flights. The second set is GDP dependent and are the aircraft whose departure airports are further than a given distance from the GDP airport. This distance is fixed at the GDP implementation and it can be a radius or a number of tier from the centre where the affected airport is located of the national airspace system (NAS).

As defined in (Ball & Lulli, 2004), in the current operations, the NAS is divided into 20 centres, and for each centre a first and a second tier are defined. The first tier is the set of all centres immediately adjacent to the centre in consideration, and the second tier is the first tier with the centres immediately adjacent to the first tier centres, and so on.

One of the main reasons for applying this exemption policy is the uncertainty when estimating the arrival capacity of the airport. These predicted capacity reductions are often caused by adverse weather conditions which, in turn, are sometimes forecast several hours ahead. Thus, too pessimistic forecasts can lead to excessive ground delays. Since flights originating farther from the airport must execute their ground delay well in advance of their arrival, if the ground delay is cancelled, all that accrued delay would be unnecessary. Therefore, most of the delay is usually assigned to shorter-haul flights by exempting flights originating outside the above mentioned radius. For more details of the effect of applying a radius of exemption on a GDP, the reader is referred to section V.5.1.

Other criteria than RBS have been analysed in other literature, such as ration-by-passenger, which maximises the passengers throughput and can decrease passenger delay by 22% with respect to RBS, ration-by-aircraft size, or even considering the fuel consumed during the ground holding at the taxi with ration-by-fuel flow (Manley & Sherry, 2010). Considering the fact that the regulations are usually cancelled before planned, ration-by-distance (RBD) policy has been suggested where prioritisation is given based on the distance of the flight plans. It has been proven that RBD minimises the total expected delay in the presence of early ground delay programs cancellation (Hoffman *et al.*, 2007; Ball *et al.*, 2010a). However, if some of these criteria can be more efficient from a passenger or an environmental point of view they have problems with equity and fairness between airlines. This is the rationale behind the work presented in (Wang *et al.*, 2012) where a combination of ration policies between RBS and RBD by weighting them is suggested to form a compromise between equity and efficiency.

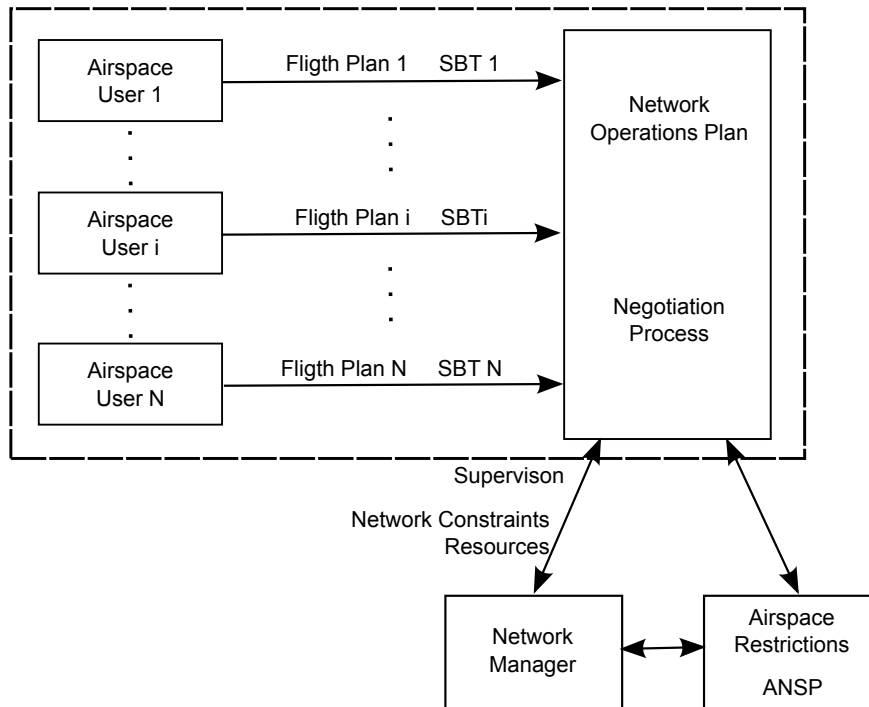


Figure II-4: Stakeholders interaction under SESAR concept of operations

In this thesis, the use of speed reduction has been applied to ground delay programs. For more details about GDP and CDM see appendix A.

II.5 SESAR and NextGen

The new concept of operations that is proposed in SESAR involves some major changes with respect to the current operational system. A similar concept is proposed in the NextGen program, but for the sake of simplicity the SESAR terminology is used and explained hereafter.

According to SESAR, the airspace user (i.e. the aircraft operator) will be the owner of the trajectories and a protocol will be established to develop and modify them. If a capacity-demand imbalance exists, a negotiation process among airlines should be made to solve the potential conflicts. The network managers will no longer be in charge of solving the imbalance in a centralised manner but of coordinating negotiations between the airspace users (see figure II-4). Thus, airspace users will be involved in the process of balancing demand and capacity and a collaborative decision making process (CDM) will become mandatory at a strategic level (SESAR Consortium, 2007).

Figure II-5 shows the processes that will be used in this new operational concept. On a long-term basis (years before the operation day), the business development trajectories (BDT) will be developed inside the user's organisation. Eventually, the BDT will become the shared business trajectory (SBT) and will be available to other users via the network operations plan (NOP), which will be distributed to the network manager and to the air navigation service providers. This process will be done on a mid/short-term basis: from 6 months up to a few hours before the flight. Using these SBTs, the ANSP will determine, among others, the airspace configuration, the available routes and their allocation of resources.

With the network constraints the airspace users will try to adapt the demand to the available capacity as much as possible. The task assigned to the network manager in the new operational

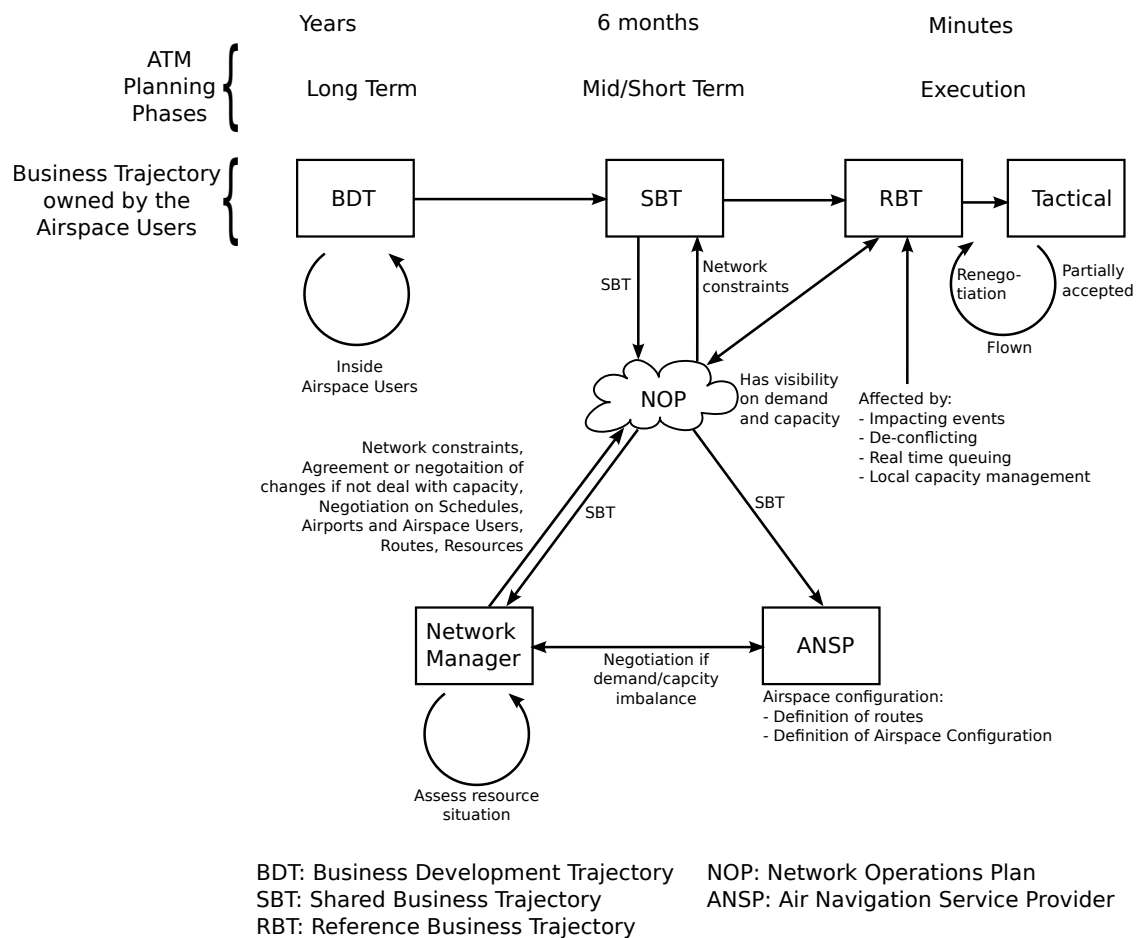


Figure II-5: Trajectory development under SESAR concept of operations.

Based on: (SESAR Consortium, 2006).

context is the coordination of the different airspace users. In this context, the negotiation process was analysed in (Ranieri & Castelli, 2009), where a market based mechanism was suggested. In this case, after an initial ration-by-schedule assignation, an auction process is initiated. The airlines are owners of their initially assigned slots, but during the auction process they may keep or sell them according to their own interests.

The airspace users will modify their SBT while fulfilling the constraints, and a new iteration will start. This iterative process of negotiations will end when an acceptable solution for all the stakeholders is found. At this point, the SBT becomes the Reference Business Trajectory (RBT), which the airspace user agrees to fly and the ANSP and airports agree to facilitate. The RBT are full 4D trajectories where a time window is attached to each waypoint.

The RBT will be need to be cleared in the execution phase and might change according to requests coming from either the airspace user or the ANSP. These changes will allow weather and trajectories uncertainties, separation and queue management, and changes in constraints or resources availability to be dealt with. When an airspace user proposes a RBT amendment the ANSP will have to accept this modification if all the constraints are met (SESAR Consortium, 2007).

Both in SESAR and NextGen, 4D trajectories are envisaged to be the base of the future of air traffic management (SESAR Consortium, 2007). Even without the collaborative mechanism design for the development of the reference trajectories, the use of 4D trajectories will enhance the predictability of the system (Korn & Kuenz, 2006). Some trial flights using this technology

have already been conducted (Kooster *et al.*, 2009; Wichman *et al.*, 2007). For the work developed in this thesis, it is especially important that controlled time of arrivals will be able to be enforced prior to arrival at over congested infrastructures (sectors or airports). In this context, in autumn 2012, the FAIR STREAM (FABEC ANSPs and AIRlines in SESAR TRials for Enhanced Arrival Management) consortium, involving major European airlines, air navigation service providers and suppliers, has started work on flight trials performed with commercial flights and existing technical systems involving the airports of Munich, Paris and Zurich. The objective of this project is the study of the use of target time of arrival (TTA) instead of calculated take off time (FABEC, 2012).

The speed reduction presented in this dissertation could be used in the process of creating the RBTs or at the moment when an RBT has already been issued, but weather constraints force its modification to deal with assigned delay.

II.6 State of the art in speed variation techniques

Speed control for ATM purposes has been the subject of several research studies and projects. The majority of the applications focus on a tactical level, where speed adjustments are used to resolve (or mitigate) aircraft conflicts. It is worth noting that the minimum speed should always be bounded by the aerodynamics constraints.

The ERASMUS project tries to strategically reduce conflict generation by speed adjustments in the 4D business trajectory in short segments of 15 minutes, reducing controllers' workloads associated with routine monitoring and conflict detection. These adjustments implemented, by changing the required time of arrival (RTA) of the aircraft at different waypoints, are not directly perceivable by the controllers and do not interfere with their actions. It has been estimated that up to 80% of the conflicts could be solved without the involvement of the controller (ERASMUS Consortium, 2007; Garcia & Gawinowski, 2006; Rey & Rapine, 2012). Variations in the interval [-6%,+6%] of the cruise speed were allowed to perform these separations. The latest results show that variations of up to -12% of the cruise airspeed can be made without the air traffic controllers realising (Avertly *et al.*, 2007).

In the SESAR operational concept, new separation modes are defined, including the trajectory control by speed adjustment (TC-SA), which will be used to minimise potential conflicts and reduce the workload of the air traffic controllers (SESAR Consortium, 2008; Loscos, 2008).

Other studies such as (Huang & Tomlin, 2009) or (Chaloulos *et al.*, 2010) try to solve air traffic management and air traffic control by using speed control. Their goal is to have conflict-free sectors, by controlling the speeds of the flights in the [-10%,+10%] interval. In this context, the CATS project (Contract-Based Air Transportation System) proposes a set of time window constraints that the aircraft must adhere to in order to guarantee the airspace capacity constraints. If the aircraft cannot make a constraint window, a negotiation process starts in order to determine a new one (CATS Consortium, 2007; Guibert *et al.*, 2008). The Innovative Future Air Transport System (IFATS) project was developed under the 6th European Union Framework Program to analyse how the new ATM system might be (Brunet *et al.*, 2005). Here 4D trajectories with time window constraints to deal with conflicts is also presented (le Tallec & Joulia, 2007).

This type of trajectory management is the basis for future implementation of 4D trajectories and enables the use of speed management for ATFM purposes and not only at a tactical level. In this context, the FAIR STREAM project studies the use of target times of arrival instead of controlled times of departure (FABEC, 2012). In (Günther & Fricke, 2006) en-route speed reductions are proposed to prevent aircraft from performing airborne holding patterns when arriving at the congested airspace. The cost to the airline, which also considers the cost of time, is no longer valid

as time has become fixed due to a limited capacity. In this case even flying slower than maximum range might lead to a benefit if holding fuel is saved. The same rationale is included in the research undertaken in a joint FAA/Eurocontrol study where it was estimated that half the terminal area inefficiency in the system today could be prevented through speed control in the cruise phase of flight, without reducing throughput efficiency (Knorr *et al.*, 2011). Instead of performing holdings at the arrival airport, aircraft could adjust their arrival time, with speed management, to prevent holding stacks. The CANSO Environment Workgroup reported seven case studies undertaken by ANSPs and industry partners related to speed control and controlled time of arrivals to manage fuel and terminal congestion (CANSO, 2011).

The service provider of the United Kingdom (NATS) has already performed trials with United Airlines flights arriving at Heathrow, coming over North Atlantic tracks, reporting significant fuel savings. The procedures are based on the absorption of delay in cruise by speed reduction instead of at holding stacks around the airport. The flights absorbed between 6 and 13 minutes in those trials. Those flights were able to bypass holding and were integrated into the arrivals. Aircraft landed at approximately the same time as if they had maintained their normal cruise speed and gone into holding. It is interesting that to absorb the delay, in some cases, flights had to fly slower than their cost index zero, therefore flying slower than their maximum range speed (see section III.1.1 for more information about the cost index). Currently NATS is working on implementing *linear holding* for North Atlantic flights, in an effort to improve overall fuel efficiency for Heathrow arrivals. (Boeing & CANSO, 2012; CANSO Environmental Workgroup, 2012).

This strategy is already implemented in Sydney airport where Airservices Australia exploits the ATM Long Range Optimal Flow Tool (ALOFT). This tool helps the controller to assign aircraft within a 1,000 mile radius of Sydney airport, an arrival time at a meter located 160 NM and 40 NM from the airport. Both times set at 160 and 40 miles allow sufficient pressure for ATC to fine-tune the sequence and manage additional flow and separations changes as needed, while guaranteeing that no slots for arrival are missed. This prevents intercontinental aircraft from arriving before the airport is open, reducing unnecessary holdings. The goal is to transfer costly holding time at low altitudes and close to airports, to the en route phase of flights (Airservices Australia, 2008). Without a coordinated approach to managing arrivals, airlines were incentivised to arrive earlier in order to improve their position in the arrival queue. The benefits of this strategy include fuel and emissions reductions, less workload for the arrival controllers and smoother sequence and transition into the Sydney terminal area. The MAESTRO system is also used for managing arrivals at major airports in Australia. Once the aircraft are approximately 200 miles from the airport, en route controllers provide a time for each flight to cross a fix located 40 NM from the airport (CANSO Environmental Workgroup, 2012).

Research has been done on the capability of aircraft to fly and meet a time over a fix. The required time of arrival function that is found on many of the sophisticated flight management systems (FMS) can provide a consistent accuracy of less than 30 seconds. While this has been proven with many of the Smiths/GE FMS on next-generation B737's, other FMS ignore this time once the aircraft has commenced descent. These technical inconsistencies across different fleets have been managed in Australia by allowing pilots to manually reduce the speed of the aircraft to achieve the time (CANSO Environmental Workgroup, 2012).

At a pre-tactical level, some research has also been conducted considering speed control as an additional decision variable (in addition to the amount of time of ground holding) to solve the ground holding problem: where aircraft are regulated in such a way that airborne traffic flows do not exceed the available capacity (Bertsimas & Patterson, 1998; Bertsimas & Patterson, 2000). These measures, however, are difficult to implement with the current concept of operations since controlled times of arrival are still not mandated and, therefore, conventional ground delays are still assigned to aircraft at their origin airport as the main pre-tactical air traffic flow management

measure.

In (Prats & Hansen, 2011), it was proposed that ground delayed aircraft could fly at the minimum fuel consumption speed (the maximum range cruise speed) and in this way, the fuel consumption (and environmental impact) of these flights was reduced at the same time as some ATFM delay was absorbed in the air. The impact of this strategy was quantified by analysing the historical data of all delayed flights to San Francisco International Airport over one year. Results showed values ranging from 5% to 15% of the initially assigned delay that could have been absorbed in the air, leading to fuel savings in the order of 4% to 7% for each individual flight, if compared with the nominal situation.

Finally, speed control is used for purposes other than conflict resolution, such as the control of continuous descent approaches (CDA), noise abatement procedures or traffic synchronisation strategies at metering points (Dravecka, 2006; Lowther *et al.*, 2008).

III

Fuel and time trade-off

As was presented in section II.6, many ATM research initiatives use cruise speed variations. When planning a flight, an airline might use more fuel than the minimum required to cover the flight duration, in order to reduce the flight duration, in this way considering the cost of time. However, when the realisation of delay is required, different options are available, and in this case, the impact on fuel consumption is important as time becomes regulated and, therefore, fixed. This chapter presents the basics of aircraft operations and the effect of cruise speed on fuel consumption, along with the definition of the cruise speed which allows airborne delay to be realised without incurring extra fuel consumption. Finally, the parameters which affect that speed are characterised.

III.1 Aircraft operations

The air transport market has been deregulated in the United States and within the European Union and therefore, competition among aircraft operators is one of its main characteristics. In the last years, the incursion of new actors such as low-cost carriers and high-speed trains has put added pressure on the market. Airlines have to react quickly to demand changes, therefore they need flexibility in the development of their networks. Nowadays, product differentiation and price are more important than ever. However, price evolution varies as a function of the business model the airline is developing. Nevertheless, the business is characterised by high fixed operating and overhead costs. Revenues are high but the high costs contribute to a poor performance and even some losses in the industry in the last years (SESAR Consortium, 2006).

In this context, the main objective of aircraft operators is to minimise their direct operating costs while maximising its incomes. Airlines have to work at different levels to achieve this objec-

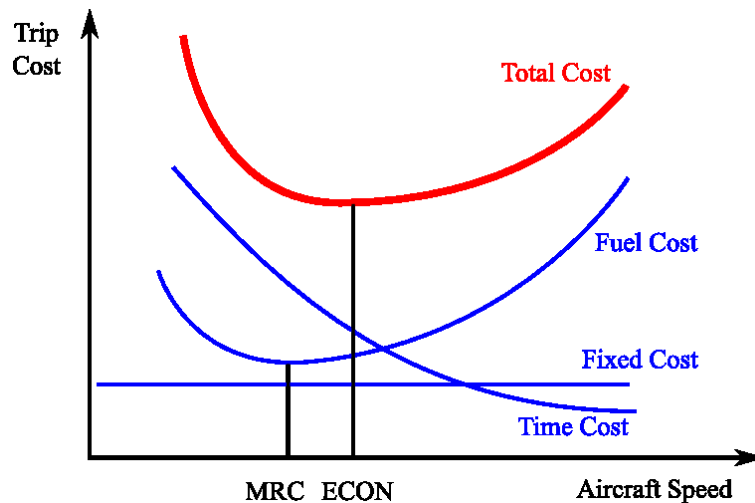


Figure III-1: Aircraft operating costs as a function of the cruise speed

tive. First, an identification of aircraft needs has to be done, this will determine how many aircraft the airline needs and with what configuration of seats. Secondly, a scheduling for the season is needed. Thirdly, as the day of operation gets closer, the yield management becomes critical as the operator has to decide at what price to sell its tickets, having in mind that the product being sold is perishable and that its activities are developed in a very competitive environment. Finally, airlines try to compute and fly efficient flight plans with the maximum load factor, which is the ratio between passengers and number of total seats in the aircraft.

Scheduling is a complex task which is done within the six months prior to execution. This process is driven by the economical situation, the airline strategy and the market estimated demand. It is usually developed in different stages: fleets are assigned to routes, then aircraft are assigned to flights and finally airlines do the crew scheduling and the assignation of crew to itineraries. In (Klabjan *et al.*, 2002) a more integrated approach is presented by solving the crew scheduling before aircraft routing. Crew assignment is paramount to have a robust network, as crew connections are critical to minimising network disruptions in the presence of delay. Moreover, many parameters need to be considered in this assignment such as, for instance, operational regulations that limit the number of hours a crew is allowed to work, scheduled maintenance that might leave a plane on ground for several days, the minimum rotation time at an airport or passenger flight connections and passenger connection times. For a review of airline crew scheduling, see (Gopalakrishnan & Johnson, 2005).

Airlines face a multi-objective problem when creating their scheduling as, on one hand, they want to maximise the use of their fleet, while on the other hand, flexibility, achieved with buffers¹, is needed in order to deal with unexpected mishaps (Rosenberger *et al.*, 2004; Klabjan *et al.*, 2001; AhmadBeygi *et al.*, 2008; AhmadBeygi *et al.*, 2010). In general, techniques such as buffeting to absorb delay are used by airlines, leading to a trade off between the robustness of the solution and the cost of implementing it (Ehrgott & Ryan, 2002). The scheduling problem is enhanced in (Schaefer *et al.*, 2005) by considering uncertainty, and in (Barnhart *et al.*, 2002), the network effects are taken into consideration.

¹In airline scheduling, the scheduling buffer time is the time allowed from when the aircraft arrives at a given airport and when it takes off in its following flight segment (Wu & Caves, 2002).

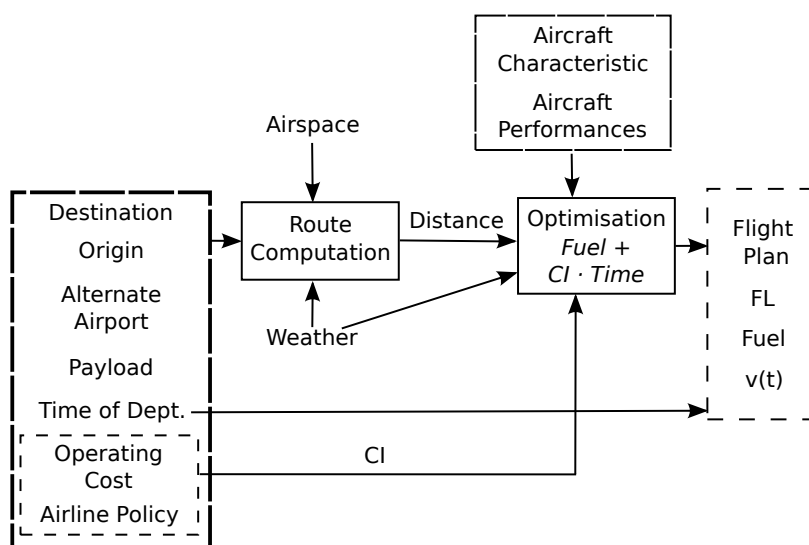


Figure III-2: Scheme of the current flight optimisation ($J = \text{Fuel} + \text{CI} \cdot \text{Time}$) realised by aircraft operators

III.1.1 Cost index

Considering the direct operating cost of a given flight, in the majority of civil aviation flights, three types of costs are present: fuel costs, time-dependent costs, which include, among others, maintenance or flight crew related costs (Airbus, 1998), and fixed costs, which are independent of the time or fuel consumption (such as landing fees or aircraft ground handling). Therefore, not only fuel consumption but time-related costs are also considered when airlines try to minimise their total operating cost. As shown in figure III-1, fuel and time-dependent costs vary as a function of the flight cruise speed. The aircraft operators have to trade-off between the amount of fuel consumed and the time needed to fly a certain route.

Aircraft equipped with flight management systems use a *cost index* (CI) parameter when optimising their flight profiles in order to consider the airline policy regarding its operating costs. The CI expresses the ratio between the cost of the flight time and the cost of fuel (Boeing, 2007)². Thus, a CI set to zero means that the cost of the fuel is infinitely higher than the cost of time and the aircraft will fly at the speed which minimises the fuel consumed per unit of distance flown: the maximum range speed (V_{MR} or MRC). The maximum value of the cost index gives priority to the flight time, regardless of the fuel needed. In this case, the aircraft will fly at the maximum operating speed (V_{MO}/MMO ³) with, in general, some safety margins. By choosing and introducing the cost index in the flight management computer (FMC), the pilot is changing the ratio of cost between fuel and time and, therefore, is determining the speed which minimises the total cost. This speed is usually called the ECONomic speed (see figure III-1). Airlines can reduce their operating costs by an efficient management of the CI settings on their scheduled flights (Boeing, 2007).

III.1.2 Flight planning

It is paramount for airlines to compute an efficient flight plan during the dispatching process. Figure III-2 presents the optimisation process that the airline does for each of its flights. Typically,

²Strictly speaking, CI is defined as the cost of time divided by the cost of fuel and multiplied by a scalar. Depending on the FMS vendor, this scalar might be different and, therefore, the actual value of the maximum CI too. Typical CI maximum values are 99 kg/min or 999 kg/min.

³VMO: Maximum Operating Speed, MMO: Maximum Operating Mach.

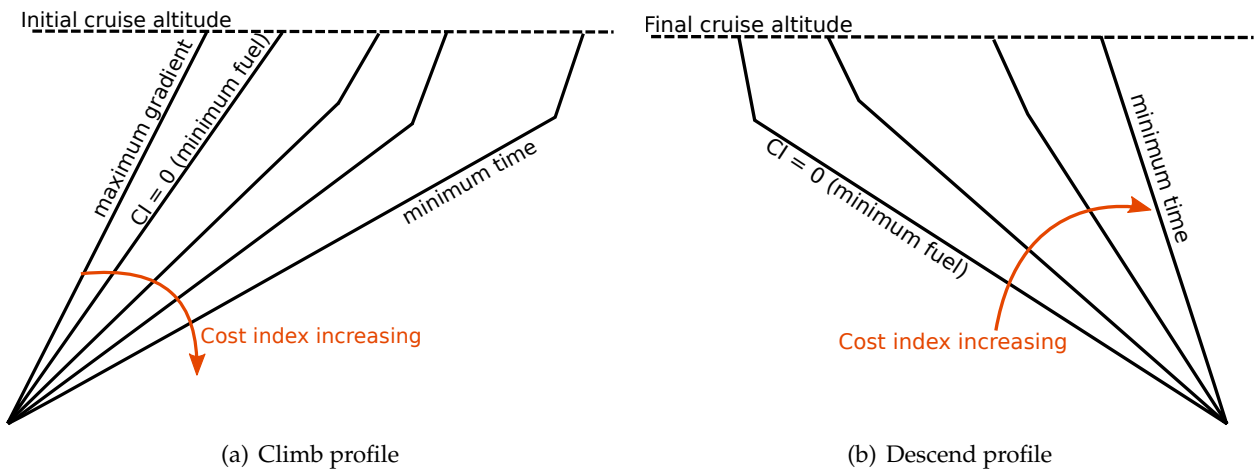


Figure III-3: Typical ascent and descent profiles as a function of the cost index

Based on: (Boeing, 2007)

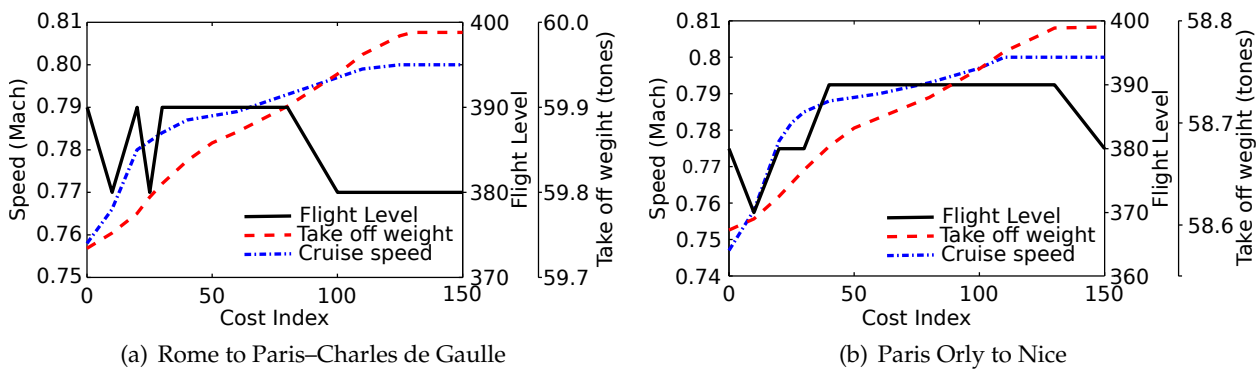


Figure III-4: Characteristics of nominal flights with A320 in no wind conditions and considering great circle distances

this optimisation is divided into a two stage optimisation process: lateral and vertical optimisation. In the flight plan optimisation, the input values are the route that the airline will fly (origin, destination and alternative airports), the intended payload and the time of departure. With the information of the airports and using the airspace configuration and the meteorological data, the route will be computed (Athans *et al.*, 1963). After this process, the distance to be flown will be obtained. The cost index is part of the optimisation function, by weighting the cost of time against the cost of the fuel. Therefore, the optimisation function is $J = Fuel + CI \cdot Time$. Using the aircraft characteristics and aerodynamic data, the payload, the distance, the weather and the CI, the optimiser computes the operational flight plan that is composed of speed and vertical profiles, as well as the fuel needed for that flight (Virtanen *et al.*, 1999; Pradines De Menezes Junior, 2006). Finally, it is worth noting that other parameters besides the ones specified in figure III-2 should also be considered such as the cost of overfly taxes, which might change the preference between routes, or the cost of fuel at origin and at destination, which might encourage fuel tankering.

As expected, changes in CI impact the profile of the flight, the optimal flight level, the speeds and, as a result, the planned consumed fuel (block fuel) and the take off weight (Rumler *et al.*, 2010). Thus, CI affects how the airline performs the climb and descent phases. As is shown in figure III-3, higher cost index values lead to a shallower climb and steeper descents (Boeing, 2007; Rumler *et al.*, 2010). The reason is that when flying at lower cost indexes, fuel is prioritised, therefore the aircraft tries to reach optimal flight level as soon as possible and descent using the

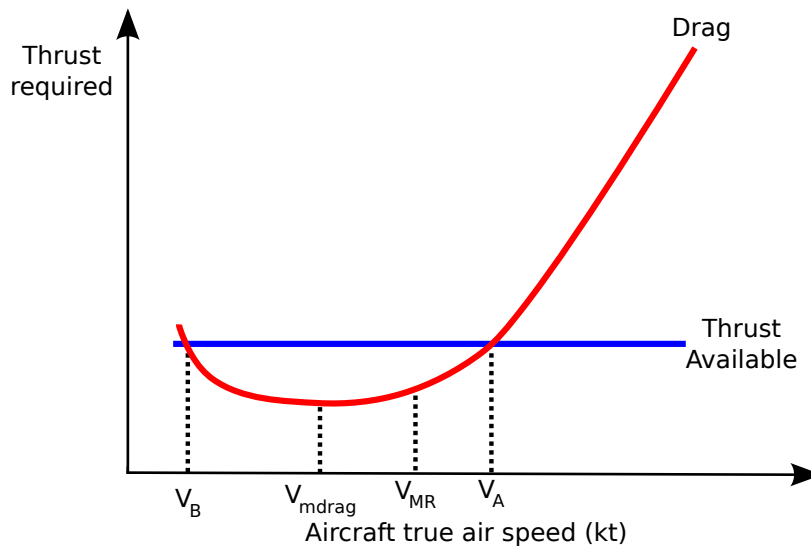


Figure III-5: Thrust required and available curve

least thrust possible. On the other hand, if priority is given to time, the thrust is used in the climb to advance, and once cruising the speed is maintained for as long as possible, leading to sharper descents.

Figure III-4 presents the optimal flight level, speed and take off weight for two flights, Rome to Paris–Charles de Gaulle (FCO–CDG) and Paris Orly to Nice (ORY–NCE), for an A320, as a function of the cost index, considering the great circle distance between the airports and zero wind situation. It is possible to observe how, as the cost index increases, the cruise speed also increases, as time has a higher impact on the total cost. As a consequence, the fuel needed and the take off weight, increase. The cost index also affects the optimal flight level, as changes in the speed and weight imply changes in the optimal cruise altitude.

The cost index, being the main parameter to manage airline operating costs and the main parameter to manage the flight, is a subject of on-going research. For instance, in (Cook *et al.*, 2009) the concept of a dynamic cost index is proposed. This strategy would allow airlines to continuously compute and change the optimal value of the cost index during the flight, taking into consideration the uncertainties of a real flight, as if a flight is delayed, there is a trade-off between the time that can be recovered and the fuel needed.

III.1.3 Aircraft performance: speed stability

Figure III-5 presents the thrust required curve for an aircraft as a function of the cruising speed. In a cruise stable flight the thrust compensates for the drag. The drag can be approximated to a function of the square of the true air speed, as is presented in section III.4. Thus, the drag required presents a minimum (V_{mdrag}), which corresponds to the maximum lift coefficient (C_L), drag coefficient (C_D) ratio (C_L/C_D maximum). For jet engine aircraft this point, V_{mdrag} in figure III-5, corresponds to the maximum endurance speed. The maximum range speed in jet aircraft is the speed which maximises the ratio $C_L^{1/2}/C_D$, and is faster than the minimum drag speed⁴ (Anderson, 2008).

With a given available thrust, there are two possible speeds which generate a compensation for the drag, V_A and V_B in the figure. In nominal conditions, the aircraft flies at V_A which is a stable

⁴Note that for propeller driven aircraft the maximum endurance is achieved flying at the maximum $C_L^{3/2}/C_D$ and the maximum range is realised when flying at maximum C_L/C_D (Anderson, 2008).

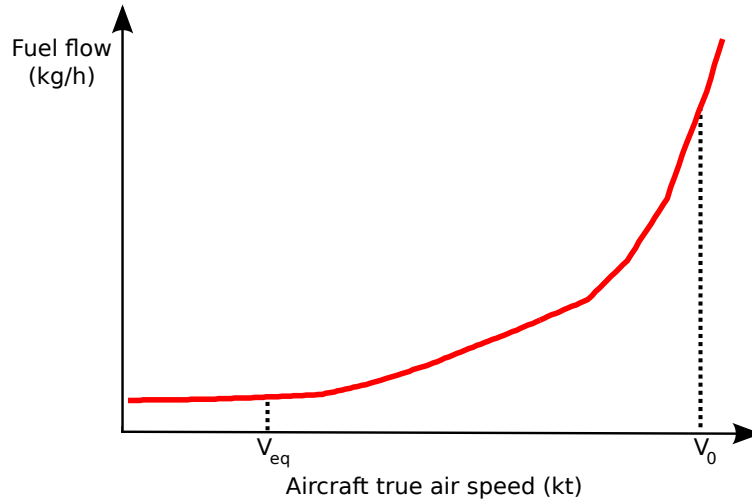


Figure III-6: Typical relationship of fuel flow as a function of the true air speed

speed with respect to small speed changes or thrust variations due to wind gusts or temperature changes. If the speed decreases, the thrust available exceeds the drag. Thus, if level flight is maintained, the aircraft speeds up until the thrust again equals the drag. On the other hand, if the speed is increased, the drag overcomes the available thrust and, therefore, a deceleration is produced, returning the aircraft to V_A . On the contrary, for speeds lower than the minimum drag speed V_{mdrag} , the aircraft is flying in an unstable speed region, as is the case for V_B speed. If the speed is increased, the thrust available exceeds the drag and thus the aircraft tends to accelerate up to V_A . If a deceleration is experienced, then the drag exceeds the thrust, and the extra drag will increase the deceleration. This region is the reverse command region or the backside of the power required curve: to fly slower more power is necessary. If the speed is reduced over V_B and the thrust is not increased, the aircraft will descend or, alternatively, may eventually depart controlled flight.

For this thesis, it is considered that autopilots are able to handle these type of unstable speed flights, and therefore the minimum speed is considered with respect to the stall speed with a safety margin.

III.2 The specific range

At typical flight altitudes and aircraft weights, the function relating the fuel flow (\dot{m}_{fuel}) as a function of the true airspeed (V) is nonlinear and increases monotonically, as seen in figure III-6. Nevertheless, aircraft operators aim at minimizing the fuel used to cover a given flight distance, and therefore, maximize the distance flown per unit of fuel consumed. Thus, the specific range (SR) is defined as:

$$SR = \frac{dx}{dF} = \frac{dx}{dF} \frac{dt}{dt} = \frac{V}{\dot{m}_{fuel}} \quad (\text{III.1})$$

where x is the distance flown, t is the time, F the fuel burnt and V is the true air speed of the aircraft, which in zero wind conditions corresponds to the true airspeed. The specific range is therefore defined as the distance flown per unit of fuel burnt and it is usually measured in NM/kg of fuel or NM/lb of fuel.

As stated in equation (III.2), the fuel flow is proportional to the selected thrust (T_r), which

compensates for the total drag force (F_D), scaled by the thrust specific fuel consumption ($\eta(\frac{\text{kg/h}}{\text{N}})$). In general, η can be considered constant during the cruise phase as it depends on the true air speed and on the altitude, and therefore on the air density (ρ): $\eta(\rho, V)$.

$$\dot{m}_{fuel} = T_r \eta \quad (\text{III.2})$$

The drag force is inverse to the flight direction and oriented towards the relative wind being perpendicular to the lift force (F_L). It can be expressed as a function of the air density, the true air speed, the surface of the wing (S), and the total drag coefficient:

$$F_D = \frac{1}{2} \rho V^2 S C_D \quad (\text{III.3})$$

And from equations III.1, III.2 and III.3, SR can be expressed as:

$$SR = \frac{2}{\eta \rho V S C_D} \quad (\text{III.4})$$

During the cruise, the lift force balances the aircraft weight (W):

$$F_L = \frac{1}{2} \rho V^2 S C_L = W \quad (\text{III.5})$$

Thus, the total lift coefficient can be expressed as: $C_L = \frac{2W}{\rho S V^2}$. As presented in section III.4, the total drag coefficient depends on the lift coefficient $C_D(C_L)$. Therefore, for an aircraft in cruise, its specific range curve, as a function of the cruising speed, varies with:

- The altitude, which affects the air density ρ and the characteristics of the η .
- The aerodynamic characteristics of the aircraft: C_D and S .
- The weight of the aircraft, as $C_D(W)$.

Due to the rapidly increasing values of the fuel flow at high operating speeds, the SR function typically presents a maximum that corresponds to the maximum range cruise speed, see figure III-7, where the SR as a function of the cruise speed is represented. When the operator defines a flight level, weight and nominal cruise speed for a flight (V_0) (i.e. when determining the cost index), the airline is fixing the value of the specific range used for the flight (SR_0). Airlines generally use a cost index greater than zero in order to consider the cost related to flight time (see section III.1). Therefore, usual operating speeds (V_0 =ECON speed) are higher than the maximum range speed as depicted in figure III-7.

III.3 Effect of speed variations on fuel consumption

In order to study the effect of speed variations on fuel consumption, it is considered that the baseline case is the nominal fuel the aircraft would consume if its nominal speed is maintained as initially planned. When the cruise speed is changed, the SR is also modified. Thus, fuel consumption is reduced as long as the new selected speed produces a SR higher than the SR achieved by flying at the intended nominal speed (SR_0), and it is increased if the new SR is lower than SR_0 .

To analyse the effect of the speed variation on the fuel consumed, two flights are studied in detail: a Rome Fiumicino to Paris–Charles de Gaulle (FCO–CDG) and a Paris Orly to Nice (ORY–NCE). The analysed flights are representative of common flights in the European region. The great

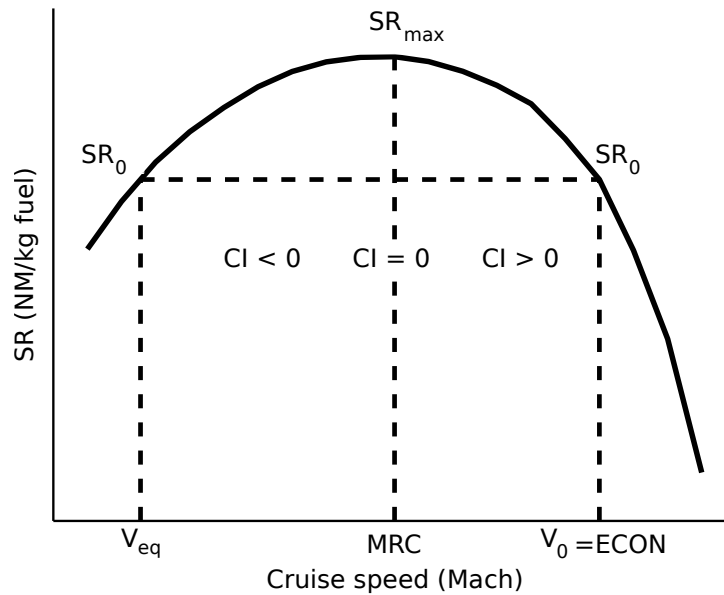


Figure III-7: Typical specific range (SR) as a function of cruise speed curve and equivalent speed (V_{eq}) definition

Table III-1: Analysed flights to study the effect of cruise speed variations on fuel consumption

Flight	Aircraft	Cost index	Flight level	Nominal Cruise Speed (V_0)
FCO-CDG	A320	25	380	M 0.78
ORY-NCE	A320	60	390	M 0.79

circle distance between each origin and destination pair is considered and the flights are analysed in a calm wind situation. A cost index of 25 kg/min and 60 kg/min is selected for the flights as they are common values used by airlines.

As was presented in section III.2, the SR varies as a function of the weight, for this reason and in order to have significant values, it is assumed that the weight of the aircraft at the calculation point is the average weight of the aircraft during their cruise. In this section it is considered that only the speed is modified, thus, the flight level is maintained as initially planned by the operator. However, it should be mentioned that the altitude has an important effect on the specific range curve, and therefore on the fuel consumption, as presented in section III.5.1. The main characteristics of the analysed flights are presented in table III-1. The Airbus Performance Engineer's Programs is used to optimise the flight level, cruise speed and fuel needed.

PEP is used to extract the aircraft performances needed to compute the results presented in figure III-8 and figure III-9. As this section is devoted to presenting the effect of speed variation on fuel consumption, the results are presented as variations in fuel with respect to variation in true air speed.

Figure III-8 presents the values of the fuel consumption as a function of percentage of speed variation over V_0 . If the new selected speed is faster than V_0 , the fuel consumption is higher than initially planned. On the other hand, if it is lower than V_0 , it can be observed that for small variations (up to about -6% of V_0 for the Rome Fiumicino to Paris-Charles de Gaulle flight (figure III-8(a)) and up to about -8% of V_0 for the Paris Orly to Nice flight (figure III-8(b)) fuel consumption is not too much affected and some fuel might be saved. This is due to the fact that the curves of SR as a function of the cruise speed are very shallow at their maximum values. However, if the speed is reduced below those values, the reduction of the SR becomes very steep and, therefore,

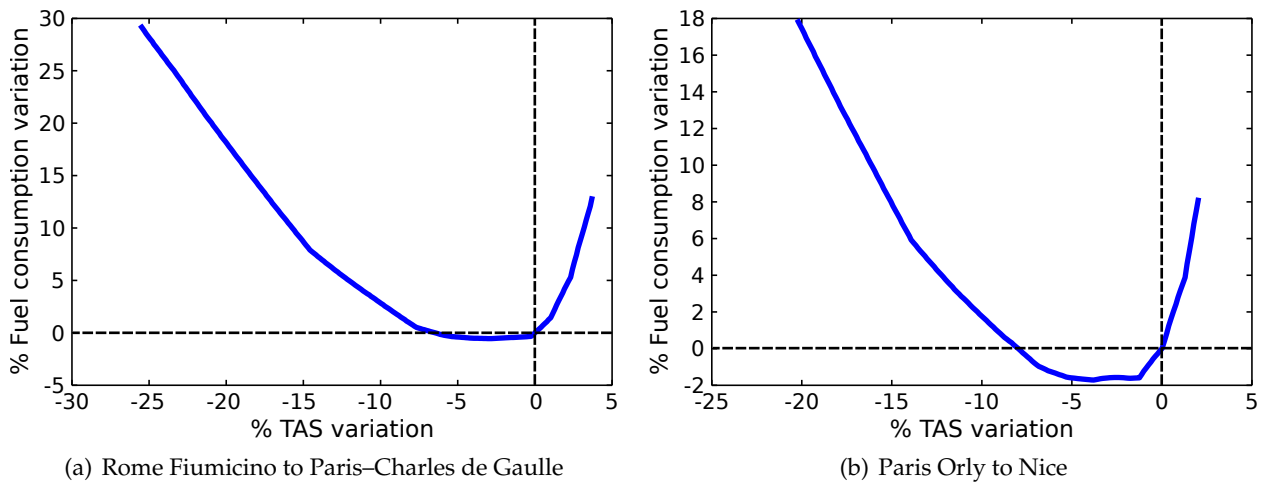


Figure III-8: Fuel consumption variation as a function of the true air speed variation

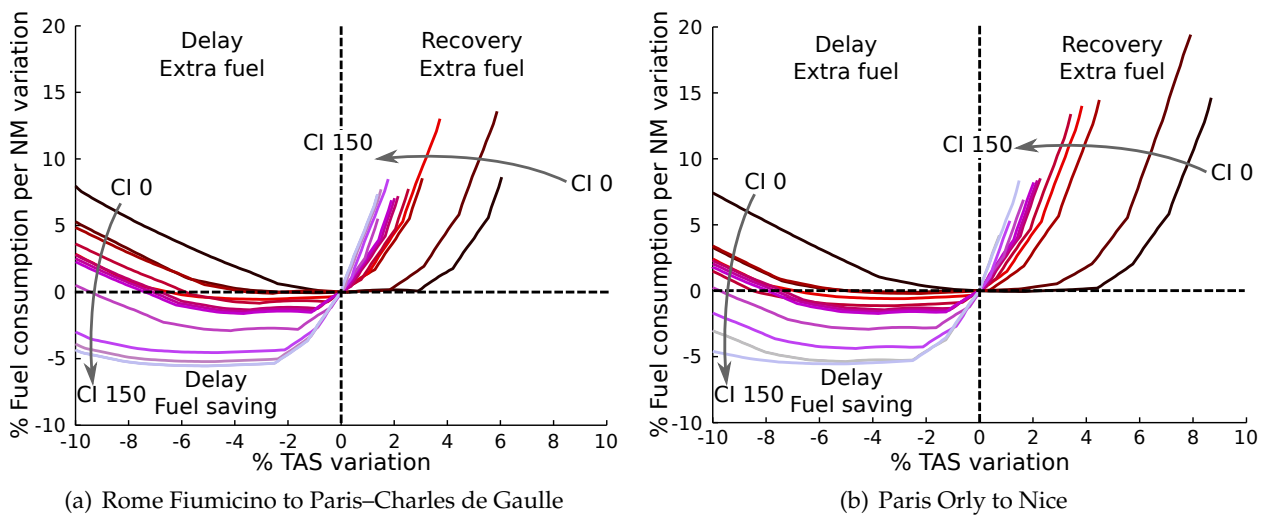


Figure III-9: Percentage of fuel consumption variation with respect to the initially planned as a function of percentage of true air speed variation

fuel consumption increases very rapidly.

Figure III-9 shows the variation in fuel per nautical mile per percentage of speed variation for different nominal cost indexes. As the cost index increases, the nominal speed is faster, and therefore, the higher the amount of fuel that can be saved if the speed is reduced and higher speed variations are possible before incurring extra fuel consumption. Speed increments lead to more fuel burned than initially planned, the higher the cost index, the higher is this effect. On the other hand, depending on the cost index value, the margin in which it is possible to change the speed of the aircraft without a negative repercussion on the fuel consumption varies from -2% to -12%. However, for realistic values of cost index this margin is reduced to values between -2% and -6%. With these examples, it is clear that the effect on fuel consumption due to a speed variation is related strongly to the intended cost index of the aircraft.

Speed variations for air traffic management have an influence on fuel consumption, however, the alternatives, such as re-routing or holding, are also expensive. Thus, cruise speed variation solutions to deal with air traffic management problems, as seen in II.6, are not cost free from a fuel consumption point of view, but they could be competitive with respect to other alternatives.

III.4 The equivalent speed: Air delay with the same fuel consumption

As presented in the previous section, due to the form of the specific range curve as a function of the cruising speed, there is a minimum speed which yields the same fuel consumption as flying at the nominal speed. Let us define V_{eq} (*equivalent speed*) as the speed with the same SR as flying at V_0 , with $V_{eq} \leq V_0$. If the aircraft flies at a speed V such as $V \in [V_{eq}, V_0]$, the fuel consumption is the same or lower than initially planned, see figure III-7. It is worth remembering that V_{eq} might be limited by V_{min} computed with a minimum margin against buffeting of 1.3g.

As was shown in equation III.4, the specific range depends on the total drag coefficient. C_D in turn depends on several terms, as the drag itself is generated by different components: lift induced drag ($C_{D,i}$), which depends on the current lift coefficient, parasitic drag ($C_{D,0}$) and compressibility effects.

For an aircraft flying at low speed ($V \lesssim M 0.6$), the compressibility effects can be neglected, up to a certain extent, and the relationship between the lift coefficient and the total drag coefficient can be expressed by the *drag polar* as: $C_D = C_{D,0} + C_{D,i}$. The lift induced drag is related to the total lift coefficient by the aspect ratio of the aircraft (Λ) and an efficient factor e which depends on the aerodynamics of the aircraft ($C_{D,i} = \frac{C_L^2}{\pi\Lambda e}$). Thus, equation (III.3) yields to:

$$F_D = \frac{1}{2}\rho V^2 S \left(C_{D,0} + \frac{C_L^2}{\pi\Lambda e} \right) \quad (\text{III.6})$$

and the SR (equation III.4) can be expressed as:

$$SR = \frac{2\pi\Lambda e\rho V^3 S}{\eta(\pi\Lambda e\rho^2 V^4 S^2 C_{D,0} + 4W^2)} \quad (\text{III.7})$$

As the specific range at the nominal speed (SR_0) is the same as the specific range at the equivalent speed (SR_{eq}), the following equation should be satisfied:

$$\begin{aligned} SR_0 &= \frac{2\pi\Lambda e\rho V_0^3 S}{\eta(\pi\Lambda e\rho^2 V_0^4 S^2 C_{D,0} + 4W^2)} \\ &= \frac{2\pi\Lambda e\rho V_{eq}^3 S}{\eta(\pi\Lambda e\rho^2 V_{eq}^4 S^2 C_{D,0} + 4W^2)} = SR_{eq} \end{aligned} \quad (\text{III.8})$$

assuming that the variations of η as a function of the speed are small. Then, equation III.8 is simplified to:

$$\frac{V_0^3 S}{\pi\Lambda e\rho^2 V_0^4 C_{D,0} + 4W^2} = \frac{V_{eq}^3 S}{\pi\Lambda e\rho^2 V_{eq}^4 C_{D,0} + 4W^2} \quad (\text{III.9})$$

Thus, V_{eq} can be computed by solving the resulting equation:

$$V_{eq}^4 - \left(V_0 + \frac{4W^2}{\pi\Lambda e\rho^2 S^2 V_0^3 C_{D,0}} \right) V_{eq}^3 + \frac{4W^2}{\pi\Lambda e\rho^2 S^2 C_{D,0}} = 0 \quad (\text{III.10})$$

For jet aircraft flying at high subsonic speeds ($M \gtrsim M 0.6$), the Mach number is used to indicate the true air speed. The Mach is defined as the ratio between the true air speed and the speed of sound (a), which in turn is related to the current static air temperature (T) as shown in the following equation:

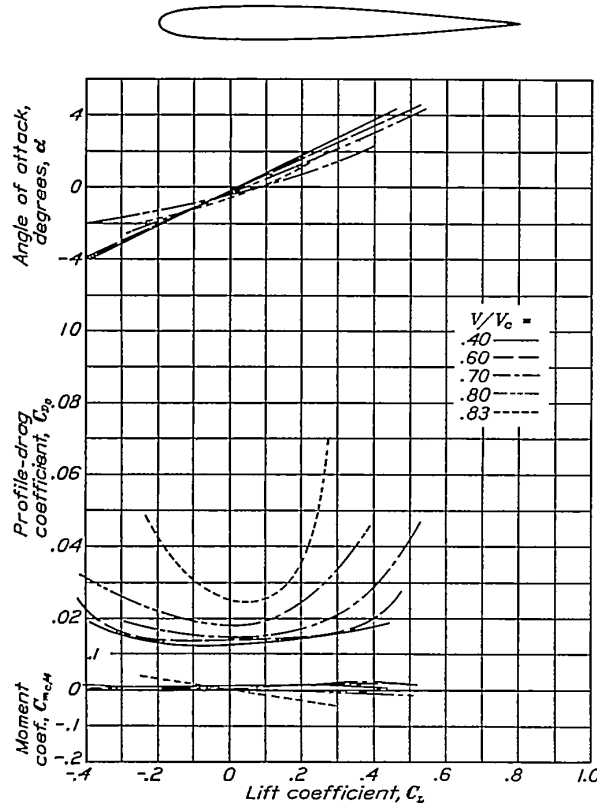


Figure III-10: Aerodynamic characteristics of the N.A.C.A. 009-93 airfoil. Note that in this graph V_c denotes the speed of sound (a)

Source: (Stack & von Doenhoff, 1934)

$$M(a, h) = \frac{V}{a(h)} = \frac{V}{\sqrt{kR_s T(h)}} \tag{III.11}$$

where k is the Boltzmann constant and R_s is the molar gas constant for the air. Note that the speed of sound is altitude (h) dependent as the static air temperature varies with h .

Nominal cruising speeds for commercial aircraft are between $M 0.78$ and $M 0.82$, and the equivalent speed is usually in the order of $M 0.6$ – $M 0.7$. For these high speed flights the compressibility effects can no longer be neglected. These effects produce an increase in the drag and, as can be seen in figure III-10, the relationship between C_L and C_D changes. This change in the relationship, as a function of the Mach, depends on the aircraft characteristics.

In these conditions, the total induced drag coefficient can be expressed as a function of the lift coefficient and the Mach number. These relationships, needed to consider the compressibility effects, are usually stabilised in the form of tables or with polynomial fitting. For example, as presented in (Kaiser *et al.*, 2011), in the form:

$$C_D = C_{D,0}(M) + k_i(M)(C_L - C_{L,0}(M))^2 \tag{III.12}$$

where the $C_{D,i}$ is defined as a function of $k_i(M)$ and the zero lift coefficient term ($C_{L,0}(M)$). Thus, drag polar coefficients can be fitted as defined in equations III.13, III.14 and III.15 in order to consider the compressibility effects.

$$C_{D,0}(M) = C_{D,min} + A_{CD0,1}M \tag{III.13}$$

$$k_i(M) = k_{i,min} + A_{ki,1}M + A_{ki,2}M^2 \quad (\text{III.14})$$

$$C_{L,0}(M) = C_{L,min} + A_{CL0,1}M + A_{CL0,2}M^2 \quad (\text{III.15})$$

Therefore, the total drag coefficient can be expressed as:

$$C_D = (C_{D,min} + A_{CD0,1}M) + (k_{i,min} + A_{ki,1}M + A_{ki,2}M^2) (C_L - (C_{L,min} + A_{CL0,1}M + A_{CL0,2}M^2))^2 \quad (\text{III.16})$$

and the specific range, defined in equation III.4, becomes:

$$SR = \frac{2}{\eta\rho VS(C_{D,0}(M) + k_i(M)(C_L - C_{L,0}(M))^2)} \quad (\text{III.17})$$

Due to the compressibility effects, equation (III.10) is not longer useful to compute the equivalent speed and the system to be solved becomes:

$$\begin{aligned} SR_0 &= \frac{2}{\eta(\rho, M_0)\rho V_0 S(C_{D,0}(M_0) + k_i(M_0)(\frac{2W}{\rho S V_0^2} - C_{L,0}(M_0))^2)} \\ &= \frac{2}{\eta(\rho, M_{eq})\rho V_{eq} S(C_{D,0}(M_{eq}) + k_i(M_{eq})(\frac{2W}{\rho S V_{eq}^2} - C_{L,0}(M_{eq}))^2)} = SR_{eq} \end{aligned} \quad (\text{III.18})$$

In order to compute the value of the equivalent speed, an accurate fitting of the aerodynamics and of the fuel flow is required, and as the specific range is weight dependent, and other parameters such as wind might affect it, simulations are needed to accurately determine the variation of V_{eq} during the flight. In this thesis, precise simulations have been conducted by using accurate aircraft performances from Airbus. Instead of realising the fitting of the aircraft characteristics, the performance data has been directly used to compute the *equivalent speed* at each simulation step.

From the analysis performed it is possible to note that the value of the equivalent speed is affected by:

- The value of the nominal speed: V_0 or M_0 .
- The weight of the aircraft: W , which varies as the aircraft flies at a rate of \dot{m}_{fuel} .
- The flight level: ρ .
- The aerodynamics of the aircraft: C_D, S .

III.5 Parameters influencing the specific range curve and the equivalent speed

As seen above, for a given aircraft, the value of the equivalent speed depends on the flight level, the weight and the value of the nominal speed, therefore, depends on the value of the cost index. It is also important to consider the effect of the wind on the air delay that can be realised. This section analyses the influence of these parameters in order to understand the importance of each of them in the fuel consumption and the equivalent speed. Thus, the parameters that are analysed are:

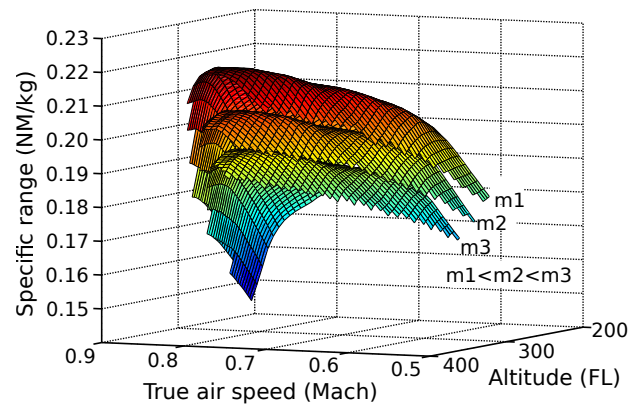


Figure III-11: Specific range as a function of speed, flight level and aircraft mass for an A320

- The flight level.
- The aircraft weight.
- The wind.
- The cost index (and the value of the nominal speed).

An A320-232 aircraft, with a nominal cruise speed of $M 0.78$ is studied using the performances from Airbus Performance Engineer's Programs. The A320 is a typical mid-range aircraft used worldwide, and representative of the vast majority of European flights, either operated by low-cost or legacy carriers. The results are also representative of a wide range of similar aircraft, like the Boeing 737.

Figure III-11 represents the specific range for this aircraft as a function of the altitude and the cruise speed. For each aircraft mass (m), the maximum specific range is achieved at a given flight level and cruise speed. As depicted in the figure, lower masses lead to higher values of specific range which are achieved at lower speeds and at higher altitudes. Therefore, in order to realise a minimum fuel consumption flight, the aircraft should continuously reduce its speed and increase the flying altitude as the fuel is burnt. This, however, is not possible for operational reasons and airlines, in general, use one or several nominal flight levels (cruise steps) (FL_0) and constant cruise speeds.

III.5.1 Influence of the cruise flight level

The cruise altitude is one of the main parameters that has a direct impact on the amount of fuel consumed on a given flight. In figure III-12, it is possible to observe how, with the same aircraft and weight, changes in altitude lead to differences in the values and shape of the specific range curve.

To study the implication of the flight level on the airborne delay that can be realised by flying at a lower speed than V_0 , some simulations are performed for a cruise distance of 100 NM. Figure III-13 shows the relationship between the airborne delay realised and the extra fuel consumed with respect to the nominal flight at V_0 . If the used speed is between V_0 and V_{eq} some fuel is saved but less delay is realised. Moreover, the amount of delay can be increased by flying slower than V_{eq} but leading to extra use of fuel. As an example, flying at FL350 and at V_{eq} almost 3 minutes can be done, while only less than 1 minute can be achieved over the same distance if the nominal flight level is set to FL390. Note that for each flight level there is a maximum air delay that can be done, achieved when the aircraft flies at its minimum speed (V_{min}) for that flight level.

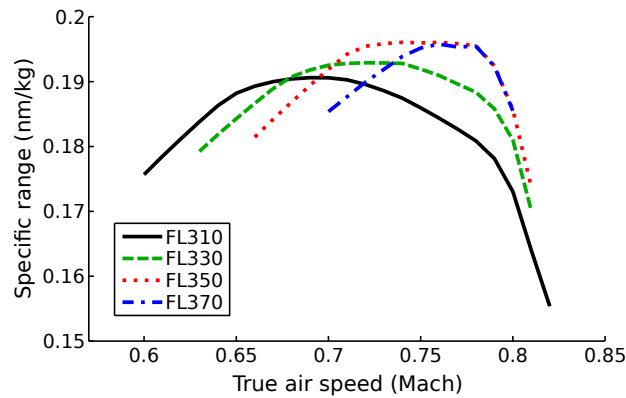


Figure III-12: Specific Range as a function of cruise speed and flight level for an A320 with constant weight

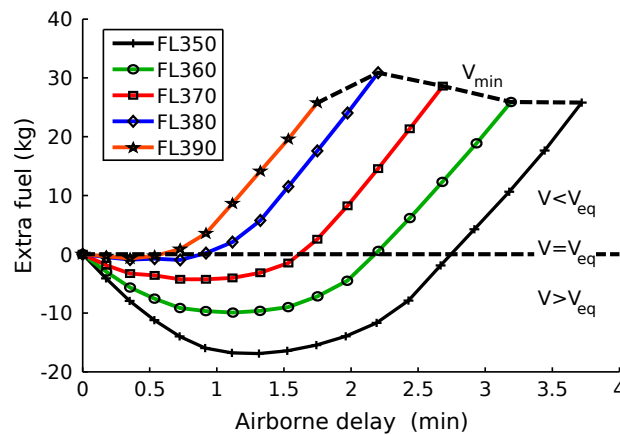


Figure III-13: Airborne delay and extra fuel burned for different Flight Levels in 100 NM

III.5.2 Influence of the aircraft weight

The weight of the aircraft reduces the value of the SR and changes the shape of the specific range curve, see equation (III.4) and figure III-11. Therefore, for a given flight, different weights will lead to different values of V_{eq} . In order to present this implication, the distance needed to perform ten minutes of air delay without incurring extra fuel (i.e. flying at V_{eq}) in calm wind conditions as a function of different flight levels and weights is computed and presented in figure III-14. As can be observed, the flown distance can be considerably different depending on the value of flight level and weight pair: ranging from less than 500 NM to more than 2,500 NM. Less distance required implies that the aircraft flies at lower speeds.

As the flight burns fuel the weight of the aircraft changes and therefore the value of the equivalent speed changes too. Figure III-15 shows the ground speed of an Orlando International to Chicago O'Hare (MCO–ORD) flight with an Airbus A320 with a CI of 60 kg/min at FL360⁵. In the nominal flight, the cruise speed is constant. However, as the weight of the aircraft decreases, V_{eq} reduces its value quite linearly. It seems possible to adjust the variation of V_{eq} as a function of the path length (i.e. as a function of the weight):

$$V_{eq} = V_{eq0} + K_e d_c \quad (\text{III.19})$$

where V_{eq0} is the value of the equivalent speed at the beginning of the cruise and d_c is the cruise

⁵Note that in the absence of wind the true air speed is equal to the ground speed.

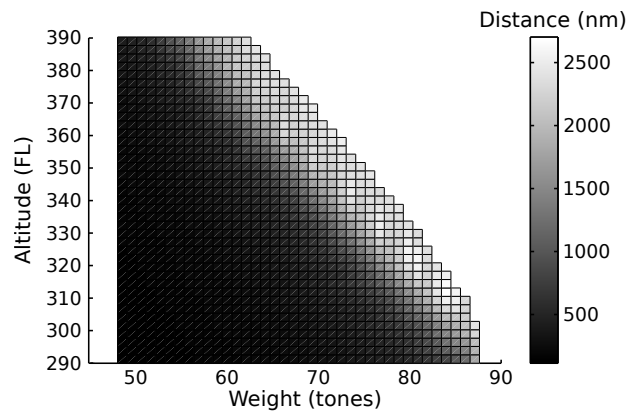


Figure III-14: Distance needed to absorb 10 minutes of delay without extra fuel burned

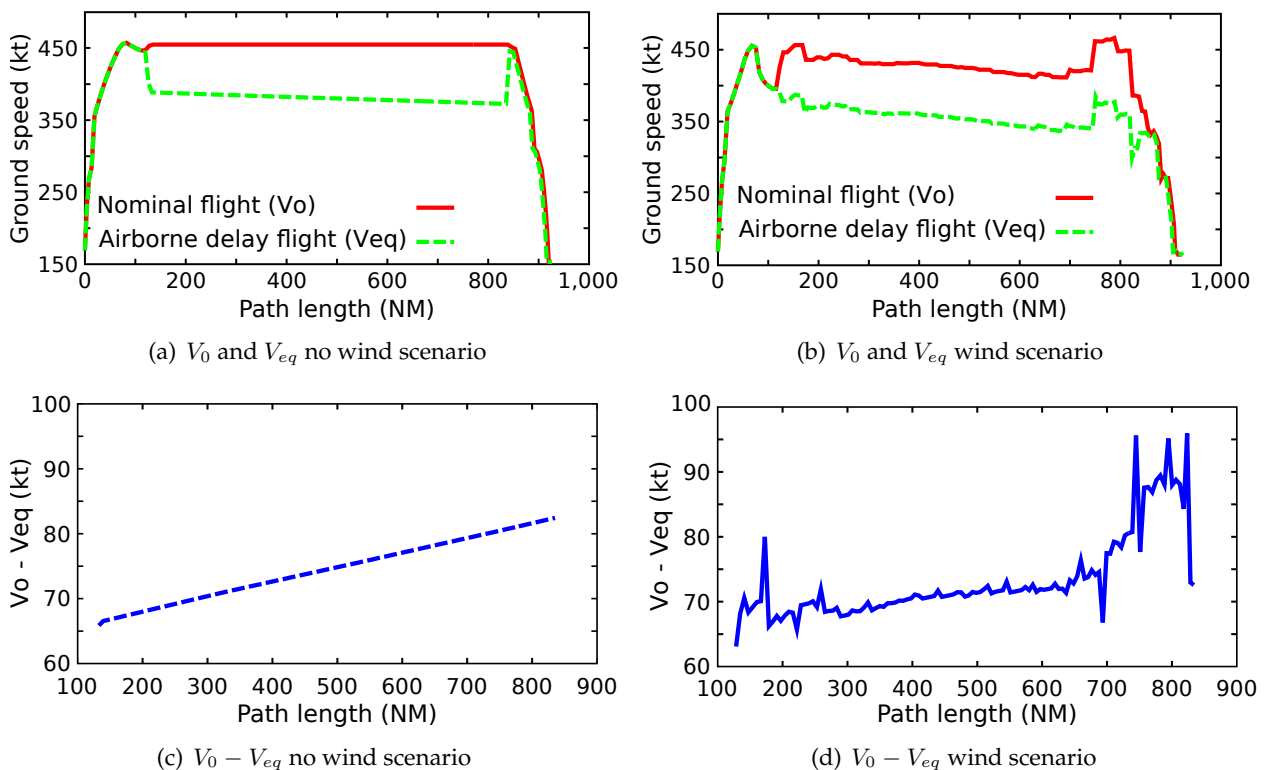


Figure III-15: Relationship between V_0 and V_{eq} for an Orlando International to Chicago O'hare flight at FL360

distance flown in hundreds of nautical miles.

For example, for the simulation depicted in figure III-15(a), the result of the fitting with least square errors has a slope $K_e = -2.26 \text{ kt}/100\text{NM}$, with $V_{eq0} = 63.5 \text{ kt}$, and an error standard deviation of $\sigma = 5.02 \times 10^{-2} \text{ kt}$.

III.5.3 Influence of the wind

The wind has a high influence on the amount of airborne delay an aircraft can realise on a given flight. It changes the available air distance to realise the airborne delay, the specific range, and it may also affect the optimal nominal flight level for a given flight.

In the presence of wind, the equivalent speed can be computed considering the specific range

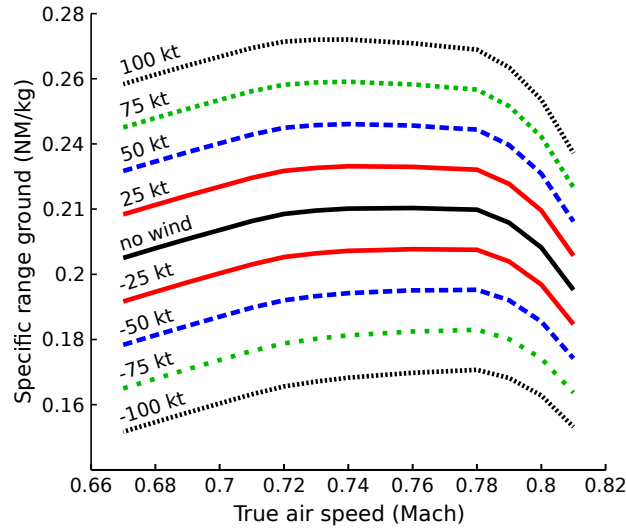


Figure III-16: Typical SR curve with different winds

with respect to the ground speed, defining the SR in *ground NM/kg* or *ground NM/lb* (SR_{ground}). Thus, the specific range becomes:

$$SR_{ground} = \frac{GS}{\dot{m}_{fuel}} = \frac{V + w}{\dot{m}_{fuel}} = SR + \frac{w}{\dot{m}_{fuel}} \quad (\text{III.20})$$

where GS is the aircraft ground speed, w is the wind component in the direction of the flight and SR is the specific range as defined in equation III.4.

Figure III-16 shows an example of a typical SR_{ground} curve with different winds. As expected, negative winds (head wind) will lead to a reduction of the SR_{ground} and positive winds (tail wind) will result in larger distances flown per unit of fuel. In no wind conditions, the SR is determined only by the aerodynamic and propulsive characteristics of the aircraft. However, in a wind environment, the shape of the SR_{ground} curve varies due to the $\frac{w}{\dot{m}_{fuel}}$ term, which is not constant as \dot{m}_{fuel} increases monotonically with the TAS for typical flight conditions (weight and altitude), as shown in figure III-6.

Increasing the cruise flight time (head wind) leads to higher amounts of airborne delay. On the other hand, tail wind conditions generally reduce the amount of airborne delay that can be realised. The effect of the Jetstream should be considered, specially in North America (Endlich & McLean, 1957), as it generates a west-east flow pattern that can increase the trip time for west bound flights up to 40 minutes. One of the main characteristics of real wind fields, is that they change with altitude and for a given route, the optimal flight level might change if wind conditions are different at different altitudes. Therefore, it is possible that in tail wind conditions, higher SR might be obtained at altitudes that are not optimal from an aerodynamic and/or propulsive point of view (SR). Results show that the margin between V_0 and V_{eq} (and therefore the maximum amount of airborne delay) is relatively small at optimal SR conditions (see section IV.1) and becomes wider as long as the flight deviates from these conditions. Thus, wind fields might help to achieve higher amounts of airborne delay without incurring extra fuel consumption.

Aiming at better illustrating this discussion, figure III-17 shows a simple example. Let us suppose that in calm wind conditions and with a given aircraft weight and V_0 , the optimal flight level is FL380, as shown in figure III-17(a). If different wind at different altitudes is present, FL370 might have a higher SR_{ground} for the same V_0 (see figure III-17(b)). Therefore, FL370 becomes more appealing than FL380 for the operator. Yet, even if at FL370 the SR_{ground} is greater than the SR_{ground} at FL380, the equivalent speed (V_{eq}) is slower, since SR curves are generally wider at lower

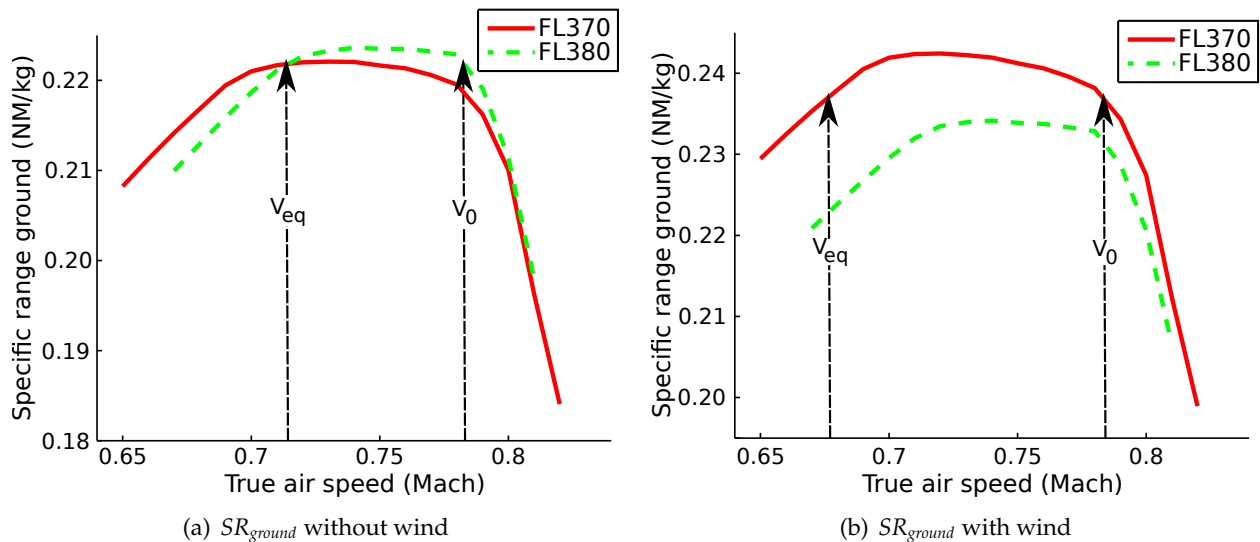


Figure III-17: Effects of wind on the optimal flight level and in the margins between V_0 and V_{eq} speeds

altitudes. Thus, if $(V_{eq}|_{FL380} - V_{eq}|_{FL370}) > (w|_{FL370} - w|_{FL380})$, more delay is done at FL370 while maintaining the same fuel consumption as in the nominal flight.

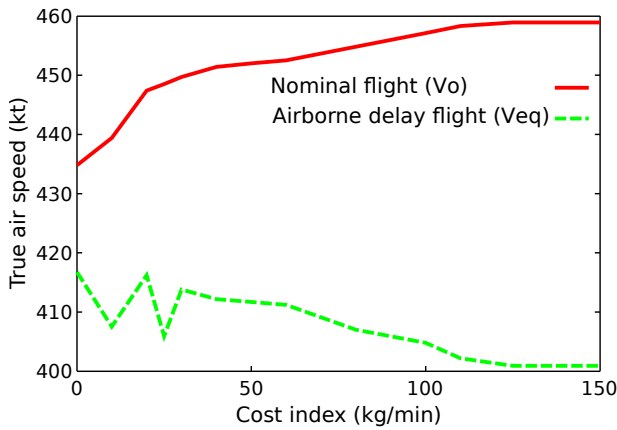
As explained in section III.5.2, figure III-15 shows two time-series graphs of aircraft speeds over a typical mid haul flight. In the no wind scenario (figure III-15(a)), in nominal conditions, V_0 remains constant during the cruise phase, while V_{eq} decreases as the aircraft reduces its weight due to fuel burnt. In the presence of wind, as seen in figure III-15(b), a similar tendency is observed, even if masked by the *noisy* effect of the wind over the ground speed. If the margin between V_0 and V_{eq} is linearly approximated, similarly to equation (III.19), the slope would be of 2.35 kt/100NM, which is very close to the reduction of V_{eq} found if no wind is present (-2.26 kt/100NM). However, the error standard deviation is higher $\sigma = 4.43$ kt, instead of 5.02×10^{-2} kt, as the variation is *noisier*.

The effects of wind on the capacity to realise airborne delay are not straightforward as the wind forecast might differ from the actual cruising wind, affecting the amount of fuel needed to meet the CTA or the deviation on the arrival time. For these reasons, wind scenarios are studied in detail in the next chapter.

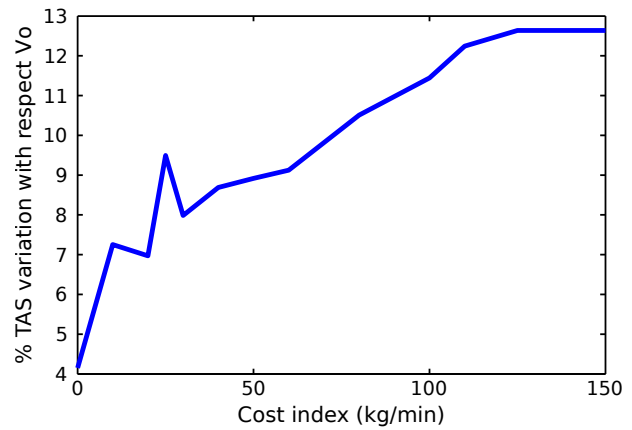
III.5.4 Influence of the intended cost index

It is worth remembering that the nominal cruise speed, the flight level and the weight, which are the main parameters affecting the value of the equivalent speed, are not arbitrarily chosen by the operators. Recalling section III.1, those parameters are determined once the operator knows its payload and decides the cost index for a particular flight. Therefore, the cost index becomes the main parameter to determine the amount of air delay that can be realised without incurring extra fuel consumption. In order to analyse the influence of the cost index, it is necessary to analyse specific flights.

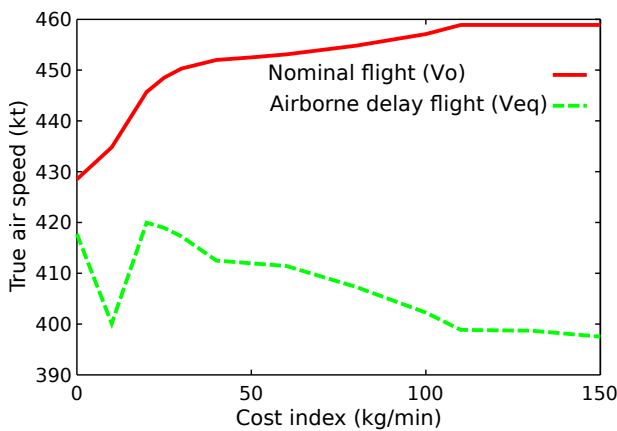
The same flights as in section III.3 are analysed in calm wind conditions (see table III-1). Figure III-18 shows the values of the nominal airspeed (V_0) and the equivalent airspeed (V_{eq}) as a function of the cost index computed with the average weight of the flight during its cruise. For the FCO–CDG, the difference between these two speeds varies from approximately 0 (at CI=0 kg/min) to M 0.15 (at CI=150 kg/min). This margin corresponds to an approximate variation of the cruise speed between [0%,-18%]. Nevertheless, for the most commonly used values



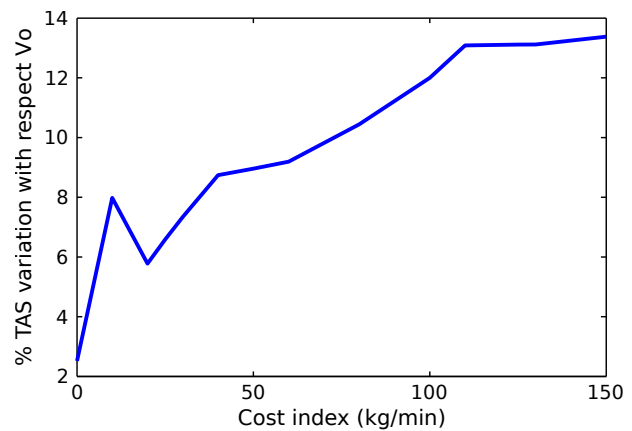
(a) Rome Fiumicino to Paris-Charles de Gaulle. V_0 and V_{eq}



(b) Rome Fiumicino to Paris-Charles de Gaulle. Percentage of $V_0 - V_{eq}$ with respect to V_0



(c) Paris Orly to Nice. V_0 and V_{eq}



(d) Paris Orly to Nice. Percentage of $V_0 - V_{eq}$ with respect to V_0

Figure III-18: Margin between V_0 and V_{eq} as function of CI in calm wind scenario

of CI (between 20 to 70 kg/min) the margins of speed reduction are between -5% to -12%. As expected, the higher the CI, the wider the margin between V_0 and V_{eq} .

Some exceptions, however, can be observed: an increment in CI leads to a reduction of the margin between the speeds. This apparent paradox is due to the fact that when changing the CI, not only is the cruise speed changed, but the optimal flight level may also change. Providing that operational flight levels take discrete values to the nearest thousand feet, a change in the flight level causes a discontinuity in the flight fuel consumption (see figure III-4). This may cause a discontinuity in the value of V_{eq} , as is seen in figure III-18.

III.6 Discussion

The *equivalent speed* has been defined as the minimum speed which results in the same fuel consumption as initially planned for the cruise, flying at the intended nominal cruise speed. If the cruising speed is modified to a new speed which is between V_0 and V_{eq} , fuel savings will be realised. However, the margin between these two speeds is generally small (around -6% of the nominal TAS speed).

The parameters which affect the specific range curve, and therefore the V_{eq} and the amount of

airborne delay that can be realised without incurring extra fuel consumption, are the flight level, the weight, the wind and the nominal speed. These parameters are not free, as the aircraft operator chooses a given route, flight level and fuel (weight) as a function of the intended payload, wind field and economic policy of the airline (cost index). However, as the effect of the compressibility cannot be neglected, instead of developing an analytical model of V_{eq} as a function of all the other parameters, simulations are undertaken. Therefore, in order to further assess the speed reduction strategy, specific flights need to be analysed.

In general, low flight levels and low weights lead to wider specific range curves and therefore more margin between V_0 and V_{eq} . As the aircraft flies, and its weight is reduced, the value of V_{eq} decreases. This reduction is quite linear as a function of the distance flown. Finally, the presence of wind adds some *noise* around the value of the V_{eq} , changes the shape of the specific range curve by adding a term to it and might change the optimal flight level from a ground specific fuel consumption point of view. In general, head winds represent an increase in the cruise flight *air* distance and, therefore, more time will be available for airborne delay. Conversely, tail winds represent a reduction in the *air* distance and flight time and, consequently, a reduction in the airborne delay. However, actual wind conditions might lead to a different optimal flight level that will represent an increase in the margin between V_0 and V_{eq} , and therefore an increase of the airborne delay.

IV

Airborne Delay by Cruise Speed Reduction

In the previous chapter, the relationship between the variations in cruise speed and fuel consumption has been presented. The equivalent speed has been defined as the speed which maximises the airborne delay while ensuring the same fuel consumption as initially planned by the airline. It has been concluded that it is necessary to study particular flights, as the parameters influencing the airborne delay are dependent on the flight plan characteristics. In this chapter the use of speed reduction to realise airborne delay with and without using extra fuel consumption, is analysed in detail. In order to simulate the flights, aircraft performances from the Airbus Performance Engineer's Programs have been used.

IV.1 Airborne delay at the equivalent speed: Calm wind situation

The use of the equivalent speed to realise airborne delay is an interesting strategy to absorb ATFM delays as it allows the aircraft operator not to use more fuel than initially planned for the flight. In order to study the feasibility of using this technique, it is firstly studied in a context where no wind is present.

IV.1.1 Initial assessment of the maximum airborne delay

This section assess the maximum airborne delay that can be realised flying at the equivalent speed. In table IV-1 the detailed analysed routes are presented: Dublin to London Heathrow (DUB-LHR), Rome Fiumicino to Paris-Charles de Gaulle (FCO-CDG), Frankfurt to Madrid (FRA-MAD) and

Lisbon to Helsinki (LIS–HEL). These routes have been extracted from (Cook *et al.*, 2009). All the flights are representative of short and mid cruise lengths and each route is analysed with different intended cost index values (ranging from 25 kg/min to 500 kg/min).

IV.1.1.1 Assumptions in the study

In order to compute the maximum air delay that can be performed by the flights, the whole cruise distance, from the top of climb (TOC) to the top of descent (TOD), is considered to be flown at V_{eq} , while the climb and descent phases are fixed to those obtained from the nominal flights. For this study, great circle distances between origin and destination airports are considered instead of using the actual en-route and terminal area procedures. These assumptions are conservative, as in a real situation more distance would be available, and airborne delays would be higher, especially for short flights, such as the Dublin to London Heathrow flight. Standard instrumental departures and arrivals, along with en-route airways, can represent, in some cases, a significant track extension with respect to the ideal great circle distance.

It should be noted that for long-haul flights it is possible to have two or more cruise altitudes: as the aircraft burns fuel, its mass decreases and therefore, the optimal flight altitude increases. For each flight of this study, the optimal flight profiles corresponding to the nominal conditions are computed. The results show that from all the analysed flights only in the Lisbon to Helsinki route at CI=200 kg/min is it preferable to have two cruise segments.

As was seen in III.5.2, the value of V_{eq} has a highly linear dependency with the weight. Therefore, as a first approximation, the mean weight for each flight is used, averaging the weight values at TOC and TOD. The V_{eq} used for these computations is the equivalent speed corresponding to this averaged weight.

A passenger occupation (load factor) of 81% is considered for all flights, being the typical value for low-cost carriers in Europe during the last few years (ELFAA - European Low Fares Association Members, 2008). Along with this value, and aiming to compute the payload mass, a cabin of 165 passengers in a single class is assumed, which corresponds to the most common cabin layout configuration for this aircraft type (A320) (Airbus, 2009). All nominal flights are optimised, setting an alternative airport at 150 NM from the destination airport when computing the required fuel according to regulations (European Council, 1991).

Finally, the performances from the Airbus Performance Engineer's Programs are used to compute the equivalent speed with the flight characteristics.

IV.1.1.2 Maximum airborne delay at nominal flight level with no extra fuel allowance

In this first study, the amount of airborne delay in the cruise phase is computed considering that the aircraft keeps the nominal flight level(s) (FL_0) and no extra fuel will be burned if compared with the nominal flight. Therefore, the flight profile is the same as intended by the airline and it is assumed that the operator only applies a cruise speed amendment to the original flight plan.

Table IV-1 shows the results in these conditions for the different routes under study. In mid-range flights the amount of airborne delay in an absolute value is higher than for short flights, as a consequence of the longest cruise distance available in which to realise the delay. However, if it is in a relative value with respect to the cruise time, the percentage of airborne delay is notably high for very short flights. This is due to the fact that short routes are not long enough to allow the aircraft to reach the optimal flight level for that given mass and therefore, the margin between V_0 and V_{eq} is wider. As expected, the higher the nominal cost index, the higher the amount of airborne delay performed (due to a larger margin between V_0 and V_{eq}), as was already presented in figure III-18. This speed reduction in percentage (computed with respect to the cruise speed in TAS) is also shown in the table (SRD). As observed before with airborne delay, in general, short

Table IV-1: Maximum airborne delay without incurring extra fuel consumption in calm wind situation

Flight (GCD)	Nominal flight				Keep FL				Change FL			
	Cost index (kg/min)	FL ₀	Flight Time (min)	Cruise Dis- tance (NM)	Cruise Time (min)	Airborne Delay (min)	(%)	SRD ‡ (%)	FL	Airborne Delay (min)	(%)	SRD ‡ (%)
DUB- LHR (243 NM)	25	320	42	53	7	2.0	28.6	21.6	320	2.0	28.6	21.6
	60	330	40	48	6	2.5	41.8	28.8	320	2.6	43.3	29.5
	100	300	39	58	7	3.9	56.1	34.7	280	4.5	64.5	37.9
	200	310	40	49	6	3.1	51.2	32.9	280	3.5	57.6	35.6
	500	310	40	49	6	3.1	51.2	32.9	280	3.5	57.6	35.6
FCO- CDG (595 NM)	25	380	90	347	46	4.1	9.0	8.2	380	4.1	9.0	8.2
	60	370	87	361	47	9.7	20.6	17.0	330	12.1	25.7	20.4
	100	370	87	353	46	9.3	20.1	16.7	330	11.6	25.1	20.0
	200	340	86	373	48	16.8	35.0	25.8	320	17.9	37.4	27.1
	500	300	85	403	51	26.4	51.7	34.0	270	30.4	59.6	37.2
FRA- MAD (769 NM)	25	390	113	504	67	4.4	6.5	6.1	370	6.4	9.5	8.6
	60	390	111	508	67	6.7	10.0	9.1	360	10.5	15.7	13.5
	100	360	110	534	70	15.9	22.7	18.5	320	18.8	26.8	21.1
	200	370	109	514	67	14.1	21.1	17.4	320	18.1	27.1	21.2
	500	280	107	589	74	44.0	59.5	37.2	260	49.9	67.5	40.2
LIS- HEL (1,819 NM)	25	390	254	1519	203	9.5	4.7	4.4	360	22.1	10.9	9.8
	60	380	251	1529	202	20.2	10.0	9.1	360	29.7	14.7	12.8
	100	370	248	1545	203	31.2	15.4	13.3	320	41.8	20.6	17.1
	200	350 †	246	767 †	100 †	21.9	21.9	18.0	300	26.7	26.7	21.1
		390 *		736 *	96 *	14.5	15.2	13.1	320	25.0	26.0	20.6
	500	300	241	1607	204	92.6	45.4	31.2	270	99.0	48.5	32.6

‡ Speed reduction with respect the nominal cruise speed
† First step of the cruise
* Second step of the cruise

flights present a higher possibility to reduce speed in relative terms.

In the Dublin to London Heathrow route the aircraft is already flying at the maximum operational speed when the cost index is set to 200 kg/min, therefore, increasing the cost index does not change the results. On the other hand, for the Frankfurt to Madrid route, the airborne delay is lower at CI=200 kg/min than at CI=100 kg/min. In this case, the optimal cruise flight levels are different for both flights, leading to slightly different performances. Moreover, since higher cost indexes involve shallower climb angles the cruise distance at CI=200 kg/min is lower than at CI=100 kg/min helping to explain this lower value in airborne delay. A similar pattern is observed for the Rome Fiumicino to Paris-Charles de Gaulle route, when comparing the flights at CI=100 kg/min and CI=60 kg/min. Although in this case the optimal flight level is the same for both flights, the cruise distance is different and therefore the airborne delay is different too. Another interesting result is the comparison between FCO-CDG and FRA-MAD routes at

CI=60 kg/min and CI=200 kg/min. In both cases the amount of airborne delay is higher for the shortest route (FCO–CDG). Once again the reason for this apparent contradiction is the dependency of aircraft performances on flight altitude. As seen in the table, optimal flight levels for the FRA–MAD flights are higher than for the FCO–CDG ones, the margin between the nominal and equivalent airspeed being narrower.

IV.1.1.3 Speed reduction with flight level change and no extra fuel allowance

The nominal flight levels are the optimal levels for the nominal flight, according to the nominal cost index. However, with the speed reduction strategy in place, these flight levels may no longer be optimal for the new (and lower) cruise velocities. In general, as the speed is reduced, the optimal flight level, the one which maximises the specific range, also decreases. For this reasons, in this section the airborne delay during the cruise phase allowing a change in the flight level with regards to the filed nominal flight plan is computed. The new flight level is the flight level that allows the amount of air delay to be maximised while not exceeding the nominal fuel consumption (i.e. by flying at SR_0). For this computation, the same cruise distances as in the previous section IV.1.1.2 are adopted.

The results are also shown in table IV-1. As expected, the amount of airborne delay increases (or remains the same) with respect to the previous case. For instance, in the FRA–MAD flight with a nominal CI=60 kg/min, if the flight level is changed from FL390 to FL360 the airborne delay in the cruise phase increases from 6.7 to 10.5 minutes at no extra fuel cost. More impressive results are found in the LIS–HEL route where, for a nominal CI=25 kg/min the airborne delay increases from 9.5 to 22.1 minutes for the same altitude change. Yet, in some flights there are almost no changes in the amount of airborne delay. When the cruise is too short, short routes flown at low cost indexes, the nominal flight level is not the optimal one for that aircraft mass because there is not enough time to reach what would be the optimal flight level. In those flights, the equivalent speed becomes limited by the minimum airspeed even if a flight level change is allowed. This is the case, for instance, of the DUB–LHR and the FCO–CDG flights at low cost index values.

IV.1.2 Detailed case study

Not all aircraft types are used by airlines to cover all distances, as aircraft are designed for a given type of market and mission. Thus, the use of realistic traffic data allows an idea of the potential benefits of the airborne delay strategy suggested in this dissertation to be obtained. Instead of using the average weight of the aircraft, a realistic variation of the mass of the aircraft throughout its cruise should be considered in order to compute the airborne delay with precision. For these reasons, the inbound traffic to San Francisco International Airport, Newark Liberty International Airport and Chicago O'Hare International Airport is simulated.

The simulations are conducted using the Airbus Performance Engineer's Programs suite, as in previous sections, and the Future ATM Concept Evaluation Tool (FACET), developed by NASA-Ames (Bilimoria *et al.*, 2000). Figure IV-1 shows the flow of aircraft flying to SFO during one of the simulations as depicted by FACET interface.

It is worth remembering that, as was presented in section I.3, the realisation of airborne delay is interesting assuming that at some point the regulation, which imposed the delay, is cancelled, and the delay being no longer needed, the airborne aircraft can recover part of their delay by speeding up to their nominal speed. The simulations realised in this case study allow the amount of delay that can be recovered with this strategy to be determined, as a function of when the regulation is cancelled with respect to the flight take off time.

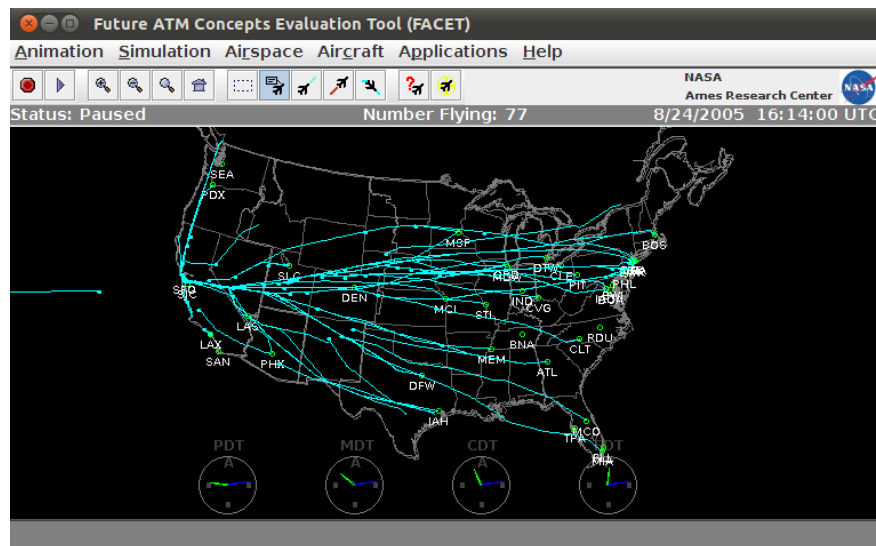


Figure IV-1: Example of FACET simulation: inbound traffic to San Francisco International Airport

Table IV-2: Aircraft grouping according to equivalent Airbus types with nominal cost index

Aircraft Family	Aircraft Types	Cost index
A300	A300, A310	80 kg/min
A319	A319, B727, B737-200, B737-300, B737-500, DC-9	60 kg/min
A320	A320, B737-400, B737-800, B737-900, MD-80	
A321	A321, B757	
A330	A330, B767, B777, DC-10	120 kg/min
A340	A340, B747	

IV.1.2.1 Simulation assumptions

In this case study, as in IV.1.1.1, it is considered that the flights use their whole cruise distance to realise airborne delay, from the TOC to the TOD.

The simulated traffic is extracted from the enhanced traffic management system (ETMS) but, as only the Airbus family performances are available, aircraft are grouped into six different families, corresponding to six different Airbus aircraft models: A300, A320, A321, A330 and A340. The families of aircraft types are created based on the performances, aircraft size and maximum take off weight, in such a way that all aircraft in the same family have similar characteristics. Table IV-2 shows this grouping with the nominal cost index used to compute the original flight plans. The cost index values selected are nominal cost indexes used by the airlines according to (Airbus, 1998). Finally, and in order to estimate the payload, an 80% of passenger load factor is assumed for A319 and A320 flights, while for the A300, A321, A330 and A340, 80% of the total payload is considered, as it is normal to also carry some freight (ELFAA - European Low Fares Association Members, 2008). As in section IV.1.1.1, all nominal flights are optimised with an alternative airport at 150 NM from the destination airport when computing the required fuel according to regulations (European Council, 1991).

In order to obtain accurate results, during the simulations, the weight of the aircraft are re-

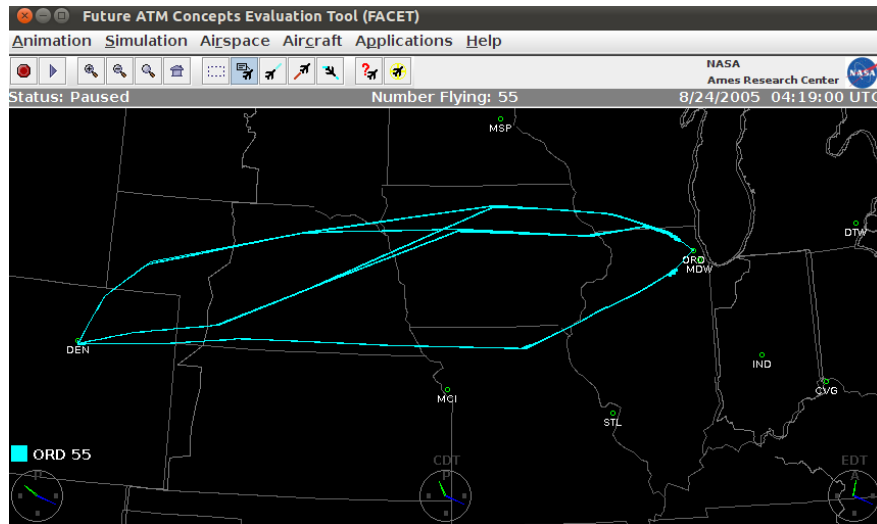


Figure IV-2: Example of different routes in FACET for flights from Denver to Chicago O'Hare



Figure IV-3: Diagram of the steps to generate the nominal traffic

duced according to the fuel consumption.

IV.1.2.2 Architecture

Figure IV-3 shows the process followed to compute the initial traffic and the nominal parameters of the flights: initial cruise weight, cruise flight level(s) and speed(s) with the required cruise steps if needed¹. As explained, aircraft types are replaced by Airbus aircraft when applicable. For these flights, the trip distances are determined. For this purpose, the flight plan of each flight, as defined in the original traffic file, is considered. Therefore, the distance between two airports might be different for two different flights depending on the actual route flown (see figure IV-2).

The initial traffic is simulated twice, as depicted in the diagram of figure IV-4. In the first simulation the speed and flight levels of the aircraft are kept to their nominal values. The result of this simulation at V_0 , is the initial arrival demand at the airport. In the second simulation, the aircraft reduces the cruise speed to V_{eq} . The second simulation represents the demand at the airport if all the aircraft fly at their equivalent speed. By comparing the arrival times, it is possible to compute the maximum airborne delay that each aircraft contributes without incurring in extra fuel consumption.

FACET uses the Base of Aircraft Data database (Eurocontrol Experimental Centre, 2011b) to compute the performances of the different aircraft. However, it is necessary to control the speed of the aircraft during the cruise with accurate aircraft performances. It has been demonstrated that BADA lacks enough precision when dealing with fuel consumption (Nuic *et al.*, 2005; Gallo *et al.*, 2006; Poles *et al.*, 2010). For more details about BADA performances and its suitability for the work realised in this thesis, see appendix B.

FACET has an application programming interface (API) which allows interaction with the

¹If in order to cover a given distance the take off weight is higher than the maximum take off weight for a given aircraft, the payload is reduced accordingly so as not to exceed this maximum weight

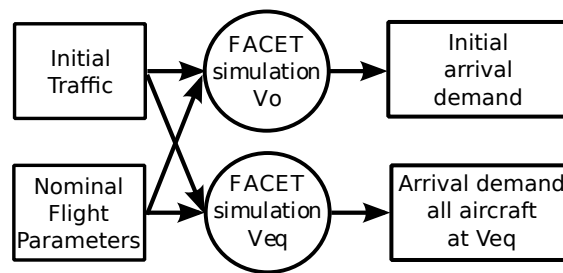


Figure IV-4: Diagram of the demand and delayed demand generation

simulation while it is being conducted. Thus, a software has been developed in order to control the simulation (require FACET to perform a simulation step of one minute) and interact with the aircraft.

As the diagram of figure IV-5(a) shows, the climb and descent are simulated directly by FACET. But in the nominal simulation, at the beginning of the cruise the flight level (FL_0), speed (V_0) and weight (W_0) are initialised with the parameters from the PEP computations. These values are kept constant during the cruise and updated only when a change in cruise altitude is needed, according to the nominal flight plan. At each iteration of the simulation, the fuel flow is computed according to the Airbus performances of the aircraft in the software specifically developed for this thesis. Recalling section III.5.2, the equivalent speed varies with the weight. Therefore, in the simulation of the reduced speed, at each simulation step, the equivalent speed is recomputed for all the airborne flights, considering their current weight, and updated in FACET using the API (see figure IV-5(b)). These computations are based on the certified performances extracted from the Airbus software PEP. In addition, if a particular aircraft has a change in cruise altitude in the nominal flight, it is also performed in the second simulation.

For more information about the quality of the simulations realised with this architecture, compared to the values obtained in the flight plan computed using Airbus Performance Engineer's Programs, the reader is referred to appendix C.

IV.1.2.3 Simulated traffic for airborne delay and delay recovery

Representative traffic, ETMS data of August 24th-25th 2005, is used to generate traffic information required to perform the simulations. A total of 3,859 flights realising airborne delay, with a total of 310 origin–destination pairs, are simulated. The 15 origin–destination pairs with more flights are presented in table IV-3, along with the average trip distances.

Figure IV-6 presents the histograms of the arrivals to SFO, EWR and ORD as a function of the flight plan distance for the two days simulated. Note that only the flights that take off during the simulation from United States of America or Canada are considered, as those are the flights that potentially can serve delay if a ground delay program is implemented. For the three airports different traffic patterns are presents.

San Francisco International airport is located on the west coast. It receives traffic from the surrounding airports, mainly from Los Angeles International Airport (LAX) and McCarran International Airport in Las Vegas (LAS). Due to its location, the amount of medium haul flights is relatively low. As presented in figure IV-6(a), there is a gap between 1,000 NM and 1,300 NM distance. However, SFO has a considerable amount of long haul flights from the east coast, for example there are 34 flights from John F. Kennedy International Airport in New York (JFK), and 35 from the Hawaii islands. Thus, for SFO the demand is divided between short and long flights. 56% of the arrival traffic is generated closer than 1,000 NM and 21.7% comes from airports located further than 2,000 NM.

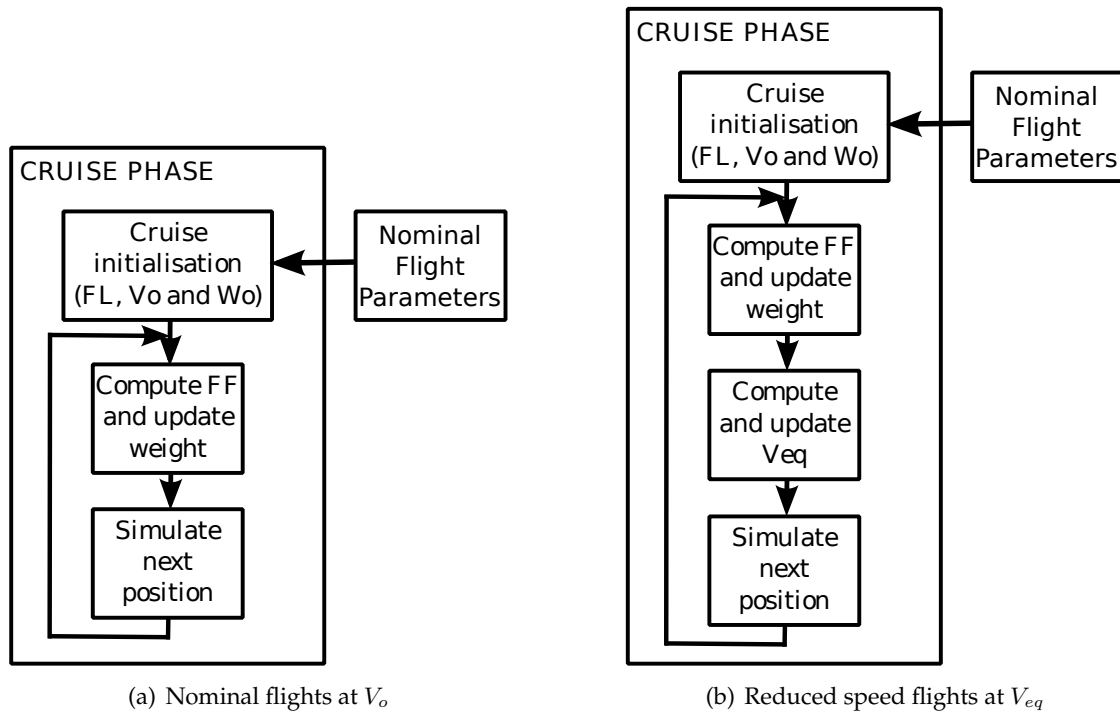


Figure IV-5: Diagram of the flight simulation in FACET

Table IV-3: Origin–Destination pairs with highest volume of traffic in the airborne delay and recovery study

Origin–Destination pairs	Average distance (NM)	Number of flights	Aggregated % of number of flights
LGA–ORD	661	71	1.8
MSP–ORD	300	62	3.4
LAX–SFO	311	61	4.9
EWR–ORD	649	52	6.2
DFW–ORD	763	51	7.5
ORD–EWR	625	51	8.8
ATL–ORD	552	45	14.6
BOS–ORD	774	44	15.7
PHL–ORD	608	49	10.0
IAD–EWR	186	48	11.2
ATL–EWR	654	46	12.4
DTW–ORD	212	45	13.5
LAX–ORD	1,559	43	16.8
DCA–ORD	553	43	17.9
CLE–ORD	287	40	18.9

Newark International Airport is located on the east coast, and similar traffic as in SFO might be expected to be found. However, as depicted in figure IV-6(b), there is more traffic from closer airports: 75.2% of the traffic comes from airports within a 1,000 NM radius. The reason for this is that there are more major airports located on the east coast than on the west coast, like Washington Dulles International (IAD), Hartsfield–Jackson Atlanta International Airport (ATL) or Chicago

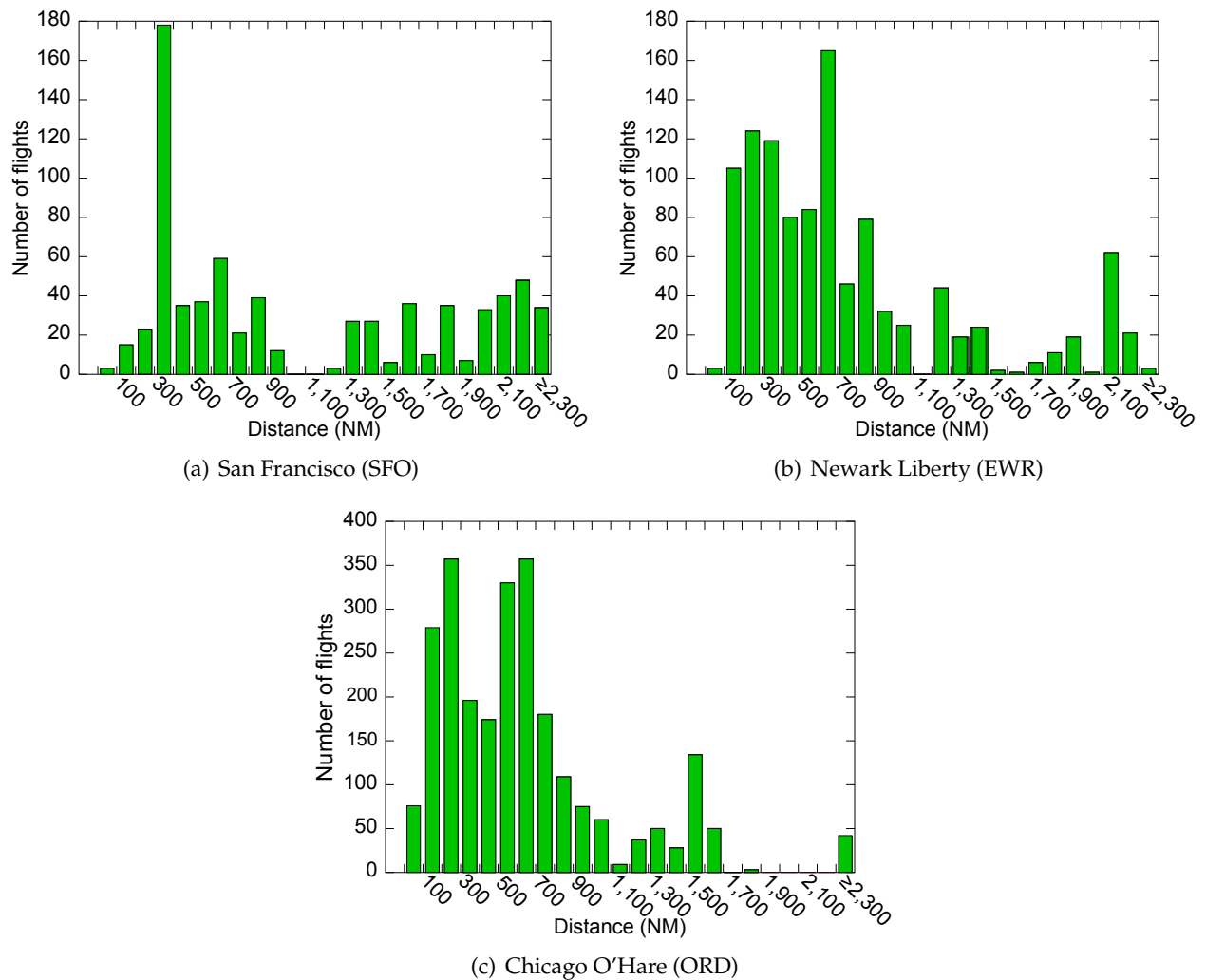


Figure IV-6: Histogram of traffic arrivals as a function of flight plan distance to SFO, EWR and ORD for August 24th-25th 2005. Only traffic taking off from United States of America and Canada.

O'Hare International. Only 9.1% of the arrival traffic comes from further than 2,000 NM, mainly coast to coast flights from Los Angeles International (28 flights), Seattle-Tacoma International Airport (SEA) (15 flights) and San Francisco International (16 flights). For these reasons, EWR mainly has short and medium traffic with some long flights.

Finally, due to its location, Chicago O'Hare International generally has short and medium flights; 82.6% of the traffic is from airports closer than 1,000 NM, only 1.8% of the traffic comes from further than 2,000 NM, all of them flights from the Hawaii islands. From ORD, SFO is located at 1,650 NM, JFK at 660 NM and ATL at 550 NM.

IV.1.2.4 Results of the case study

Figure IV-7 presents the airborne delay as a function of the distance of the flight plan for the simulated flights. In the figure the non uniform distribution of flights, as aircraft types are related to the intended mission (mainly flight distance and payload), is explicit. Thus, small aircraft such as the A319, are mainly used up to 1,300 NM, and bigger aircraft, such as the A340, are used for longer flights.

The results presented in figure IV-7 show that there is a strong relationship between the flight

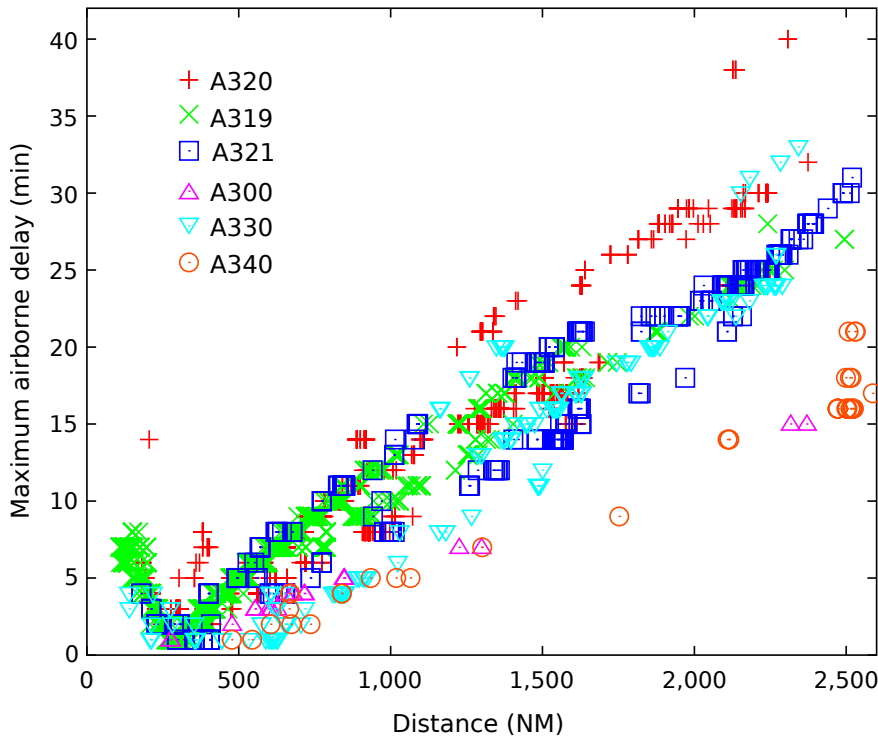


Figure IV-7: Airborne delay as a function of the flight plan distance for flights with destination EWR, ORD and SFO

plan distance and the amount of airborne delay realisable. In general terms, the longer the flight, the higher the amount of airborne delay. This tendency is inverted for very short flights (up to around 250 NM), because they do not have the minimum required length to achieve an optimal flight level. This leads to flights at non-optimal altitudes which allow wider distances between V_0 and V_{eq} . The relationship between the flight plan distance and the airborne delay realisable is analysed in detail in section IV.1.3, where flight plans between 100 NM up to 3,500 NM have been systematically simulated at 50 NM intervals.

Figure IV-8 shows, for the three scenarios, the distribution of airborne delay realisable without incurring extra fuel consumption (i.e. the difference between the flight time at its nominal conditions and cruising at the equivalent speed). For the three origin airports the distribution is similar, the maximum being around five minutes of delay. However, in the inbound traffic to San Francisco International, figure IV-8(a), there are a high number of flights that can realise around 25 minutes of airborne delay, in Newark Liberty International there are very few (figure IV-8(b)) and in Chicago O'Hare International there are none (figure IV-8(c)). The explanation for this behaviour is the fact that in these simulations the whole NAS is considered. Thus, coast to coast flights, such as flights originating in Washington Dulles or Philadelphia with destination San Francisco, are long enough to realise an average airborne delay of around 25 minutes. By their location, these long flights are limited in Newark Liberty and Chicago O'Hare airports where an airborne delay between 5 and 7 minutes is more common. The effect of the location of the airport on the airborne delay and its use in air traffic flow management initiatives is studied in section V.5.

The results of the amount of airborne delay that can be recovered if the aircraft speed up to their nominal cruise value are presented in figure IV-9. It should be noticed that for these simulations the whole flight is simulated. Therefore, if the regulation is cancelled while the aircraft is still climbing, all the delay can be recovered (flat part of the curves at the beginning of the flight), as the aircraft has not started to fly at the reduced speed. On the other hand, if the regulation is cancelled once the aircraft has started its descent, then no recovery is possible as all the airborne

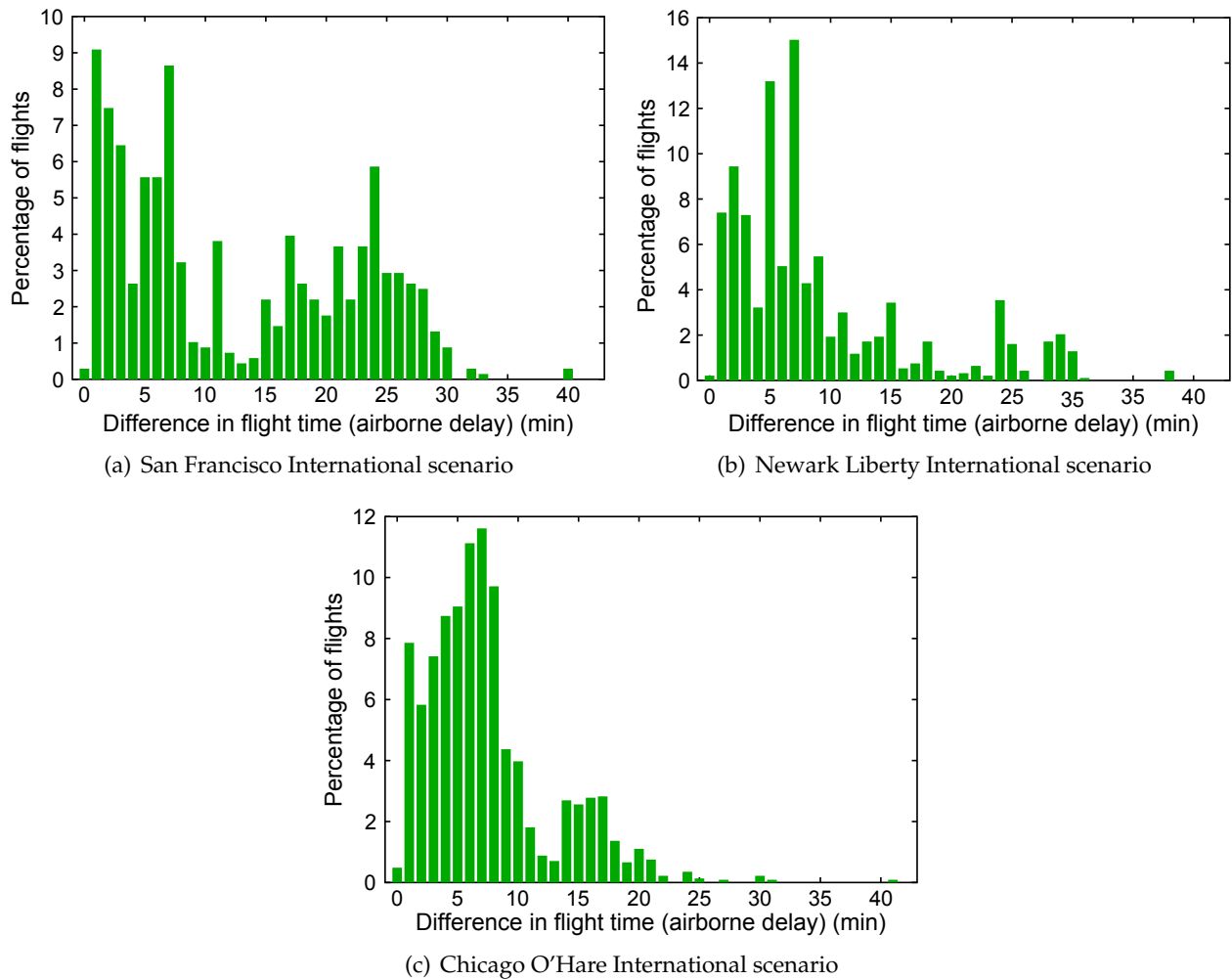


Figure IV-8: *Difference in flight time (airborne delay) between the simulated nominal flight and the speed reduction flight*

delay has already been accrued (flat line at the end of each flight).

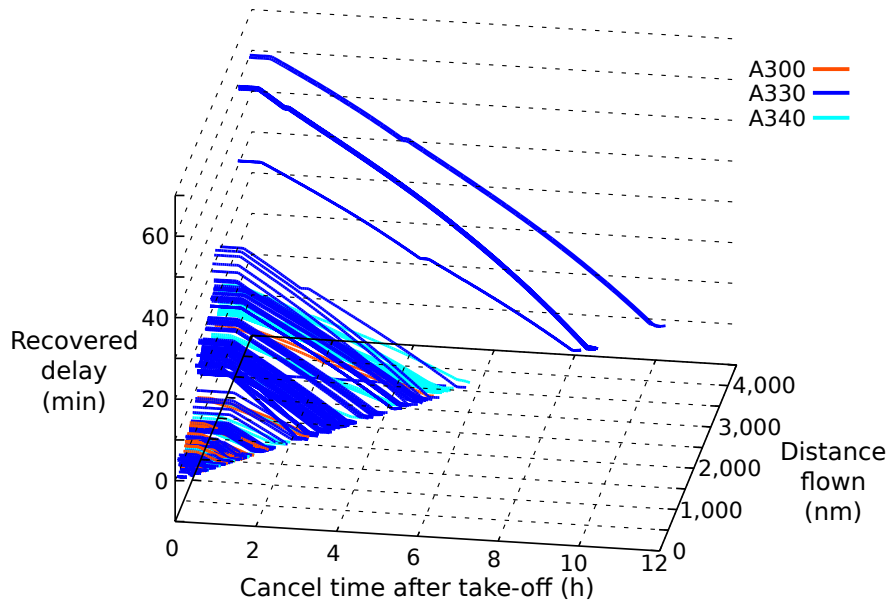
Another characteristic present in these graphs is the effect of realising a climb step during the cruise on the airborne delay recovered, for example, for all the A330 flights for distances between 3,000 NM and 4,500 NM (see figure IV-9(a)). When the cruise step is performed the amount of airborne delay that can be recovered is not reduced with the flight, as no airborne delay is done while the aircraft is climbing, and the slope of the delay recovered as a function of the flight time changes as the margin between V_{eq} and V_0 changes with the modification of the flight level.

Finally, it seems that there is a relationship between the flight plan distance, the time when the aircraft is allowed to increase its speed to V_0 and the amount of delay that can be recovered without incurring extra fuel consumption. These relationships are analysed in detail in section IV.1.4

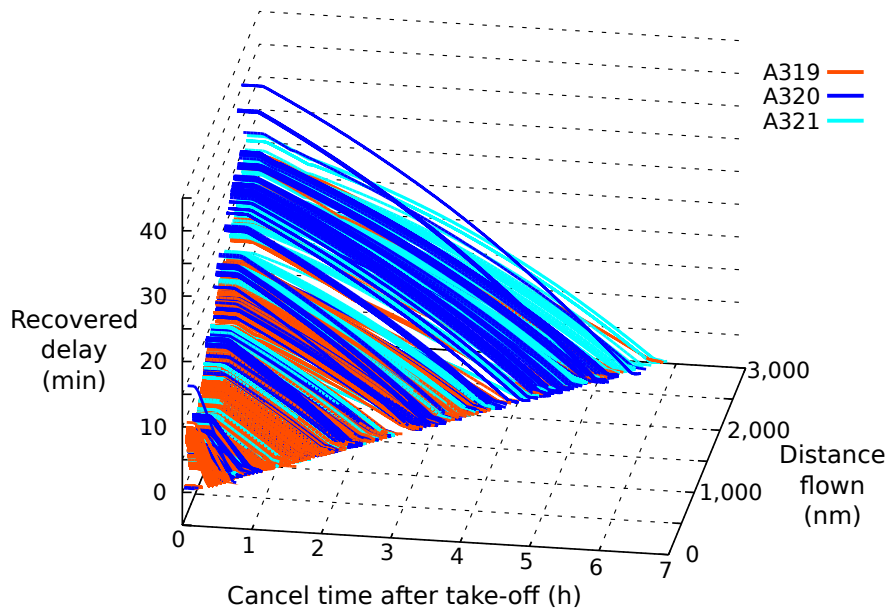
IV.1.3 Relationship between airborne delay and the flight plan distance

From the results presented in the previous section, it is observed (see figure IV-7) that there is a relationship between the flight distance and the amount of airborne delay that can be realised by reducing the speed. In general terms, the longer the flight the longer the distance available to reduce the speed and therefore the higher the amount of airborne delay realised.

In order to study this relationship, the airborne delay for representative flights in normal



(a) A300, A330 and A340 flights



(b) A319, A320 and A321 flights

Figure IV-9: Potential delay recovered as a function of flight time and the length of the flight plan for flights with destination EWR, ORD and SFO

operations is analysed. Thus, with the same assumptions as in the previous section, for each aircraft type, flight plans are computed from 100 NM to 3,500 NM or until the take off weight is limited, in 50 NM intervals.

Figure IV-10(a) shows the results for the A320 aircraft type. The plot presents for each flight plan distance which is (are) the optimal flight levels(s) for the flight and the amount of airborne delay that is realised for each flight. As expected, the tendency is that the longer the flight, the higher the amount of airborne delay realisable. However, there are some exceptions. It is interesting to notice that for very short distances (less than 250 NM), it is possible to realise more airborne delay than for longer distances, such as 400 NM. The reason is that the aircraft does not have enough distance to achieve an optimal flight level, as was the case in the DUB-LHR flight in section IV.1.1. For example, if the distance is 100 NM, the optimal flight level is FL100, leading

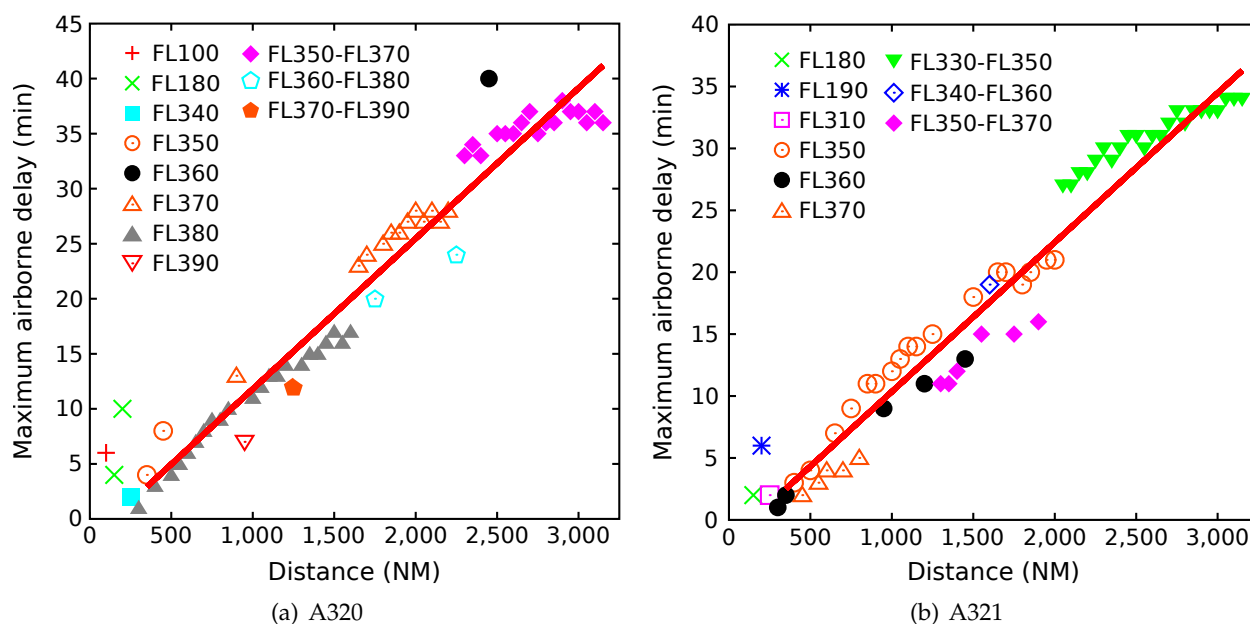


Figure IV-10: Airborne delay and optimal flight level as a function of flight plan distance for A320 and A321 aircraft types

to 6 minutes of airborne delay. If the distance is increased by 50 NM, the flight level increases to FL180, leading to better aerodynamic conditions and therefore less margin between the nominal and the equivalent speed, the maximum airborne delay being reduced to 4 minutes. For 200 NM, the flight level is maintained at FL180 and therefore, as there is more distance available than in the 150 NM flight and the flight level is not optimal, the amount of airborne delay is increased rapidly to 10 minutes. From 250 NM on, the distance is long enough to an optimal flight level to be reached, and from there, in general, the maximum airborne delay increases with the distance, as is the case for almost all the flights between 250 NM and 1,600 NM.

In figure IV-10(b), the same results are presented for the A321 aircraft type. It is interesting to analyse these results in detail, as in this case there are two cruise altitude options that are preferred over the others for flights between 1,200 and 2,300 NM (FL350 and FL350 with a step to FL370). The optimality between them is alternated, as the flight plan distance increases, which leads to differences in the airborne delay for similar flight distances. For longer flight plans an initial cruise at FL330 followed by a cruise at FL350 is then optimal.

These results stress the importance of the flight level on the amount of airborne delay that can be realised without incurring extra fuel consumption. In this case there are around five minutes difference of airborne delay between using FL350 or FL350 with a step to FL370. The optimality of a given flight level is related with the total cost of realising the flight at that altitude ($Cost = Fuel + CI \cdot Time$), and in some cases the difference in cost between choosing one flight level or another can be very small. For example, in the 950 NM flight, the cost of using FL360 is 82,156 kg (2h14 minutes of flight and 74,116 kg of fuel), but there are only 39 kg of difference with respect to using FL350 (2h14 minutes of flight and 74,155 kg of fuel), which is optimal for 900 NM and for 1,000 NM. It is worth noting that the Airbus Performance Engineer's Programs computes the time of the flight plan rounded to the nearest minute. This rounding is responsible of some of the changes of the optimal flight level as flight plan distance increases, and consequently on the fluctuations of airborne delay realisable. Therefore, small variations in cost when choosing the optimal flight level for a given flight can lead to airborne differences of more than five minutes.

Finally, if the very short flights are dismissed (flight plans shorter than 250 NM), the airborne delay, as a function of the distance, can be parameterised with a linear fitting function:

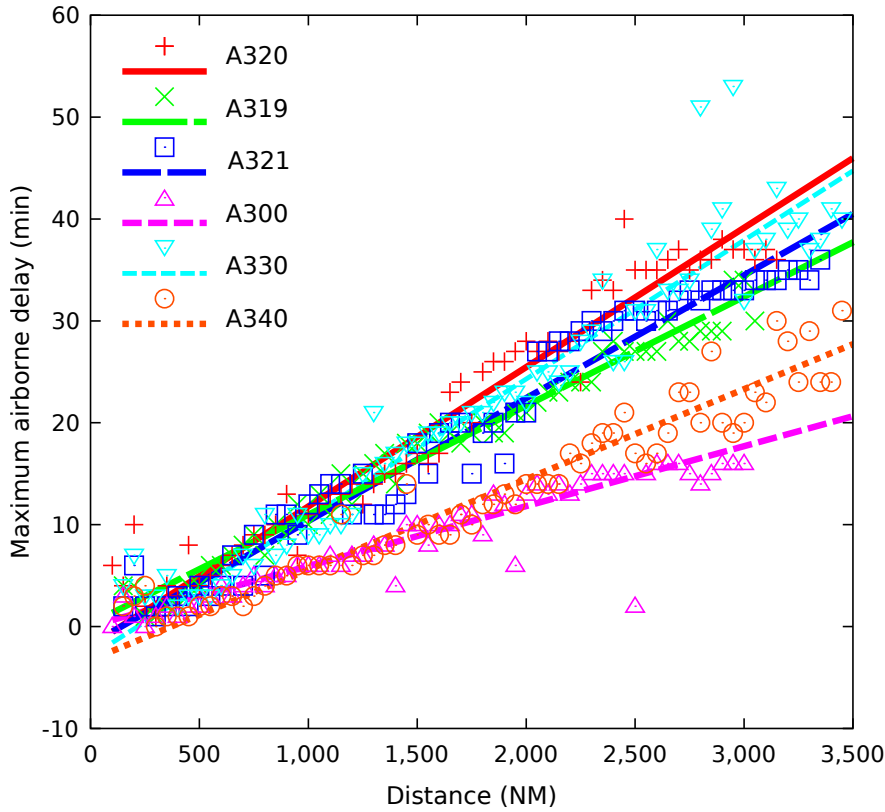


Figure IV-11: Airborne delay as a function of flight plan distance for Airbus aircraft with fitting lines

Table IV-4: Parameters of fitting air delay as a function of flight plan distance ($d_f > 250$ NM)

Aircraft Family	AD_0 (min)	K_D (min/100NM)	σ_D (min)
A300	7.63×10^{-3}	0.59	0.99
A319	2.64×10^{-2}	1.06	1.43
A320	-1.87	1.37	2.45
A321	-1.71	1.21	2.32
A330	-2.94	1.36	3.69
A340	-3.29	0.88	2.06

$$AD = AD_0 + K_D d_f \quad (\text{IV.1})$$

where d_f is the total flight plan distance. The results of this fitting are presented in figure IV-10 and IV-11 and the values of the fitting function for each aircraft type (the slope of the curve and the standard error deviation) are shown in table IV-4. From those values, it is possible to observe that there are two categories of aircraft, the A319, A320, A321 and A330 types which have a K_D between 1.06 (min/100NM) and 1.37 (min/100NM), and the A300 and A340 with a smaller slope of 0.59 (min/100NM) and of 0.88 (min/100NM) respectively. One reason for this differentiation, is that it is more common to have climb steps for the A300 and the A340 aircraft types than for the others, probably due to the greater weight of the aircraft.

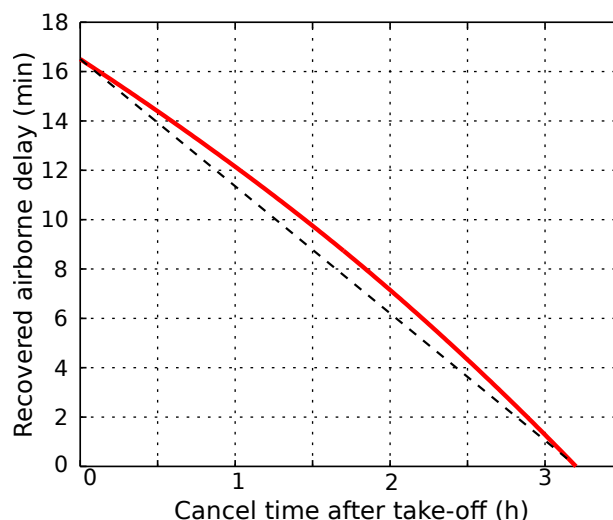


Figure IV-12: Recovery delay as a function of cruise time when aircraft speeds up to V_0 for an A320 with a flight plan of 1,600 NM

IV.1.4 Assessment of the potential airborne delay and the delay recovery

In this section, the airborne delay that can be potentially recovered if the regulation which imposes the delay is cancelled before planned, as presented in figure IV-9, is analysed in detail. Recalling figure I-3, note that the part of the delay that can be realised airborne is the one that can be recovered. As in the previous section, the flights analysed are computed at fixed 50 NM intervals.

Figure IV-12 presents the delay that can be recovered for an A320 aircraft with a 1,600 NM flight, if the regulation is cancelled after the aircraft starts cruising. Note that, in this case, only the cruise is simulated and, therefore only the cruise is represented in the figure. During the climb and descend phases it is assumed that the aircraft is flying following the nominal flight plan. Therefore, if the regulation is cancelled while the aircraft is climbing, all the airborne delay is recovered, but if it is cancelled once the aircraft has started the descent, then no recovery is possible. Thus, if the aircraft is allowed to speed up at the moment it reaches the beginning of its cruise (time=0), all the airborne delay (around 17 minutes) can be recovered, as the flight progresses, less delay can be recovered as more delay has already been accrued. As is depicted in the figure, the savings are not linear with the cancellation time. The reason is that the equivalent speed decreases as the aircraft cruises due to the weight reduction. Thus, the delay is not spread equally along the flight.

Figure IV-13 depicts the delay recovered as a function of the cancellation time after the aircraft reaches the cruise for all the simulated A320s when no cruise step is present. For example, a 850 NM flight which is allowed to speed up to V_0 27 minutes after starting its cruise can recover a total of 7 minutes of delay, while a 1,000 NM flight speeding up to V_0 at the same time after starting its cruise can recover around 9 minutes.

Even if, as previously noted, the RD as a function of the cancellation time is not linear, it can be approximated with a linear fitting function. As in the previous section the airborne delay fitted was parametrised with a linear function, it is possible to fit the airborne delay recovered as a function of the time elapsed since the aircraft started flying its cruise (t_c) and as a function of the flight distance as a plane in the form:

$$RD = RD_0 + K_D d_f + K_t t_c \quad (\text{IV.2})$$

The coefficients of the fitting of equation IV.2 for the aircraft types analysed in the interval between 250 NM and 2,200 NM when no cruise step is done are presented in table IV-5.

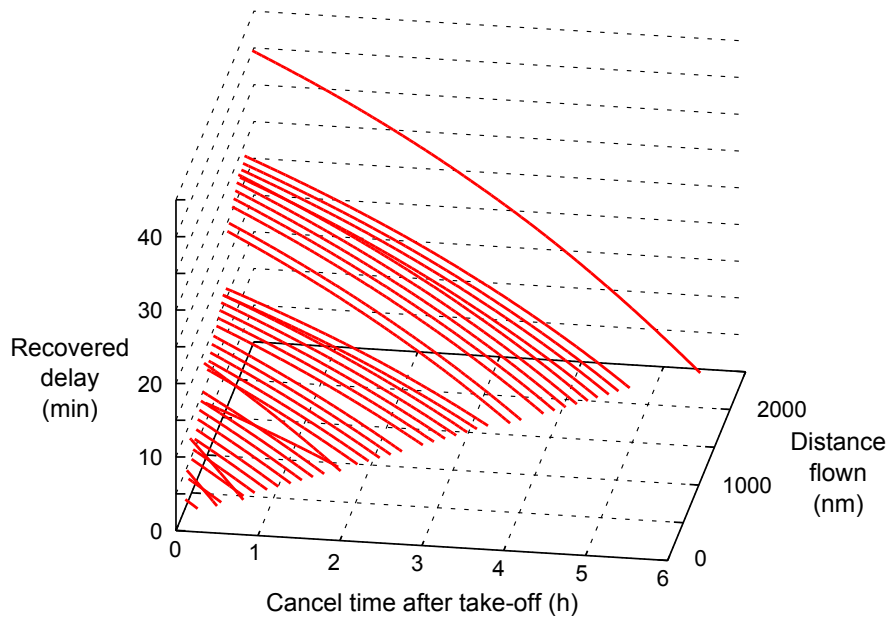


Figure IV-13: Recovery delay as a function of cruise time when aircraft speeds up to V_0 for an A320 with flight plans up to 2,500 NM

Table IV-5: Parameters fitting air delay recovered as a function of flight plan distance and cruise time when speeding up to V_0

Aircraft Family	RD_0 (min)	K_D (min/100NM)	K_t (min/h)	σ_D (min)
A300	-1.12	0.71	-3.20	0.18
A319	-2.80	1.44	-5.96	0.69
A320	-4.42	1.61	-6.18	1.34
A321	-2.43	1.31	-5.50	1.07
A330	-3.55	1.42	-6.18	1.05
A340	-1.43	0.69	-3.22	0.24

IV.1.5 Discussion of the airborne delay in calm wind situation

From analysis of the results, it can be highlighted that the airborne delay is directly proportional to the intended cost index and the available distance in which the speed reduction can be applied. On a general basis, the higher the distance and the higher the cost index, the higher is the amount of airborne delay. A few exceptions are observed to these general trends, where an increment of the cost index or the flight plan distance leads to a reduction of the airborne delay realisable, see for instance the FRA–MAD routes at $CI=200$ kg/min (table IV-1) or the simulations of the A320 for 1,200 NM and 1,250 NM (figure IV-10(a)). These irregular discontinuities are caused by the operational constraint of having a finite and discrete set of cruise altitudes to choose from (flight levels).

It has been shown that in the absence of wind, the maximum realisable airborne delay as a function of the flight plan distance for nominal flights can be fitted to a linear curve, and that the potential delay recovered as a function of the flight plan distance and the time when the regulation is cancelled can be approximated by a plane. However, as presented in section IV.1.3, small variations in the cost of a flight (i.e. the amount of fuel or the time required) might change the optimal flight level which can be used, and this can lead to changes of up to five minutes in the amount of airborne delay realisable. Hence the importance of precisely determining the nominal

flight plan characteristics. In this section it has been identified that **the intended flight level is one of the main parameters affecting the amount of airborne delay realisable by a given flight.**

By changing the cruise speed on a given flight, the optimal conditions for that flight are also changed. For this reason, as presented in IV-1, the optimal cruise flight level(s) for the equivalent speed may be different than for the nominal speed. When a change in cruise altitudes is allowed, it is observed that lower flight levels are used, leading to an increase of airborne delay for the same fuel consumption. Even without extra fuel consumption, more than 12 minutes are absorbed in the air for the FCO–CDG flight at CI=60 kg/min. This highlights how choosing the right flight level for the right speed is crucial.

It must be noted that high cost index values are not generally used by aircraft operators, typical values being between 20 kg/min to 70 kg/min for short and mid range flights. Therefore, in table IV-1, the most significant values are the first two rows of each different route. For short haul flights, such as the DUB–LHR, the amount of airborne delay is too small for this speed reduction concept to be practical, even if the percentage of delay with respect to the whole cruise time is high. For medium haul flights, airborne delay can easily be around 10 minutes, and at no extra fuel cost than initially planned.

IV.2 Airborne delay at the equivalent speed: Wind situation

Wind affects the amount of airborne delay that can be realised without incurring extra fuel consumption. Its influence is due to the variation in the specific range curve, the air distance available and the optimal flight level for a given flight (see section III.5.3).

In this section the effect of the wind on the maximum airborne delay and the effect of uncertainty on the wind forecast are analysed.

IV.2.1 Assessment of airborne delay: Constant wind approximation

In order to present the effect of wind on the maximum amount of airborne delay that can be realised, without incurring extra fuel consumption with respect to the nominal flight conditions, an Airbus A320, with a typical commercial load factor of 80% (ELFAA - European Low Fares Association Members, 2008) is simulated for different flight distances (500 NM, 700 NM, 900 NM and 1,300 NM), with seven different altitudes and constant cruise winds ranging from -80 kt to 80 kt. Flight distances correspond to the whole flight and therefore, the cruise distance varies as a function of the cruise flight level chosen. The nominal cost index is set to 60 kg/min (Airbus, 1998). In these simulations, the reduction of the weight during the flight is also considered, and therefore the changes of V_{eq} throughout the cruise are simulated. Figure IV-14 presents the results of the obtained airborne delay for each simulation where the amount of airborne delay has been rounded to the closest minute.

As expected, the stronger the head wind, the greater the airborne delay that can be realised. For example, around 10 minutes of airborne delay can be done in a 500 NM flight, flying at FL370 with a constant head wind of 80 kt (see figure IV-14(a)). For the same altitude and the same distance, but with 80 kt of tail wind, only 4 minutes of airborne delay can be realised.

From these figures (or the equivalent tabulated data), the aircraft operator could get a quick approximation of the airborne delay that can be realised by reducing the cruise speed without using extra fuel for a given set of flight conditions. However, airborne delay is strongly related to the optimal cruise flight level which depends, in turn, on the actual wind. Since wind fields change significantly with the altitude, each particular flight has to be studied separately.

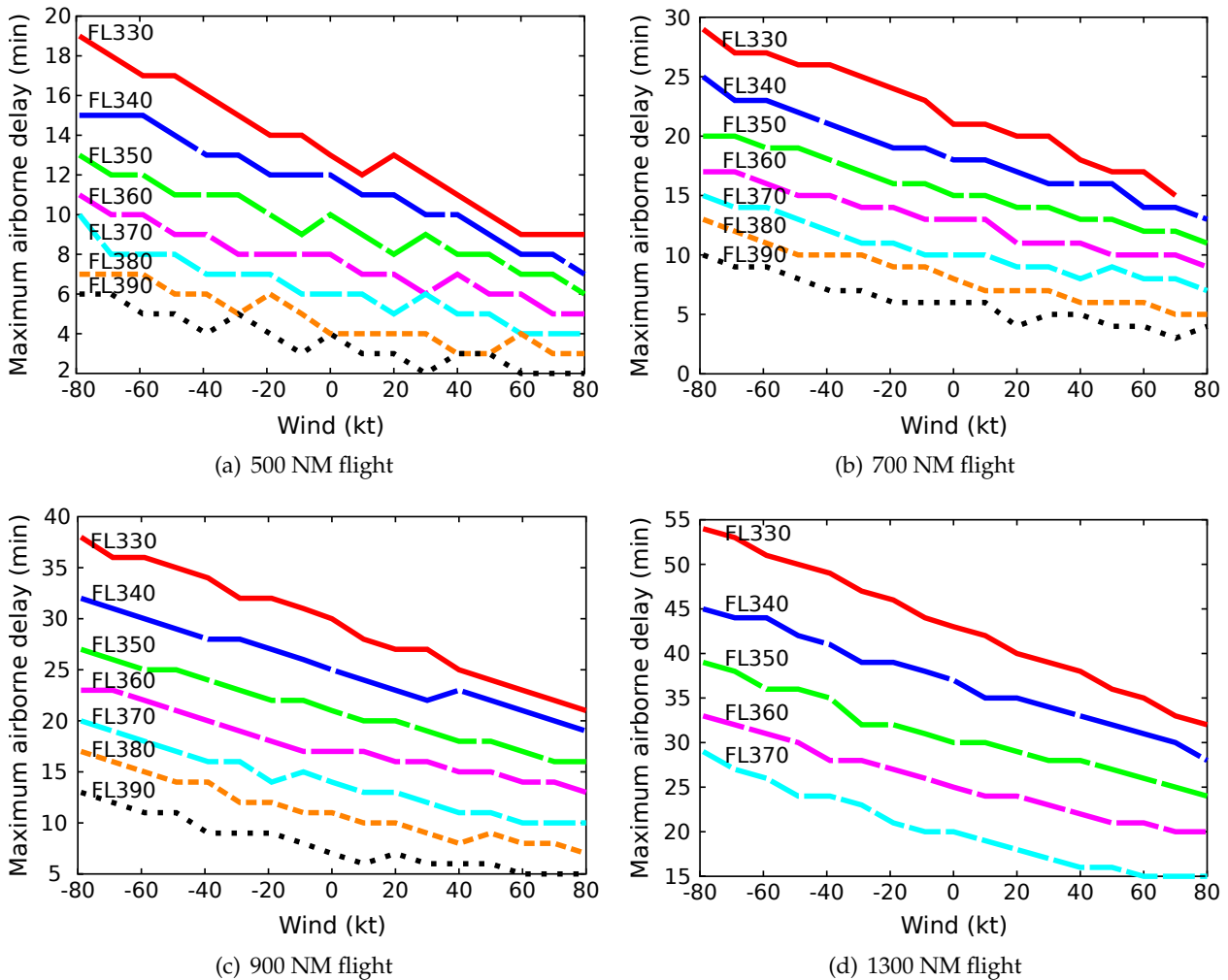


Figure IV-14: Maximum airborne delay as a function of flight level and wind (constant wind during the cruise)

IV.2.2 Realistic wind field analysis: Case study

In the previous section, the effect of wind has been analysed in a general manner. In this section, specific flights are considered in order to analyse the effects of realistic wind fields.

IV.2.2.1 Definition of the simulations

Of all the flights arriving at ORD on August 24th, 2005, those that originated at an airport within a 1,200 NM radius centred at ORD and that were flown by A320 aircraft or by an aircraft with similar performance (B737-400, B737-800, B737-900 and MD-80) are analysed with the same assumptions as in the case study without wind in section IV.1.2.3. Table IV-6 contains a summary of these flights. The table also shows the number of different routes that were used that day between each particular origin-ORD pair. The eighteen airports with the most traffic to ORD represent more than 75% of all the traffic studied. As wind might change during the day, in order to define this scenario, from each origin the take off time of the first flight of the day is selected.

As was presented in section I.3, the speed reduction strategy is useful if ATFM delay are assigned to the aircraft. When an ATFM initiative, such as a ground delay program (GDP) is implemented, a radius of application is typically set. Therefore, the aircraft closest to the airport are the ones that are most affected. Moreover, it is interesting to study the effect of wind on short

Table IV-6: *Flights to Chicago O'Hare performed by A320 aircraft types originated within a 1,200 NM radius*

Origin	Average Distance Distance	Number of routes available	Flights	Aggregated % of flights
LGA	661	3	25	10.5
DFW	763	3	18	18.0
BOS	774	3	12	23.0
MCO	925	3	12	28.0
MSP	300	3	12	33.1
ATL	552	3	11	37.7
PHL	608	2	9	41.4
BDL	720	2	8	44.8
DCA	553	2	8	48.1
DEN	800	5	8	51.5
DTW	215	2	8	54.8
EWR	649	2	8	58.2
IAH	830	3	8	61.5
STL	230	2	8	64.9
CYYZ	380	2	7	67.8
MCI	365	1	7	70.7
TPA	915	1	7	73.6
AUS	890	1	6	76.2

and medium flights as they are the ones which, without wind, are able to perform less airborne delay (see table IV-1). Thus, a 1,200 NM radius filter is set, which in addition means it is only necessary to simulate only one cruise altitude, as all the flights are short enough not to need a climb step.

The wind data is obtained from the November 28th 2007 rapid update cycle (RUC) files from the National Oceanic & Atmospheric Administration ([National Oceanic & Atmospheric Administration \(NOAA\), 2012](#)). The wind field is non-uniform in altitude nor in position and is updated every hour during the simulation. By using this weather forecast it is possible to compute the average wind of all the flight levels of all the studied routes from a first simulation. This information is used to compute, using the Airbus Performance Engineer's Programs, the cost of each possible route and flight level and determine the nominal route, flight level, nominal speed and weight.

It should be noted that RUC data format is chosen because it offers a very realistic set of meteorological conditions that are easy to integrate with FACET simulations (see figure IV-15). In a real operational implementation, the best available wind forecast at the creation of the flight plan would instead be used.

The results from the simulations of the inbound flights to ORD with wind can be divided in two: general results that are interesting regardless of the airport and represent flights with head, tail and cross wind, and the value of the air delay that can be realised in the presence of wind in this particular simulation. In general, the main wind streams in North America are west-east flows ([Endlich & McLean, 1957](#)). Thus, flights to Chicago from the west usually have tail winds and are generally medium or long haul flights. On the other hand, flights from the east coast are shorter flights but with heavy head winds. Finally, flights from the south have roughly cross wind components. Three airports, each one representative of one of these situations, are studied: Austin-Bergstrom International (AUS), Washington Dulles International and Orlando

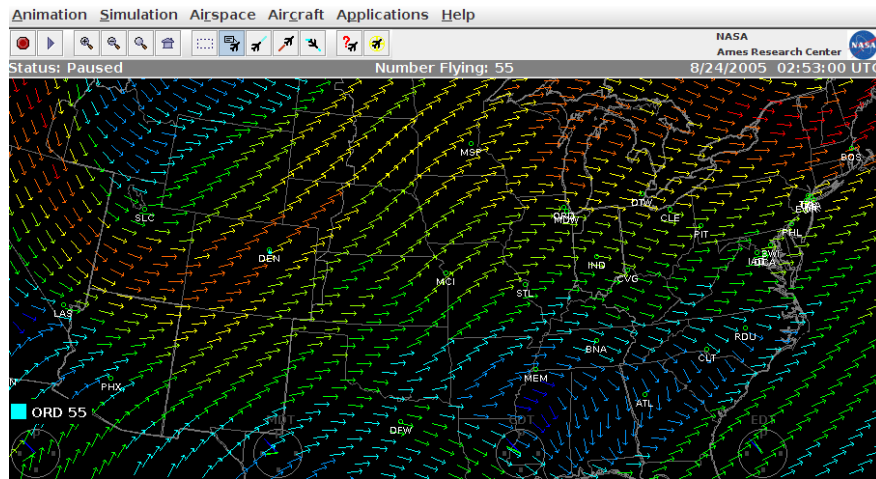


Figure IV-15: Example of FACET screen-shot simulation with RUC wind loaded

International (MCO).

IV.2.2.2 Characteristic results of the wind field analysis

In this section the three characteristic origins are analysed in detail without considering wind uncertainties. Figure IV-16 presents, for the MCO–ORD flights, the total cost² of each possible route and flight level³; and the maximum amount of airborne delay that can be realised for each of the different flight levels and routes using the same fuel consumption as in their nominal flight plan (i.e. flying at V_{eq}). The values of airborne delay range from 10 to 40 minutes. However, as the airline would choose the flight level and route which minimise the total cost, route 2 and FL370 in this case, the maximum airborne delay is fixed to 16 minutes. As different winds are present at different altitudes, slight variations in wind might lead to variations in the total cost and changes in the preference of different routes and flight levels. For example, if a lower head wind were present in route 3, it might be preferable to use that route at FL350.

As can be seen in figure IV-17, only one route was flown the day of study from Austin to Chicago. The cost and average wind of each flight level are also represented in the figure. As can be observed, the flight level with lower cost is the FL390, where an average tail wind of 46 kt is present. With that flight level, 6 minutes of airborne delay can be performed without extra fuel consumption.

Finally, for the IAD–ORD flight, there are two different routes. From figure IV-18, it can be deduced that the second route is more efficient than the first one, and that the FL380 is the one with a lower cost. At this flight level, 9 minutes of airborne delay can be realised.

Table IV-7 summarises the optimal flight level, route and maximum amount of airborne delay that can be realised for the flights. In order to assess the effect of the wind on the amount of airborne delay realised, the airborne delay is compared with the case when no wind is present. In the same table these results are shown too. When no wind is present, the optimal flight level (and even the optimal route), might change. This leads to big differences in airborne delay even in the presence of relatively weak winds, as is the case for the MCO flight.

However, if the flight level and route are maintained, as in the wind situation (values between brackets in the table), as expected, the amount of airborne delay is almost the same in the case of perpendicular wind (MCO flight), in the head wind situation (IAD flight), the amount of

²Total cost is computed as: $\text{Cost} = \text{Fuel} + \text{CI} \cdot \text{Time}$

³No ATM restrictions have been assumed for the different flight levels, like the typical odd/even flight level restrictions.

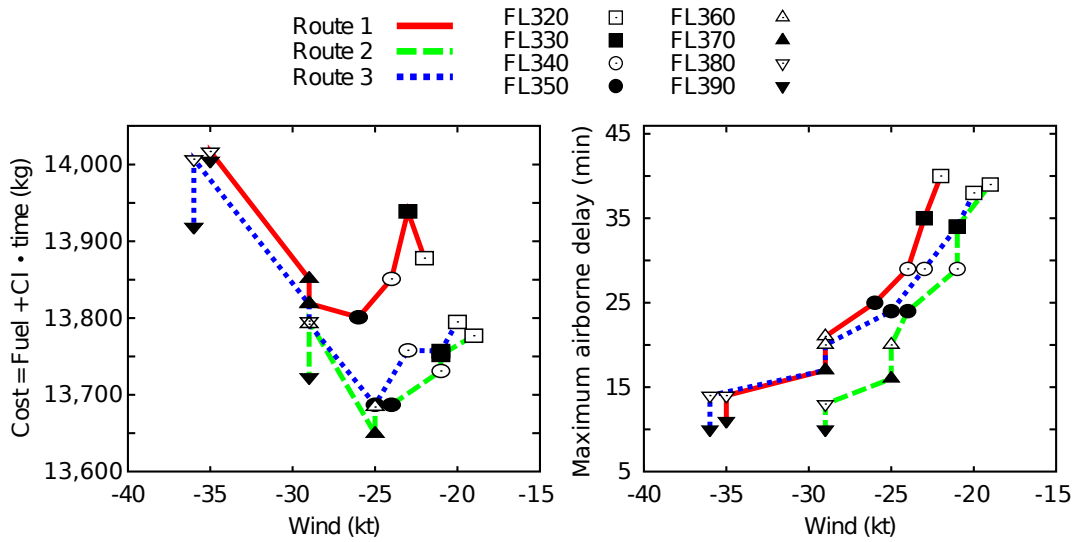


Figure IV-16: Optimal flight level, cost and maximum airborne delay as a function of route for Orlando International to Chicago O'Hare flights

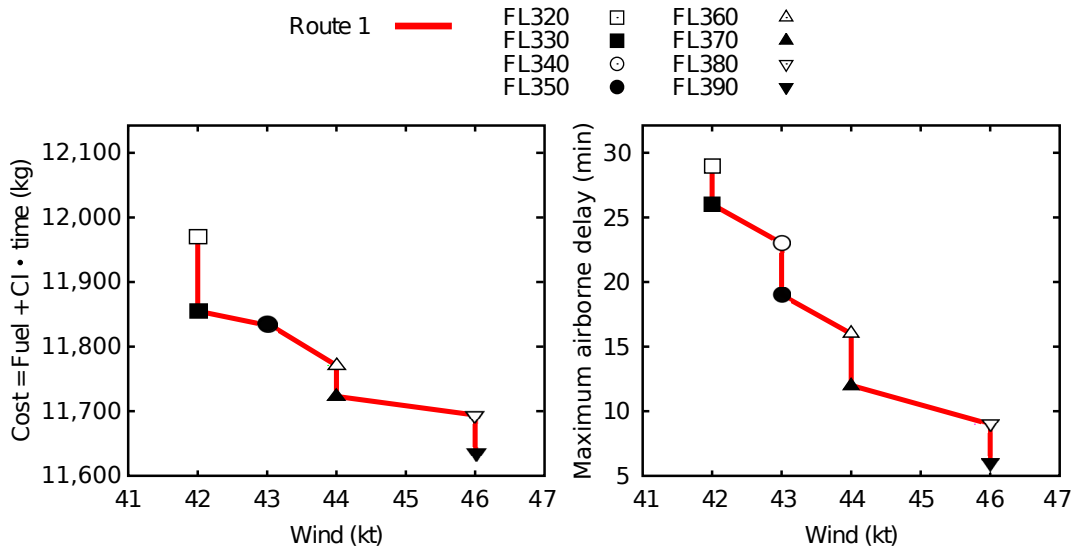


Figure IV-17: Optimal flight level, cost and maximum airborne delay as a function of route for Austin-Bergstrom International to Chicago O'Hare flight

Table IV-7: Average wind, optimal flight level and airborne delay for characteristic analysed flights (same FL and route but without wind between brackets)

Origin	Wind Situation				No Wind Situation		
	Wind	Optimal FL	Optimal Route	Airborne Delay (min)	Optimal FL	Optimal Route	Airborne Delay (min)
MCO	-26	370	2	16 (15)	390	3	8
AUS	46	390	1	6 (7)	370	1	14
IAD	-83	380	2	9 (5)	370	2	7

airborne delay is increased, and in the case of tail wind (AUS flight), the amount of airborne delay is reduced.

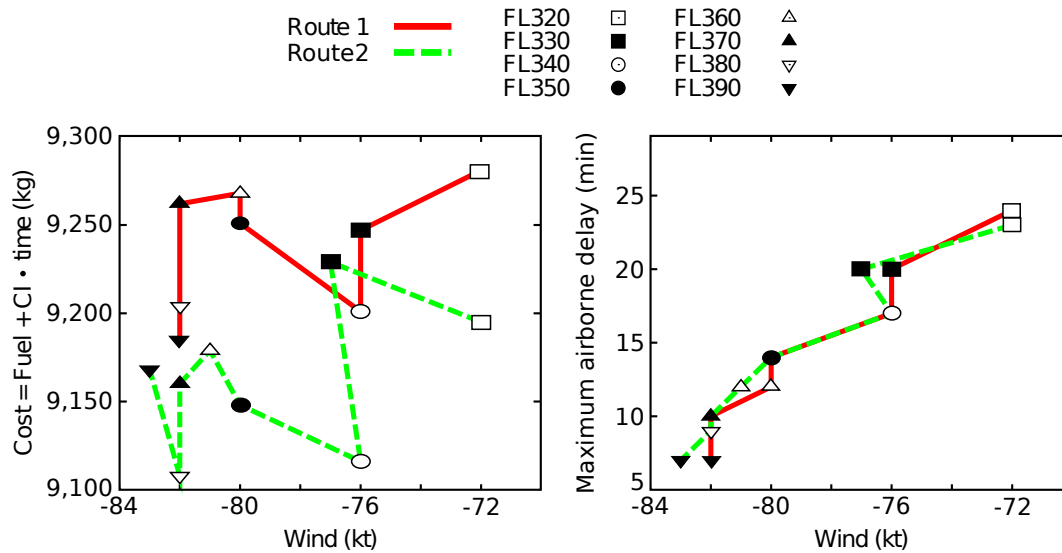


Figure IV-18: Optimal flight level, cost and maximum airborne delay as a function of route for Washington Dulles International to Chicago O'Hare flight

All these simulations are done using the recorded wind in the RUC file using FACET. However, it is possible to assess the amount of airborne delay, with a faster computation, by assuming that during the cruise the wind is constant and equal to the average wind the airline will face, on that route and flight level. Results show that there is less than one minute of error for the three flights between the two techniques. In the AUS flight the same value of airborne delay is obtained. For the IAD, using the average wind, the amount of airborne delay computed is 8 minutes versus the 9 of the RUC simulation; and for the MCO flight, 15 minutes using the average wind instead of 16 minutes of airborne delay with the accurate wind simulation.

Therefore, by using the average wind value without needing the detailed wind profile, as done in section IV.2.1, it is possible to obtain an accurate approximation of the amount of airborne delay that can be realised without incurring extra fuel consumption.

IV.2.2.3 Case study results

Following the same principle as in section IV.2.2.2, the best route, flight level, and airborne delay are selected for all the flights of table IV-6. These results are presented, in turn, in table IV-8, where three extra origins are added: Washington Dulles International (530 NM, 2 routes and 4 flights (1.7%)), Louis Armstrong New Orleans International Airport (MSY) (725 NM, 2 routes and 8 flights (3.3%)) and Salt Lake City International Airport (SLC) (1,100 NM, 1 route and 2 flights (0.8%)). They are added because MSY follows a route with an average wind which is almost perpendicular to its track, and the routes from SLC are long and have heavy tail winds.

In general, head winds represent higher airborne delays, the only exception is the flight from Reagan National Airport (DCA), where the airborne delay is the same with and without wind, due to the change in the optimal flight level.

On the other hand, when tail wind is present, in general, less airborne delay can be performed than without wind. However, this is not always the case, for instance from Kansas City International Airport (MCI), even with 99 kt of average tail wind, more airborne delay can be done with wind than without wind. Once again, the change in the optimal flight level is the cause. In this example, the wind leads to a situation similar to the one shown in figure III-17. For the flights with perpendicular wind, the variations are generally very small, as in the MSY case, or explained due to variations in the flight level or the optimal route.

Table IV-8: *Optimal flight level, route, average wind and maximum airborne delay for flights inbound to Chicago O'Hare International within a 1,2000 radius (airborne delay for the no wind scenario displayed between brackets)*

Origin	Optimal FL	Optimal Route	Wind (kt)	Airborne Delay (min)	Δ Airborne Delay (min)	Δ Airborne Delay (%)
EWR	380 (380)	1 (1)	-107	13 (7)	6	85.7
CYYZ	380 (380)	1 (1)	-105	5 (3)	2	66.7
LGA	390 (380)	1 (1)	-100	10 (8)	2	25.0
BDL	390 (380)	1 (1)	-98	12 (9)	3	33.3
BOS	390 (380)	1 (1)	-95	13 (9)	4	44.4
IAD	380 (370)	2 (2)	-83	9 (7)	2	28.6
PHL	340 (390)	1 (1)	-86	20 (5)	15	300.0
DCA	390 (370)	1 (1)	-82	7 (7)	0	0.0
ATL	370 (370)	1 (1)	-43	9 (8)	1	12.5
MCO	370 (390)	2 (3)	-26	16 (8)	8	100.0
TPA	310 (380)	1 (1)	-22	43 (11)	32	290.9
IAH	370 (380)	3 (3)	5	12 (10)	2	20.0
MSY	390 (390)	1 (1)	8	6 (6)	0	0.0
STL	300 (300)	1 (1)	16	3 (4)	-1	-25.0
DFW	390 (380)	2 (1)	26	5 (8)	-3	-37.5
AUS	390 (370)	1 (1)	46	6 (14)	-8	-57.1
MSP	320 (340)	1 (1)	92	4 (4)	0	0.0
MCI	320 (360)	1 (1)	101	5 (4)	1	25.0
DEN	380 (380)	4 (4)	103	6 (10)	-4	-40.0
SLC	380 (380)	1 (1)	110	10 (14)	-4	-28.6
DTW		Too short - no cruise				

It is worth noting that the values of the amount of airborne delay are, in the majority of cases, over 10 minutes for flights with head wind, which are in general short flights, and over 5 minutes for longer flights with tail or perpendicular wind.

IV.2.3 Sensitivity of airborne delay and controlled time of arrival to forecast inaccuracies

In general, during the flight the aircraft faces a different wind field than the forecast used during the flight planning process. Two different situations are considered in the work of this thesis: the aircraft keeps the cruise speed as initially planned or it adjusts the speed in order to fulfil the CTA compensating for the wind forecast errors. In both cases, a variation in the fuel burnt, with respect to the initially computed quantity, will exist. Yet, in the first case, the trip time will also be affected and the CTA will not be respected. This is usually the case in the current concept of operations, where CTAs are still not enforced. It is expected, however, that in SESAR and NextGen scenarios airlines will compensate for the wind variations in order to comply with the assigned CTAs (4D trajectory management).

IV.2.3.1 Flight at cruise airspeed computed with forecast wind

This case supposes that the aircraft maintains the cruise airspeed profile as a function of the distance that was initially computed at the flight planning stage (when using wind forecast data),

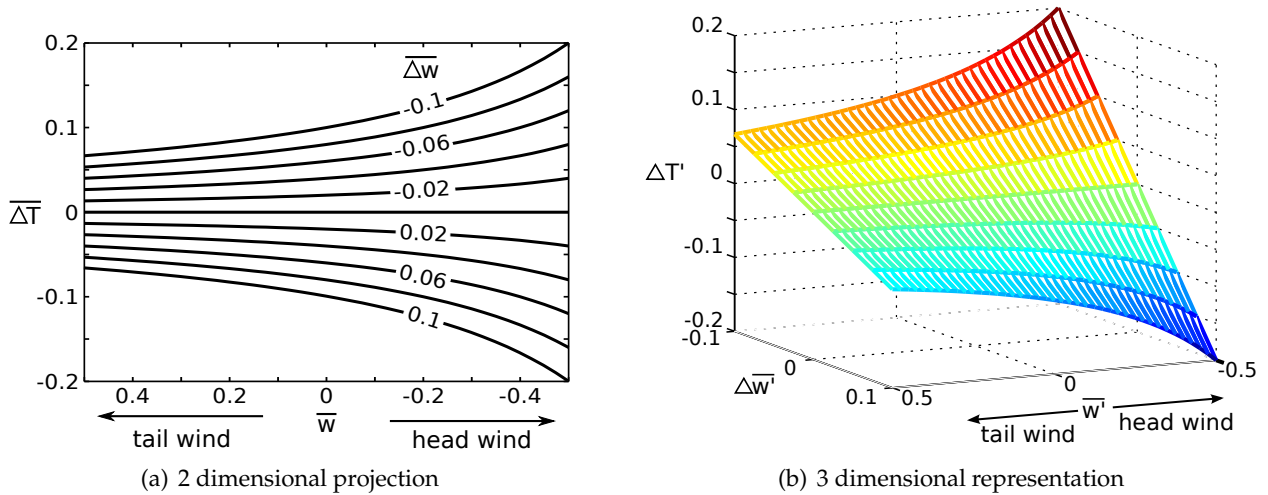


Figure IV-19: Normalised trip time difference as a function of the normalised values of wind forecast and its error

regardless of the actual wind encountered once the aircraft is airborne. Let D_c be the cruise distance and $GS = V + \bar{w}$ be the ground speed computed from the desired true airspeed and an average forecast wind \bar{w} along this distance. Then, the trip time difference (ΔT), as a function of the wind forecast error $\Delta \bar{w}$, can be written as:

$$\Delta T = -\frac{D_c}{GS} \frac{\Delta \bar{w}}{GS + \Delta \bar{w}} \simeq -\frac{D_c}{GS^2} \Delta \bar{w} \quad (\text{IV.3})$$

where it is considered that $GS \gg \Delta \bar{w}$ to obtain a linear relationship between the trip time difference and the wind forecast error⁴.

If we define normalised values for the forecast wind and forecast error such as $\bar{w}' = \bar{w}/V$ and $\Delta \bar{w}' = \Delta \bar{w}/V$, and substitute them in equation IV.3 it yields:

$$\Delta T' = \frac{\Delta T}{T} = -\frac{\Delta \bar{w}'}{1 + \bar{w}'} \quad (\text{IV.4})$$

where the trip time difference is also normalised with the trip time computed at the flight planning stage $T = D_c/GS$ (see figure IV-19).

As expected, the effects of wind uncertainties have a higher impact over $\Delta T'$ in headwind conditions than in tailwind conditions: the slower the ground speed, the longer the cruise time and, therefore, the higher the effect of the wind on the trajectory.

If the variations in aircraft mass are neglected during the ΔT period, the fuel flow can be considered constant for a given cruise airspeed and flight level. Thus, the difference in fuel burnt on the actual flight, with respect to the planned one, can also be written as a linear function of the wind prediction accuracy: $\Delta F = \dot{m}_{fuel}(V, \rho) \Delta T$.

This relationship, along with equation (IV.3), gives a good approximation of the fuel and time error, respectively, due to wind forecast inaccuracies. For example, an Airbus A320 performing a medium haul flight of 700 NM experiences around 5 to 7 minutes of error in the CTA, for strong headwind conditions (around 100 kt) and a forecast error of 30kt. On the other hand, the impact on fuel consumption is around 200 kg of extra or less fuel depending if the forecast underestimates or overestimates the headwind respectively.

⁴In general, wind forecast differences with actual wind are usually lower than 20 kt (Benjamin et al., 2002).

Since wind effects are more noticeable at lower aircraft ground speeds, for a given error in wind forecast ($\Delta\bar{w}$), the error on the CTA will be more significant for an aircraft realising airborne delay (by flying slower at V_{eq}) than the same flight at the higher nominal cruise speed V_0 . Even if the equivalent speed decreases during the flight, its variation is almost linear (see section III.5.2). Thus, for flights performing airborne delay with this strategy it is fair to approximate them as aircraft flying at a constant average equivalent speed \bar{V}_{eq} for the whole cruise distance. With this assumption, the trip time for a flight at \bar{V}_{eq} , with respect to the planned one with forecast winds, can be expressed as:

$$\Delta T_{V_{eq}} = \Delta T_{V_0} \left(\frac{V_0 + \bar{w}}{\bar{V}_{eq} + \bar{w}} \right)^2 \simeq \Delta T_{V_0} \left(\frac{V_0}{\bar{V}_{eq}} \right)^2 \geq \Delta T_{V_0} \quad (\text{IV.5})$$

where ΔT_{V_0} is the trip time error for the nominal flight at V_0 .

Typically, \bar{V}_{eq} represents 80% of the nominal speed V_0 . Therefore, the error in the CTA when cruising slower at the equivalent airspeed, can be up to 50% higher than in nominal conditions. However, since ΔT_{V_0} is already very little for typical flights, the CTA error will only be around 2-4 minutes worse than the same error in nominal conditions, and for strong headwind and high forecast inaccuracies. The same rationale follows for differences in the amount of extra (or less) fuel needed between nominal conditions and reduced speed flights, which would be around 70 kg for typical medium haul flights performed with an A320.

In order to particularise the assessment of the effect of the uncertainties in the forecast and actual wind on the amount of airborne delay, detailed simulations are conducted using the average wind over the routes, changing the wind the aircraft actually faces in the simulations. Figure IV-20 presents the variation in the CTA for the MCO-ORD flight, if the wind is different than forecast. Flying at V_{eq} leads to higher variations in flying time and fuel consumption. However, if $\Delta\bar{w}$ is small, it is observed that the differences between flying at V_0 and flying at V_{eq} are small; less than 2 minutes on the CTA and less than 65 kg on the fuel consumption for the three analysed flights with $\Delta\bar{w} \in [-30, 30]$ kt.

As was presented in equation (IV.3), the error in the flying time can be approximated linearly, as a function of the wind forecast uncertainty. Table IV-9 presents the value of the slope of this relationship ($\frac{D_c}{V_{GS}^2}$) when flying at V_0 and at V_{eq} , respectively for the flights simulated in section IV.2.2.1 adding the wind uncertainty. As is presented, there are very small differences in time error in the CTA if flying at V_0 or flying at V_{eq} .

Similarly, with the linear approximation of the error in the fuel burnt as a function of $\Delta\bar{w}$, it is possible to compute the error in kg of fuel per wind knot deviation with respect to the forecast value. Results are also presented in table IV-9, for the V_0 and the V_{eq} cases, showing again that the differences between flying the nominal flight plan or realising airborne delay are small for a typical $\Delta\bar{w}$. As expected, the higher differences are observed on the longer flights, like Austin-Bergstrom International or Orlando International to Chicago O'Hare.

IV.2.3.2 Flight adapting cruise airspeed in order to fulfil the CTA

In this case, the ground speed remains the same as initially computed at the flight planning stage. Thus, CTA will be fulfilled but actual wind differences will produce variations in the cruise true airspeed and, consequently, a different fuel consumption with respect to the initially planned flight.

At typical flight altitudes and aircraft weights, the fuel flow is a non linear monotonically increasing function with respect to the true airspeed (see figure III-6). Therefore, more fuel is needed to compensate for stronger head winds or weaker tail winds ($\Delta\bar{w} < 0$), i.e. an increase in the cruise speed is needed; while some fuel is saved if $\Delta\bar{w} > 0$ (more tail wind or less head wind

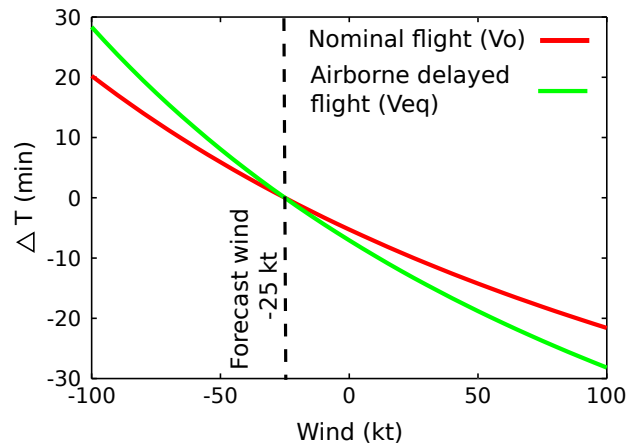


Figure IV-20: ΔT if speed is maintained as initially planned if wind is not as forecast for Orlando International to Chicago O'Hare flight

Table IV-9: Slopes of the linear approximations of the controlled time of arrival error and fuel burnt difference for flights maintaining the cruise speeds computed with the forecast winds

Origin	Slope of the CTA error (min/10 kt)			Slope of the fuel burned error (kg/10 kt)		
	V_0	V_{eq}	Difference	V_0	V_{eq}	Difference
EWR	-2.0	-2.8	0.8	-76.9	-87.3	10.4
CYYZ	-0.8	-1.2	0.3	-31.9	-35.8	3.9
LGA	-2.0	-2.6	0.6	-72.3	-83.2	11.0
BDL	-2.3	-3.0	0.8	-86.0	-96.0	9.9
BOS	-2.4	-3.1	0.7	-85.2	-98.3	13.1
IAD	-1.3	-2.0	0.7	-48.8	-61.5	12.7
PHL	-1.8	-3.1	1.3	-66.1	-89.3	23.2
DCA	-1.4	-1.8	0.4	-50.3	-55.5	5.2
ATL	-1.2	-1.7	0.6	-45.2	-52.5	7.3
MCO	-2.2	-3.0	0.8	-83.4	-90.5	7.1
TPA	-2.2	-4.5	2.3	-97.2	-127.5	30.3
IAH	-1.6	-2.1	0.5	-54.3	-64.2	9.9
MSY	-1.4	-1.7	0.2	-48.1	-53.4	5.3
STL	-0.1	-0.3	0.2	0.0	-9.5	9.5
DFW	-1.2	-1.4	0.3	-37.8	-45.1	7.2
AUS	-1.5	-1.7	0.2	-50.2	-53.6	3.4
MSP	-0.1	-0.3	0.2	-7.5	-8.3	0.8
MCI	-0.2	-0.5	0.3	-5.2	-15.2	10.0
DEN	-1.0	-1.2	0.2	-30.8	-36.9	6.0
SLC	-1.6	-1.7	0.1	-50.3	-51.3	1.0
DTW	Too short - no cruise					

than forecast and, consequently, a decrease in the initially planned cruise speed). Moreover, due to its non linearity, the impact on the final fuel consumption in absolute value (increase or savings) is higher when speed variations are performed at high cruise airspeed. Thus, these fuel burnt variations, due to wind forecast errors, are less significant if flying at V_{eq} than at V_0 . For example, for the flight presented in figure III-6, if V_0 is $M 0.79$, the equivalent average speed is $M 0.705$. If

the cruise speed is incremented by 10 kt, the fuel flow is increased by 246 kg/hour if the aircraft is flying at V_0 , and only by 16 kg/hour if flying at \bar{V}_{eq} . Similarly, if the speed is reduced by 10 kt, to compensate for extra tail wind, 92 kg/hour are saved in the V_0 flight, while the variation is -4 kg/hour in the \bar{V}_{eq} scenario.

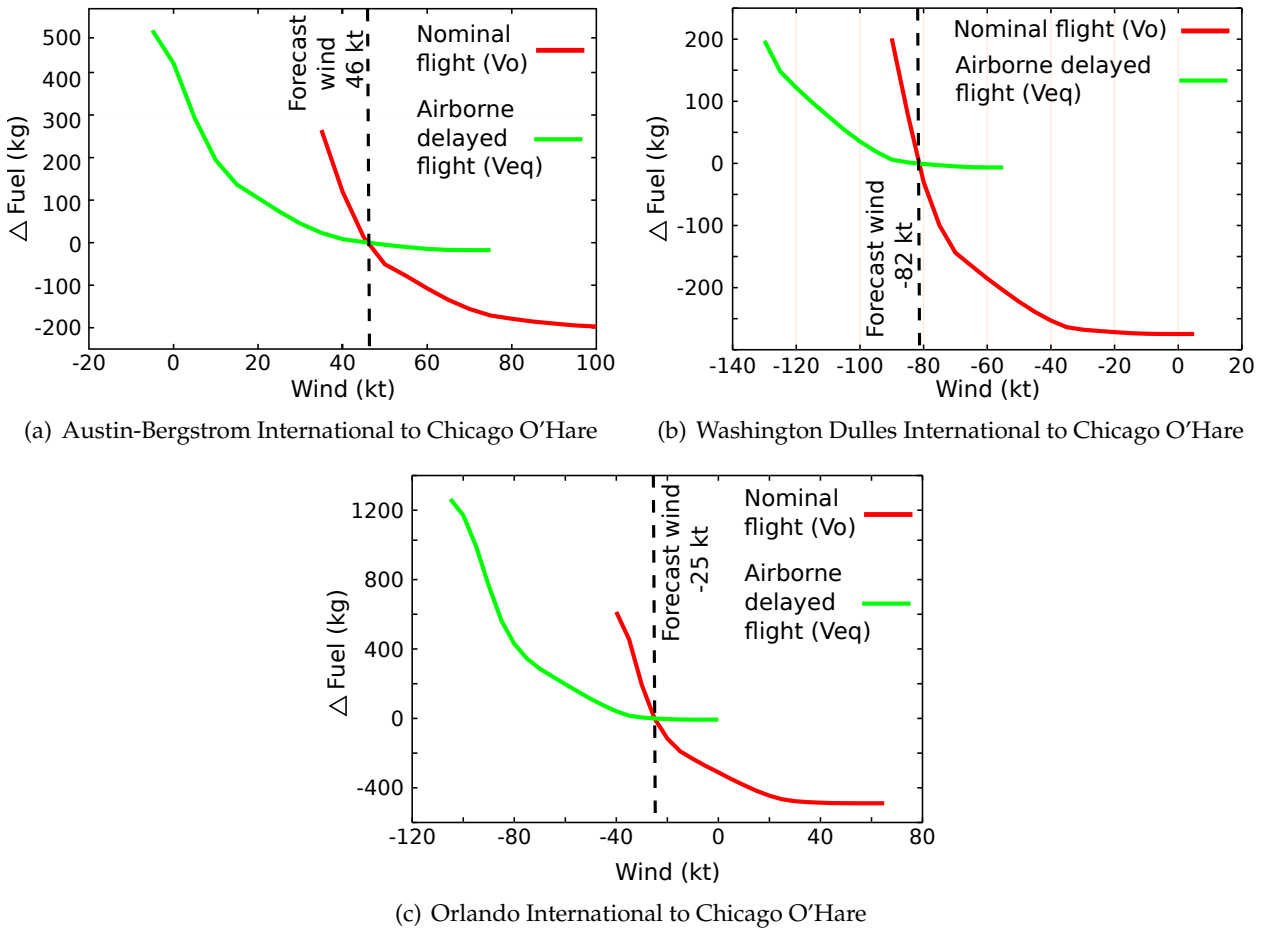


Figure IV-21: Differences in fuel consumption if the CTA is respected and the wind is different than forecast as a function of wind forecast error

The fuel burnt, as a function of the actual wind encountered, for the three characteristic flights simulated in section IV.2.2.2 is computed and presented in figure IV-21. In these simulations the wind is constant during the entire flight, as in the previous section. Therefore, the wind forecast inaccuracies are assumed to be distributed uniformly across the flight. In the results of the simulations, it is possible to observe that fuel burnt variations due to wind forecast errors are less significant if flying at V_{eq} than at V_0 , as explained before. Results show that with a little $\Delta \bar{w}$, flying at V_{eq} has almost no impact on fuel consumption, while when flying at V_0 , the variations in fuel consumption are significantly higher.

Some example values for the flights from section IV.2.2.1 are presented in table IV-10. In these results the amount of extra fuel consumed or saved is presented for each flight with $\Delta \bar{w} = \pm 5$ kt, at V_{eq} there is almost no variation in the amount of fuel used (less than 10 kg). Moreover, with only 5 kt of originally forecast wind, it is possible to have more than 5 times more error in the forecast wind if flying at V_{eq} in order to have the same fuel error as flying at V_0 (values presented between brackets in table IV-10). Therefore, realising airborne delay, by flying slower, is more robust against the variation in the fuel used if the cruise speed needs to change in order to meet the CTA.

Table IV-10: Differences in fuel burnt for flights adapting the cruise airspeed in order to fulfil the CTA (between brackets it is shown the $\Delta\bar{w}$ needed, if flying at V_{eq} , to have the same fuel deviation as if flying at V_0)

Origin	V_0		V_{eq}	
	$\Delta\bar{w} = -5$ kt	$\Delta\bar{w} = 5$ kt	$\Delta\bar{w} = -5$ kt	$\Delta\bar{w} = 5$ kt
EWB	184 kg (-37 kt)	-105 kg (29 kt)	7 kg	-4 kg
CYYZ	77 kg (-37 kt)	-42 kg (29 kt)	3 kg	-1 kg
LGA	117 kg (-27 kt)	-106 kg (29 kt)	7 kg	-6 kg
BDL	121 kg (-26 kt)	-115 kg (27 kt)	9 kg	-7 kg
BOS	123 kg (-26 kt)	-126 kg (24 kt)	9 kg	-7 kg
IAD	128 kg (-39 kt)	-72 kg (27 kt)	3 kg	-2 kg
PHL	142 kg (-31 kt)	-86 kg (30 kt)	8 kg	-5 kg
DCA	100 kg (-32 kt)	-75 kg (24 kt)	5 kg	-4 kg
ATL	105 kg (-34 kt)	-57 kg (22 kt)	4 kg	-2 kg
MCO	192 kg (-34 kt)	-116 kg (25 kt)	5 kg	-4 kg
TPA	168 kg (-46 kt)	-122 kg (16 kt)	-2 kg	2 kg
IAH	127 kg (-33 kt)	-80 kg (25 kt)	4 kg	-2 kg
MSY	116 kg (-29 kt)	-53 kg (27 kt)	8 kg	-6 kg
STL	9 kg (-58 kt)	-6 kg (4 kt)	0 kg	-1 kg
DFW	82 kg (-26 kt)	-44 kg (24 kt)	5 kg	-4 kg
AUS	98 kg (-25 kt)	-56 kg (29 kt)	7 kg	-6 kg
MSP	8 kg (-49 kt)	-6 kg (8 kt)	0 kg	-6 kg
MCI	15 kg (-48 kt)	-12 kg (5 kt)	0 kg	-12 kg
DEN	71 kg (-32 kt)	-44 kg (20 kt)	2 kg	-2 kg
SLC	114 kg (-31 kt)	-69 kg (20 kt)	4 kg	-4 kg
DTW	Too short - no cruise			

† Unable to match the same extra fuel consumption than in the V_0 case since V_{min} is reached before. Instead, $\Delta\bar{w}$ at V_{min} is shown

Note that the Tampa (TPA) flight has an unexpected behaviour when flying at V_{eq} and the CTA is respected: a positive Δw produces more fuel consumption, while a negative Δw produces fuel savings. Due to the vertical wind profile, the minimum cost flight level is low (FL310). For these flight characteristics, an increase in speed represents a reduction of fuel flow for slow speeds (values between 330 kt and 340 kt). As stated previously, aircraft typically operate at altitudes where an increase of true air speed implies an increase of the fuel flow, as shown in figure III-6, for this reason TPA is an exception.

Finally, it is worth mentioning that true air speed modifications are always bound by the flight envelope of the aircraft. Therefore, airspeed increases are quickly limited by the aircraft's maximum speed if flying at V_0 , while a greater margin is available if flying at V_{eq} . On the other hand, if the cruise air speed is reduced, it is limited sooner when flying at V_{eq} rather than at V_0 .

IV.2.4 Discussion of the airborne delay in wind situations

In general, head winds lead to increases in airborne delay and tail winds mean a decrease in the maximum airborne delay. The variations in airborne delay with respect to flying without wind are due to the differing duration of flights, but also because the specific range function is changed by adding a term depending on the wind ($\frac{w}{\dot{m}_{fuel}}$), see equation (III.20). However, the main effect

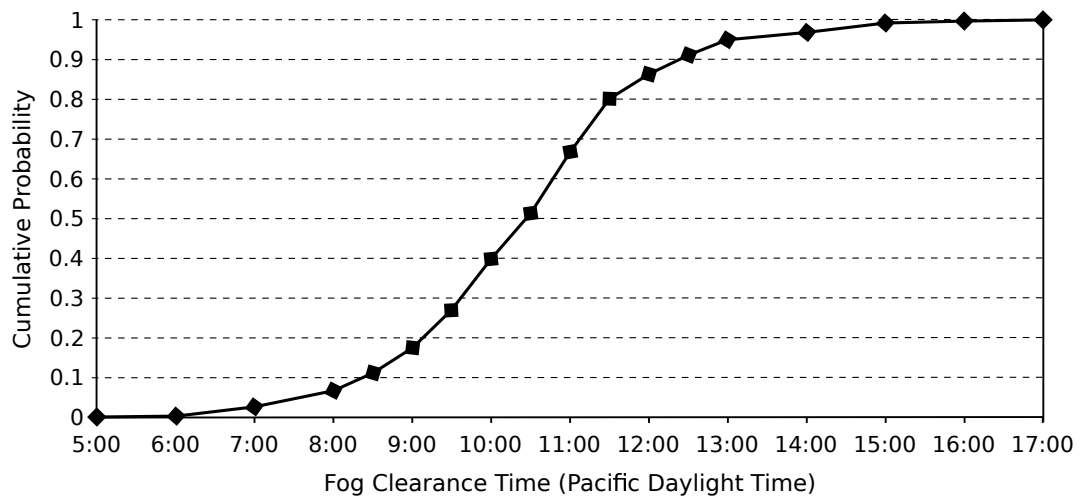


Figure IV-22: Cumulative probability distribution of fog clearance time at SFO

Source: (Mukherjee et al., 2012)

of wind on the amount of airborne delay is that it might change the optimal flight level. And as has been previously presented, changes in the flight level lead to big changes in the amount of airborne delay that can be realised without incurring extra fuel consumption.

If differences are present between the forecast and the actual wind, two scenarios have been analysed. If the speeds are maintained as previously planned, the variation in the arrival time and fuel consumption are higher if the aircraft is realising airborne delay. However, this variations does not seem very great. In the order of 2-4 minutes and 70 kg. On the other hand, if the time of arrival is maintained by adjusting the speed to compensate for wind forecast errors, as aircraft are expected to do in SESAR and NextGen, the airborne delay strategy leads to a more robust situation from a fuel variation point of view.

IV.3 Airborne delay with extra fuel consumption

The early cancellation of a ground delay program is common, especially when dealing with weather related causes, as presented in section I.2. Figure IV-22 presents the cumulative probability distribution of fog clearance time at SFO computed from observed fog clearance times on 387 summer days between 2004–2007 (Mukherjee et al., 2012). The probability of clearing increases with time, but there is still a possibility that the low ceiling will remain longer than forecast. Thus, regulations are usually planned to last longer than actually needed (Cook & Wood, 2010). For this reason, in San Francisco International Airport, GDPs are generally cancelled about 2 hours before planned, as presented in table I-1. The same behaviour is encountered in other airports.

For this reason, in this section the option of using extra fuel in order to realise airborne delay is analysed. Recalling figures III-7 and III-13, this means that the aircraft would fly at a speed lower than V_{eq} and so produce a SR lower than SR_0 . More fuel to cover the same distance will be used. This strategy might be useful for the airline as long as it considers that there is a high probability that the regulation which generated the ATFM measure is cancelled before planned, as in that case the aircraft in the air will be in a better position to recover part of the delay. It would be possible to speed up, even faster than the initial nominal speed, and trade fuel for delay recovered.

For this study, the same flights, with the same conditions as in section IV.1.1.2 and IV.1.1.3, are analysed.

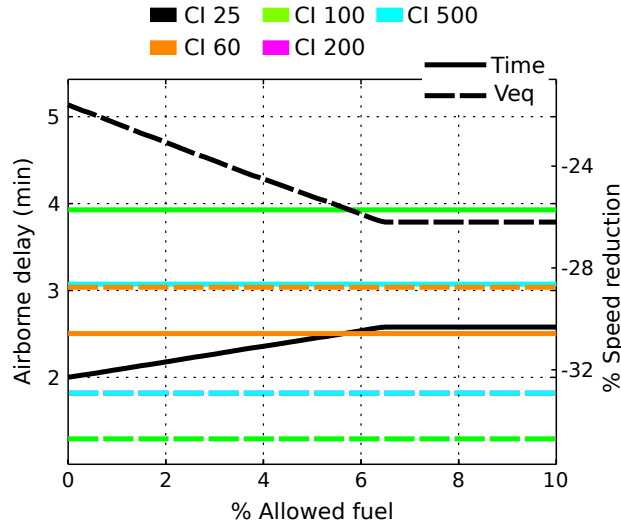


Figure IV-23: Airborne delay and speed reduction for the Dublin to London Heathrow route as a function of the extra fuel allowance

IV.3.1 Speed reduction at nominal flight level with extra fuel allowance

It should be noted that the values obtained in section IV.1.1.2 correspond to the particular situation where the allowed extra fuel is set to 0%. Figures IV-23 to IV-26 show the results for the analysed routes allowing extra fuel consumption. As the extra fuel allowance increases, the amount of airborne delay also increases. However, the airborne delay reaches a maximum value, which in some flights is even attained with no extra fuel consumption (horizontal lines in the figures). This saturation in the airborne delay is due to the fact that, at that point, the aircraft is flying at the minimum operational speed for that flight level and weight. The lower value of V_{eq} is limited by V_{min} (recall figure III-13) and not by the extra fuel consumption. As seen from the figures, this usually happens with the higher values of cost index, since they involve higher nominal cruise speeds (V_0) and consequently lower equivalent speeds (V_{eq}).

If comparing this case with the one studied in IV.1.1.3, where the change of flight level was allowed but the fuel consumption was maintained as in the nominal planned flight, it is observed that, on several occasions, the airborne delay of case IV.1.1.3 is higher than the maximum airborne delay achieved in this case where extra fuel is allowed but the flight level maintained, even though in case IV.1.1.3 the extra fuel consumption with respect to the nominal flight was 0%. This shows the importance of optimising the cruise altitude if changes in speed are made.

Finally, it is observed that the airborne delay (and the speed reduction) follow a linear dependency with the amount of extra fuel allowed. As seen in figures IV-23 to IV-26, this proportionality (the slope of the lines) remains constant for each route regardless of the cost index. If these magnitudes are expressed in relative terms the proportionality is also constant regardless of the route. For each flight considered in this study airborne delay and speed reduction data were fitted to linear equations as a function of the extra fuel allowance by using a standard least squares method:

$$AD(\%) = AD_{0f}(\%) + K_{Df} \cdot EF(\%); \quad SRD(\%) = SRD_{0f}(\%) + K_{Sf} \cdot EF(\%) \quad (IV.6)$$

AD_{0f} and SRD_{0f} are, respectively, the airborne delay and speed reduction when fuel consumption is equal to the nominal flight and EF is the percentage of extra fuel consumption allowed. These values are route and cost index dependent. For all the flights involved in this study, the mean values of the slopes are: $K_{Df} = 1.26$ and $K_{Sf} = -0.92$, with standard deviations of $\sigma_D = 0.049\%$ and $\sigma_S = 0.111\%$ respectively. These linear approximations are valid from a zero percentage of extra fuel up to the maximum amount of extra fuel which implies that the aircraft cruises at its

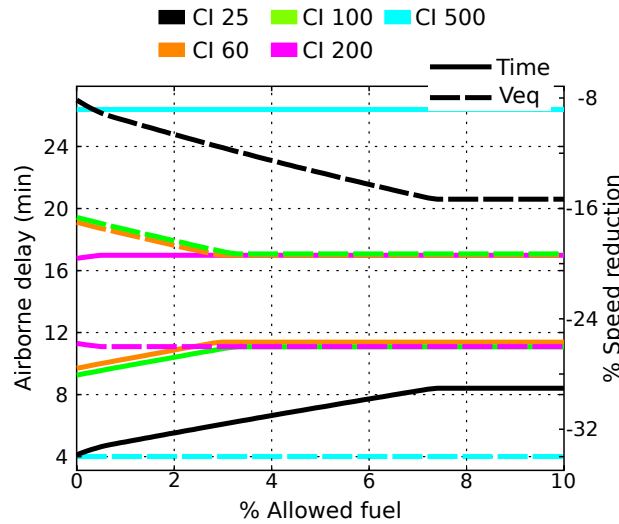


Figure IV-24: Airborne delay and speed reduction for the Rome Fiumicino to Paris–Charles de Gaulle route as a function of the extra fuel allowance

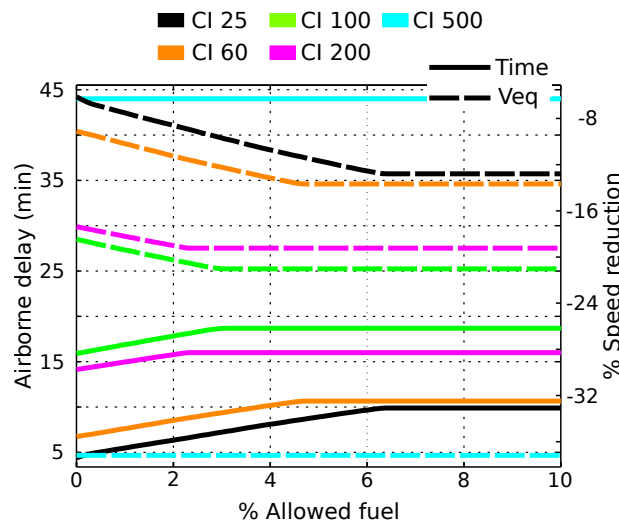


Figure IV-25: Airborne delay and speed reduction for the Frankfurt to Madrid route as a function of the extra fuel allowance

V_{min} , this value is flight and cost index dependent.

IV.3.2 Speed reduction with flight level change and extra fuel allowance

In this case, the results already obtained in section IV.1.1.3 are expanded by allowing more extra fuel consumption than initially planned. Figures IV-27 to IV-30 show, as a function of the extra fuel consumption, the airborne delay, the percentage of cruise speed reduction and the flight level changes for the routes under study. Once again, the higher the extra fuel consumption, the higher the airborne delay. In this case, a saturation is not observed, since it is always possible to fly at lower speeds if the cruise altitude is suitably reduced⁵. This means that airborne delay can be increased at the expense of burning more fuel and flying at lower altitudes. However, at a given point, the flight level is too low and/or the extra fuel consumption is too high to make this

⁵For a given mass, the stall speed of an aircraft decreases as altitude decreases too, due to a progressive increase of the air density

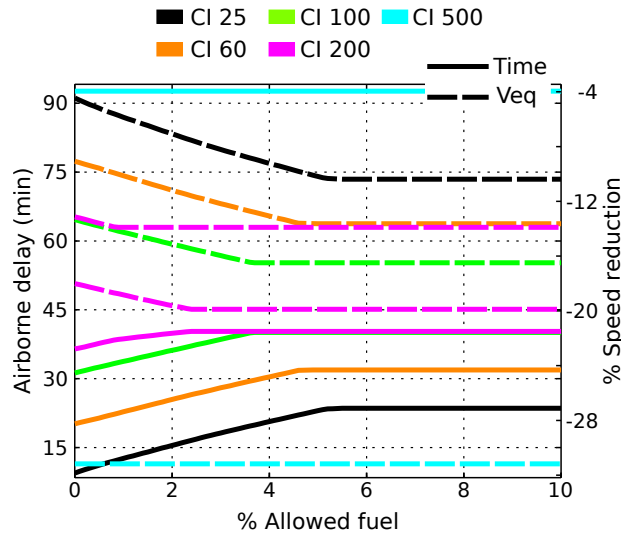


Figure IV-26: Airborne delay and speed reduction for the Lisbon to Helsinki route as a function of the extra fuel allowance

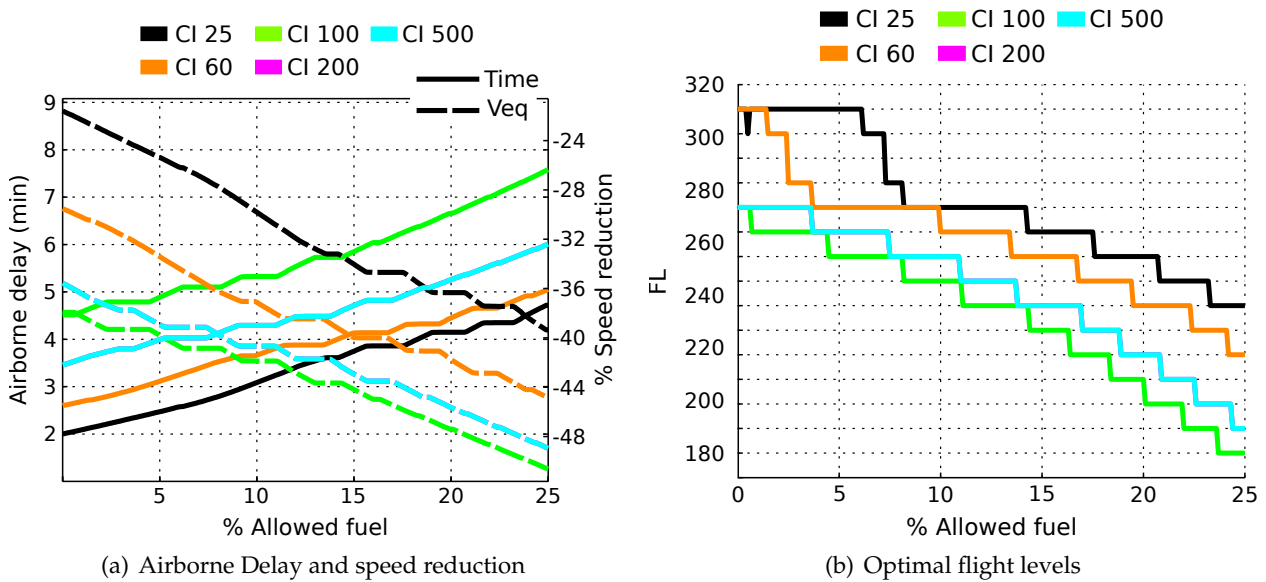


Figure IV-27: Airborne delay, speed reduction and flight level for the Dublin to London Heathrow route as a function of the extra fuel allowance

strategy appealing to the operator. For this reason, the figures are truncated at 25% of extra fuel consumption allowance.

From these figures, the dependency of airborne delay (and speed reduction) versus extra fuel allowance seems quite linear, with some discontinuities caused by the discrete changes in the optimal flight levels. Following the same procedure as in the previous case, data from each flight is fitted to linear equations, obtaining a mean value for the slopes of $K_{Df} = 1.68$ and $K_{Sf} = -0.87$, with standard deviations of $\sigma_D = 0.217\%$ and $\sigma_S = 0.113\%$. As expected, for a given amount of fuel allowance, the amount of airborne delay is higher if cruise altitudes are allowed to change. From the analysed flights, it is observed that an additional 0.42% of AD per percentage of extra fuel consumption allowed is achieved with respect to the case where the flight level is maintained as initially planned ($K_{Df} = 1.68$ instead of $K_{Df} = 1.26$). Conversely, the equivalent speed is reduced by a lower proportion -0.05% than if maintaining the initially computed flight level for

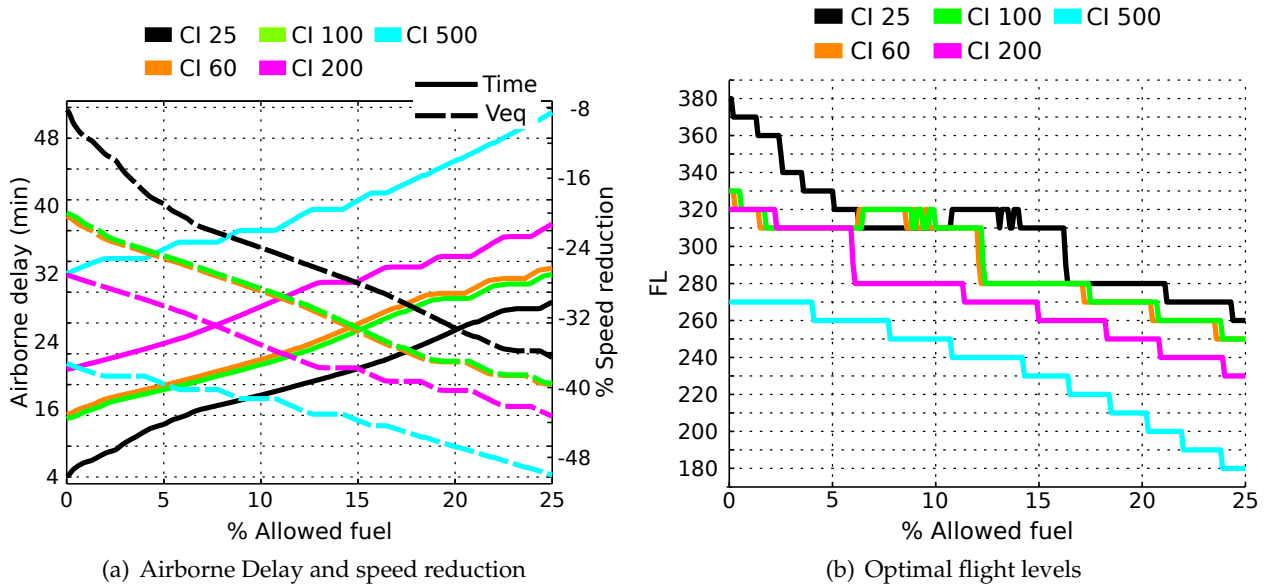


Figure IV-28: Airborne delay, speed reduction and flight level for the Rome Fiumicino to Paris-Charles de Gaulle route as a function of the extra fuel allowance

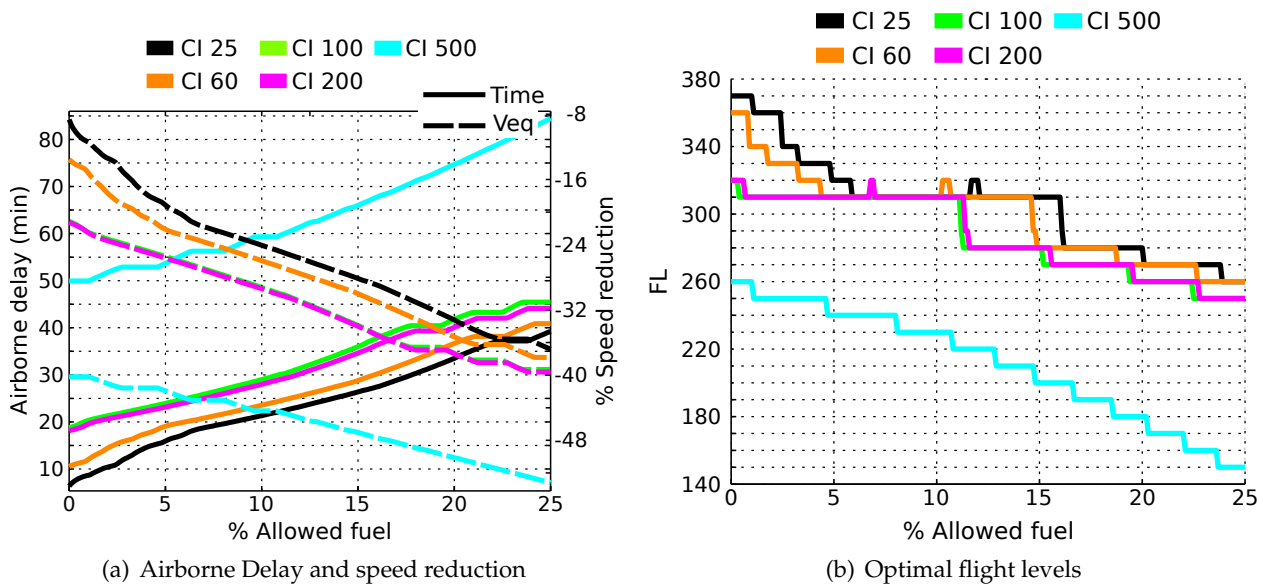


Figure IV-29: Airborne delay, speed reduction and flight level for the Frankfurt to Madrid route as a function of the extra fuel allowance

the same fuel allowance ($K_{Sf} = -0.87$ instead of $K_{Sf} = -0.92$).

IV.4 Discussion of the results

As has been presented in chapter III, the amount of airborne delay that can be realised without incurring extra fuel consumption depends on the specific range. This means that the airborne delay varies with the weight, the flight level and the nominal intended speed of the aircraft and, therefore, it depends on the cost index the airline chooses to plan its flights.

From the simulations of the flights without wind, it is possible to infer that the amount of

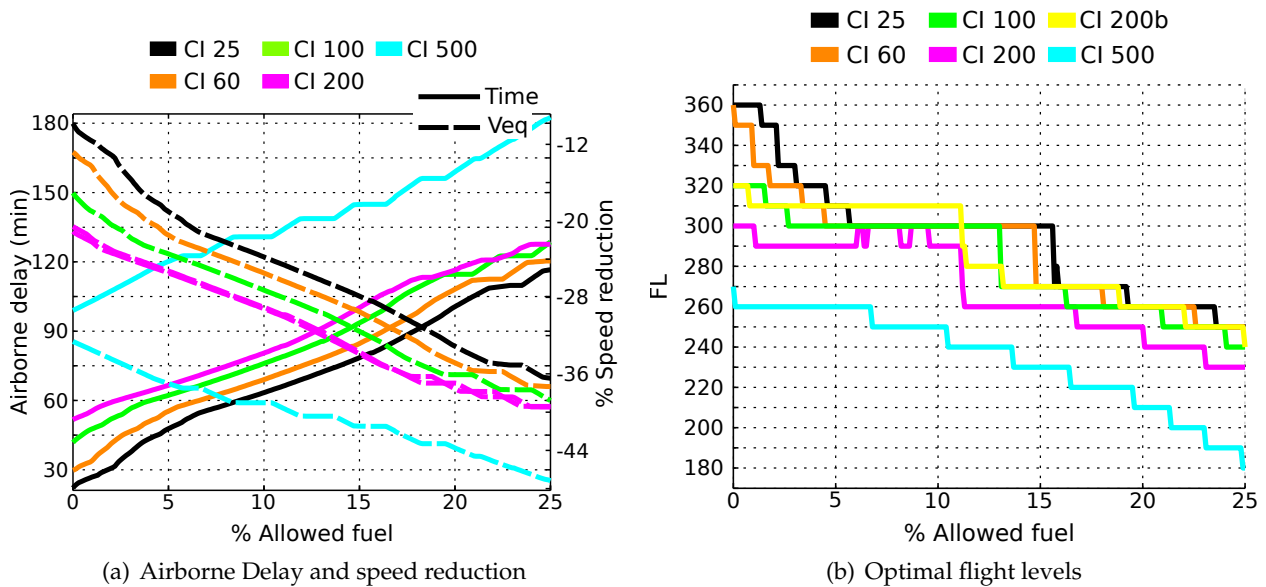


Figure IV-30: Airborne delay, speed reduction and flight level for the Lisbon to Helsinki route as a function of the extra fuel allowance

ground delay that can be absorbed in the air, as well as the potential delay that can be recovered without extra fuel consumption directly depends on the flight distance, the nominal flight level used being paramount. The relationship between all the analysed parameters is quite linear. The amount of airborne delay that can be recovered at no extra fuel cost by speeding up to V_0 decreases with time as the later the regulation is cancelled, the less distance is available to recover delay and more delay has already been realised.

The presence of wind affects the amount of airborne delay that can be realised because it directly affects the specific range. Results show how, when flying at the aerodynamic/propulsive optimal flight level, the amount of airborne delay is very small. Therefore, changes in the optimal flight level due to winds, in general, will represent an increment in the amount of airborne delay with respect to a zero wind situation. This effect is observed even in tail wind situations. In general, the presence of wind produces a reduction in the amount of airborne delay for tail wind situations and an increment in the delay realisable for head wind situations. However, usually the increment in airborne delay for head wind is higher than the reduction produced for tail wind, due to the changes in the optimal flight level.

The values of airborne delay that have been obtained for flights in a radius of 1,200 NM with forecast winds are consistent with the airborne delay we obtain if an average constant wind during the whole cruise is assumed. This means that by knowing the average wind it is possible to get a good approximation of the airborne delay that can be done without needing the detailed wind profile the aircraft will face.

When there are wind forecast errors, if the speed profile computed before the flight is maintained, variations in the flying time and fuel consumption are produced. These variations are higher when the aircraft are performing airborne delay, as the effect of the wind error is longer. However, for the studied flights, and for small forecast errors, the differences between flying at the nominal speed and at the equivalent speed are small: around -0.04 minutes and around -1 kg of fuel per knot error in the forecast. Finally, if the airline adjusts its true air speed in order to meet the controlled time of arrival, as they are expected to do in SESAR and NextGen, variations in fuel consumption will arise. These variations are produced because the fuel flow changes as a function of the *TAS*. The fuel flow dependency among the *TAS* is non linear and therefore lower variations are present at lower speeds (around V_{eq}) than at higher speeds (around V_0). This means that by

realising airborne delay with the proposed strategy, adjusting the speed to meet the controlled time of arrival is more robust against fuel consumption than flying at nominal cruising speed.

If extra fuel is allowed more air delay can be realised with a ratio of 1.2% of extra delay per percentage of extra fuel consumed. It has also been observed that the influence of the flight level is even more important than the allowance of extra fuel consumption, as more airborne delay can be achieved by choosing the appropriate flight level rather than just reducing the speed below V_{eq} and maintaining the nominal altitude.

The values of airborne delay found in these simulations are high enough to suggest that this speed reduction technique might be useful in a real operational scenario, incurring less variation in the fuel consumed, if the controlled time of arrivals are met, as predicted in SESAR and NextGen, and the forecast has uncertainties. However, long cruise distances are needed in order to obtain high values of airborne delay, and most of the regulated areas in Europe, are located in central Europe leading to regulated sectors close to the airports of origin. Therefore, in a European context, the amount of airborne delay achieved by reducing the cruise speed without incurring extra fuel consumption is too small to be operational. On the other hand, in the United States, the regulation of traffic due to ATFM initiatives is mainly due to low capacity at the destination airports and the consequently definition of GDPs. These circumstances maximise the available distance in which to realise the delay. Therefore, this strategy seems more suitable for the current operational scenario in the United States. In the next chapter, this airborne delay strategy is simulated in realistic GDP scenarios in the United States of America.



Application of Cruise Speed Reduction to ATFM initiatives

The speed reduction technique proposed in this dissertation becomes interesting when applied to air traffic management initiatives. In this chapter the effect of this strategy applied to the North American GDPs is analysed. GDPs are candidates for this cruise speed reduction approach since the distance between the origin airport and the regulated area (the destination airport) is maximised, and therefore more delay can be absorbed in the air. For more details about GDPs the reader is referred to appendix A.

As has been presented in section I.3 and in figure I-3, the speed reduction technique (flying at V_{eq} during the cruise) allows the assigned ATFM delay to be divided between in ground and airborne delay. For a particular flight, if the GDP is not cancelled before the aircraft arrives at the destination airport the same amount of delay occurs in the baseline and in the speed reduction scenarios. Moreover, it does not have any effect on the fuel consumed (according to the V_{eq} definition). However, if the regulation is cancelled before planned, it is possible to recover part of the delay by speeding up to V_0 without incurring extra fuel costs over the initially planned flight, since flying at V_0 has the same fuel consumption per distance flown as flying at V_{eq} . Note that the fuel is maintained as initially planned, but not necessarily the total operating cost, as there are costs associated with the block time, such as maintenance and crew costs. These extra costs should be considered in a realistic implementation of the suggested technique.

In this chapter it is only the change of speed during the cruise that is considered, therefore, the flight levels are maintained as defined in the original optimal flight plan. On the other hand, the recovery of the delay is computed assuming that no extra fuel consumption is produced, thus, the speed is not increased over V_0 once the regulation is cancelled.

V.1 Speed reduction and ATFM initiatives

Two options are available to implement the speed reduction concept: a centralised system and a distributed one.

In a centralised approach, the network manager solves the ATFM problem and assigns delayed waypoint over-fly times to all the 4D trajectories affected by the regulation. An advantage of this solution is that the network manager has information about all the submitted flight plans and can prevent possible network effects derived from the delay allocation algorithms. It is therefore easier to find an acceptable solution for all the aircraft involved. However, this approach suffers from a major drawback: the network manager needs to know some sensitive data from the aircraft operators. In particular, fuel consumption models and the actual weight of the aircraft which, in general, is kept in strict confidence by the operators.

A distributed system would overcome these drawbacks and reduces the chances of collision. In this scenario, the network manager computes the ground delay for the affected aircraft, as is done in the current system. Then the different operators, who have all the sensitive data related to their flights, can do the necessary calculations to establish the best way to deal with the imposed delay: doing it completely on ground or defining the best speed profile to realise some airborne delay. A newly generated flight plan is then sent to the network manager for consideration. This flight plan includes the different times attached to the waypoints while fulfilling the total delay imposed. This process might require negotiation and the convergence of the iterations may become an issue.

The main idea of SESAR and NextGen is to involve the different stakeholders in the decision making process. Therefore, a distributed solution where the airspace user suggests the best speed profile, is more suitable recalling figure II-5.

In the future it may also be possible for airspace users to negotiate amongst themselves in order to solve the capacity-demand imbalance problems, with their SBTs, as proposed in (Ranieri & Castelli, 2009; Castelli *et al.*, 2011). In that case, the speed reduction technique is useful during this negotiation phase, adding a new way for airspace users to develop their trajectories in order to obtain the RBT.

Finally, it should be mentioned that, in both options, the strategy suggested in this thesis is only valid if there is a compliance of the trajectories and the CTAs. Thus, the fulfilment of the controlled time of arrival and the minimisation of collusion should be considered in a possible implementation of the system.

V.2 Study and clustering of ground delay programs

During 2006, a total of 1,052 GDPs were implemented by 49 airports in the United States, according to the CDM archival database. Table V-1 presents the statistics of the airports with the most GDPs for that year. The five airports with the most GDPs represents more than 55% of all 2006 GDPs. Newark Liberty International was the airport where most GDPs were implemented, followed by San Francisco International and Chicago O'Hare International Airport. As the GDPs of these three airports represent more than 37% of all the GDPs defined in 2006, they are analysed in more detail in this thesis. Note that the three airports are also interesting as they present different traffic patterns, as presented in section IV.1.2.3.

In table V-1, it is observed that when a GDP is implemented and the nominal capacity of the airport is already small compared to the nominal demand, as is the case in EWR, the average delay assigned per aircraft is high. Other airports, such as Hartsfield-Jackson Atlanta International Airport or Chicago O'Hare are big hubs of Delta and United Airlines respectively, and, therefore,

Table V-1: Statistics of the 10 airports with the most GDPs in 2006. Source: (Melgosa, 2012)

Airport	Number of GDPs implemented	% GDPs over total	Total delay assigned (min)	Average number of aircraft per GDP	Average delay per aircraft (min)
EWR	148	14.07	2,591,987	354	49
SFO	131	12.45	855,438	190	34
ORD	120	11.41	4,533,341	773	49
LGA	107	10.17	2,286,558	379	56
PHL	98	9.32	1,823,049	359	52
BOS	76	7.22	1,077,669	279	51
ATL	64	6.08	1,969,485	804	38
CYYZ	45	4.28	185,519	220	19
JFK	40	3.80	590,186	282	52
CYYC	29	2.76	89,875	138	22

when a GDP is applied in those airports, a high number of aircraft are affected, leading to high quantities of accrued assigned delay.

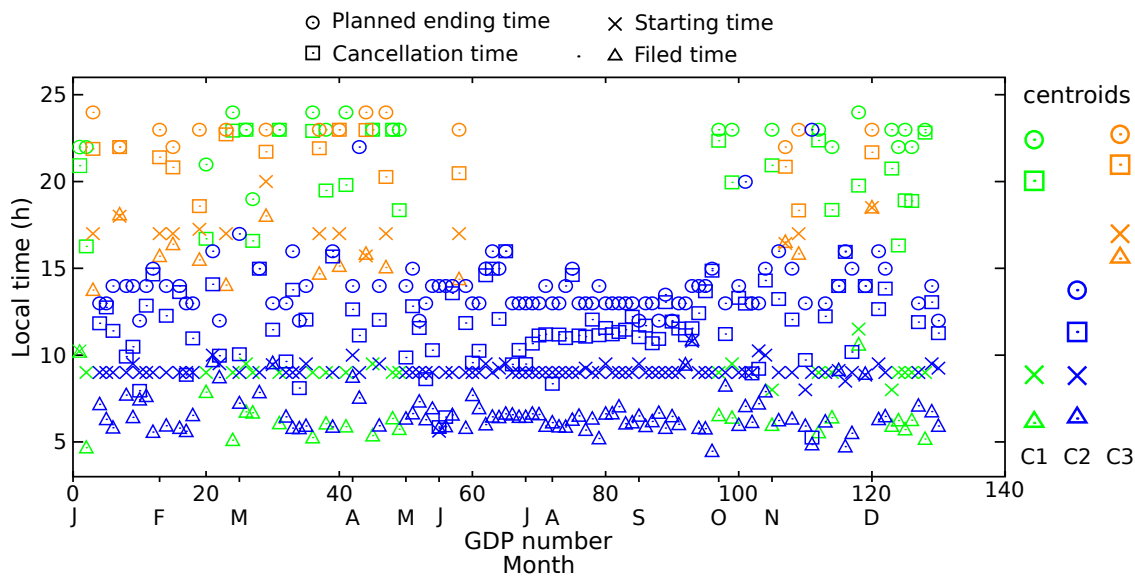
Approximately 75% of all the GDPs are applied due to weather related issues, as can be identified from the analysis of GDPs in 2006. Different scenarios of airport arrival acceptance rates reflect, in most cases, well-identified weather patterns in the regions where the airports are located (Liu *et al.*, 2008). For example, in the case of SFO, it is common to have marine stratus which usually burn off around the middle of the day. There are days, however, when the capacity remains at reduced values throughout the day. In addition, in SFO, some reductions in the airport arrival acceptance rate are produced due to the rainy periods in the winter season. These well defined meteorological patterns lead to patterns in the airport capacity and, consequently, in the duration of the GDPs implemented. For these reasons, it is possible to analyse the GDPs in order to determine how the representative GDPs of a given airport are.

As a set of GDPs are most probably implemented for common reasons, it is expected that they will have similar characteristics. The *K*-means clustering algorithm (Macqueen, 1967) is used in this dissertation to group the GDPs of 2006 in different categories. In order to cluster the GDPs, they are characterised by their filed time, starting time, planned ending time and actual cancellation time and the Euclidean distance between these times is considered. The clustering is computed with an iterative process from two to eight clusters and the silhouette and the *pseudo-F*-statistic coefficient used to determine the best clustering (Calinski & Harabasz, 1974). Other techniques as the hierarchical clustering can also be used, but the analysis done ensures a good clustering (Murtagh, 1983; Day & Edelsbrunner, 1984; Jain, 2010). The centroids of each cluster are considered representative of their category.

The 131 GDPs that were issued in SFO during 2006, after being analysed, are clustered in three categories, as it is the number of clusters which maximises the silhouette coefficient. The centroids of the three clusters are shown in table V-2 and all the 2006 GDPs are shown with their cluster in figure V-1, where the definition, start, planned ending and cancellation times are depicted for each of the GDPs. The first cluster contains the majority of the year's GDPs (91) corresponding to *Morning* GDPs caused by low ceilings. These GDPs are typically declared early morning and cancelled when the fog burns off which, on average, is around 2h25 before initially planned. The second group are *All-day* GDPs that are also filed in the early morning, but expand during the whole day because the meteorological conditions do not improve, having a planned duration of 13h34 and being cancelled, on average, 2h24 ahead. Finally, the third category of GDPs, correspond to *Afternoon* GDPs with an average duration of 5h43 and cancelled around

Table V-2: Cluster centroids for the 2006 GDPs of SFO, EWR and ORD (hours in local time)

Airport	GDP group	Number of GDPs	Filed time	Starting time	Planned ending time	Cancellation time
SFO	Morning GDPs	91	6h31	8h59	13h55	11h30
	All-day GDPs	24	6h12	8h58	22h32	20h08
	Afternoon GDPs	15	15h42	17h08	22h51	21h06
EWR	All-day-night GDPs	68	10h20	12h36	00h18	22h58
	All-day-evening GDPs	64	11h59	13h30	21h49	19h59
	Afternoon GDPs	16	16h53	16h55	23h14	21h20
ORD	All-day GDPs	65	8h28	9h52	22h19	20h13
	Afternoon GDPs	43	14h58	15h26	22h15	19h58
	Early cancel GDPs	12	7h49	9h02	18h33	9h53

**Figure V-1:** Clustering of GDPs implemented in San Francisco International Airport during 2006

1h45 before planned.

As can be observed in figure V-1, GDPs in the first category are found during the whole year, whilst the GDPs of the second and third category are mainly declared only during the winter season. The duration and cancellation times that are obtained for the centroids of the clusters of the GDPs are consistent with the values from table I-1 (Cook & Wood, 2010). Moreover, this clustering is in line with the results presented in (Liu *et al.*, 2008), where airports were characterised by their AAR during the day. It should be noted, however, that in the clustering realised in this thesis, the AAR are not used, and only times related to the GDP definition and cancellation are considered.

The same cluster principle is applied in (Melgosa, 2012) for all the GDPs implemented in all the airports during 2006. The results for EWR and ORD are presented in table V-2. In this work, the silhouette coefficient is computed in order to determine the quality of the clustering, the results are 0.70 for SFO, 0.35 for EWR and 0.46 for ORD. The silhouette coefficient ranges from -1 to 1 which represents the best clustering possible. Therefore, the results show that in SFO the three categories are clearly identified, while in the other two airports the clusters are less compact and, even if the centroids are representative of the population, there is more interrelation between

the groups. This means that the causes of the implementation of the GDPs probably do not form such well defined patterns as the fog in SFO.

In EWR, the three clusters correspond to *All-day-night* GDPs, GDPs that are declared in the morning and planned to last until midnight, *All-day-evening* GDPs, which are GDPs filed in the morning, as in the first category, but planned to end around ten in the evening, and finally *Afternoon* GDPs implemented in the afternoon. The layout of EWR airport means that the arrivals at runway 11 need ceilings of 2,500 feet at least and visibility of 5 miles or more, if this is not possible, the capacity is reduced to 29 aircraft per hour in low IFR conditions. Runway 11 is usually needed in the afternoon as the traffic is higher (Snell & Tamburro, 2011), thus, the three GDPs are extended during the afternoon. It is worth noting that on average, for the three cluster categories, the GDPs are cancelled between 1h20 and 1h50 before planned.

The ground delay programs implemented in Chicago O'Hare during 2006 are also clustered in three categories. The first cluster includes the GDPs planned to last during the whole day. The second group is formed of the GDPs implemented in the afternoon. These two categories are, on average, cancelled around 2h00 ahead of plan. Finally, the third category clusters ground delay programs which are declared but probably were not needed, and are, in some cases, even cancelled before their start time, their average cancellation time is 7h40 minutes before planned, only 3h14 after being filled and 1h51 after their start.

V.3 Assumptions for the study and simulation set up

As done previously in this thesis, simulations are performed using the Future Air Traffic Management Concepts Evaluation Tool, along with performance data from the Airbus Performance Engineer's Programs suite which allows accurate data of specific range and fuel consumption to be obtained.

For these simulations, the same assumptions defined in IV.1.2.1 and used in section IV.1.2, are considered. Enhanced Traffic Management System data from the 24th and 25th of August 2005 is used to generate traffic information required to perform the simulations. In this case, when aircraft are already flying at the beginning of the simulations or their performances are notably different from any of the Airbus models available (i.e. small business jets, turboprops and propeller driven aircraft), they are not considered for the speed reduction strategy, and therefore they are not categorised with Airbus models as presented in table IV-2. All these aircraft, however, are simulated to correctly represent the demand at the airport, but are excluded from the speed reduction strategy. If any of those flights has some assigned GDP delay, it is realised completely on ground, as in the current concept of operations. The aircraft that are already flying when the simulation starts are kept in their original aircraft type, even if they have an Airbus equivalent, when simulated with FACET, as it is not necessary to know their accurate cruise performance, since they are exempt from the GDP.

In order to simulate the GDPs, it is considered that the centroids of each cluster are representative of their category and therefore are used for the simulations. Only two airport acceptance rates are defined for each airport, a reduced one, which is considered while the capacity is limited, and a nominal airport acceptance rate used otherwise. It is worth noting, however, that there are more possibilities for AARs during GDPs as each of them has a wide variety of runway configurations. For San Francisco International Airport, the reduced capacity is considered to be 30 aircraft per hour and the nominal airport acceptance rate is fixed to 60 aircraft per hour; as the two parallel arrival runways of SFO cannot be independently operated when the visibility is reduced (Janić, 2008; Federal Aviation Administration, 2012g). For Newark Liberty International Airport, the AAR is considered to be 46 aircraft per hour and the PAAR 29 aircraft per hour (Fed-

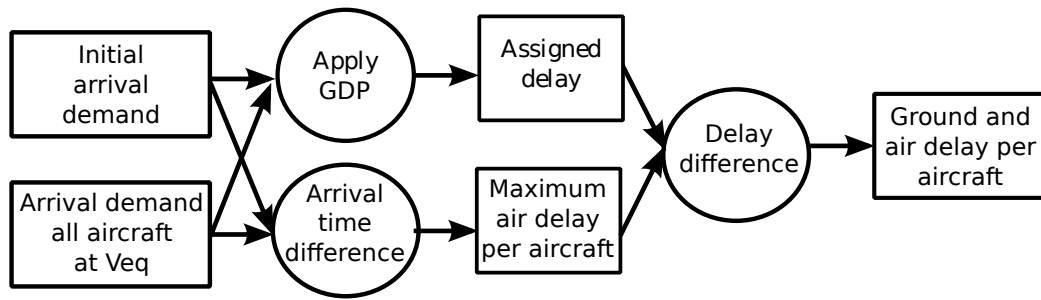


Figure V-2: Diagram of the computation of the ground and airborne delay

eral Aviation Administration, 2012e), and for Chicago O’Hare International Airport, a nominal total of 112 aircraft per hour and 84 aircraft per hour in reduced capacity are assumed (Federal Aviation Administration, 2012d). These values are in accordance with the runway capacities and operations defined by the FAA. The time in the simulation when it is considered that the capacity changes from the PAAR to the AAR is computed in order to end the GDP (the controlled traffic demand is equivalent to the available capacity at the airport) at the time defined by the cluster as the GDP definition, start and end time are fixed by the clusters (see figure II-2). For more information about the application of the centroids of the GDPs to the traffic see appendix D.

Finally, it is assumed that once the GDP is cancelled, the capacity at the airport is unconstrained, see section I.5. This is not always true however since the GDP shifts the demand and, at the cancellation time, the forecast arrival demand at the airport might occasionally exceed the airport new arrival capacity. Finally, the maximum delay that can be recovered is computed assuming that the aircraft that are delayed on ground, at the cancellation time, can immediately take off and that the airborne aircraft, which are flying at V_{eq} , can speed up immediately to V_0 .

The amount of delay assigned to each aircraft is computed by applying the GDP to the initial arrival demand. Having previously computed the maximum airborne delay that each flight can perform by flying at V_{eq} , the assigned delay is divided into ground and airborne delay as depicted in figure V-2. In the case that a particular flight has been assigned a delay smaller than the maximum airborne delay realisable by flying at V_{eq} , a new speed (between V_{eq} and V_0) is selected. This new speed is adequately chosen in order to fulfil the CTA, and consequently, for those flights, all the assigned delay is done in the air while saving some fuel with respect to the nominal situation.

The ground delay programs with the speed reduction technique has been applied to the three airports without considering the wind, in order to reduce the uncertainty associated with this meteorological parameter.

V.4 Assessment without radius of exemption

Firstly, the GDPs are applied over the three airports without considering a radius of exemption. Therefore, for these simulations all the flights taking off from North America or Canada are potentially controlled. These simulations present a limit of the maximum effect of the airborne delay technique realised by reducing the cruise speed without incurring extra fuel consumption. However, as the use of a radius of exemptions has advantages and is always employed, the effect of the radius is presented and discussed in section V.5. For each airport the following is analysed:

- The inbound traffic of 24th-25th August 2005, to the airport: the type and amount of traffic.
- The application of the GDP over the demand: Each of the centroids of the GDP’s cluster is applied to the demand at the airport. After this process, the amount of delay assigned to

Table V-3: Number of aircraft inbound to SFO, EWR and ORD on the August 24th-25th 2005 and their grouping according to equivalent Airbus types (in brackets number of aircraft which take off during the simulation)

Aircraft Family	Aircraft Types	SFO		EWR		ORD	
		Absolute number	Relative number	Absolute number	Relative number	Absolute number	Relative number
A300	A300, A310	2 (2)	0.2 %	24 (21)	1.7 %	11 (11)	0.4 %
	A319, B727, B737-200 B737-300, B737-500						
A319	DC-9, MD-90, E-145 CRJ-200, CRJ-700 CRJ-900	284 (280)	28.1 %	594 (584)	43.0 %	1,397 (1,391)	49.1 %
A320	A320, B737-400, B737-800, B737-900 MD-80	191 (178)	18.9 %	190 (185)	13.7 %	638 (626)	22.4 %
A321	A321, B757	147 (144)	14.5 %	86 (84)	6.2 %	161 (161)	5.7 %
A330	A330, B767, B777 DC-10	81 (77)	8.0 %	71 (63)	5.1 %	119 (107)	4.2 %
A340	A340, B747	18 (15)	1.7 %	10 (6)	0.7 %	44 (32)	1.5 %
	Total Airbus-like aircraft simulated	723 (696)	71.4 %	975 (943)	70.5 %	2,370 (2,328)	83.3 %
	Aircraft without equivalence	289	28.6 %	407	29.5 %	476	16.7 %
	Total of simulated aircraft	1,012	100 %	1,382	100 %	2,846	100 %

the aircraft due to the GDP, and the potential division of the delay between ground and air delay that can be realised, is computed.

- The results obtained as a function of the cancellation time, in terms of extra delay that can be recovered with the speed reduction technique, over the delay that is saved if all the delay is realised on ground.
- The results obtained if the GDPs are cancelled according to the centroid value.

V.4.1 Traffic

A total of 1,012 flights inbound to SFO are simulated to generate the airport's demand. Table V-3 shows the grouping of the flight into Airbus families: 723 flights are simulated with Airbus performance, representing 71.4% of the total traffic. From those, 696 aircraft take off during the simulation and therefore can potentially have delay assigned and realise part of it airborne. The 28.6% of remaining aircraft are not considered for the speed reduction strategy either because they are already flying when the simulation starts, or because they are notably different from any of the Airbus models available

In the same table, it is presented that in August 24th and 25th 2005, a total of 1,382 flights arrived at EWR. From this simulated traffic, 70.5% can be considered as an Airbus aircraft type and 96.7% of that traffic (943 flights) takes off during the simulation. Finally, table V-3 incorporates the information about inbound traffic to Chicago O'Hare International, 2,846 flights for those

Table V-4: Results of the delay assigned for the simulated GDPs

Airport	GDP group	Number of affected aircraft †	Total assigned delay (min)	Maximum delay assigned (min)	Average delay assigned per aircraft affected (min)
SFO	<i>Morning</i> GDPs	117 (115)	4,798	60	41.0
	<i>All-day</i> GDPs	347 (336)	9,363	65	27.0
	<i>Afternoon</i> GDPs	116 (111)	1,615	29	13.9
EWR	<i>All-day-night</i> GDPs	385 (381)	30,505	129	79.2
	<i>All-day-evening</i> GDPs	288 (288)	8,211	61	28.5
	<i>Afternoon</i> GDPs	147 (147)	9,188	117	62.5
ORD	<i>All-day</i> GDPs	933 (922)	25,716	63	27.6
	<i>Afternoon</i> GDPs	406 (400)	15,691	52	38.6
	<i>Early cancel</i> GDPs	769 (754)	8,070	26	10.5

† Between brackets number of aircraft with delay assigned

days. 2,370 of those are similar to Airbus aircraft (83,3%). Therefore, ORD is the airport with the highest demand from the three scenarios analysed, and also with the highest number of Airbus and Airbus-like aircraft in absolute and relative value.

V.4.2 GDP application

Table V-4 presents the results of the application of the different clusters of the GDPs defined at each of the airports to their inbound traffic. The table shows the total, the maximum and the average delay assigned. This delay is divided between airborne and ground delay as a function of the maximum airborne delay each flight can realise. The results of this division are presented, in absolute and relative value, in table V-5.

For San Francisco International GDPs, the amount of delay that can be done airborne varies between 15.7% (*Morning* GDP) and 47.9% (*Afternoon* GDP) with respect to the whole assigned delay. In the *Afternoon* GDP the average assigned delay is usually smaller than in the other GDPs, and since the amount of airborne delay that an aircraft can realise is usually small, the percentage of air delay assigned in the *Afternoon* GDP is larger than in the other scenarios. In the three clusters, more than 71% of all the aircraft with assigned delay can realise part of it airborne. However, only 9.8% of the total traffic in the *Morning* GDP doing airborne delay can realise all of its assigned delay in the air (i.e no ground delay is needed), while in the *Afternoon* GDP, 38.5% of the traffic which does airborne delay is in that situation. The main reason for this difference, is that *Afternoon* GDPs have smaller average delays for each flight (as seen in table V-4) and maximum airborne delays can reach up to 20 minutes in the best case as shown in chapter IV.

According to table V-2, the *Morning* GDPs and the *Afternoon* GDPs have a similar duration. As a consequence, the amount of airborne delay that can be realised is also similar (see table V-5). However, the total amount of delay is higher in the *Morning* GDP due to the fact that the arrival demand is greater. As the maximum airborne delay realisable is limited by the flight characteristics, if the average delay assigned is high, the percentage of airborne delay simulated with respect to the assigned delay is small. Therefore, in general, the smaller the total delay assigned in the GDP, the more important the effect of the speed reduction strategy. For this reason, in the *Afternoon* GDP almost half of the delay can be realised airborne.

Table V-5: Division between ground and airborne delay for the simulated GDPs

Airport	GDP group	Total ground delay (min)	Total airborne delay (min) †	Aircraft realising airborne delay ‡	Aircraft realising only airborne delay *
SFO	<i>Morning</i> GDPs	4,046	752 (15.7%)	71.3%	9.8%
	<i>All-day</i> GDPs	6,997	2,366 (25.3%)	76.8%	26.4%
	<i>Afternoon</i> GDPs	842	773 (47.9%)	82.0%	38.5%
EWR	<i>All-day-night</i> GDPs	27,766	2,739 (9.0%)	78.5%	5.0%
	<i>All-day-evening</i> GDPs	6,518	1,693 (20.6%)	79.2%	11.8%
	<i>Afternoon</i> GDPs	8,459	729 (7.9%)	75.5%	2.7%
ORD	<i>All-day</i> GDPs	20,250	5,466 (21.3%)	85.2%	14.5%
	<i>Afternoon</i> GDPs	13,374	2,317 (14.8%)	85.0%	1.8%
	<i>Early cancel</i> GDPs	4,389	3,681 (45.6%)	85.3%	31.7%

† Between brackets percentage of airborne delay over the total delay
‡ Percentage over the total number of aircraft serving ground delay
* Percentage over the total number of aircraft doing airborne delay

It is interesting to notice that in EWR the number of aircraft affected by the GDPs is higher than in SFO and that the average assigned delay is also higher for the three studied scenarios. This leads to the conclusion that when the division of the delay is done between on ground and airborne delay, even if the number of aircraft realising airborne delay is similar (around 78%) and in absolute value the minutes of airborne delay realised are equivalent, only between 8% and 21% of the assigned delay can actually be realised in the air by flying at V_{eq} (see table V-5).

Finally, as Chicago O'Hare International Airport is the one with the most traffic, the absolute number of aircraft involved in the GDPs is higher than in the other two scenarios, as shown in table V-4. However, as the capacity of the airport is also higher, the delay assigned per aircraft is not as important as in the EWR case, and the maximum and average assigned delay is equivalent to the simulations of the SFO GDPs. As presented in the division between ground and air delay, the percentage of aircraft realising part of the delay in the air is very high (more than 85%). However, the number of aircraft that can do all their assigned delay in the air by flying at V_{eq} is lower than in the San Francisco International Airport case. Due to the location of Chicago O'Hare International Airport, in general, flights are shorter than in the San Francisco scenarios. For this reason, the amount of airborne delay realisable by aircraft is also smaller. This effect is studied in more detail in section V.5, where the definition of the radius of exemption in the GDPs is analysed.

The centroid of the third cluster of the ORD scenario, *Early cancel* GDPs, is planned to end at 18h33. This means that the total assigned delay is lower than in the other two clusters as the late afternoon arrival demand is excluded from this GDP and the capacity increases to the nominal AAR before 18h33. However, the number of aircraft affected is approximately the same as in the first cluster (*All-day-evening*), as both GDPs start approximately at the same time and are extended during the whole day. Therefore, similar values of total airborne delay can be realised in both scenarios but, as less delay is assigned in percentage per aircraft in the third scenario, on average more delay can be completely absorbed in the air.

V.4.3 GDPs cancellation results

In this section, the scenario where airborne delay is realised is compared with the baseline scenario where all the delay is served on ground as is done nowadays. The delay that can be saved if the GDP is cancelled before initially planned is computed. The results for the SFO, EWR and ORD scenarios, are presented in figures V-3, V-4 and V-5 respectively. Notice the two different scales in the y-axis. As a function of the time, the accrued delay realised by all the aircraft is represented. The recovered delay achieved if the GDP is cancelled at each time is also presented for both scenarios. The extra delay recovered due to the speed reduction strategy is the difference between these recovered delays and is presented in the figures. If all the delay is realised on ground, the recovered delay can only be the delay that is not accrued yet. For a given flight, see figure I-3(a), the delay recovered will be all the initially assigned delay if the cancellation time is before the flight's ETD. It will be the difference between the cancellation time and the CTD if the GDP cancels between the ETD and the CTD. If the flight has already taken off, however, no delay is recovered for that flight since it is assumed that the flight cruises at V_0 . With the speed reduction strategy, the recovered delay is increased by the time that can be gained by speeding up to V_0 (i.e. not using extra fuel) for the aircraft that are already flying at V_{eq} when the GDP is cancelled.

At the beginning of the GDP, none of the delay is accrued and, therefore, if the GDP is cancelled all the assigned delay can be recovered. As time advances, more delay is already realised and therefore less delay can be saved if the GDP is cancelled. The benefit of the speed reduction strategy applied to the GDP programs depends on when the GDP is actually cancelled. If the GDP is not cancelled before initially planned, this strategy only implies a change in where all the assigned delay is realised. In addition, the graphs in figures V-3, V-4 and V-5 show the filed, start, ending and actual cancellation times of each GDP according to the centroids of table V-2.

The amount of extra delay that is recovered with respect to the case when all the delay is realised on ground depends on the number of aircraft that are at that time in the air realising airborne delay. Figure V-6 shows this dependency. There is a correlation between the number of aircraft in the air flying at V_{eq} and the extra savings of delay if the GDP is cancelled. The curve showing the number of aircraft is shifted to the right: when the aircraft are flying at V_{eq} , the later the GDP is cancelled the more delay is already realised and the smaller the distance available to recover delay is. For this reason, close to the GDPs ending time, there are aircraft in the air that are doing airborne delay but there is no extra delay recovered. The reason is that those aircraft are already on their descending phase and have already realised the whole assigned delay. Table V-6 shows the maximum number of aircraft that are at the same time in the air doing the speed reduction strategy and the maximum extra delay recovered with respect to the baseline scenario for the simulated GDPs.

In the SFO cases, even if the total airborne delay that can be done in the three GDPs is very different, the maximum extra delay recovered with the speed reduction strategy is very similar for the three cases, ranging between 379 and 437 minutes. These similarities are explained because the extra time that can be recovered depends on the number of aircraft that are flying at V_{eq} at the cancellation time, which it is very similar among the three GDPs. For the *Morning* and the *Afternoon* GDPs there is a maximum value of the extra delay that can be recovered (around 9h00 and 18h30 respectively) and then, a decrement until the end of the GDP. Conversely, for the *All-day* GDP, two peaks of extra delay recovered are observed: one in the morning and the other in the afternoon (see figures V-3 and V-6). These results show the dependency between the amount of extra delay that is recovered and the actual demand at the airport. The maximum extra delay recovered is achieved before the maximum demand is reached at the airport, which is around 10h00 in the morning and 21h00 in the afternoon.

For EWR airport, the minutes of extra delay recovered are different for the three clusters, being higher for the *All-day-night* and the *All-day-evening* GDPs. In those scenarios, the number of aircraft in the air realising airborne delay at the same time is higher and more constant than in

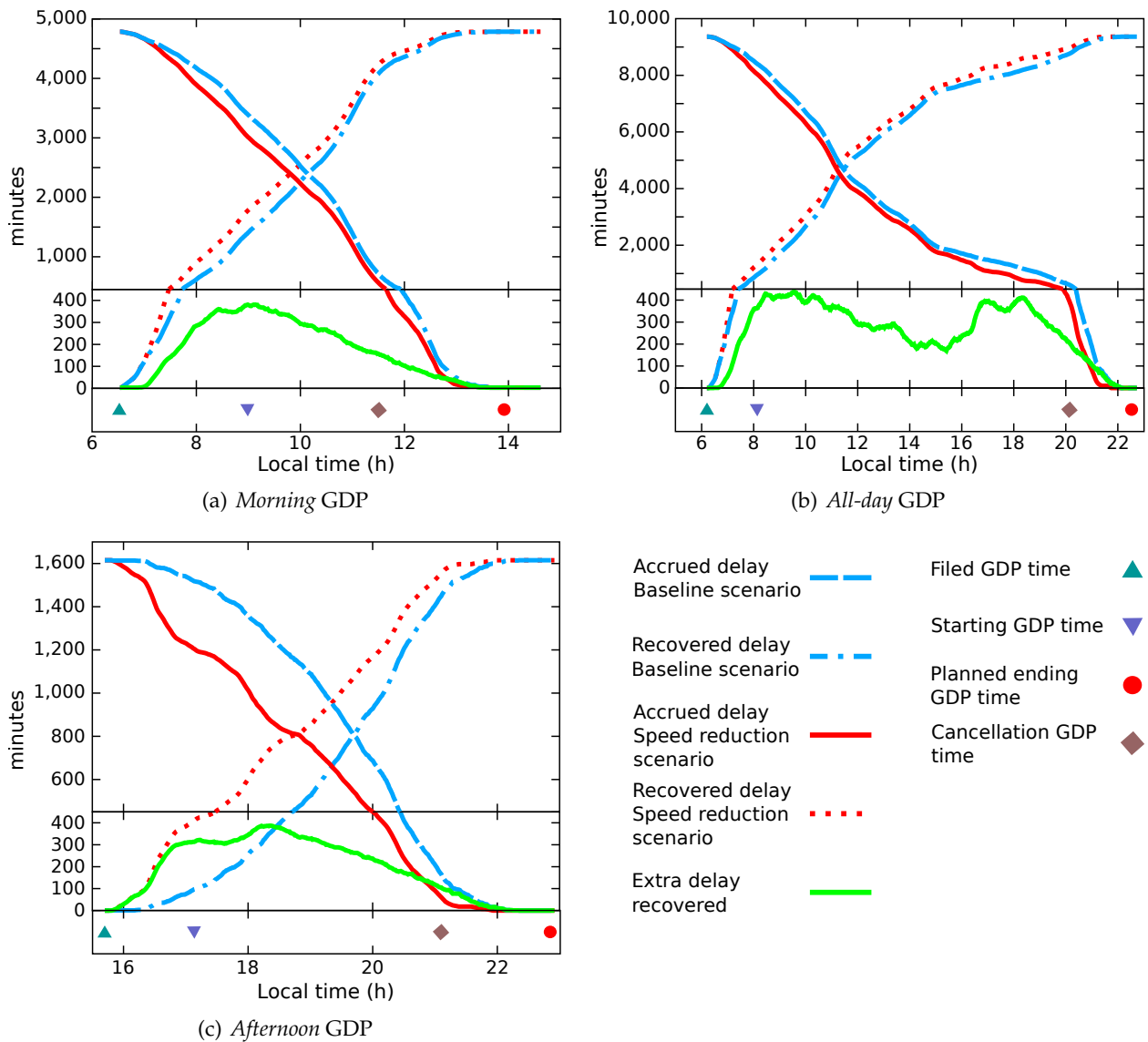


Figure V-3: Delay accrued and saved for the baseline and speed reduction scenarios for SFO airport

the third cluster, *Afternoon* GDPs. Once again, it can be observed that the maximum extra delay recovered is in concordance with the demand at the airport during the day.

Finally, the total number of aircraft affected in the ground delay programs applied to ORD is higher than in all the previous simulations, but due to the large capacity of the airport, the average delay per aircraft is relatively small, as presented in table V-4. This means that the amount of aircraft realising part of the assigned delay airborne is very high, and, therefore, if the regulation is cancelled before initially planned, there are a significant amount of aircraft in the air which can potentially increase their speed to their nominal one and recover part of the delay. Thus, as shown in figure V-5 and in figure V-6, the airborne delay recovered can be up to 717 minutes; and, as presented in table V-6, the maximum number of aircraft flying at the same time at a reduced speed is more than 119 aircraft for the three ground delay programs simulated.

The application of the speed reduction strategy implies that some aircraft are in the air, while otherwise they would be still grounded. The number of flight in this situation is small, as presented in table V-6. However, gate availability would be improved and ground congestion reduced at the departure airport, as those aircraft are in the air rather than waiting at their gates.

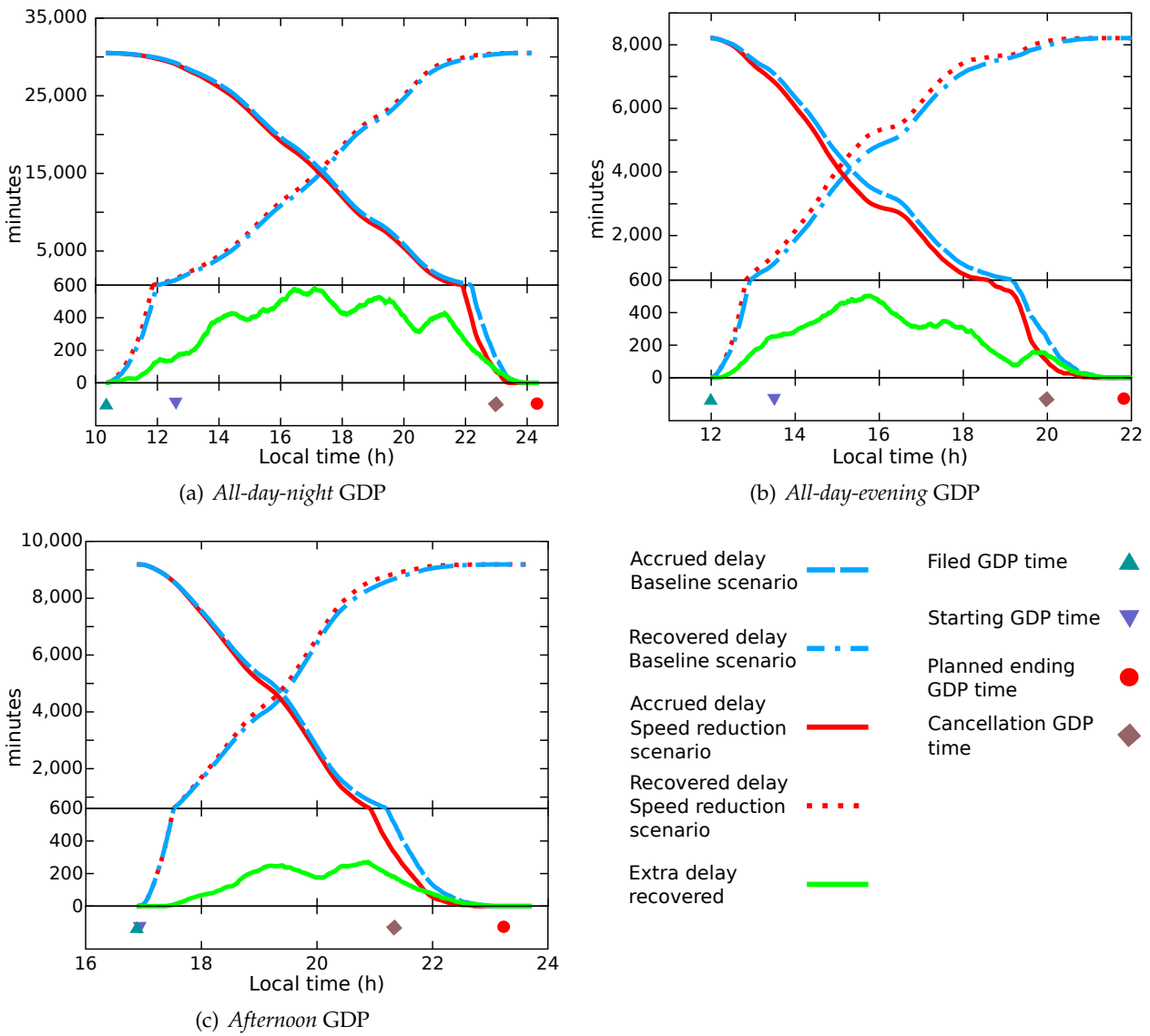


Figure V-4: Delay accrued and saved for the baseline and speed reduction scenarios for EWR airport

V.4.4 Results at the actual cancellation time according to the centroids

It is possible to use a probability distribution of the weather improvement, like the one presented in figure IV-22, to compute the benefit of the speed reduction strategy. However, not all the clusters simulated have the same cause, and in this thesis it has been considered that the centroids are representative of the GDPs in their clusters. For these reasons, the cancellation time, according to the centroids of table V-2, is considered for all the simulations as an average value for their cluster. Table V-7 shows the extra delay that is recovered with respect to the baseline scenario, where all the delay is realised on ground, at the actual cancellation time according to those centroids.

In SFO, in the *Morning* GDP, 155 minutes of extra delay are recovered, representing 27.6% of the total ground delay that can be saved in the baseline case. This percentage is increased for the GDPs that have a forecast duration of the whole day to 52.5% (208 minutes of extra delay recovered) and becomes very significant for the *Afternoon* GDP, with 172.1% of extra delay recovery (105 minutes).

In EWR, even if, for the two first clusters the maximum extra delay that can be recovered is very close (582 minutes in the first cluster and 503 minutes in the second), the fact that the

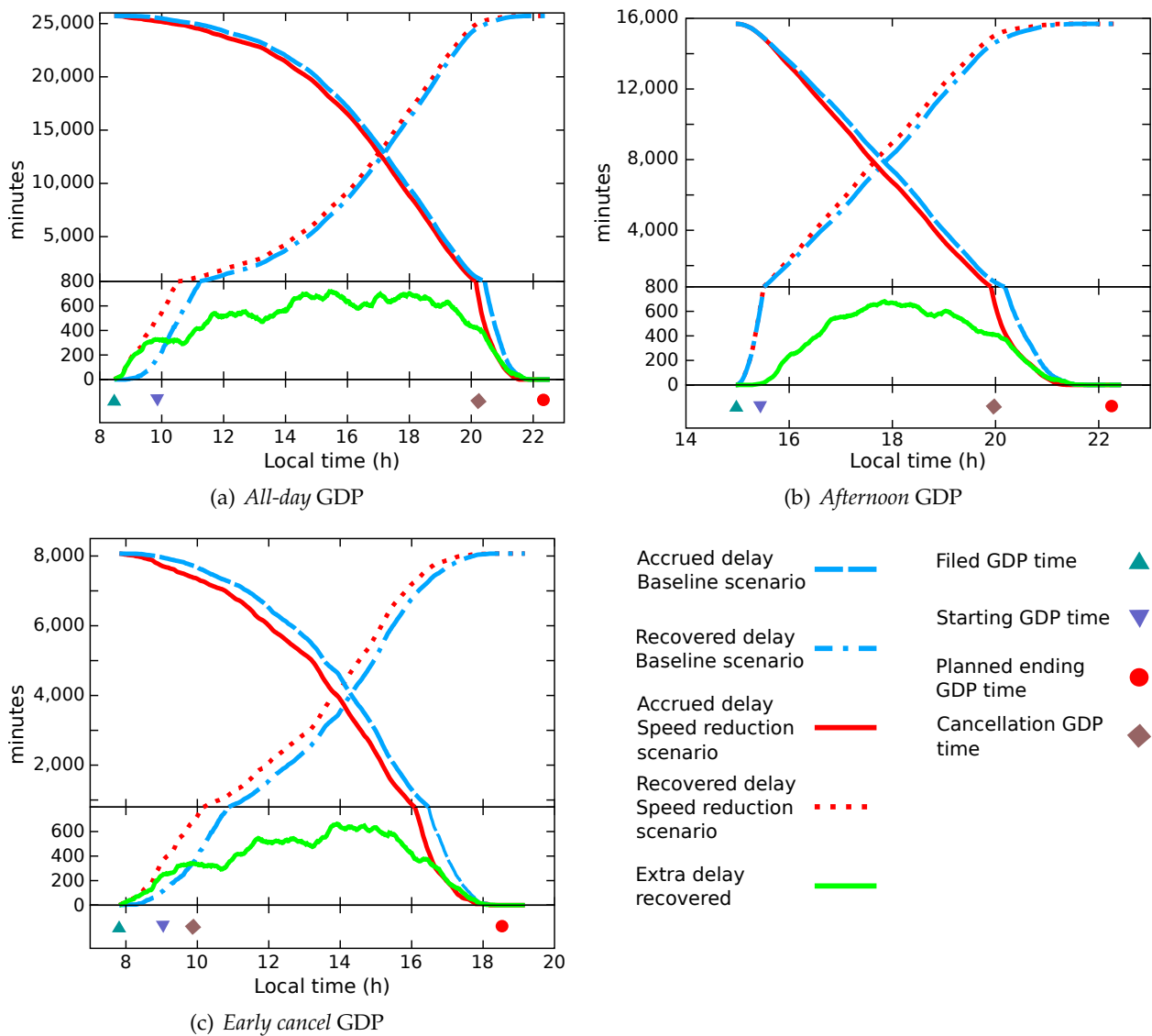


Figure V-5: Delay accrued and saved for the baseline and speed reduction scenarios for ORD airport

second cluster is cancelled earlier, when the airport is still experiencing a high demand, means that the benefit of the strategy is higher in minutes of extra delay recovered (141 minutes instead of 84 minutes). In these results it is clear that the time when the regulation is actually cancelled is of paramount importance in determining the benefits of the speed reduction strategy. Thus, the third cluster, which has a very bad performance with respect to the maximum airborne delay that can be recovered compared with the other two clusters (only 271 minutes instead of 582 minutes and 503 minutes for the first and second cluster respectively), has the maximum benefit at the cancellation time (180 minutes of extra recovery instead of 84 minutes and 141 minutes), and the highest average extra delay recovered by aircraft (3.5 minutes).

A similar pattern is found in ORD simulations, where the benefits of the speed reduction strategy are maximised, as it is the scenario with the highest number of aircraft realising airborne delay. In ORD, the *Early cancel* GDPs cluster, which is the one including the GDPs that are cancelled because they were probably not needed, or because the drop in capacity which generated them was solved very early¹, is not the cluster with the highest benefit of this speed

¹The GDPs in this cluster are on average cancelled only 1h51 minutes after the start time.

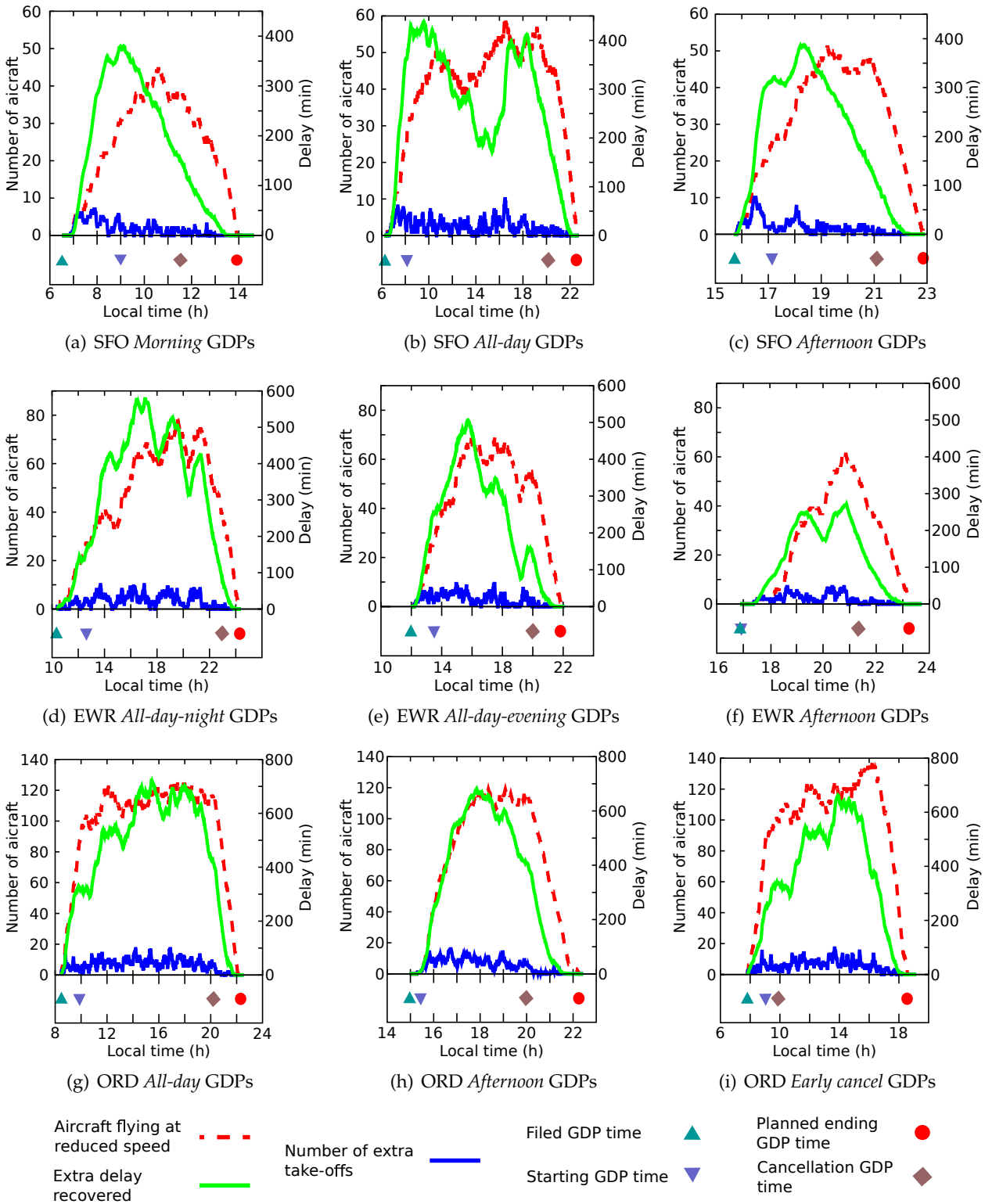


Figure V-6: Extra delay recovered, aircraft flying at V_{eq} and extra take-offs

reduction strategy. Even if the total delay recovered in that cluster is the highest of the three GDPs (7,721 minutes), as almost all the initially assigned delay is cancelled, the difference between realising airborne delay or doing it completely on the ground is relatively small in comparison with the other two clusters (340 minutes instead of more than 410 minutes). Thus, in order to maximise the benefits of the speed reduction strategy, the GDP needs to be cancelled earlier than initially

Table V-6: Maximum number of aircraft flying and doing airborne delay at the same time, number of extra take-offs and extra delay recovered

Airport	GDP group	Maximum number of aircraft realising airborne delay at same time	Maximum number of extra take offs	Maximum extra delay recovered † (min)
SFO	<i>Morning</i>	45	7	379
	<i>All-day</i>	60	10	437
	<i>Afternoon</i>	51	10	387
EWR	<i>All-day-night</i>	79	10	582
	<i>All-day-evening</i>	69	10	503
	<i>Afternoon</i>	61	7	271
ORD	<i>All-day</i>	125	17	717
	<i>Afternoon</i>	119	16	682
	<i>Early cancel</i>	138	18	662

† With respect the baseline scenario where no airborne delay is realised

Table V-7: Results of the simulated GDPs at the actual cancellation time

Airport	GDP group	Aircraft flying at V_{eq}	Delay saved in the baseline scenario (min)	Delay saved in the speed reduction scenario (min)	Extra delay recovered (min)	% Extra delay recovered †	Average extra delay recovered * (min)
SFO	<i>Morning</i>	37	562	717	155	27.6%	4.2
	<i>All-day</i>	45	396	604	208	52.5%	4.6
	<i>Afternoon</i>	42	61	166	105	172.1%	2.5
EWR	<i>All-day-night</i>	38	75	159	84	112.0%	2.2
	<i>All-day-evening</i>	52	104	245	141	135.6%	2.7
	<i>Afternoon</i>	51	331	511	180	54.4%	3.5
ORD	<i>All-day</i>	115	693	1,108	415	59.9%	3.6
	<i>Afternoon</i>	113	694	1,104	410	59.1%	3.6
	<i>Early cancel</i>	100	7,381	7,721	340	4.6%	3.4

† With respect the baseline scenario where no airborne delay is realised
* By aircraft recovering part of its delay by speeding up to V_0

planned, but it is even more important to consider the number of aircraft realising airborne delay at the cancellation time.

The extra delay recovered is achieved by the aircraft that are flying at V_{eq} at the cancellation time, therefore, by dividing the extra amount of delay saved by the number of aircraft that are

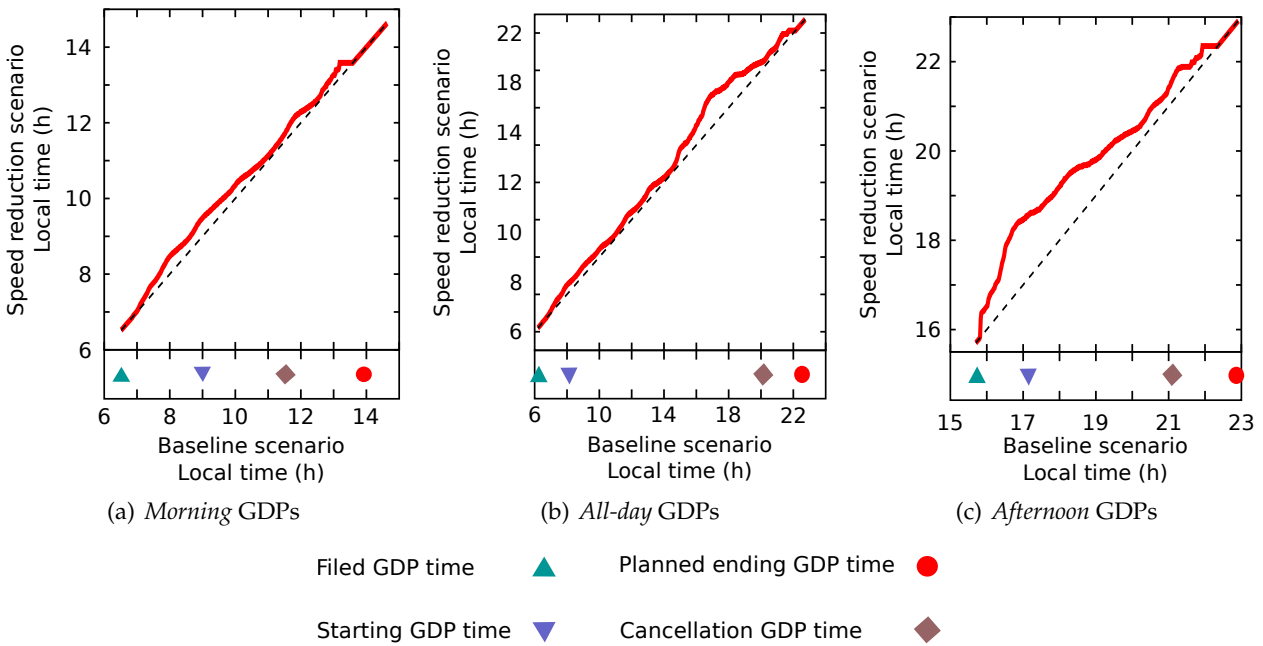


Figure V-7: Hour when delay accrued is the same in baseline and speed reduction scenarios for SFO airport

doing airborne delay at the cancellation time, an average recovered delay per aircraft recovering delay is computed. This metric allows to estimate the average recovered delay per aircraft is presented in table V-7. Results are similar for all the simulated scenarios. In SFO, in the *Morning* and *All-day* GDP, the average delay recovered per aircraft flying at the cancellation time at V_{eq} is around 4.5 minutes. Conversely, in the *Afternoon* GDP, this value is reduced to 2.5 minutes. In general, for EWR, the average recovery delay per aircraft is smaller than in the San Francisco and the Chicago O’Hare scenarios, this is because, due to the location of Newark Liberty, the inbound traffic usually comes from closer airports than in the other cases, and therefore, the maximum airborne delay is also smaller. This is especially the case for the *Afternoon* GDPs. For more details about the effect of the location of the airport on the airborne delay realised and recovered, see section V.5. Finally, note that in ORD the average recovered delay is similar between the three clusters and even if the amount of recovered delay is different the recovered airborne delay per aircraft recovering delay is around 3.6 minutes in all cases.

As seen in the previous results, with the speed reduction scenario, more delay than in the baseline scenario can be recovered. Therefore, in the speed reduction scenario, the same amount of delay recovery as in the baseline scenario by cancelling the GDP later can be obtained. Figure V-7 shows this difference for SFO simulations, which can reach values of up to two hours in the *Afternoon* case.

V.4.5 Discussion of the results

The amount of airborne delay that can be performed for an individual flight, using the suggested speed reduction strategy, is not very high, and therefore the potential delay recovered, if the ground delay program is cancelled ahead of plan, is relatively low. The average delay recovered by aircraft speeding up from V_{eq} to V_0 at the cancellation time, for the three airports, is only 3.5 minutes.

However, at an aggregate level, considering that all the GDPs in the cluster are similar to the centroid and, multiplying the extra delay recovered for each GDP centroid by the number

Table V-8: Amount of delay recovered at aggregate level by GDP cluster

Airport	GDP group	Aggregate delay recovered (min)
SFO	<i>Morning</i>	14,105
	<i>All-day</i>	4,992
	<i>Afternoon</i>	1,575
	Total:	20,672
EWR	<i>All-day-night</i>	5,712
	<i>All-day-evening</i>	9,024
	<i>Afternoon</i>	2,880
	Total:	5,712
ORD	<i>All-day</i>	26,975
	<i>Afternoon</i>	17,630
	<i>Early cancel</i>	4,080
	Total:	48,685

of GDPs present in each cluster, this strategy leads to a significant increase of the delay that is recovered if the GDPs are cancelled before planned, as is usually the case, without incurring extra fuel consumption. Table V-8 presents these aggregate results for each of the simulations, and for the three airports shows that the use of the speed reduction technique can lead up to almost 87,000 minutes of extra delay for the three airports considering 2006 GDPs: 20,672 minutes for SFO, 17,616 minutes for EWR and 48,685 minutes for ORD.

As has been presented, the distance between the flight and the destination airport, and the average delay assigned per aircraft is of paramount importance in order to determine the limitations and positive effects of the cruise speed reduction. All these parameters are affected by the radii of exemption defined for the GDPs, thus the effect of this radius is analysed in the next section V.5.

V.5 Assessment with radius of exemption

As presented in II.4.3, when a ground delay program is issued, typically an exemption radius is defined. In this section the effect of this radius on the GDPs applied to San Francisco, Newark Liberty and Chicago O'Hare is analysed. Notice that in the *ground holding problem* literature, when the term *airborne delay* is used, it is usually with reference to fuel consumption, undesired holdings and path stretching. However in this thesis the term *airborne delay* is used to define the delay that can be realised during the cruise by flying at the equivalent speed without incurring extra fuel consumption and the term *holding delay* is used to define the delay realised at the arrival at the airport due to lack of capacity.

V.5.1 Implication of applying a radius of exemption in GDPs

When a radius of exemption is issued in a GDP, all enclosed airports are included in the program, and, consequently, all the flights whose departure airport is within the circle and whose arrival

time is within the GDP time period, might be served ground delay. For the flights taking off outside that distance, a slot is reserved for them at the arrival airport but no delay needs to be served. Therefore, it is possible to define alternative programs by changing this radius. If the radius is small, then the majority of the aircraft are exempt from realising ground delay. Thus, if the AAR does not increase, holding delay must be realised. As the radius of exemption increases, the pool of flights that receive ground delay increases and, therefore, there is a decrease in the holding delay needed. Beyond a certain distance, the holding delay remains almost constant. A program distance shorter than the point where holding delay is minimised is not optimal since unnecessary and expensive holding delay could be transferred to safer and cheaper ground delay. As the radius of exemption is increased, the average and maximum delays are reduced, as the total amount of delay is divided between more participants, however, the unrecoverable and the unnecessary delay tends to increase.

The unrecoverable delay is the part of the delay that will be incurred even if the program is cancelled and the unnecessary delay is the delay that is realised when it was not needed because the regulation is cancelled before planned (Ball & Lulli, 2004). If the delay is divided between aircraft originating from airports further away, at a given time, more delay has already been accrued, as the delay needs to be realised a long time before the arrival slot time. Therefore, in this case, less delay can be recovered if the ground delay is cancelled. Thus, there is a trade off between the holding delay needed (high costs), the maximum and average delay assigned (fairness of the GDP) and the potentially recovered delay if the GDP is cancelled ahead of plan (maximising the benefit of uncertainty).

The application of an exemption radius has two major impacts on the use of the speed reduction strategy. Firstly, the average assigned delay is increased, as less slots are available for the aircraft performing the delay, and secondly, the flying distances available to realise airborne delay are consequently reduced. Thus, it is expected that the application of a radius of exemption has a negative influence of the maximum delay that can be realised airborne.

V.5.2 Assumptions for the radius of exemption study

As stated in (Ball & Lulli, 2004), for each GDP, there are an infinite number of distances that can be selected for the exemption radius. However, the finite set of airports to be included or excluded from the program naturally reduce these possibilities into a discrete set of options. And, there is no interest in considering an additional distance if it does not encompass a new set of airports. However, the information regarding the radii of exemption is not in the records of the GDPs used in this thesis. Thus, three different radii are considered in nautical miles from the analysed airports: 400 NM, 800 NM and 1,200 NM, as depicted in figure V-8. The distance of the flight plan is considered, to decide if an aircraft is affected by the radius of the ground delay program. These radii are selected to present a progressive increment in the distance, in order to analyse the effect of the length of the radius.

The same ground delay programs as defined in section V.2, with the same traffic as in section V.4.1 are used in these studies, along with the assumptions defined in section V.3.

V.5.3 Delay assignment and division for the GDPs with radius of exemption

Figure V-9 shows the division between holding delay, ground delay and airborne delay for each of the distances and each of the GDPs defined for the three airports under study. The percentage shows, for each GDP implementation, the relative value of the airborne delay with respect to the ground delay realised. It is worth noting that, as expected, the total amount of delay needed to accommodate the demand to the airport capacity is approximately constant, as was presented in figure II-2. With the increment of the radius, a transfer of where the delay is served is produced.

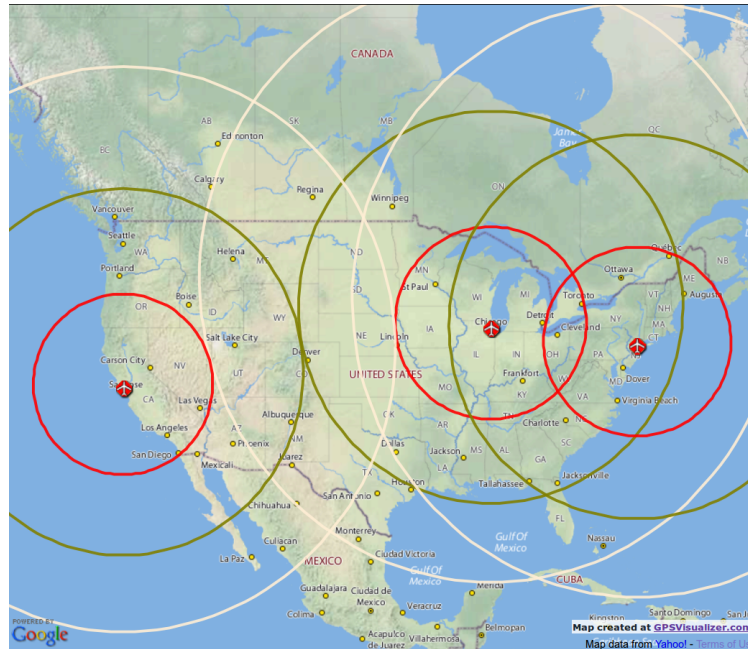


Figure V-8: Equidistant radius around SFO, EWR and ORD airports with 400 NM, 800 NM and 1,200 NM lengths

For San Francisco International, figure V-9(a) shows that a radius larger than 800 NM does not reduce any more the holding delay. For example, in the *Morning* GDP, the total holding delay decreases from 508 minutes for a 400 NM to 88 minutes for a 800 NM, decreasing to 75 minutes for a 1,200 NM and only reducing its value by 34 minutes, to 41 minutes of holding delay, if all the NAS is considered in the GDP. In ORD similar values of holding delay as in SFO are assigned as depicted in figure V-9(c) (178 minutes for the 800 NM exemption radius in the *All-day* cluster), however, even with the reduced 400 NM radius the holding delay is already small in comparison with the Newark Liberty and the San Francisco scenarios (182 minutes of holding delay in the *Afternoon* GDP for a 400 NM radius and 5 minutes for the 800 NM radius). Conversely, in EWR higher values of holding delay are generally found (see figure V-9(b)), for example, in the *Afternoon* GDPs cluster, with a radius of exemption of 800 NM, 735 minutes of holding delay are required to accommodate the demand to capacity.

The rest of the delay (ground and airborne delay) would be the amount of ground delay assigned if the speed reduction technique is not applied. However, if the cruising speed is adapted to V_{eq} , it is possible to realise part of that delay airborne without incurring fuel consumption. The increment of the radius leads to more aircraft in the pool of aircraft which can potentially have delay assigned and that can realise part of that delay airborne, as depicted in figure V-10. Those aircraft are the ones which can potentially recover part of their assigned delay without incurring extra fuel consumption by speeding up to their nominal speed once the ground delay program is cancelled. Moreover, flights coming from greater distances are able to realise more airborne delay.

As an example, in Chicago O'Hare airport for the *Afternoon* GDPs, the ground delay and the airborne delay assigned is 14,876 minutes and 408 minutes respectively for the 400 NM radius, 14,317 minutes and 1,326 minutes for the 800 NM, 13,946 minutes and 1,726 minutes for the 1,200 NM and 13,374 minutes and 2,317 minutes when no radius of exemption is defined. Another effect of the increment of the radius of exemption is that the maximum and the average delay is reduced as the total amount of delay is divided between more flights. As a consequence, the number of flights that can realise all their assigned delay airborne, i.e. flying at a speed between V_0 and V_{eq} and therefore saving fuel, increases. Figure V-10 shows these tendencies. Once again, there is a direct relationship between the type of traffic an airport generally has and the amount of aircraft

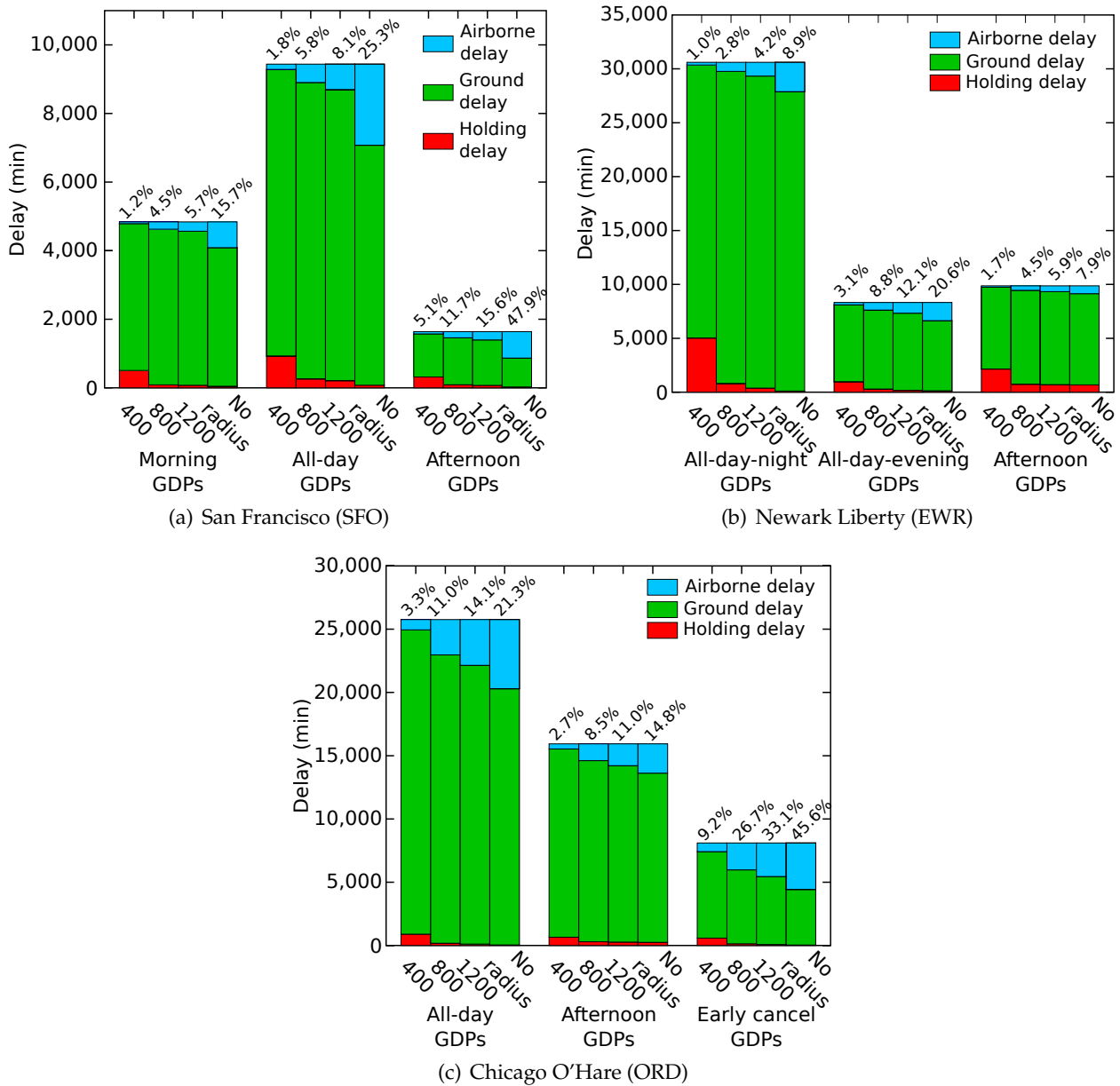


Figure V-9: Division between holding, ground and airborne delay. Percentage of airborne delay over the total assigned delay (ground and airborne)

which are able to realise all their assigned delay airborne.

The increment of the amount of airborne delay with the radius is a tendency but it is not proportionally related. In some airports, as in Chicago O'Hare, the division between ground and airborne delay increases gradually, while in others, as in San Francisco, there is a large increment when switching from 1,200 NM radius to no radius of exemption. The underlying reason is that, the increment of the radius is only of interest if the number of airports from where the flights originate also increases. Figure V-11 presents the assigned delay for four of the simulated ground delay programs, and the division between ground and airborne delay for all the affected aircraft as a function of their flight plan distance. For some airports, such as Chicago O'Hare, due to their location there is a progressive increment of airports as distance increases, see figure V-8. Thus, as depicted in figure V-11(a), the augmentation of the radius of the GDP implies a proportional inclusion of airports and aircraft which can potentially realise airborne delay.

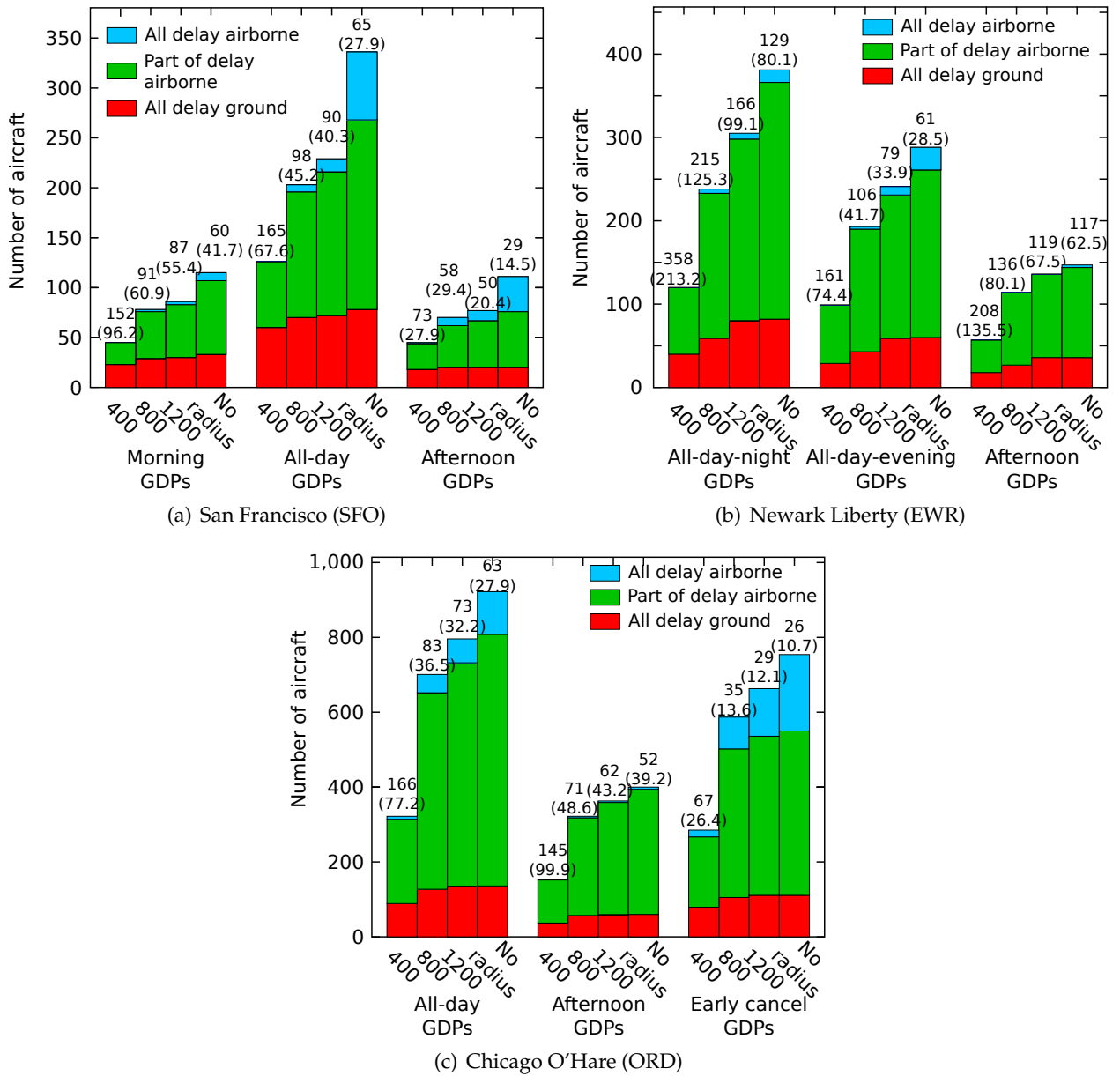


Figure V-10: Aircraft affected by GDP, maximum delay assigned in minutes and, between brackets, average delay per aircraft serving delay in minutes

However, for San Francisco International, as shown in figure V-11(b), there is a gap between 900 NM and 1,200 NM, and there is a significant amount of long haul flights coming from the east coast, Hawaii, and important hubs, such as Hartsfield-Jackson Atlanta International Airport, which are excluded in the 1,200 NM radius, see figure IV-6(a). For this reason, it is possible to observe a big difference in the amount of airborne delay realisable between having a 1,200 NM radius or not applying it (from 745 minutes to 2,366 minutes in the *All-day* cluster), as shown in figure V-9(a). Finally, the east coast airports, such as EWR, are in general also affected by the long haul flights as in San Francisco, but their effect is more limited as the demand on the east coast is composed by shorter flights. Thus, as depicted in figure V-11(c), with a majority of short and medium haul flights, the amount of airborne delay is relatively small, the effect of the long haul flights is clear in the *All-day-evening* GDPs (figure V-11(d)). These effects were expected from the analysis of traffic presented in section IV.1.2.3.

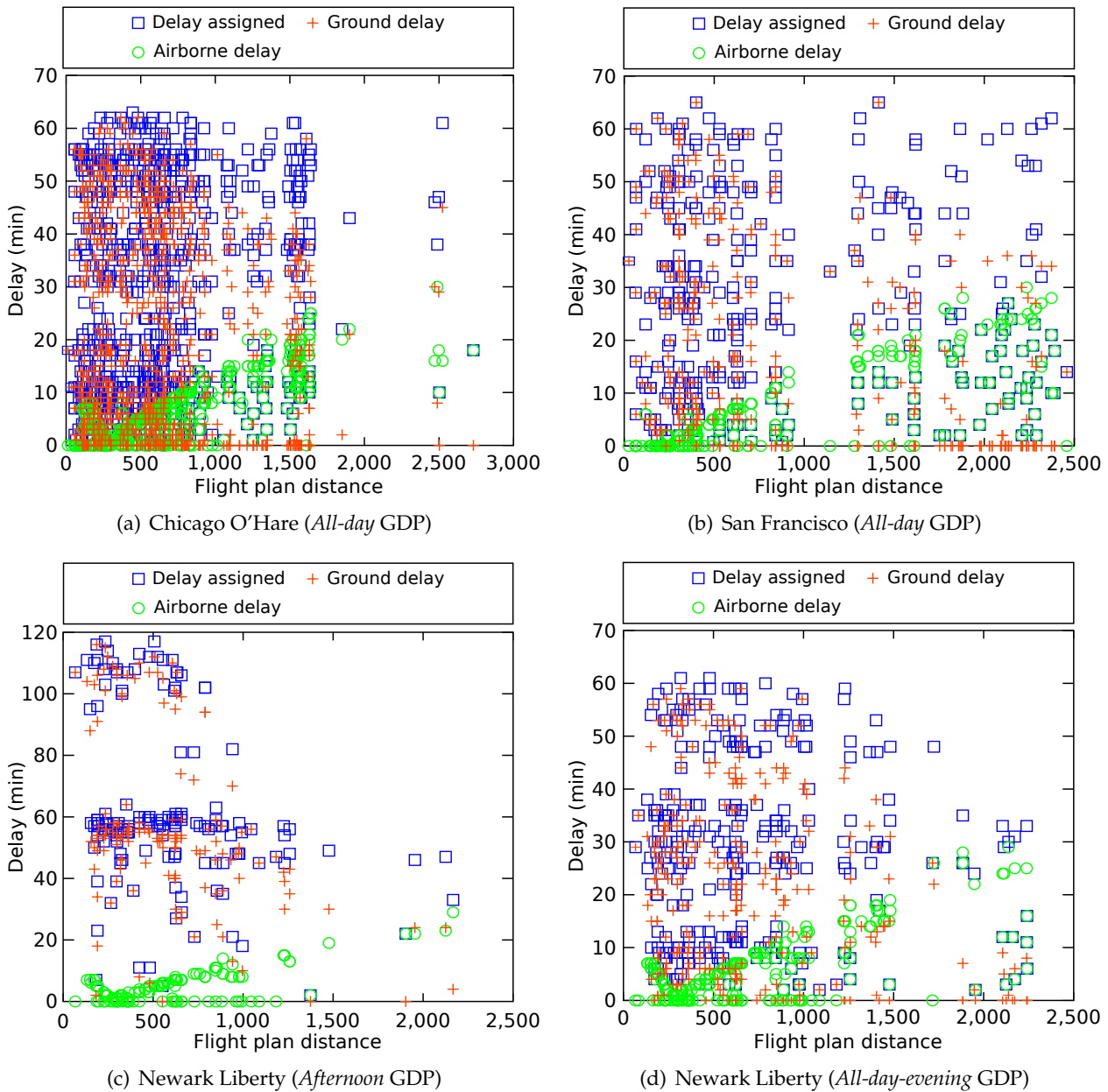


Figure V-11: Delay assigned, ground delay and airborne delay realised as a function of the flight plan distance

V.5.4 Delay saved if GDP is cancelled with radius of exemption

As done in section V.4, for each simulated GDP, the amount of delay that is recovered if the regulation is cancelled before planned is computed, and the aircraft flying at V_{eq} speed up to their nominal speed. Figure V-12 shows the results for the three airports and the four radii under study. In each plot it is indicated, at the cancellation time according to the GDP clusters from section V.2, the amount of extra delay that is recovered when compared to the case of no airborne delay being realised.

As expected, the longer the radius of exemption, the more airborne delay is absorbed and the more flights are in the air flying at V_{eq} when the ground delay program is cancelled. Therefore, the higher the extra delay recovered with respect to realising all the delay on ground. As shown in the previous section V.5.3, the increment of airborne delay as a function of the radius, depends on the traffic and location of the airport. Thus, for Chicago O'Hare the benefit of using the speed

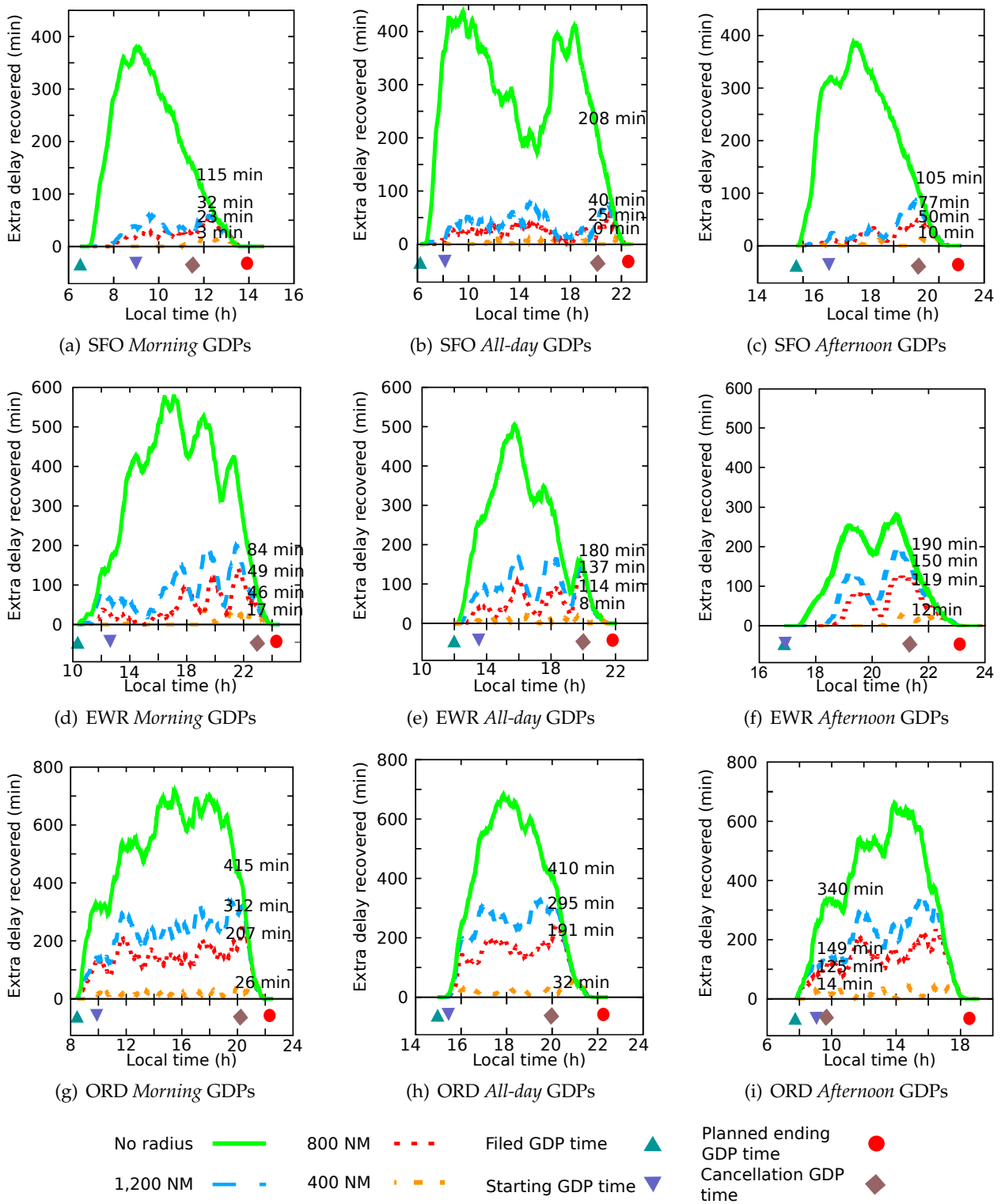


Figure V-12: Extra delay recovered as a function of cancellation time and radius of exemption

reduction strategy increases gradually with the radius of exemption, while for other airports, such as San Francisco, there is, in general, a gap of more than 200 minutes of extra delay recovered between using a 1,200 NM radius or the whole NAS. Finally for Newark, it is possible to see how the influence of having a radius is more or less important as a function of the time of day when the GDP is issued.

From these results, it could be concluded that the longer the distance of the radius, the higher the delay recovered. However, this is only the case if the extra benefit of using airborne delay with respect to a classical ground based GDP is considered. When deciding the optimal radius for a given ground delay program, the total delay saved when cancelled before planned should be considered (saved ground and holding delay that are not realised), as stated in (Ball & Lulli, 2004). Figure V-13, presents the total delay recovered if the ground delay programs are cancelled at their cancellation time according to their clustering. As depicted, the extra airborne delay recovered can represent up to more than 150% of the total ground delay recovered. As a direct implication of the use of an exemption radius, the greater the radius, the lower the holding delay, and, therefore, less holding delay is recovered if the GDP is cancelled ahead of plan. Similar behaviour is seen for the ground delay, as more ground delay is accrued with a longer exemption radius due to the longer flight distance the aircraft need to fly to attain their assigned slots. Thus, there is a trade off between the holding delay realised and the amount of delay that can be recovered at the cancellation time.

V.5.5 Discussion of the results

The use of a radius of exemption has implications on the ground delay programs and on the use of the speed reduction strategy. When defining a GDP with a radius of exemption, an air navigation service provider has to consider the associated trade offs. On one hand, it is better to define a small radius as the unrecoverable delay is minimised. Thus, if the regulation is cancelled before planned, more delay can be recovered. On the other hand, a large exception radius ensures a reduction of the maximum and the average assigned delay as the pool of affected aircraft is increased. This leads to a fairer and less costly² solution and the expensive and undesired holding delay is minimised, as more delay is served on ground. The speed reduction allows a higher radius of exemption to be used, minimising the negative impact on the total amount of delay recovered, in this way dividing the total delay fairly between more aircraft, reducing the maximum and average assigned delay per aircraft.

Considering the speed reduction strategy, the higher the radius the more distance is available for the aircraft to realise airborne delay and therefore more delay can be absorbed during the cruise phase without incurring extra fuel consumption. Moreover, more aircraft realising airborne delay implies that the number of flight which can potentially recover extra delay by speeding up during their cruise if the regulation is cancelled, is maximised. Finally, as higher radii imply lower average assigned delays, the number of aircraft that can realise all their assigned delay in the air, and by doing so, save some fuel with respect to their initially planned flight plan, is also maximised.

Finally, it is worth remembering that the effects of the use of a radius of exemption are airport and demand dependent. The location of Chicago O'Hare airport leads to a proportional increment of the airborne delay realised as a function of the radius, while in San Francisco International, there is a gap between distances, as the middle part of the United States does not accommodate any big airport with numerous flights to SFO.

The aggregate extra delay saved using the speed reduction strategy is computed for each airport and for all the GDPs and radius are presented in table V-9.

Even if the total benefit of using the speed reduction strategy once a radius of exemption is defined is relatively small, the use of this technique has an interesting benefit: the difference in recovered delay when the regulation is cancelled beforehand is reduced between two consecutive

²As stated in (Ball & Lulli, 2004): "the total ground delay and the total cost may not be related in a simple manner. As the delay assigned to a flight increases, it becomes more likely that passengers will miss connections, that crews will timeout, that the delayed availability of aircraft will cause delays on subsequent flights, etc. Thus, the cost to an airline of 20 flights, each incurring 15 minutes of delay, as a rule, is less than the cost of 5 flights each incurring 60 minutes of delay".

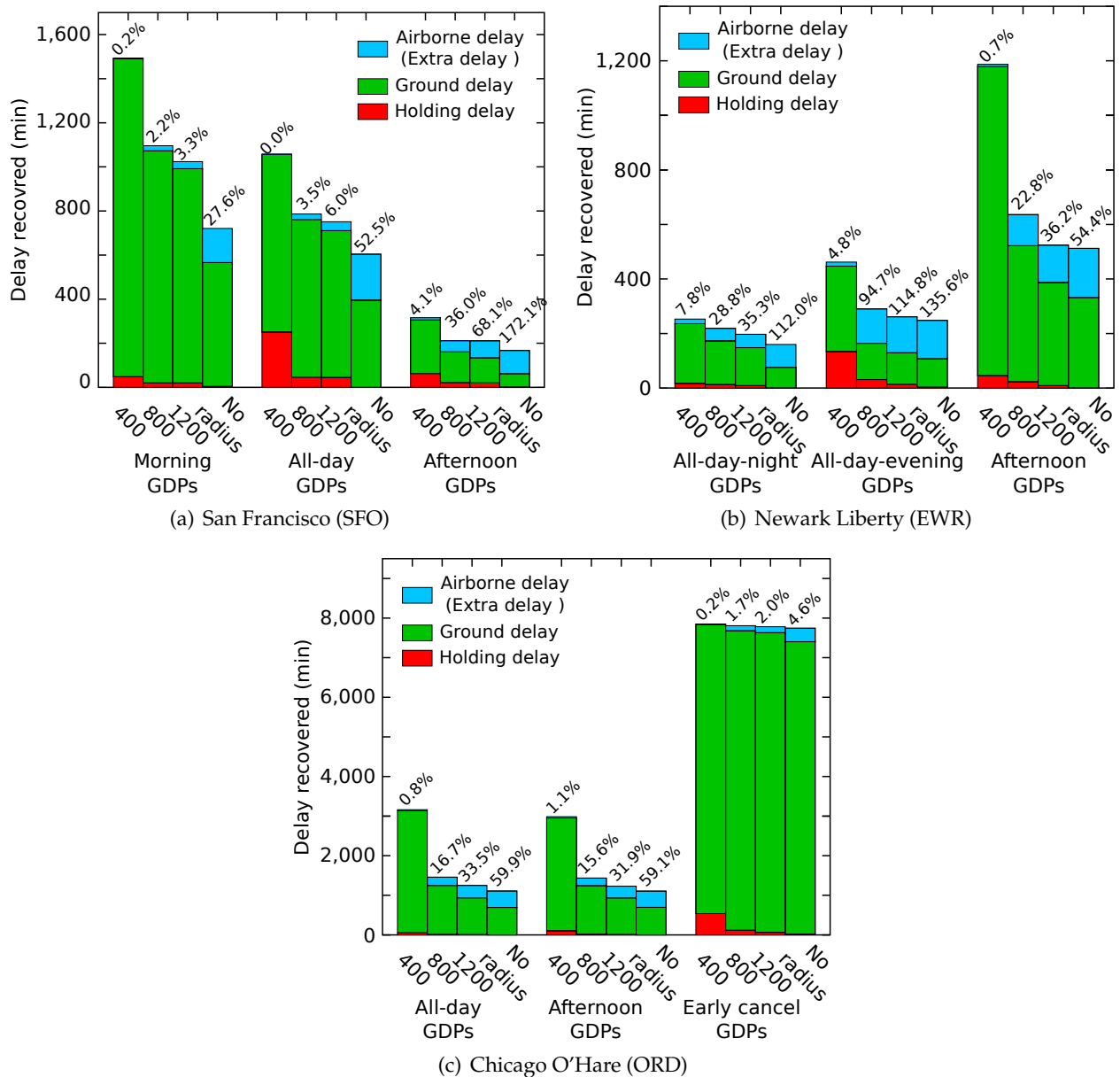


Figure V-13: Delay recovered at cancellation time with radius of exemption. Percentage of extra delay saved due to speed reduction with respect to the delay saved (holding and ground delay) with only ground delay

Table V-9: Aggregated extra delay saved for all GDPs during one year per airport and radius of exemption

Airport	400 NM radius (min)	800 NM radius (min)	1,200 NM radius (min)	No radius (min)
San Francisco International	423	3,443	5,027	20,672
Chicago O'Hare International	3,246	23,168	34,753	48,685
Newark Liberty International	2,244	13,016	13,972	17,616

studied radii. For example, as depicted in figure V-13, in Newark Liberty airport, for the *All-day-night* GDPs, when the radius increases from 400 NM to 800 NM, if no speed reduction is realised,

there is a difference of 63 minutes of delay recovered. However, if the aircraft are doing part of their delay airborne, the total delay recovered if the GDP is cancelled and the radius is set to 400 NM is only 34 minutes higher than for the 800 NM radius. Moreover, having a 800 NM radius for that GDP and using speed reduction leads to only 17 minutes less delay recovered than doing the GDP with a 400 NM radius and realising all the assigned delay on ground.

If the 400 NM radius GDPs are dismissed due to their high holding delay, in general, realising a higher radius and airborne delay lead to the same amount, or even more, delay recovered than doing a smaller radius without speed reduction. As an example, in the *All-day* GDP cluster of Chicago O'Hare airport, only 2 minutes of extra delay is saved with an 800 NM radius and no speed reduction implemented with respect to a 1,200 NM exemption radius where the cruise speed reduction technique is realised (see figure V-13). In the *All-day* GDP cluster of ORD case, 172 minutes of extra delay are recovered if the whole NAS is used with the speed reduction technique with respect to the total delay recovered with a 1,200 NM radius and no speed reduction.

V.6 Ration policies for speed reduction in GDPs

Figure V-10 presented the aircraft affected by the simulated GDPs as a function of the GDP cluster and the radius of exemption used. As can be observed, there are a number of aircraft which can realise all their assigned delay airborne. In those flights the assigned delay is lower than the maximum airborne delay realisable by flying at V_{eq} during the cruise. The difference between the maximum airborne delay realisable and the assigned delay for those flights can be considered as potential airborne delay which is unused. Figure V-14 shows, for the previous simulations, the airborne delay realised and the amount of potential delay that could have been done in the air but was not assigned.

Firstly, it is worth noting that the amount of airborne delay that can be potentially done and is not assigned is relatively small for all the radii of exemption except when the whole NAS is selected. For example, in the *All-day* GDPs of San Francisco International airport when no radius is selected the potential airborne delay unused is 27.1% of the airborne delay which is actually flown. However, if a 1,200 NM radius of exemption is used, the percentage decreases to 8.9%. Secondly, this extra airborne delay which is not realised is airport and flight characteristics dependent. Thus, by its location, it is higher in the SFO cases when no radius of exemption is used, or in ORD, but it is quite marginal for the EWR scenarios.

In order to maximise the benefits of the speed reduction strategy, in term of potentially recovered delay, different ration policies rather than ration-by-schedule are analysed, aiming at maximising the airborne delay used.

V.6.1 Ration-by-schedule, ration-by-inverse-distance and ration-by-distance policies

It is interesting to use a ration policy which prioritises flights with short flight distances (or flight times), as they are the ones which can realise less airborne delay, see section IV.1.3. This policy is a ration-by-inverse-distance (RBiD). However, in order to assess the benefits of different ration policies, it is considered necessary to compare the results of the ration-by-schedule and the ration-by-inverse-distance with the ration-by-distance policy suggested in (Ball *et al.*, 2010a), as it has been proven that in its *pure form* it minimises the total expected delay under early termination models. Thus, these three ration policies are simulated for the three airports, for each of the GDP clusters and for each of the radius of exemption under study.

In figure V-15 the histograms of the delay distribution for the three policies for Chicago

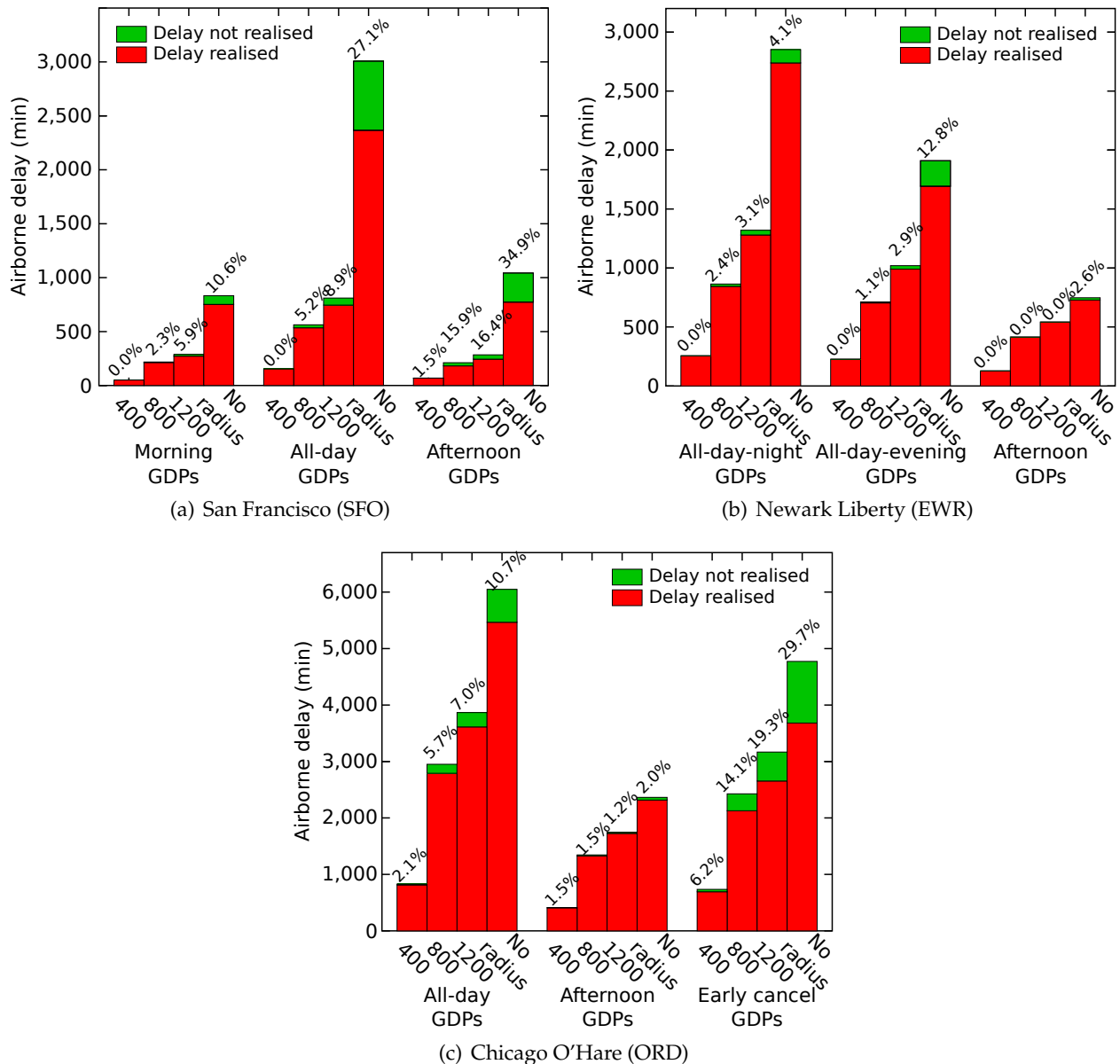


Figure V-14: Airborne delay realised and un-realised with RBS policy. The value is the percentage of airborne delay un-realised over airborne delay realised

O'Hare's *Afternoon* GDPs are presented for RBS, RBD and RBiD policies. The use of different ration policies does not modify the total delay assigned nor the average delay, as the number of aircraft affected and excluded by the ground delay program is the same. However, it changes the distribution of the delay.

In the RBS case a total of six controlled aircraft have a delay of zero minutes assigned to them, meaning that the slot coinciding with their estimated time of arrival at the airport is available and no delay is needed; and the maximum delay served by an aircraft is of 52 minutes. Note that the highest bin contains 190 flights and is the bin ranging from 30 minutes to 40 minutes of assigned delay, which correspond to the average delay of the GDP (39.2 minutes of delay per aircraft serving delay). Thus, RBS gives a good distribution of the delay on all the affected aircraft.

On the other hand, RBD and RBiD present a similar behaviour which is different from RBS. Many aircraft that are controlled by the GDP receive zero minutes of delay (79 aircraft for the RBD and 62 aircraft for the RBiD), the reason is that as the flights are ordered by their flight distance,

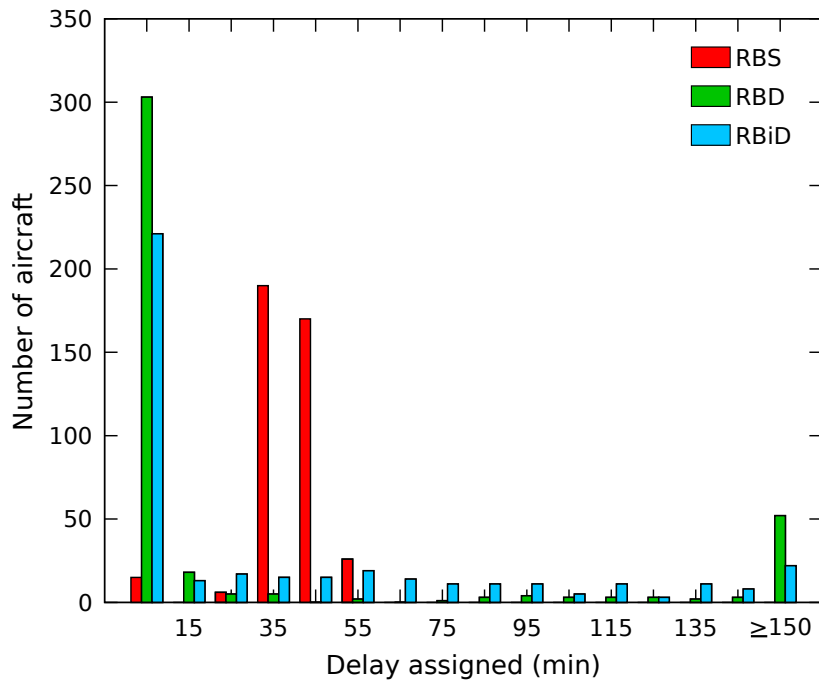


Figure V-15: Delay distribution histogram with different ration policies for Chicago O'Hare Afternoon GDPs. 10 minutes bins.

the probability that the slot is available is high (303 flights are in the 0–10 minutes bin for the RBD case and 221 for the RBiD). However, the maximum assigned delay are higher than in the RBS policy (364 minutes for the RBD and 235 minutes in the RBiD case). This means that the average delay per aircraft serving delay is also higher than in the RBS case (48.0 minute in the RBD and 45.6 minutes in the RBiD). The big difference between the average and the maximum assigned delay, for these policies, implies that they are not very equitable as they differ notably from RBS which is considered the fairest approach. For this reason in (Hoffman *et al.*, 2007; Ball *et al.*, 2010a) an equity variation of the RBD in order to decrease the difference between the slot the aircraft would receive if no GDP is implemented and the one it is finally assigned, is suggested. These enhancements of rationing policies are out of the scope of this dissertation and thus the nominal form of RBS, RBD and RBiD are analysed with respect to the use of the speed reduction technique.

Figure V-16 presents the division of the assigned delay between airborne delay and ground delay. As expected, RBD allows only a very reduced quantity of airborne delay to be realised. Surprisingly, with the RBiD policy the percentage of airborne delay with respect the ground delay served is smaller than in the RBS case. The underlying reason is the distribution of the delay with the RBiD. The potential airborne delay which was not used in the RBS simulations is relatively small and mainly due to long haul flights. However, the RBiD policy increases the delay on those flights more than the maximum airborne delay that they can realise, while it decreases considerably the delay for short and medium flights. Therefore, RBiD is transferring delay from short and medium flights, which could be done partially as airborne delay, to long flights that are already realising their maximum airborne delay, in this manner increasing the total ground delay served.

Figure V-17, presents the same information as figure V-14, airborne delay realised and airborne delay realisable, but for the different ration policies in the case where no radius of exemption is used. The case where all the NAS is included in the GDP is presented, as it is the case where there is the most potential of airborne delay not used. As expected, RBD is the policy which has the maximum quantity of potential airborne delay which is not used. In addition, it should be noted that the number of aircraft which can potentially realise airborne delay is different for the

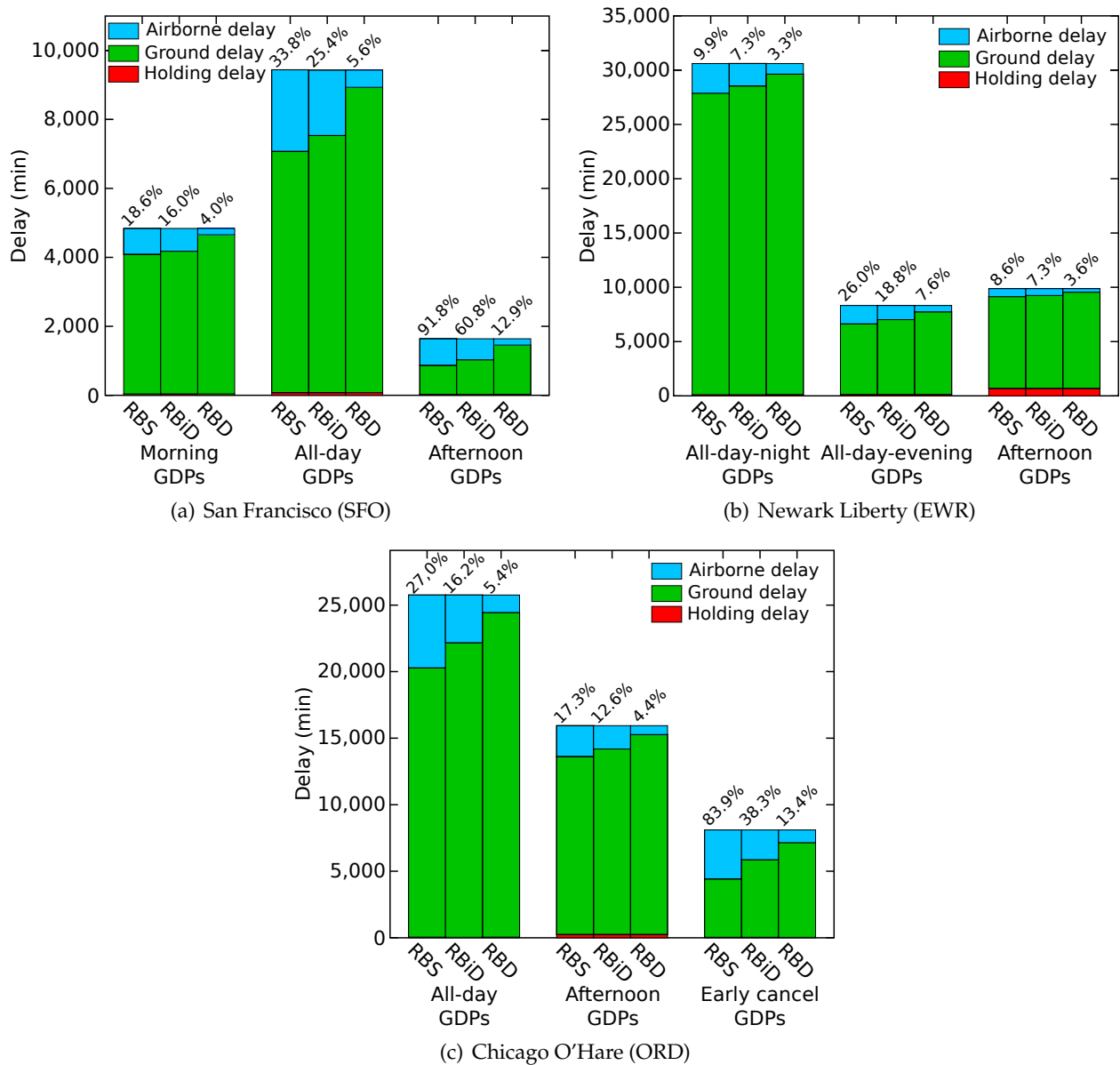


Figure V-16: Delay division by ration policy for GDPs without radius of exemption. Percentage of airborne delay over ground delay

three policies³. In the figure, the number of aircraft that are affected is presented for each ground delay program, and between brackets is the number of aircraft which have delay assigned. For example, in the *Afternoon* GDPs from ORD, a total of 406 aircraft are controlled by the GDP, but the number of aircraft serving delay ranges from 327 in the RBD policy to 344 for the RBiD or 400 for the RBS. As more aircraft are serving delay, the potential airborne delay that can be realised is higher.

The figure also shows the number of aircraft that are realising all their delay airborne and the number of flights which divide their assigned delay between ground and airborne delay. For the same example (*Afternoon* GDPs from ORD), the number of aircraft with a maximum airborne delay higher than their assigned delay is 7, 111 and 158 for the RBS, RBiD and RBD policies respectively. In general, the RBiD and the RBD concentrate the delay in less aircraft with higher delay, and therefore the potential airborne delay of the mid range aircraft is not completely used.

³In this figure only the airborne delay of the aircraft which have a ground delay assigned are considered.

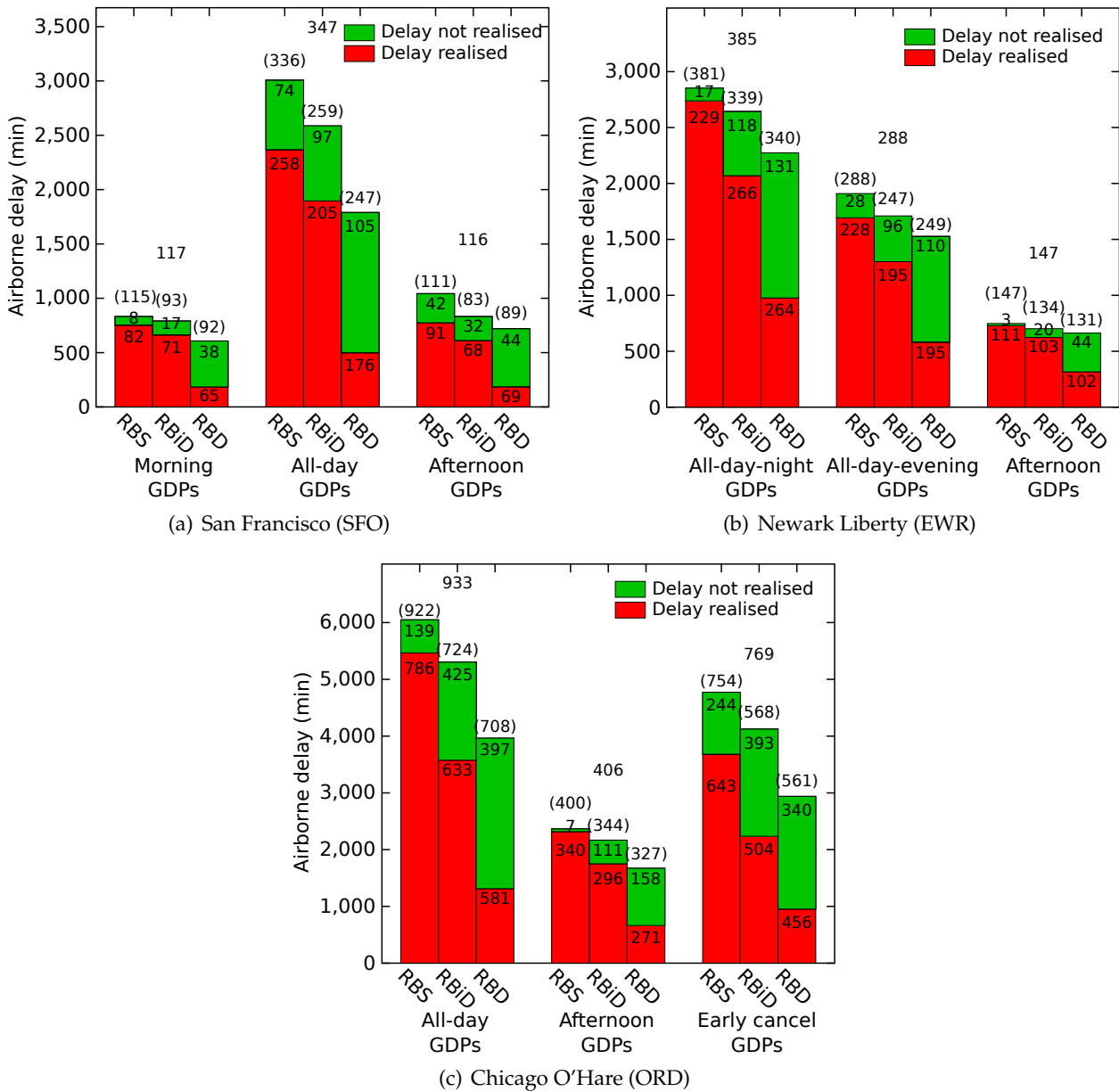


Figure V-17: Airborne delay realised and un-realised by ration policy for GDPs without radius of exemption. Per GDP the number of aircraft affected is indicated. And, per ration policy: between brackets the number of aircraft serving delay, and the number of aircraft that could realise more airborne delay than the assigned delay and the number of aircraft realising their maximum airborne delay

As was discussed in section V.5.4, when considering the early cancellation of the ground delay program, the delay that is globally saved should be considered. In figure V-18, the results for the case when no radius of exclusion is defined are presented. The ration-by-distance is the policy which performs the best from a ground delay recovery point of view, but the benefit of using the speed reduction strategy is practically marginal. The delay recovered due to the increment of speed of the aircraft flying at V_{eq} at the cancellation time, represents only between 0.7% and 1.8% of the ground delay recovered for the three clusters of ORD.

Conversely, if RBD maximises the ground delay recovered, RBiD minimises this value. RBiD maximises the amount of delay recovered due to the speed reduction but the ground delay recovered is so reduced that this strategy cannot be considered a good candidate for operational

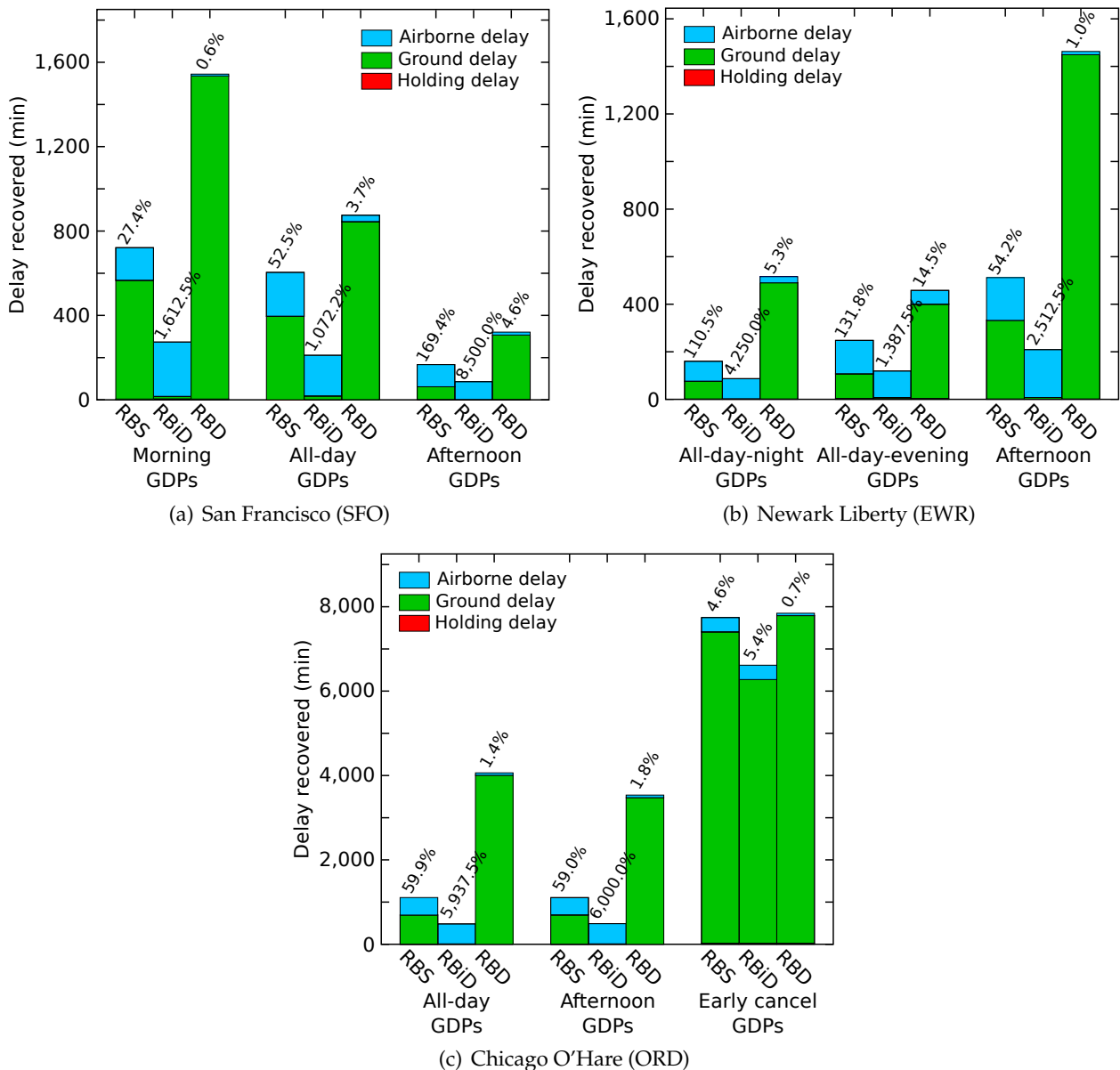


Figure V-18: Delay recovered at cancellation time by ration policy for GDPs without radius of exemption. Percentage of extra delay saved due to speed reduction with respect to the delay saved (holding and ground delay) with only ground delay

purposes, due to its low fairness and equity performances and due to the recovered delay results.

V.6.2 Ration-by-schedule and ration-by-distance delay recovered comparison

In general terms, RBD recovers the maximum total delay at the cancellation time, but the effect of the speed reduction strategy proposed in this thesis is marginal. However, RBS with speed reduction achieves an amount of delay recovered which is close to the one obtained by RBD, as is the case in the *All-day* GDPs of San Francisco International (see figure V-18). For this reason, in this section, the RBS technique is analysed with respect to the RBD policy with different radii of exemption. The results are presented in figure V-19.

One remarkable fact is that the RBD policy is not affected significantly by the exemption radius, considering the amount of delay recovered at the cancellation time of the GDP. The reason

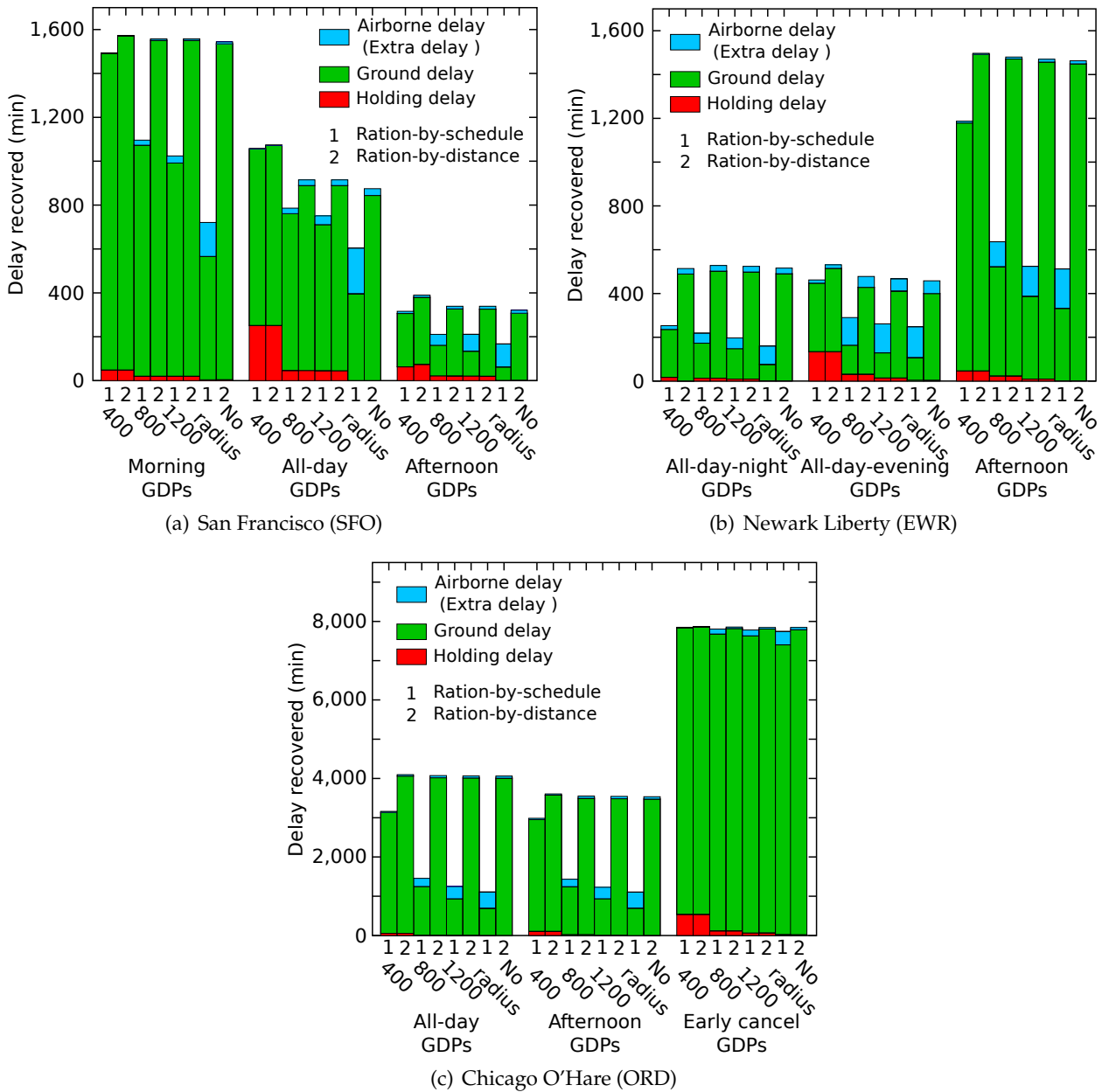


Figure V-19: Delay recovered at cancellation time comparing RBS and RBD for GDPs without radius of exemption

is that the RBD policy assigns more delay to aircraft closer to the airport. Thus, when the ground delay is cancelled, the aircraft recovering the ground delay are approximately the same when the radius decreases. On the other hand, the amount of delay recovered in the RBS case is affected by the radius of exemption, and the speed reduction strategy allows more delay to be recovered. The results, however, are still small with respect to the RBD.

V.6.3 Discussion of the results

RBS gives a better distribution of the assigned delay with lower average delay. As stated in (Ball & Lulli, 2004), the cost of the delay is non-linear with the amount of delay. Thus, an average lower assigned delay leads to lower related total costs, and the use of speed reduction allows some extra delay to be recovered, even if the RBD still performs better with respect the total amount of delay

recovered if the ground delay program is cancelled before initially planned.

On the other hand, ration-by-inverse-distance allows a considerable amount of extra delay to be recovered by the aircraft speeding up to their nominal speed when the GDP is cancelled, but there is still some potential airborne delay which is not used and the total delay recovered is very limited. A different approach is needed, in this context RBiD does not provide an acceptable solution to the problem, as it does not assign the delay with equity, nor perform adequately once the ground delay is cancelled; and RBS is the policy which minimises the potential airborne delay unused. Different approaches to try to minimise the airborne delay unused, while being close to the RBS solution could be considered. It could be possible to apply a modification of the RBiD in order to maintain a certain degree of equity with respect to the RBS, as was done in (Ball *et al.*, 2010a) with the RBD algorithm. Another option could be to weight the ration-by-schedule solution with the ration-by-inverse distance as suggested in (Wang *et al.*, 2012) in order to reach a compromise between RBS and RBiD, even if it is likely that, the increment in airborne delay recovered will be compensated for by a decrease in the ground delay recovered.

In the current implementation, when two aircraft cannot both get a slot because their estimated time of arrival is the same, one of them is randomly prioritised. A possible idea could be to use the information of the maximum airborne delay that each aircraft can realise, in order to assign the slot maximising the airborne delay. This modified RBS policy will, however, need information about the maximum airborne delay each aircraft can realise. If all that information is available to the network manager, it might be possible to realise an optimisation of the slot allocation (i.e. a ground holding problem) in order to maximise the airborne delay, while maintaining the solution closest as possible to the RBS, as it is considered to be the rationing policy which maximises fairness between the aircraft. Whatever the rationing policy used, the airline will always have the option to interchange its flights once the assignment of slots has been done in order to maximise the airborne delay in the CDM part of the GDPs.

V.7 Impact on the air traffic management

The use of the cruise speed reduction technique suggested in this dissertation for air traffic flow management initiatives, such as the GDPs, might also have an impact on air traffic management and air traffic control. These effects can be summarised in three different aspects:

- the difference between the position of the aircraft flying at equivalent speed and where it would be if the whole assigned delay were served on the ground and the speed maintained to the nominal one;
- the number of aircraft that are in the air when in the nominal operational scenario, they would still be on ground serving their delay;
- and the effect of having aircraft flying at unusually slow speed during their cruise phase, mixed with flights cruising at nominal speeds.

Flying slow during the cruise implies that the aircraft is at a different position to where it would have been if all the delay were realised on ground. This might have an effect on the air traffic control as the aircraft will be behind their initially scheduled position. However, the main objective when flying at the reduced cruise speed is to arrive at the destination airport at the controlled time of arrival, regulated by the GDP, as they would if they realised the delay on ground and flew at the nominal flight plan speed; hence this difference is reduced as the flight goes on. Actually, the fact that the reduced speed is only controlled during the cruise implies that the

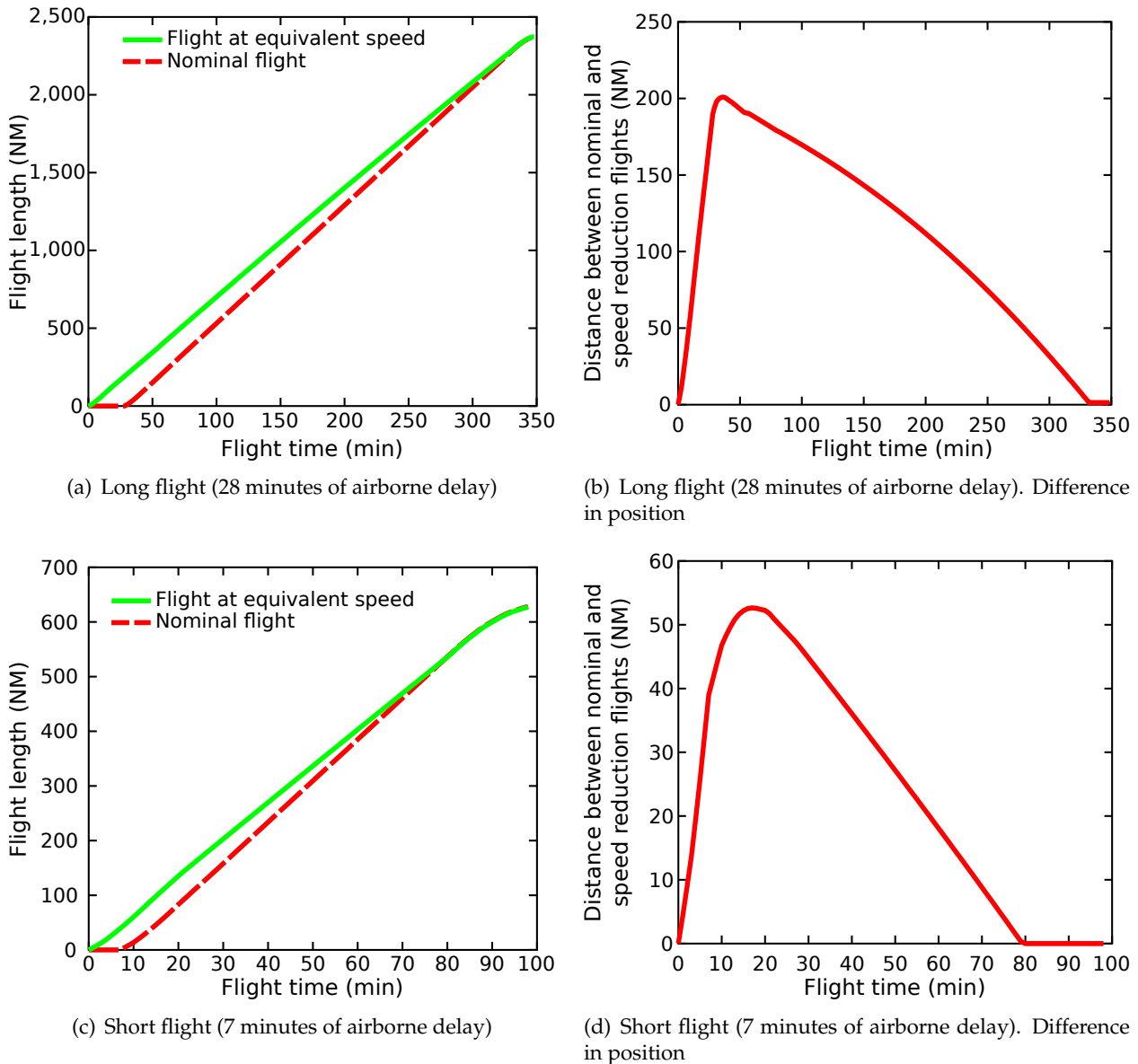


Figure V-20: Difference in trajectory position flying at V_{eq} or only doing ground delay and flying at V_0

aircraft will reach the TOD at the same time as it would have done if the delay had been realised solely on ground.

Figure V-20 shows the distance between the nominal and the speed reduced trajectory for a long and a short flight. As can be seen, the distance between the two trajectories increases rapidly when the grounded aircraft is still realising its delay at the airport of origin and the speed reduced one is already flying. However, as soon as this second aircraft takes off, as its speed is faster than in the reduced speed case, the difference in position decreases rapidly, and is in the same position during the descent. It should be noted that the amount of airborne delay realisable is relatively small, for the example flights it is 28 minutes for the long flight, and only 7 minutes for the short flight. Thus, the maximum difference in distance is achieved when the aircraft is still in its ascending phase or during its early cruise. And when the aircraft is reaching the congested TMA of the destination airport with the reduced capacity, there is almost not difference between flying at V_{eq} or at the nominal speed. For the example of the short flight the distance is less than 55 NM and for the long one around 200 NM. These distances are achieved by realising the

maximum airborne delay in the air, which for long flights is not always the case as the assigned delay might be lower than the maximum airborne delay realisable.

The fact of having aircraft in the air that would otherwise be on the ground, might be an issue from an ATC point of view, as sectors might get saturated due to these aircraft. In addition, if there is a redefinition of the GDP, for example, due to changes in the PAAR or an extension of the GDP, those aircraft that are in the air and otherwise would be on the ground would be exempted from this replanning. Figure V-6 shows the number of aircraft that are flying at V_{eq} at every moment during the simulations and the number of extra take-offs, if compared with the scenario where all the delay is realised on ground, for the San Francisco International, Newark Liberty International and Chicago O'Hare International airports respectively. As shown in those figures (and also in table V-6), the number of aircraft that are in the air flying at V_{eq} varies with the GDP and can be at its maximum value between 46 and 60 aircraft for the SFO's scenarios, between 61 and 79 for EWR's cases and between 119 and 138 aircraft for the ORD's simulations. However, this does not imply that that number of extra aircraft are airborne when they would otherwise be on the ground. There will be an overlap between the time when both aircraft are in the air. In fact, almost all the time both flights will be airborne at the same time. Thus, the number of extra take-offs, i.e. the number of aircraft that are in the air with the speed reduction technique that would be on ground in the baseline scenario, is very small (as shown in the same figures and tables). During the entire simulations there are less than 10 aircraft in the air that otherwise would be on the ground for SFO and EWR scenarios and less than 18 for the ORD simulations. It is worth noting that by studying these cases without a radius of exemption, the worse case with respect to the number of extra take off and aircraft realising airborne delay is studied, as when the radius of exemption decreases the aircraft able to fly at V_{eq} and the maximum airborne delay they can realise decreases.

Another concern with respect to the impact of the speed reduction on the ATM and ATC network is the fact that aircraft are flying at an unusual reduced speed during the cruise and that this might affect the number of conflicts generated and their resolutions. However, it has been shown that the increment of aircraft in the airspace is very reduced and therefore, the impact on the number of conflicts should be marginal. If required some offset tracks could be implemented for those slow aircraft. More research is required in order to fully assess this last concern.

Finally, the gate availability would be slightly improved and ground congestion reduced at the departure airport, as aircraft are in the air sooner rather than waiting at their gates.

V.8 Discussion of the results

If a GDP is cancelled as predicted when filed, the realisation of the speed reduction strategy only leads to a division on where the delay is accrued. The same amount of delay is totally realised and the same fuel is burned as in the nominal case when all the delay is served on ground. However, if the ground delay program is cancelled before planned, as is usually the case, the aircraft in the air flying at the reduced speed are able to increase their cruising speed to their nominal one, in this way recovering some extra delay that in the completely ground based scenario is lost. In this chapter, it has been shown that this extra benefit is airport and demand dependent. The benefit is directly related with the number of aircraft which are at that time flying at their equivalent speed. In general, an average of around 3.5 extra minutes of delay per aircraft is recovered flying at V_{eq} at the cancellation time.

For the speed reduction strategy it is interesting to have long flights, as they are able to absorb a higher amount of delay during the cruise. Thus, the longer the radius of exemption the better the performance of this strategy. Ultimately, the use of the whole NAS reveals values up to more than 40% of extra delay recovered with respect to the delay which would be recovered if all the delay

were realised on the ground, as a function of the airport and time of the day. As longer radii of exemption lead to better performance of the speed reduction strategy, in some cases, it is possible to obtain results of delay recovered similar to those obtained with a shorter radius, without the speed reduction technique. Therefore, when defining a ground delay program, longer radii of exemption might be used with the advantages that less holding delay is realised and therefore, less fuel is used leading to less cost. Moreover, as with longer radii of exemption more aircraft are included in the program, the delay is better distributed, leading to a lower average delay per aircraft. However, there is a trade off, as the unnecessary delay recovered with shorter radii might be significantly higher than with longer radii of exemption.

The amount of airborne delay that each individual aircraft is able to realise is high enough to make this strategy interesting at an aggregate level but small enough to not increase significantly the number of aircraft in the air and therefore not result in a significant increase in the number of aircraft controlled by the ATC.

It is very unlikely that a GDP is cancelled a short time after its implementation. Therefore, it is very probable that the initial demand will have to perform all the assigned delay, and no benefits will arise from the cruise speed reduction strategy for these flights. Therefore, a possibility is to apply a ration-by-schedule strategy and to realise all the delay on ground at the beginning of the GDP. Then, from a certain moment when the probability of cancellation of the GDP increases, change to the speed reduction strategy with a ration policy or aircraft slot assignment algorithm, which maximises the airborne delay, in this way maximising the potentially recovered delay if the GDP finally cancels.

It should be mentioned that in the simulations conducted in this chapter the flight levels were maintained as initially planned. If flight levels are allowed to be changed the maximum airborne delay increases significantly and, therefore, this strategy would increase its potential.

Finally, it should be remembered that the fuel is maintained as initially planned but not necessarily the total cost.



— Das Rheingold - Richard Wagner

VI

Concluding Remarks

The air traffic management system is reaching its capacity and issues like fuel consumption and the environmental impact of aviation are becoming more important in the ATM community. The use of cruise speed variation is envisaged for different purposes, such as conflict resolution. In this thesis, the effect of cruise speed variations on fuel consumption was analysed in detail and its use for pre-tactical delay management in air traffic management initiatives was studied. A brief summary and conclusions of the achieved results, along with future work that could be undertaken from the research accomplished in this thesis, are presented in this chapter.

VI.1 Summary of contributions

The main contributions of this PhD thesis are summarised as follows:

- The analysis of the effect of cruise speed modifications on fuel consumption was presented in chapter III. Generally, in the literature, speeds lower than maximum range (MRC) speed are identified as non-operational speeds, as they use more fuel than the minimum required to cover a given distance. However, in this thesis it was shown that the optimality of a speed should be considered with respect to the nominal speed and fuel consumption intended by the flight. The first contribution of this thesis is the definition of the *equivalent speed* (V_{eq}) as the minimum speed which has the same *specific range* (NM/kg fuel) as flying at the intended nominal speed (V_0). This equivalent speed, by definition, is lower than the MRC speed. As a function of the cost index, this speed reduction without incurring extra fuel consumption can be up to 12% of reduction over the nominal speed, for nominal cost indexes being values

between 2% and 6%. In a real implementation of the system the safety aspects regarding flying at unstable speeds on the backside of the power curve should be considered.

- One of the objectives of this work was to determine the relationship between speed variations and fuel consumption. The fact that the equivalent speed varies as a function of the flight level, the aircraft weight, the cost index and the cruise wind was identified. If the aircraft flies at a sub-optimal flight level from an aerodynamic point of view, the margin between V_0 and V_{eq} increases. Generally, lower weights lead to lower equivalent speeds. Thus, the fuel consumption during the cruise implies that V_{eq} decreases with the flight. This variation could be linearly approximated as a function of the distance flown.
- The weight, flight level and nominal speed are not free parameters for a given flight, as they are optimised once the cost index is determined. Higher cost indexes lead to bigger differences between the nominal and the equivalent speed, even if some exemptions can be found, as an increment in the cost index can lead to a discontinuous change in the optimal flight level.
- In order to assess the maximum airborne delay that can be realised during the cruise without incurring extra fuel consumption, representative European flights were analysed in chapter IV. It was proven that the amount of airborne delay ranges from 4 minutes to 30 minutes as a function of the flight characteristics. However, for nominal values of cost index, the airborne delay is reduced to between 5 minutes, for short and mid-range flights, and up to 25 minutes for long flights.
- One of the contributions of this thesis is the analysis of the airborne delay realisable if extra fuel consumption is allowed, in order to reduce the speed even more. Results show that if the flight level is maintained, the speed is soon limited by the minimum stall speed. It was determined that there is a linear relationship between the extra percentage of airborne delay realisable, the percentage of true air speed reduction, and the percentage of extra fuel consumption allowed. These results might be interesting for researchers working on the use of speed variation to deal with air traffic management and conflict resolution initiatives, as it establishes a relationship between the extra fuel consumed and the extra airborne delay realisable.
- This dissertation also examines the amount of airborne delay realisable, if the flight level is adapted in order to select the cruising altitude which has the minimum speed with the same specific range as in the nominal conditions. Results show that by optimising the optimal flight level in this manner, the airborne delay is increased significantly. It is worth noting that the optimisation of the flight level without incurring extra fuel consumption leads to similar, or even higher, amounts of airborne delay than allowing extra fuel consumption but maintaining the nominal altitude.
- Another contribution of the work presented in this thesis is that if the flight parameters are fixed (payload and cost index), the amount of airborne delay has a linear dependency with the flight plan length. This relationship is explained due to the fact that there is a relationship between the flight distance, the fuel needed and the optimal flight level for a given flight. Two categories of aircraft types have been determined: aircraft which are used mainly for short and medium distances where there is generally a single cruise flight level (A319, A320, A321 and A330 aircraft types) and aircraft which are used for long flights and which, due to their high payload, generally, do a climb step during their cruise (A300 and A340 aircraft types). The climb step leads to shallower variations of airborne delay as a function of the flight distance, as the aircraft spend more time flying close to their aerodynamic optimal flight level. Results show that for extremely short flights, the relative amount of airborne delay is high as the aircraft does not have time to reach its optimal altitude.

- The effect of wind was thoroughly studied in order to completely assess the amount of airborne delay realisable without incurring extra fuel consumption in realistic scenarios. Two effects of wind on the equivalent speed were determined: first, it modifies the shape of the specific range curve as a function of the cruising speed, as it adds a wind dependent term. Secondly, as wind is not constant at different altitudes, it might change the optimal flight level from a ground speed point of view. This change in the flight level leads to cruising altitudes which are not optimal from an aerodynamic point of view, and, therefore, to an increase in the margin between the nominal and the equivalent speed. As expected, head winds lead to the possibility of realising more airborne delay, while tail winds decrease the maximum airborne delay for a given flight with respect to a calm wind situation. However, the flight level change might lead to more airborne delay in the presence of wind, even with tail wind, compared to a still situation.
- Another contribution of this thesis is the verification, with the simulations, that the estimation of the amount of airborne delay realisable by flying at the equivalent speed is very similar, whether the average wind the aircraft encounters on its route, or the detailed wind field, is considered.
- In order to contribute to the research community in the current and foreseeable concept of operations, two situations were studied when the actual wind differs from the forecast: to keep the flight speed profile as initially planned (as done in the current concept of operations) or to adapt the speed in order to compensate for the wind error and fulfil the controlled time of arrival (as foreseen for SESAR and NextGen). Results show that in the first case, the difference between realising airborne delay or flying at the nominal speed, is very small. Conversely, the use of speed reduction leads to a more robust solution with respect to fuel consumption, if the wind forecast errors are compensated for. This contribution is important for airlines, as they might be willing to realise part of their assigned delay airborne, even if the air traffic management initiative is not expected to be cancelled, as their fuel consumption will be more predictable.
- One of the main applications of the speed reduction concept suggested in this dissertation is the possibility of dividing the assigned delay, between ground and airborne delay, which will be absorbed during the cruise. If at a certain moment the regulation is cancelled, the aircraft might be able to increase its speed to the nominal cruise speed, in this way recovering some delay while using no more fuel than the initially planned. The assessment of this airborne delay recovery without incurring extra fuel consumption, was defined as one of the objectives of this thesis. It has been determined that it is possible to linearly approximate the delay that can be recovered by a single flight as a function of the flight plan distance, and the amount of time the aircraft has been realising its cruise before speeding to V_0 .
- The application of the centroid of the clusters of the GDPs of 2006 of San Francisco, Chicago O'Hare and Newark liberty, in the inbound traffic August 24th-25th 2005, show that around 80% of all the traffic is able to realise, to a certain extent, part of their assigned delay airborne. And, as a function of the GDP, the total airborne delay varies between 8% and 48% of all the assigned delay.
- The extra delay that can be recovered if the ground delay programs are cancelled before planned was computed assuming that airborne traffic realising delay by flying at V_{eq} can speed up to their nominal cruise speed, recovering delay without impacting the fuel consumption. If the ground delay programs are cancelled according to their centroids, on average 3.5 minutes of airborne delay per aircraft flying at that moment at the equivalent speed is recovered. Thus, it was demonstrated how it is possible to recover delay without incurring extra fuel consumption, just by transferring part of the assigned delay to the air.

- The simulations were extended in order to include the use of radii of exemptions, usually defined when a ground delay program is set. The airspace manager has to deal with the trade off of using a larger radius where more aircraft are affected, reducing the unsafe and expensive holding delay and having a better distribution of the delay between the affected aircraft and therefore reducing the cost, or using a shorter radius, which, if the ground delay program is cancelled, will mean the less delay is realised. This thesis has proven that the speed reduction technique can improve the delay recovered with longer radii of exemptions, and thus allow the airspace manager to define a longer radius.
- In chapter V different ration policies other than ration-by-schedule (RBS) were analysed. RBS with the speed reduction technique obtains, with a fairer distribution of the assigned delay, results of delay recovered that are closer to ration-by-distance, which is considered the policy which recovers the maximum assigned delay, than just RBS. The strategy of ration-by-inverse-distance, suggested in this thesis, increases the delay recovered due to the speed reduction but performs inadequately with respect to the total delay recovered.
- Finally, one of the objectives of this dissertation is the assessment of the effect of this speed reduction strategy on air traffic management and air traffic control. In chapter V, it was determined that the distance between the position where the aircraft is located in the airspace if flying at the equivalent speed, and where it would be if flying the nominal flight plan and realising delay solely on ground, is relatively small and decreases as the aircraft flies. Moreover, the number of extra take-offs is not significantly high. Thus, this thesis contributes to demonstrating that this technique should not represent a significant increment on the workload of the controllers, considering the number of aircraft per sector. However, further research is needed to study if adding this slow traffic to the en-route sectors affects the air traffic control at a tactical level. It is also worth mentioning that the use of the speed reduction technique will improve the gate availability and reduce ground congestion, as aircraft are in the air sooner.

VI.2 Future Research

During this thesis new questions and research lines arose. The following work items are proposed for the future:

- As was shown in this thesis, it is possible to parameterise the airborne delay with linear expressions. Thus, by extending these relationships, it could be possible to develop a parametric model of the amount of airborne delay and the potential delay recovered as a function of the flight characteristics.
- In this thesis, in order to analyse the benefit of the speed reduction strategy applied at air traffic management initiatives, and considering that the extra fuel consumption is determined with respect to the nominal flight plan, nominal values for the flights were adopted. However, these nominal parameters might change as the air traffic and economical situation change. Nowadays, as the cost of fuel increases, airlines tend to use lower cost index values and higher load factors. Therefore, the studies undertaken in this work should be extended to consider different payloads and cost indexes. Different types of airlines, with different economic policies, could also be analysed in order to assess the benefit of this technique by airline type.
- It has been demonstrated that the optimisation of the flight level can lead to more airborne delay than even the use of extra fuel consumption. Therefore, it is interesting that at the

pre-tactical phase, an optimisation of the flight level could be realised along with the computation of the equivalent speed profile. This will definitively lead to a higher amount of airborne delay potentially being realised.

- A natural extension of the work done in the simulation of the ground delay programs is the inclusion of wind. It is expected that wind will, in general, represent an increment in the total amount of airborne delay realisable, even if it will be highly dependent on the airport location.
- This thesis focuses on the recovery of the delay without incurring extra fuel consumption. However, it could be possible to increase the speed over the nominal one, once the regulation is cancelled, in order to trade fuel for delay. This decision would be airline dependent. Another interesting idea that should be further studied is the realisation of airborne delay by flying at maximum range speed, in order to minimise fuel consumption while realising some airborne delay. This strategy might be interesting when the ground delay program is not expected to be cancelled early, and thus it is not as important to have the aircraft airborne to recover delay if an early cancellation occurs.
- It is worth mentioning that new ration methods could be studied in order to maximise the airborne delay realised, while maintaining a degree of fairness, and to maximise the delay recovered if an early cancellation of the ground delay program occurs. A first approach is the prioritisation of aircraft with the same estimated time of arrival, considering their maximum realisable airborne delay under a ration-by-schedule policy. Another approach could be the modelling of a ground holding problem to be solved using linear integer programming, or the exploration of other policies such as ration-by-minimum-airborne-delay.
- Finally, total cost and not only the fuel consumption should be considered when optimising the trajectories in order to deal with the assigned delay.



Ground Delay Program

As defined in (Ball & Lulli, 2004): *ground delay program (GDP) is a mechanism to decrease the rate of incoming flights into an airport when it is projected that arrival demand will exceed capacity [...] The motivation for doing so is that as [...] delay is unavoidable, it is safer and cheaper for the flight to absorb this delay on ground before take off.* The ground delay programs are extensively used in the United States by the Federal Aviation Administration (FAA). In this appendix the main characteristics of ground delay programs is detailed.

In order to deal with capacity demand imbalances, the air traffic management experts have different initiatives that can be applied (Federal Aviation Administration, 2012b):

- Ground delay programs to strategically manage the arrivals at an airport. Generally, a GDP is issued in two situations: when the capacity of an airport is reduced and cannot handle the demand, and when the demand at an airport is unusually high. Ground delay programs are issued when long periods of capacity reduction are forecast.
- Ground stops (GS) are used tactically and are extreme forms of ground holding. When a ground stop is implemented, all departure of aircraft bound for a particular destination are postponed. A ground stop typically only applies to a set of airports, usually the ones that are close to the affected destination airport. Ground stops are implemented for a number of reasons, the most common ones being: to control air traffic volume to airports when the demand is expected to exceed the airport's acceptance rate for a short period of time; to temporarily stop traffic, allowing for the implementation of a longer-term solution such as a ground delay program; and when the acceptance rate of the affected airport is reduced to zero.
- Airspace flow programs (AFP) are similar to ground delay programs but used to control the

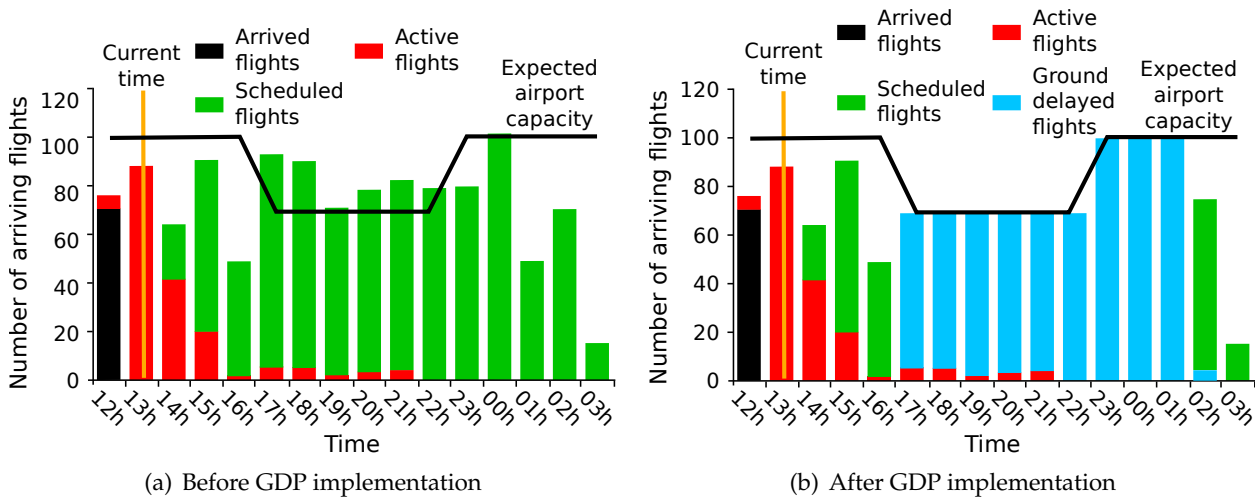


Figure A-1: Projected demand and capacity
Based on: (Manley & Sherry, 2010)

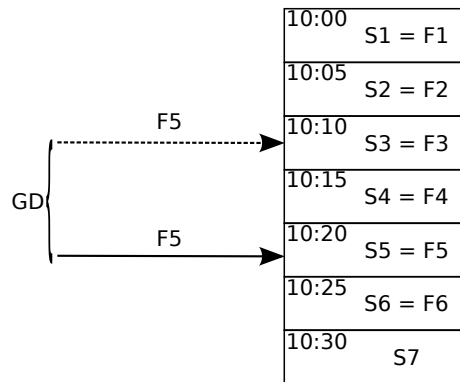


Figure A-2: Example of a regulated area with 5 slots every five minutes

demand over flow constrained areas (FCA). For example, to reduce the flow rate of flights to a centre with low capacity due to severe weather events. Until recently AFP were included in the GDP category.

In figure A-1 an example of a typical situation where a ground delay program is implemented is presented. Figure A-1(a) shows how the forecast demand for the forthcoming hours greatly exceeds the airport acceptance rate, which has been reduced. This capacity reduction is expected to last for almost seven hours. If no action is taken, the accommodated demand will experience holding delay at the arrival airport. In order to avoid this situation, a ground delay program is implemented, leading to the situation depicted in A-1(b). It is worth remembering that some traffic have to realise delay even when the capacity is restored, as otherwise the nominal capacity would be critically exceeded. Thus, the GDP needs to be properly defined in order to avoid holding delay, while keeping the capacity of the airport as high as possible to minimise unnecessary ground delay.

In order to apply a ground delay program, a ration-by-schedule (RBS) policy is used. The idea is that the first available slot is assigned to the aircraft with the closest scheduled time of arrival to that slot. Figure A-2 presents an example of a regulation with one slot every five minutes. As presented, flight F5 has a scheduled time of arrival which is within slot S3. However, aircraft with earlier schedule arrival times have already been assigned to slots S3 and S4. Thus, in order

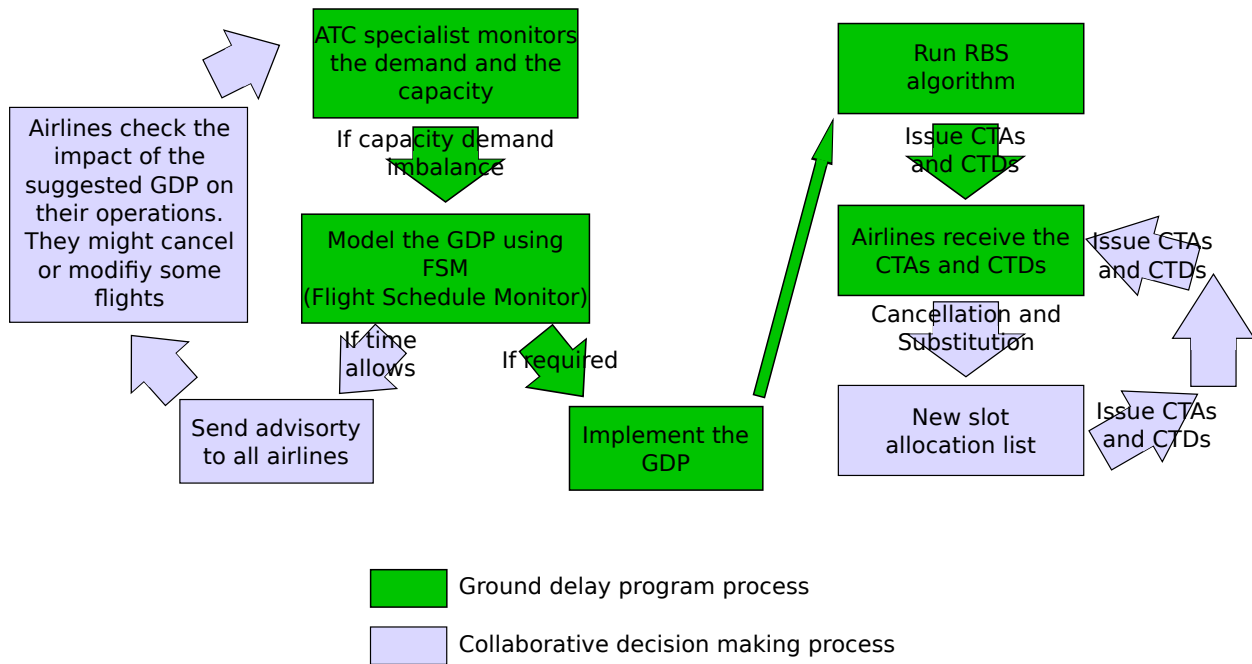


Figure A-3: Ground delay program implementation phases

to offset the arrival time to S5, it will be assigned a given ground delay than will be served on ground at the departure airport.

As an incentive to airlines to provide up-to-date data to the FAA during the formulation of a GDP, the ration-by-schedule algorithm considers the original gate time of arrival, without the taxi time, instead of the estimated time of arrival, and the collaborative decision making process (CDM) is designed to benefit airlines by promptly updating their flight status, as will be explained in this appendix (Ball & Lulli, 2004). Initially, the air traffic service provider was the sole decision maker, assigning ground delay to airlines to manage the capacity demand imbalance. However, it has been demonstrated that the associate cost of delay is airline and flight dependent, and they are not related in a simple linear manner. By including the airlines in the slot allocation process, the cost of incurring the delay can be more effectively managed. Moreover, the real time operations leads to uncertainty in the definition of the flights, which can produce dynamic delays and modifications of flight plans. All these changes might modify the time of arrival of the flights, leading to slot assignments that are not optimal. For these reasons, there is a need to involve the stakeholders in the decision process of assigning the slots. Since 1998, the ground delay program has been enhanced with the introduction of collaborative decision making procedures. CDM implies a cycle of feedback between the service providers and users of the NAS. Once a GDP has been implemented, airlines react to the new situation in a cancellation and substitution process. This is an iterative process which improves the understanding of the situation that the service provider has, while optimising the cost of the required delay. Improved data exchange and communication between aviation transportation organizations will lead to better decision making in ATFM (Wambsganss, 2001).

Figure A-3 presents the diagram of the implementation of a ground delay program. Air traffic control specialists monitor the current and forecast situation at North American airports in terms of demand and capacity. Whenever the number of flights expected to arrive over a 15 minute time interval exceeds the predicted arrival capacity of the airport, the air traffic control system command centre (ATCSCC) undertakes some corrective actions. When the imbalance is foreseen for a long period, then the implementation of a GDP is envisaged (Ball & Lulli, 2004). The ATCSCC uses the flight schedule monitor (FSM) to monitor the demand and the capacity and to model the

Table A-1: Example of application of a GDP with substitution, cancellation and compression phases

Original demand			Original RBS assignment		Cancellations and substitutions		Compression	
Flight ID	Scheduled time	Slot	Flight ID	Delay (min)	Flight ID	Delay (min)	Flight ID	Delay (min)
A1_F1	10h00	10h00–10h02	A1_F1	0	A1_F2	0	A1_F2	0
A2_F1	10h02	10h03–10h04	A2_F1	1	A2_F1	1	A2_F1	1
A1_F2	10h02	10h05–10h06	A1_F2	3	A1_F1	4	A1_F1	4
A3_F1	10h02	10h07–10h08	A3_F1	5	A3_F1	5	A3_F1	5
A1_F3	10h03	10h09–10h10	A1_F3	6	A1_F3	6	A1_F3	6
A2_F2	10h03	10h11–10h12	A2_F2	8	A2_F3	7	A2_F3	7
A2_F3	10h04	10h13–10h14	A2_F3	9	A2_F2	cancelled	A3_F2	7
A3_F2	10h06	10h15–10h16	A3_F2	9	A3_F2	9	A2_F4	0
A1_F4	10h10	10h17–10h18	A1_F4	7	A1_F4	7	A1_F4	7
A1_F5	10h12	10h19–10h20	A1_F5	7	A1_F5	cancelled	A4_F1	4
A4_F1	10h15	10h21–10h22	A4_F1	6	A4_F1	6	A1_F6	0
A3_F3	10h15	10h23–10h24	A3_F3	8	A3_F3	8	A3_F3	8
A4_F2	10h15	10h25–10h26	A4_F2	10	A4_F2	10	A4_F2	10
A2_F4	10h16	10h27–10h28	A2_F4	11	A2_F4	11		
A1_F6	10h21	10h29–10h30	A1_F6	7	A1_F6	7		

ground delay initiative. At this stage, if time allows, a collaborative decision making process is started, advisories are sent to all airlines that would be involved in the ground delay program. Those airlines might decide to modify their flight plans, for instance cancelling some flights, and therefore modifying the demand for the restricted airport capacity period. In that case, the air traffic management specialist will re-evaluate the situation and consider if the program stills needs to be implemented. Once the GDP is implemented, the ration-by-schedule assignation algorithm is run. The controlled time of arrival and the consequently controlled time of departure are distributed to the airlines which at that moment *own* the slot. At this stage, an airline is able to both interchange any two flights, as long as it is possible for them to reach the slots, and to cancel any flight. The cancellation of flights will eventually generate empty slots which cannot be filled by airline's flights. At that moment a compression algorithm is applied. The compression algorithm is an inter airline slot swapping system to fill unused slots created in the previous phase. Airlines are encouraged to update their status as, if a slot is vacant, it might be used by another airline and, in that case, the original company receives control of the slot vacated by the flight which moves into its slot (Ball & Lulli, 2004). At the end of this process, a new iteration starts. Finally, it should be noted that the parameters defining the GDP might need to be revised as the situation at the airport might change. Thus, it is not uncommon to cancel a ground delay program earlier than initially planned, if the situation improves or, on the other hand to extend its duration. All the interchanges of messages between the stakeholders are recorded in the enhanced traffic management system (ETMS), which is used as a database and communications system for traffic management.

In order to clarify the operation of the ground delay programs, in table A-1 an example of GDP implementation, with its different phases, is presented. In this example, it is assumed that the capacity of an airport is reduced to thirty aircraft per hour. This means, that there is a slot every two minutes. The first two columns show the arrival demand of the airport. As can be observed,

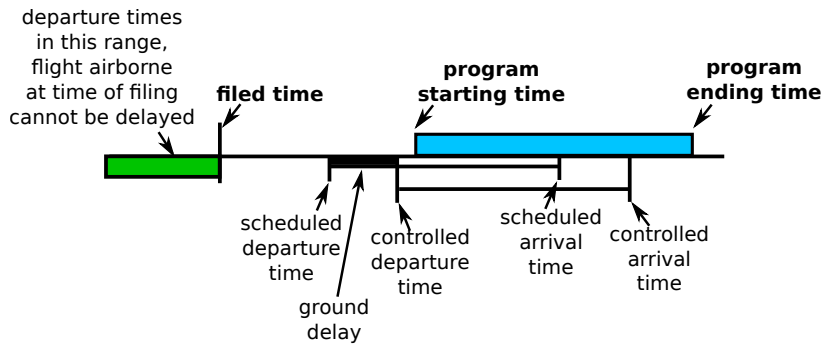


Figure A-4: Ground delay program parameters

Based on: (Ball & Lulli, 2004)

there are four different airlines with a total of fifteen flights. Firstly, a ration-by-schedule policy is applied to assign the slots to the different flights and airlines. The results are presented in the next two columns. Once the airlines receive the information about their assigned delay and slot, it is possible for them to make pertinent substitutions and cancellations. In this example, the first airline decides to swap its first flight (A1_F1) with its second (A1_F2) and to cancel flight number five (A1_F5). It is interesting to note that the total amount of delay served by flight A1_F1 and A1_F2 is actually increased (from three minutes to four), however, the delay assigned to A1_F2 is reduced, allowing the flight to arrive on time. If, for instance, A1_F2 is a connecting flight this process might be more economical. Also, there is now a vacant slot created by the cancellation of A1_F5, as none of the further flights of the first airline is able to arrive at the airport soon enough to use the empty slot. Airline number two decides to cancel its second flight (A2_F2) and to use the vacant slot for its third flight (A2_F3), therefore reducing its assigned ground delay. The cancellation of A2_F2 might be due to reasons exogenous to the GDP, but has a positive impact on the delay served by the second airline. After this cancellation and substitution phase, the compression algorithm is applied in order to use the slots that are vacant, as it will allow the total served delay to be reduced. Firstly, the 10h13–10h14 slot which is vacant and *owned* by the second airline is assigned to the next flight which is able to use it according, to the ration-by-schedule planning, in this case it is a flight from the third airline (A3_F2). By making this modification the delay of A3_F2 is reduced by two minutes, but now the slot that was previously used by that flight is available to the second airline which is able to fill it with the A2_F4 flight, completely reducing the 11 minutes of delay initially assigned to that flight. A similar process is done for the 10h19–10h20 slot which will be assigned to A4_F1, releasing the 10h21–10h22 slot which can be consequently assigned to A1_F6. These examples demonstrate why it is worth while for an airline to update the status of its flights as soon as possible, as with a cancellation, even if a concurrent airline is favoured, the slots released by that airline can be used by another of its own flights.

When issuing a ground delay program, three parameters are mainly needed: the start and end time, the scope of the program, which origin airports are included based on tier-scope or distance scope, and the program airport acceptance rate (PAAR). The start and end time of the program can be considered as exogenous parameters, as they are mainly based on capacity forecast and airline schedules. However, it is possible to define the set of flights included in the program by, for instance modifying the scope of the program or the time when the ground delay program is issued. The flights that are scheduled to arrive at the airport between the start and end time are the ones in the GDP range, as presented in figure A-4. However, only a restricted set of aircraft from the ones in the program serve some delay. In (Ball & Lulli, 2004) the following notation was defined in order to understand the different types of aircraft involved in a ground delay program:

- \mathcal{F} = set of flights in the GDP range

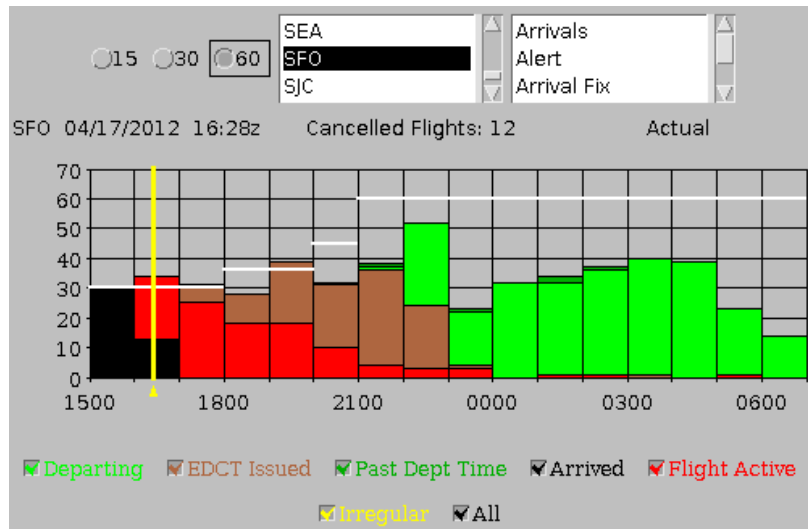


Figure A-5: Demand and capacity at San Francisco International Airport with a GDP implemented

Source: (*Federal Aviation Administration, 2012c*)

- \hat{F} = flights in \mathcal{F} that are exempt
- $\tilde{F}(t)$ = flights in \mathcal{F} that are airborne at time t .
- \bar{F} = flights included in the GDP
- \hat{t} = file time of the program

Thus, with this notation the aircraft included in the GDP are defined as $\bar{F} \subseteq \mathcal{F} - \hat{F} - \tilde{F}(\hat{t})$. It is worth remembering that the total amount of delay required to accommodate the demand is practically constant and that by modifying the parameters which define the ground delay program, there is a redistribution of which aircraft serve the delay, and how much delay is realised on ground and in holding form. As stated in (*Ball & Lulli, 2004*), there are some basic trade-offs involved in the election of when the GDP is defined. If \hat{t} increases, \bar{F} decreases as more aircraft are already airborne at the definition time. Thus, as the pool of flights that are assigned some delay gets smaller, the average assigned delay increases. And bigger delays represent higher associated costs. Also, as more aircraft are exempt, the holding delay needed is increased. Conversely, as \hat{t} decreases \bar{F} increases. Therefore, the pool of flights that are assigned delay increases but long haul flights with earlier departure times are also included, this leads to an assignment of delay based on less accurate weather forecast, therefore it is more likely that delays are assigned and served unnecessarily. A similar principle is found in the definition of the exemption radius, including further airports leads to lower average delay assigned and less costly solutions, however, if the ground delay program is cancelled, the unrecoverable unnecessarily realised delay increases (*Ball et al., 2010a*).

Moreover, in realistic air traffic management initiative implementations, there is a stochastic component that cannot be neglected. The airport acceptance rate is a parameter which changes dynamically during the day. Figure A-5 presents a ground delay program defined at San Francisco International Airport, as can be observed, the forecast capacity at the airport is not a fixed parameter but increases gradually during the day. These variations will inevitably lead to variations in the controlled time of departure. In particular, as stated in (*Hoffman et al., 2007*), the time at which the AAR is restored is not known precisely until it happens. The minor variations of AAR produced during the ground delay program implementation are usually swamped by the uncertainty of the demand.

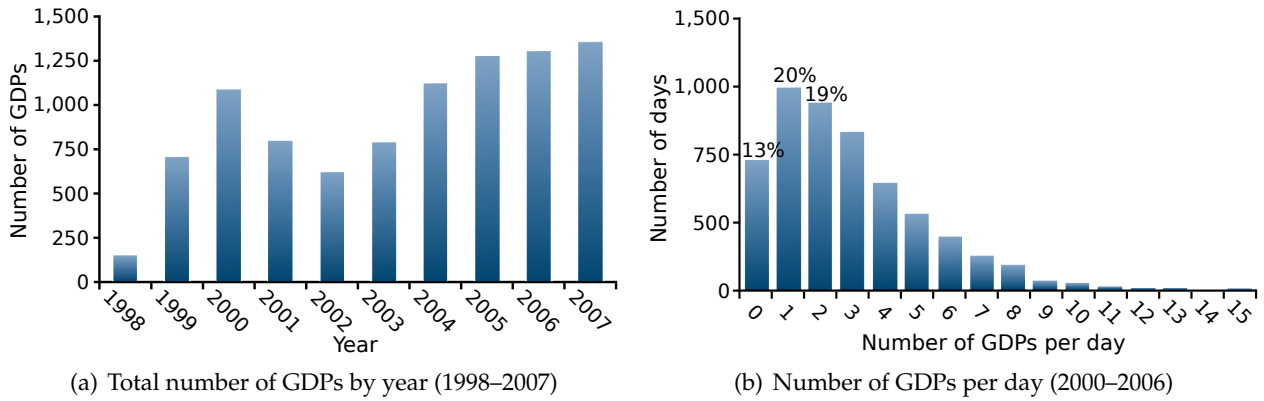


Figure A-6: Ground delay program statistics

Based on: (Manley & Sherry, 2010)

Table A-2: Direct cost of air transportation delay in 2007 in the NAS. Source: (Ball et al., 2010b)

Cost Component	Cost (\$ billions)
Cost to airlines	8.3
Cost to passengers	16.7
Costs from lost demand	3.9
Total direct cost	28.9
Impact on GDP	4.0
Total cost	32.9

For these reasons, it is not unusual to issue ground delay programs that are extended longer than required, leading to early cancellations. In (Ball et al., 2010a), it was identified that there are two possibilities when cancelling a GDP. In the first case, at the cancellation time, it is assumed that grounded aircraft are allowed to depart without any further delay and that when these flights arrive at the airport they can land without any additional delay. The natural spread of flight times and schedules allows this cancellation policy to be used quite extensively. The second option is to augment the existing slot set and reassign aircraft based on their current controlled time of arrival to potentially earlier slots. The statistical analysis of San Francisco International ground delay programs from the first quarter of 2009 period realised in (Ball et al., 2010a), shows that about 77% of all the GDPs were cancelled according to the first case, 13% under the slot reallocation principle and the remaining 10% of the programs were cancelled very early when very few flights had served any delay.

The first time GDPs were implemented was due to major weather related capacity reduction at airports after the air traffic controllers strike in the United States of America in 1981. The analysis of 2006 GDPs show that approximately 74% of the ground delay programs are issued due to weather related situations, 6% the runway and equipment are behind the decision to implement a GDP, in 4% of cases the expected traffic is unusually high compared with the infrastructure capabilities and in 2% of cases special events greatly increase the demand at an airport. For the remaining 14% of the ground delay programs there was no information as to its cause. This is the case of all the GDPs defined in the Canadian airspace. It can be assumed, however, that for those GDPs a high percentage are also related to weather issues.

In general, the issue of GDPs is increasing, as depicted in figure A-6. Between 2000 and 2007, on any given day, there was an 87% probability of having a GDP declared at least at one airport (Manley & Sherry, 2010). As is stated in (Manley & Sherry, 2010), where more than ten GDPs per day are depicted in figure A-6(b) it is because, in the past, GDPs were also used to deal with airspace capacity problems. Nowadays, those air traffic management initiatives are under the AFPs. In general, more than 16.8 million minutes of delay, affecting over 530,000 flights per year, are assigned due to GDPs and, as presented in table A-2, this can represent up to almost 33 \$ billion per year.

B

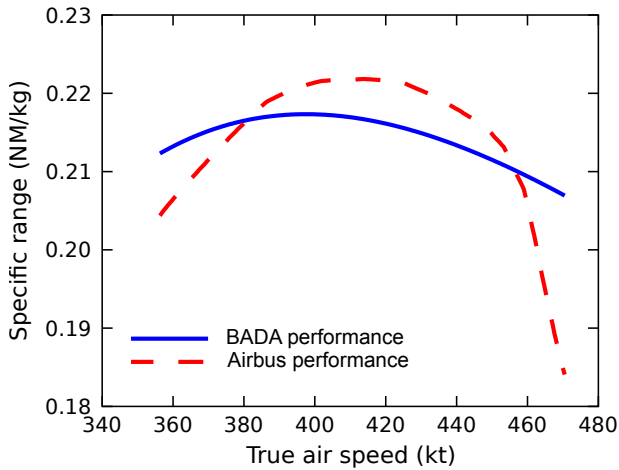
Airbus and BADA Performance

In the air traffic management community, the Eurocontrol's base of aircraft data (BADA), which is a set of aircraft models, is extensively used, from aircraft trajectory simulation, and research and development studies to the modelling and planning of traffic flows. BADA provides information of geometric, kinetic and kinematic aspects of aircraft behaviour. It is based on a mass-varying, kinematic approach to aircraft performance modelling (Poles *et al.*, 2010). In its most recently released version (BADA v3.9), the performances and operating procedure coefficients for 338 different aircraft types are available. From those, for 117 aircraft data is directly provided, the remaining 221 aircraft types are specified to be the same as one of the directly supported 117, being identified as *equivalent* to the original aircraft models. The coefficients include those used to calculate thrust, drag and fuel flow, and those used to specify nominal cruise, climb and descent speeds (Eurocontrol Experimental Centre, 2011b).

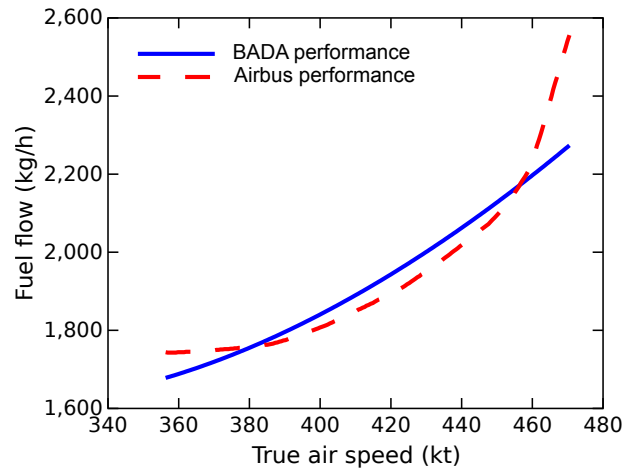
According to the study undertaken in (Eurocontrol Experimental Centre, 2011a), BADA v3.9 covers 89.7% of the European air traffic. This coverage study was undertaken considering the central flow management unit (CFMU) statistics for the ECAC airspace from January to December 2010.

The domain of validity of BADA 3 includes the part of the flight envelope corresponding to nominal operating conditions: minimum and maximum speeds in the range of speeds used by airlines, weight ranging from minimum to maximum nominal values, and standard atmospheric conditions from zero to 20 degrees. Under these conditions, BADA 3 has demonstrated an accuracy with a mean root square error in vertical speeds lower than 100 feet per minute and fuel flow error less than 5%. (Poles *et al.*, 2010). However, the error increases towards the edges of the flight envelope, where the *equivalent* speed defined and used in this PhD dissertation is.

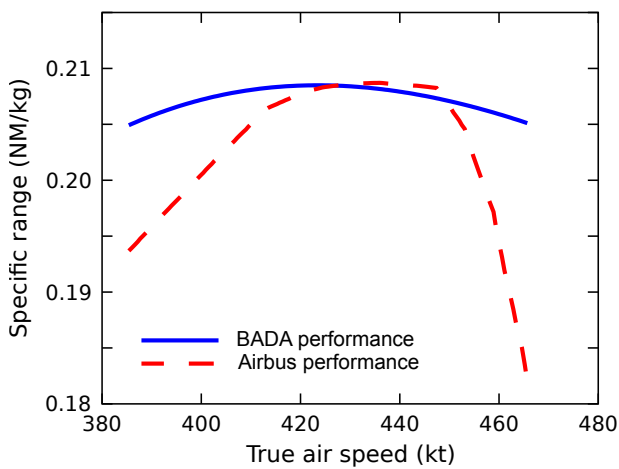
On the other hand, with the Airbus Performance Engineer's Programs (PEP) suite, it is pos-



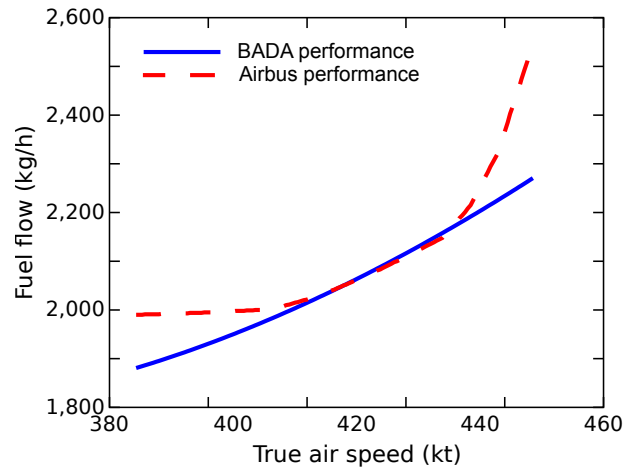
(a) Specific range – FL360, weight 55 tons



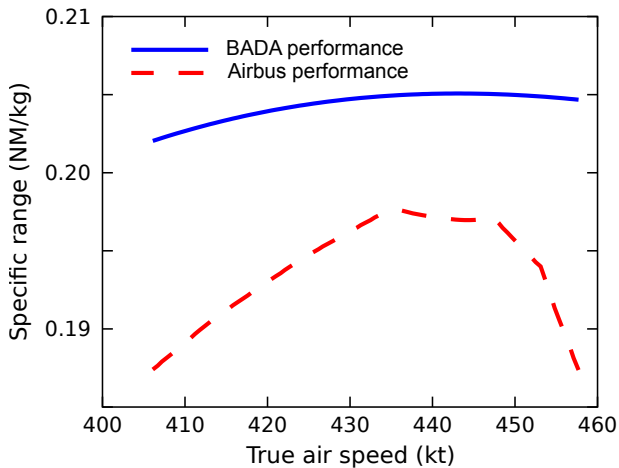
(b) Fuel flow – FL360, weight 55 tons



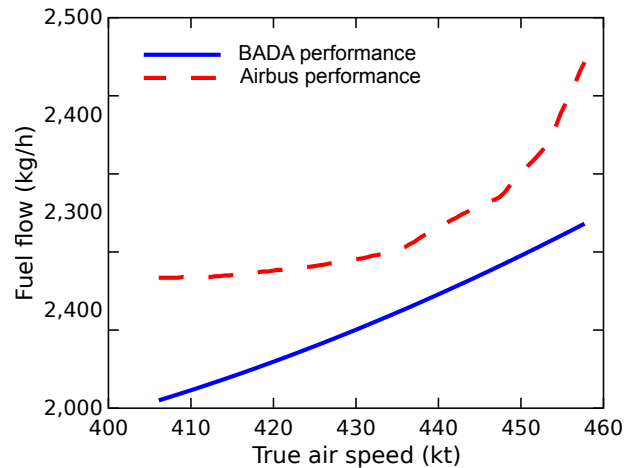
(c) Specific range – FL370, weight 60 tons



(d) Fuel flow – FL370, weight 60 tons



(e) Specific range – FL380, weight 63 tons



(f) Fuel flow – FL380, weight 63 tons

Figure B-1: Medium size twin jet engine Airbus model. BADA and PEP performances comparison as a function of cruise speed

sible to obtain accurate performances for Airbus type aircraft. These performances have been validated by the manufacturer and therefore can be assumed to be correct. The main drawbacks of using the values obtained from this software is that, firstly, an analytical model of the perfor-

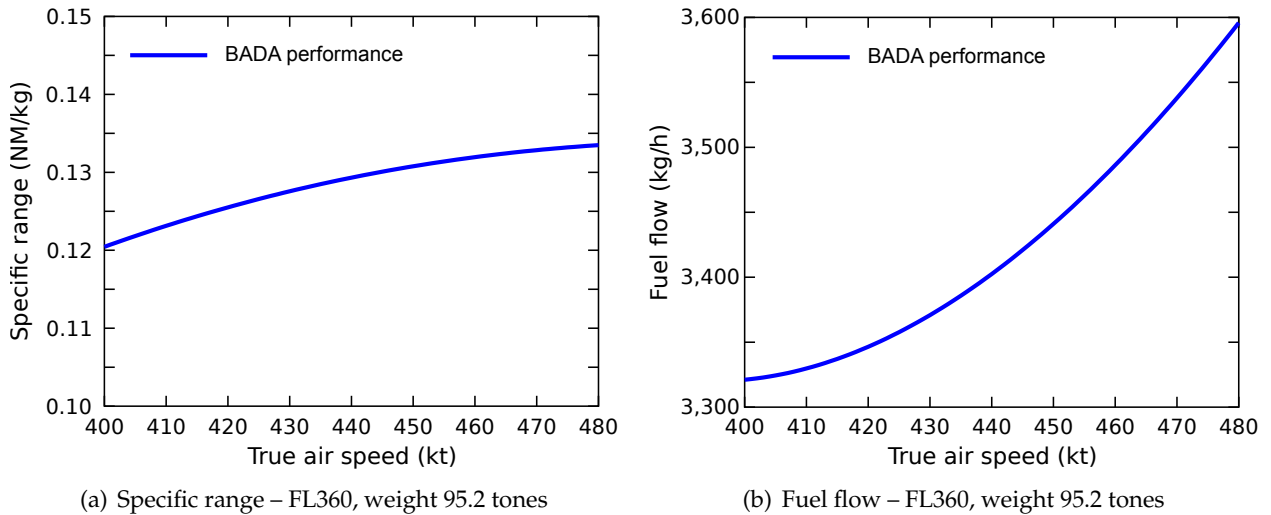


Figure B-2: BADA B757-200 performances as a function of the cruise speed

manances is not directly available, and, secondly, only Airbus aircraft can be simulated. This second drawback has been overcome by assimilating non-Airbus aircraft to Airbus types according to the aircraft characteristics. In this manner, only small aircraft are not considered during the simulations. This means that between 70.5% and 83.8% of all the simulated flights in the different scenarios have been simulated with accurate performances, covering a percentage of traffic similar to the one presented by BADA for the European traffic (89.7%).

Figure B-1 presents a comparison of BADA 3.9 and PEP performances, looking at the specific range and fuel flow, as a function of the cruise speed for a medium size twin engine Airbus model. As presented in figures B-1(b) and B-1(d), the BADA model generally approaches the value of the fuel flow when the speed is close to nominal values ($M 0.78 \sim 447.5$ kt). However, the fitting becomes less accurate for lower speeds which implies that the specific range curve as a function of the cruise speed is close to the Airbus values at nominal speed, but does not match the variations for lower speeds. In some cases as in B-1(e) and B-1(f), the fitting does not match the values provided by the Airbus software.

BADA 3.9 does not consider the compressibility effects. For this reason, for some aircraft, as is the case for the B757-200 (figure B-2), the specific range curve does not present an accurate behaviour. In this case, with the information provided by BADA 3.9, the aircraft is always flying at a speed lower than its maximum range speed, which is not correct.

Figure B-3 depicts the specific range as a function of the flying altitude with respect to different weights, for a cruise speed of $M 0.78$. The optimum altitude computed with BADA 3, for all values of weight, is equal to the highest altitude, which is not the expected behaviour. The main reason for this is a limitation in the BADA 3 drag model, which does not take into account the compressibility effect that appears at high altitudes and speeds (Poles *et al.*, 2010).

For these reasons, Eurocontrol is developing BADA version 4. BADA 4 presents better capabilities, as the domain of validity is the entire flight envelope, and the error levels in accuracy remains similar to the error levels in goodness-of-fit (Poles *et al.*, 2010). As an example, the number of coefficients needed to model the performance of an aircraft are increased from less than 20 in BADA 3 to more than 50 coefficients in BADA 4. The fact that BADA 4 is based on accurate manufacturer data reduces the coverage of aircraft to major airliners (Nuic *et al.*, 2005; Gallo *et al.*, 2006; Poles *et al.*, 2010).

Thus, BADA 4, when released, might be a good performance database candidate to undertake optimisations similar to the ones computed in this dissertation, whereas BADA 3 is not, as it

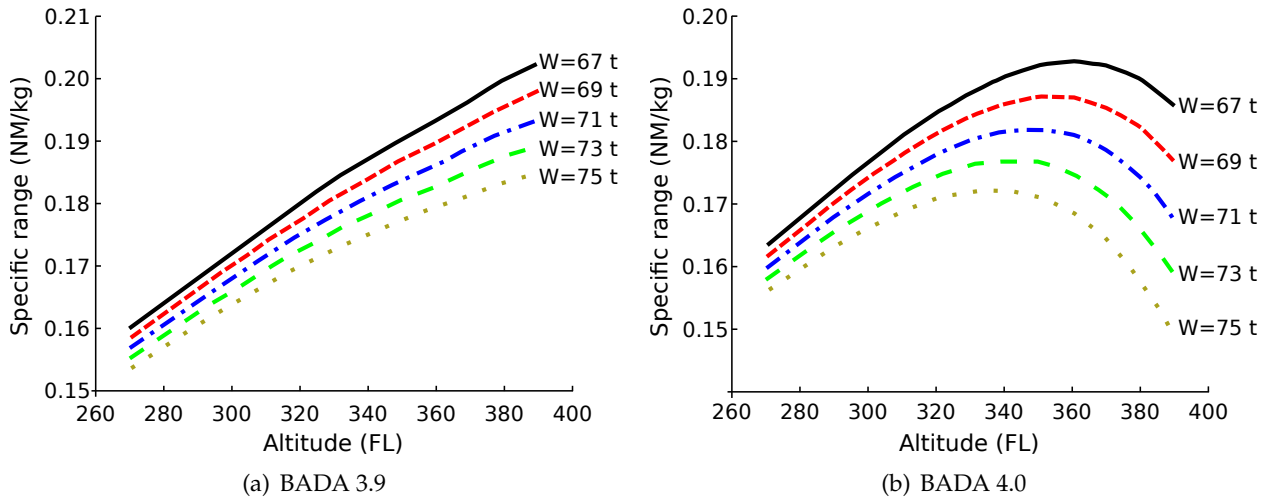


Figure B-3: Specific range as a function of altitude for typical twin engine aircraft at M0.78
 Based on: (Poles et al., 2010)

does not produce accurate information for lower speeds.



Quality of the simulations

As explained in section V.2, San Francisco International, Newark International Airport and Chicago O'Hare International are three of the airports where the most ground delay programs are implemented in the United States. They are also interesting due to their location, as different traffic patterns are observed. Thus, in chapter V the inbound traffic to these airports is analysed, applying the speed reduction strategy proposed in this thesis.

When studying GDPs, as previously presented in section V.3, the traffic only needs to be simulated twice per airport under study. Once with the flights at their nominal characteristics and once with all the aircraft flying at their equivalent speed during the cruise.

In order to obtain representative results, some of the main assumptions defined for this work include the mapping of non-Airbus aircraft to Airbus aircraft with similar performances (see table IV-2), and the assumption that all the aircraft use nominal cost index values and payload to optimise their nominal flight plan (see section IV.1.2.1). This flight plan optimisation is realised by using the Airbus Performance Engineer's Programs (PEP) suite. However, the simulations are conducted using FACET (Bilimoria *et al.*, 2000), which relies on Eurocontrol's base of aircraft data (BADA) performances. As presented in appendix B, BADA is not suitable for the type of simulations undertaken in this thesis. To overcome this, the performances of PEP suite is used during the cruise of the flight, see section IV.1.2.2. Thus, in this thesis, during the climb and descent phases the aircraft are simulated by FACET considering BADA performances, and during the cruise the flight characteristics are initialised according to the previously optimised flight plans and the PEP suite performances are used to compute the fuel consumption and the specific range equivalent speed.

In this appendix a comparison between the fuel consumption simulated with FACET, as presented in section IV.1.2.2, with the cruise simulated using the performances of PEP suite, and

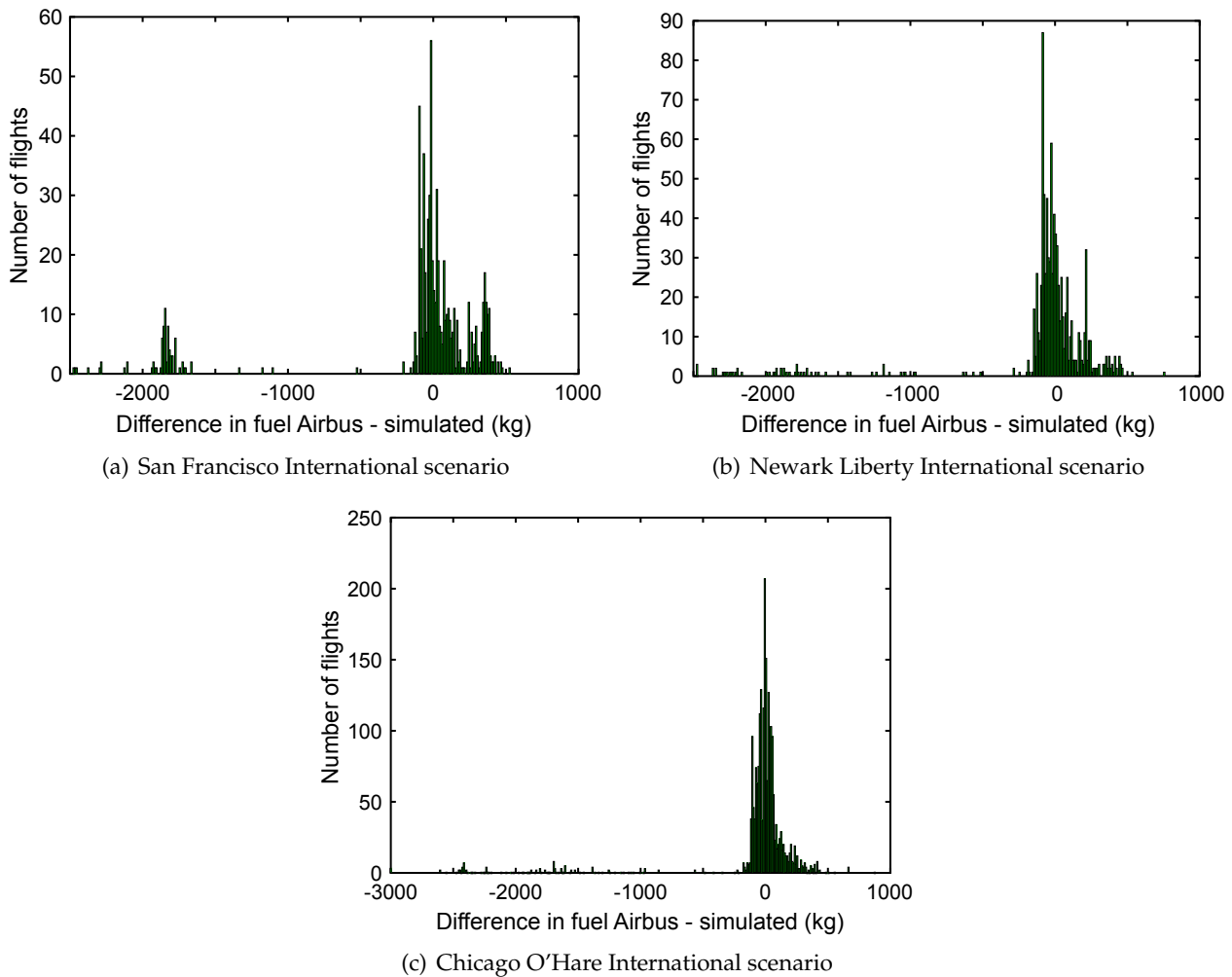


Figure C-1: Difference in total fuel burnt between Airbus PEP computation and simulation

the values of the flight plans pre-computed with Airbus PEP suite is presented. This comparison serves to validate the simulation of the nominal flight plans in FACET.

In this thesis, the August 24th and 25th, 2005 Enhanced Traffic Management System data is used to generate traffic information required to perform all the simulations. Table V-3 presents the flights that are simulated in each of the scenarios.

Figure C-1 depicts a histogram of fuel difference between the fuel planned according to the nominal flight characteristics by using Airbus PEP suite and the simulated flight in FACET, with the architecture described in section IV.1.2.2. In general the fuel computed during the simulation is very close to that planned, the majority of the flights are close to zero fuel difference. However, there are a reduced number of flights with a higher fuel consumption in the simulation, compared to the optimised flight plans. In general, these big differences are observed in flights that have a high optimal flight level according to the PEP suite. In those cases, the simulation of FACET might use a high amount of time in the climb phase and, in some cases, for very short flights, the aircraft does not reach its optimal flight level and the cruise is reduced to zero. For example, in the San Francisco International scenario, the aircraft with a higher difference in fuel consumption between the planned and the simulated is an A330 aircraft type flying from Seattle with an optimal flight level of FL410. According to the flight plan, the flight should cruise for 39 minutes, but in the simulation, due to performance during the climb phase included in BADA, the cruise is only for 13 minutes. Thus, this extra time expended in the climb implies that there is more fuel consumed than in the PEP flight plan, and the cruise is shorter. Therefore, the amount of airborne delay

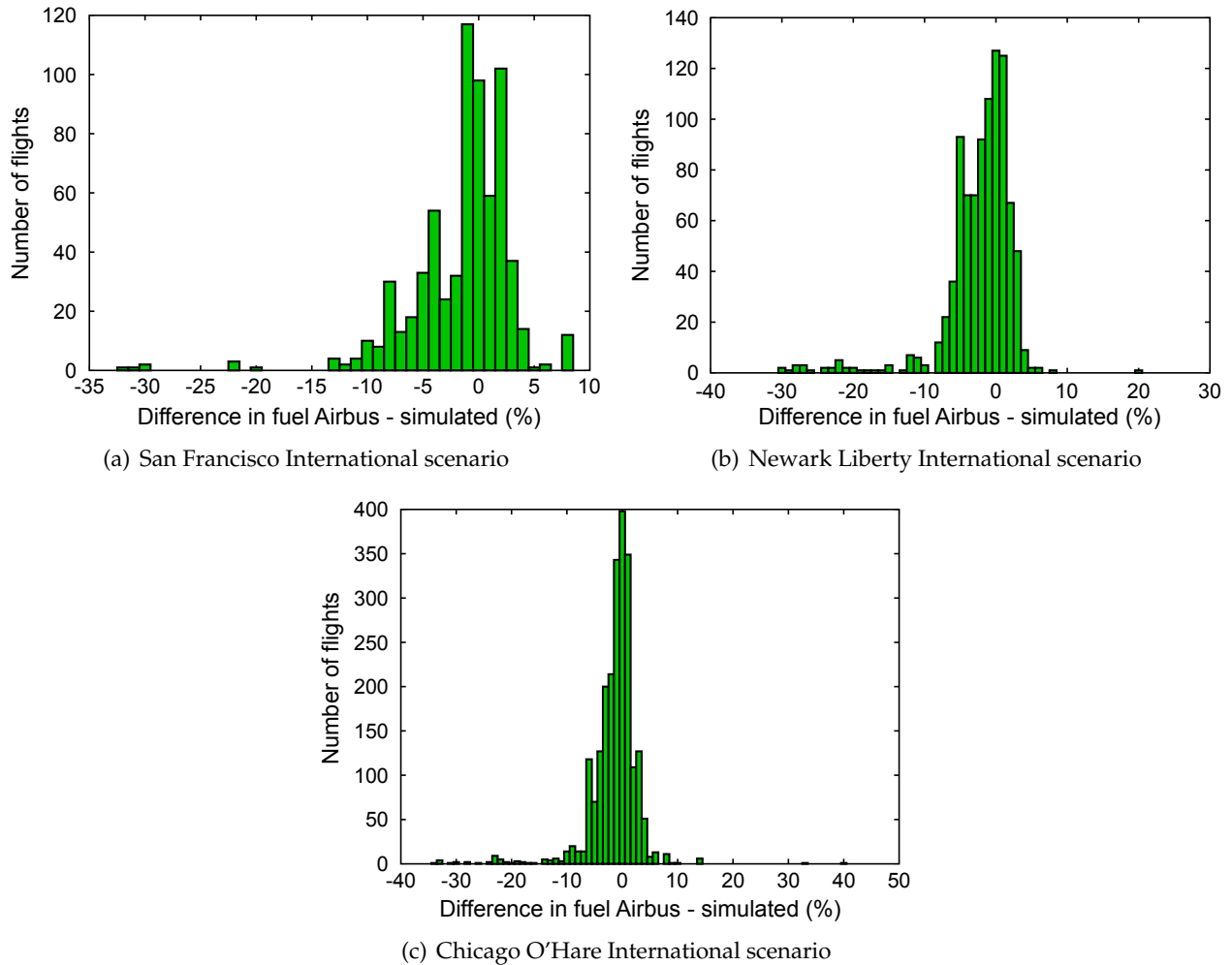


Figure C-2: *Difference in total fuel burnt between Airbus PEP computation and simulation in percentage with respect Airbus fuel*

realisable is also reduced. However, the number of flights in that situation is relatively small, only 11.7%, 6.8% and 5.5% for SFO, EWR and ORD respectively have more than -200 kg of fuel difference between the planned and the simulated flights. 69.2%, 80.3% and 87.5% for SFO, EWR and ORD respectively, of the simulated traffic has an error between ± 200 kg of fuel.

In figure C-2 the differences in fuel simulated are presented in percentage of fuel variation with respect to the fuel computed with Airbus software for the flights. As presented, the majority of the flights are in the $\pm 10\%$ of fuel difference. Only 3.3% of all the simulated flights have a difference greater than 10% in the fuel optimised with PEP and simulated (2.6% of the SFO flights, 4.8% of the EWR flights and 2.8% of the ORD ones).

The difference between the flight time computed according to the Airbus PEP suite flight plans and the simulated flight time, is presented in figure C-3. As can be observed, the differences are small with a tendency of simulated flights that are slightly longer than planned according to PEP. On average, the time difference for the three scenarios is lower than 1.7 minutes. Once again, this difference is due to the climb and descent phases simulated with FACET and helps to explain the difference observed in fuel consumption.

These studies prove the importance of using accurate performance databases and also that in nominal conditions the flight time is similar using PEP or FACET computations. In general, flights simulated with FACET tend to be slightly longer but with shorter cruises than in PEP. These flights

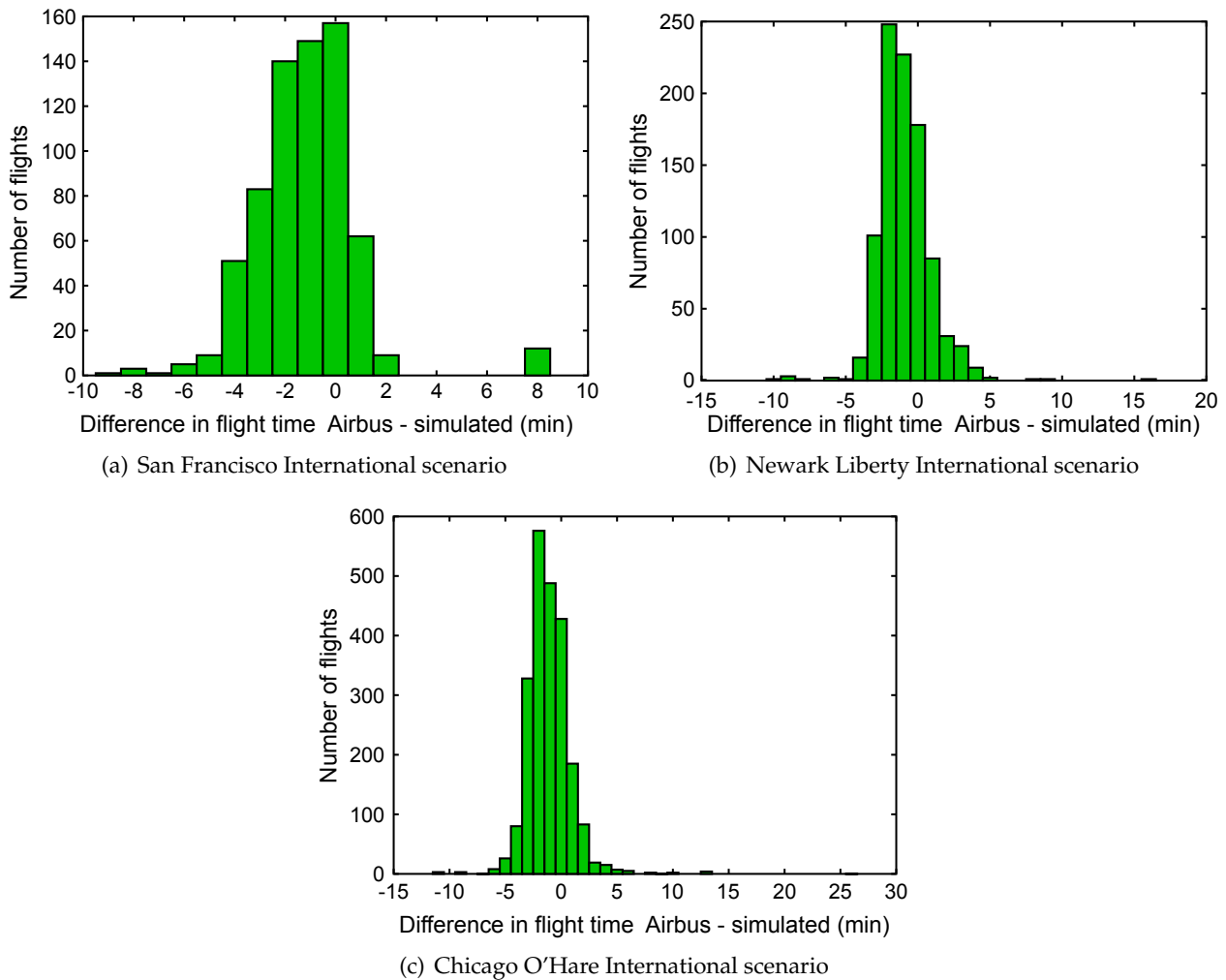


Figure C-3: Difference in total flight time between Airbus PEP computation and simulation

define what is considered the nominal flight demand in this work which has been proven to be representative of nominal optimised flights.

In order to complete the validation of the simulations, the fuel difference between flying at nominal speed and using the equivalent speed suggested in this thesis is computed. By definition, the difference between the cruise fuel used in both simulations should be zero. The results, presented in figure C-4, show that the majority of the flights (92.7% of all the flights) have an error smaller than 5%. In absolute value, the fuel differences encountered in all the simulated flights is in the order of the fuel consumption of one minute, which is the step used in the simulation process, as depicted in figure C-5. For SFO, EWR and ORD the average cruise fuel difference are 15.9 kg, 13.9 kg and 13.9 kg. Thus, the simulations of the equivalent speed are validated.

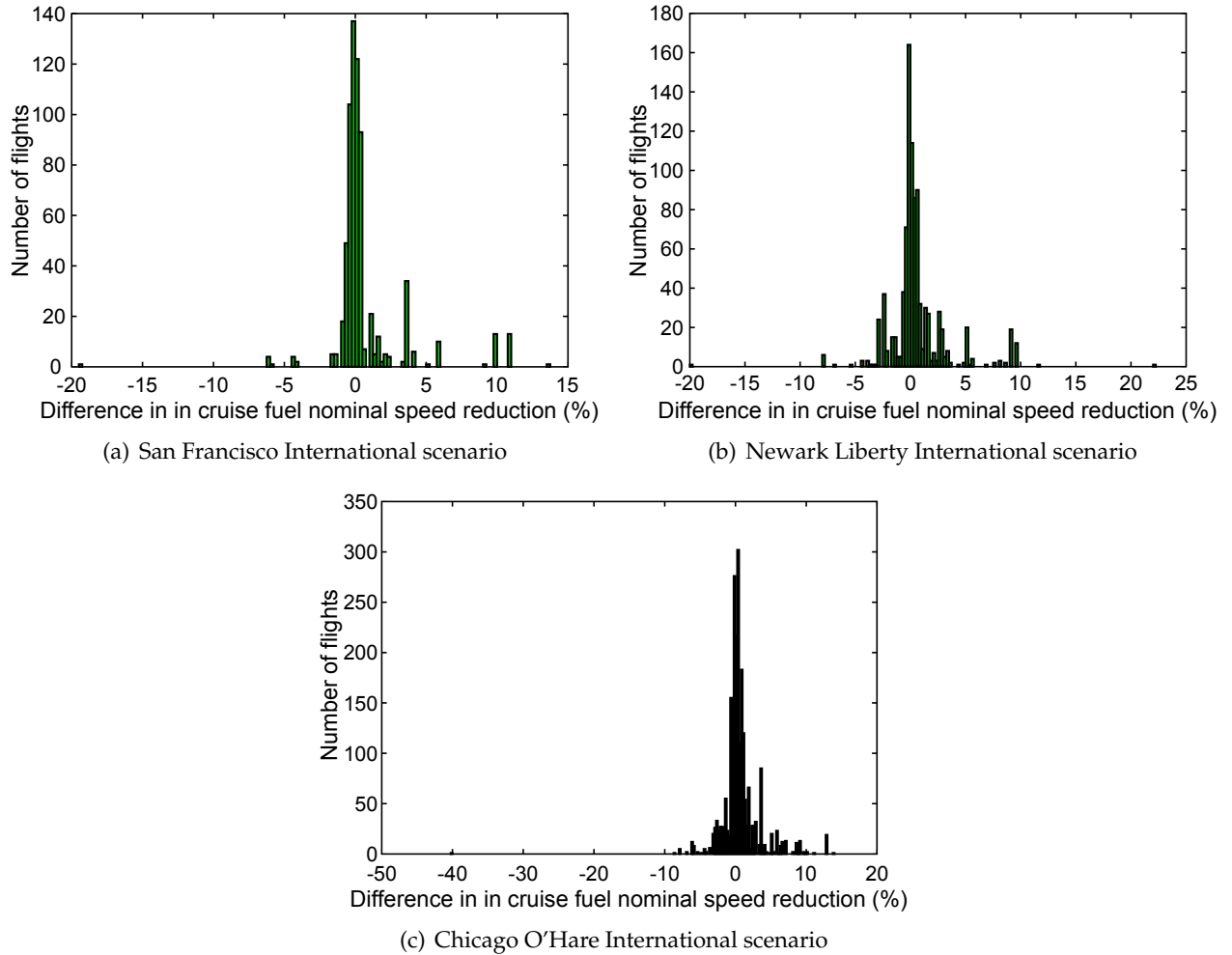
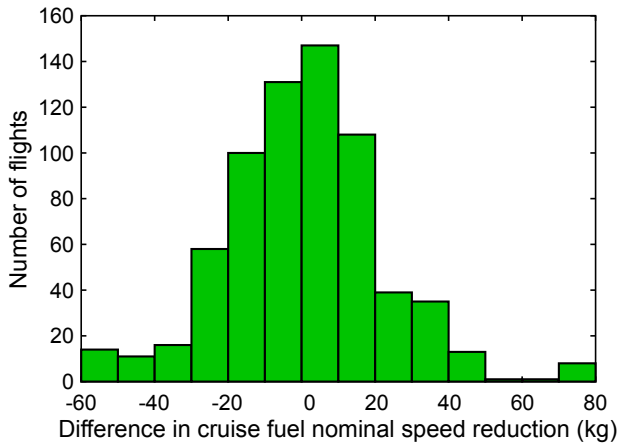
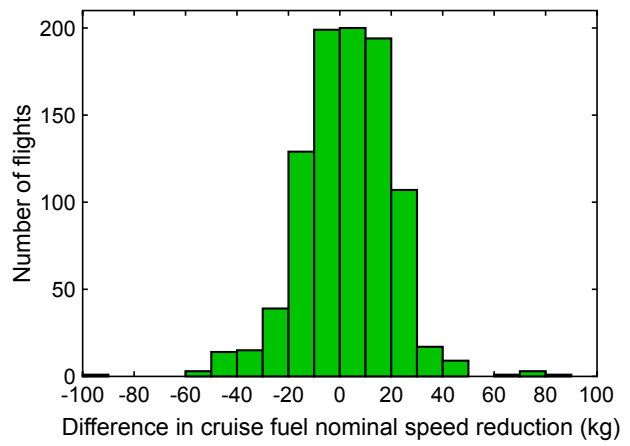


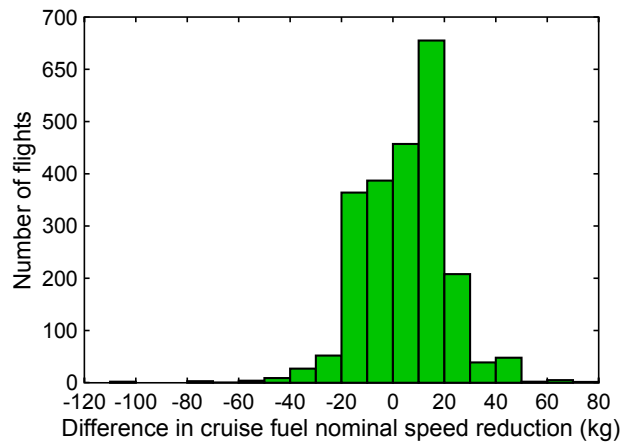
Figure C-4: *Difference in cruise fuel between simulated nominal flight and speed reduction flight in percentage with respect nominal flight*



(a) San Francisco International scenario



(b) Newark Liberty International scenario



(c) Chicago O'Hare International scenario

Figure C-5: *Difference in cruise fuel between simulated nominal flight and speed reduction flight*

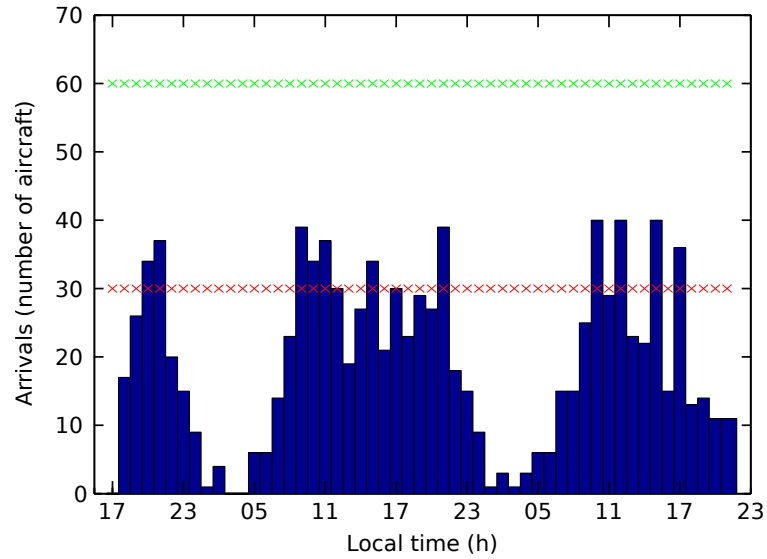
D

Application of the GDP in the analysed scenarios

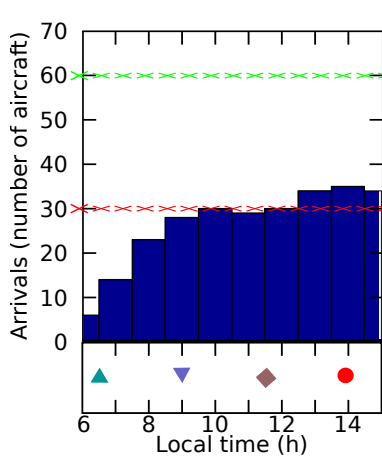
This appendix contains the figures of the aggregate demand as a function of time, for the three scenarios simulated (San Francisco International, Newark Liberty International and Chicago O'Hare airports). The reduced (PAAR) and nominal capacity (AAR) of the airport during the time each GDP is implemented is depicted for each scenario.

As presented in section II.4.1 and figure II-2, the area contained between the airport demand and capacity is the minimum delay that is needed to accommodate all the arriving traffic. And, as explained in V.3, the time when it is considered that the capacity changes from the PAAR to the AAR is computed in order to end the GDP at the time defined by the GDP clusters, computed in section V.2. Thus, in figures D-1, D-3 and D-5, the time when the capacity at the airport at an AAR rate meets the arrival demand corresponds to the GDP ending time according to the clustering.

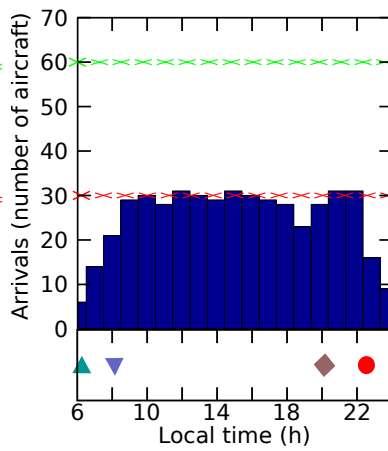
In this appendix, the histograms of the original arrival demand and the controlled arrival demand at the three airport are also presented (figures D-2, D-4 and D-6). The AAR and PAAR capacity are also depicted in those figures. It is possible to observe how the arrivals are limited during the duration of the GDP, showing the adequate assignment of delay, in order to avoid a saturation of the infrastructure.



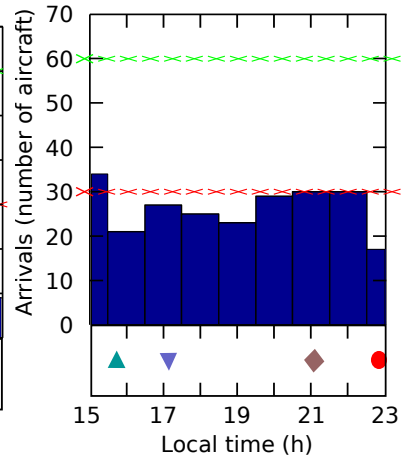
(a) Original demand



(b) Morning GDP



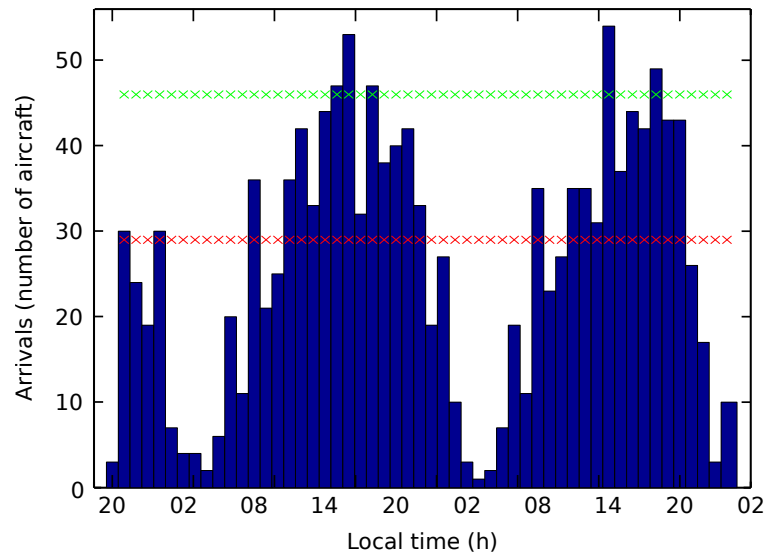
(c) All-day GDP



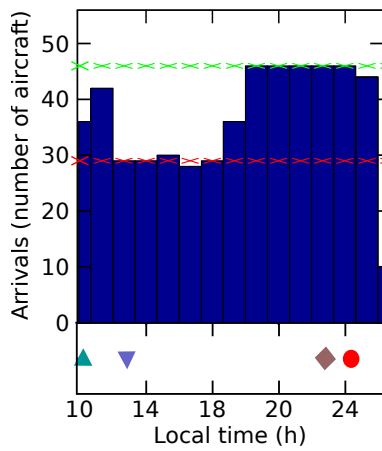
(d) Afternoon GDP



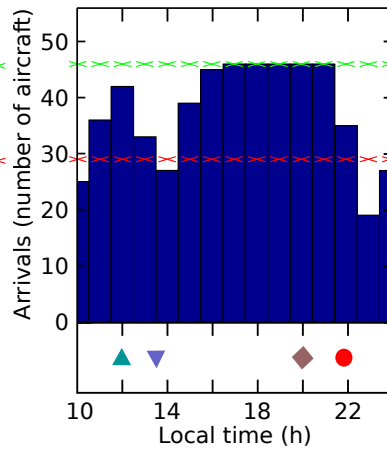
Figure D-2: Histogram demand regulated traffic San Francisco International



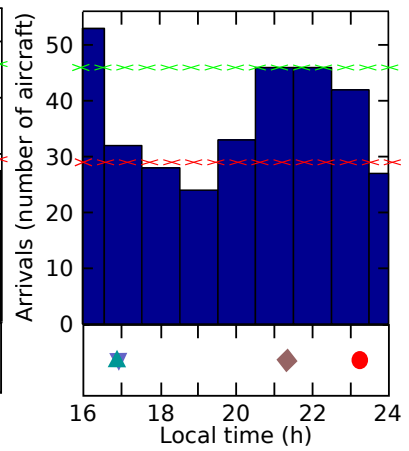
(a) Original demand



(b) All-day-night GDP



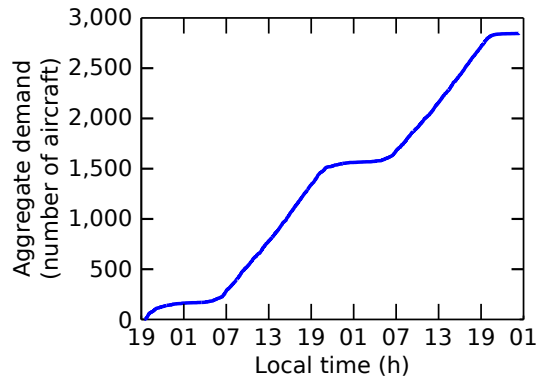
(c) All-day-evening GDP



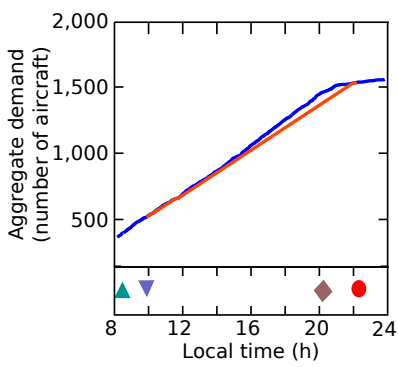
(d) Afternoon GDP

Nominal Capacity (AAR)	xxxxxxx	Filed GDP time	▲	Planned ending GDP time	●
Reduced Capacity (PAAR)	xxxxxxx	Starting GDP time	▼	Cancelled ending GDP time	◆

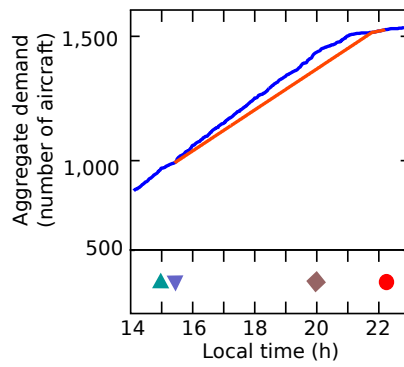
Figure D-4: Histogram demand regulated traffic Newark Liberty International



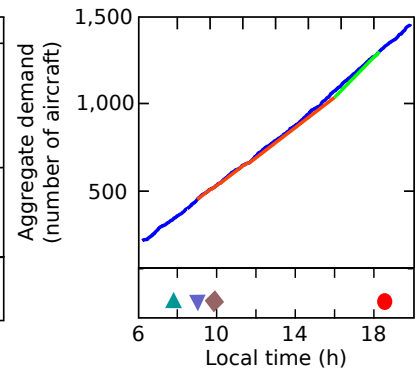
(a) Original Demand



(b) All-day GDP



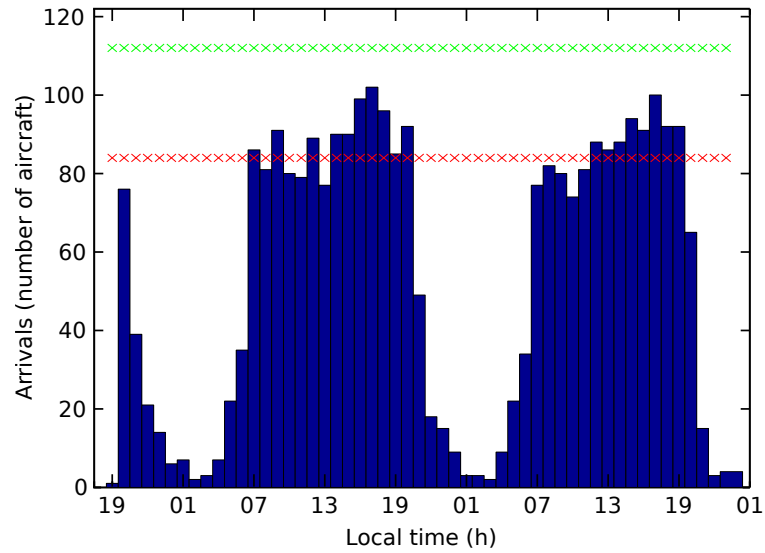
(c) Afternoon GDP



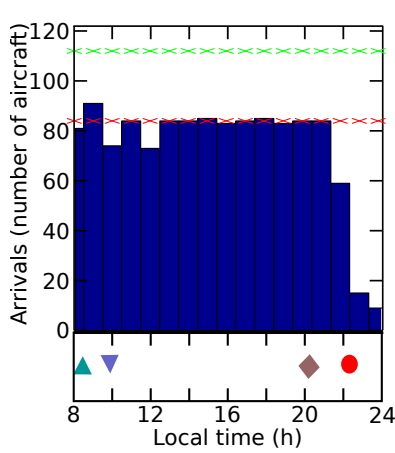
(d) Early cancel GDP



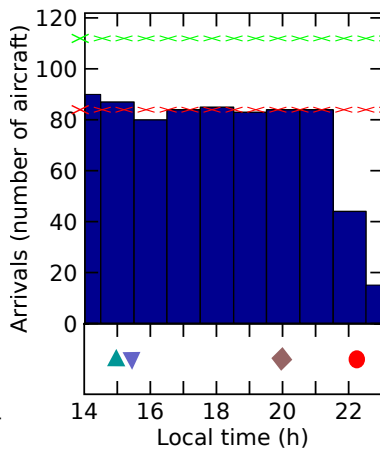
Figure D-5: Aggregated arrival demand and regulated traffic Chicago O'Hare International



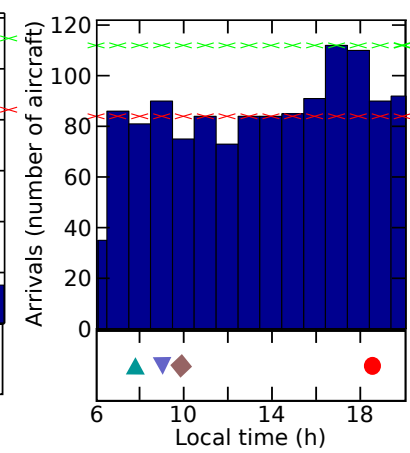
(a) Original demand



(b) All-day GDP



(c) Afternoon GDP



(d) Early cancel GDP



Figure D-6: Histogram demand regulated traffic Chicago O'Hare International

References

- AHMADBEYGI, SHERVIN, COHN, AMY, GUAN, YIHAN, & BELOBABA, PETER. 2008. Analysis of the potential for delay propagation in passenger airline networks. *Journal of air transport management*, **14**(5), 221–236. 26
- AHMADBEYGI, SHERVIN, COHN, AMY, & LAPP, MARCIAL. 2010. Decreasing airline delay propagation by re-allocating scheduled slack. *IIE transactions*, **42**(7), 478–489. 26
- AIR TRANSPORT ACTION GROUP (ATAG). 2012 (Mar.). *Aviation benefits beyond borders*. Tech. rept. Air Transport Action Group, Oxford Economics, Geneva (Switzerland). 1
- AIRBUS. 1998. *Getting to grips with the cost index*. Tech. rept. Airbus, Blagnac, France. 27, 49, 61
- AIRBUS. 2009 (May). *A320 Technical Appendices*. Tech. rept. Airbus. 46
- AIRSERVICES AUSTRALIA. 2008. *Annual Report: 2007-2008*. Tech. rept. Airservices Australia. 23
- ANDERSON, JOHN D. 2008. *Introduction to flight*. Sixth edn. 29
- ARCHAMBAULT, NICOLAS, & DURAND, NICOLAS. 2004. Scheduling heuristics for on-board sequential air conflict solving. *Pages 481–3.1–9 of: 23rd digital avionics systems conference (IEEE Cat. No.04CH37576)*, vol. 1. Salt Lake City, UT: IEEE. 16
- ATHANS, M, FALB, P., & LACOSS, R. 1963. Time-, fuel-, and energy-optimal control of nonlinear norm-invariant systems. *IEEE transactions on automatic control*, **8**(3), 196–202. 28
- AVERTLY, PHILIPPE, JOHANSSON, BJÖRN, WISE, JOHN, & CORINNE, CAPSIE. 2007 (June). Could ERASMUS speed adjustments be identifiable by air traffic controllers? *In: 7th USA/Europe air traffic management research and development seminar (ATM2007)*. 22
- BALL, MICHAEL O., & LULLI, GUGLIELMO. 2004. Ground delay programs: Optimizing over the included flight set based on distance. *Air traffic control quarterly*, **12**(1), 1–25. 16, 19, 98, 104, 112, 123, 125, 126, 127, 128
- BALL, MICHAEL O., HOFFMAN, ROBERT, CHEN, CHIEN-YU, & VOSSEN, THOMAS. 2000. *Collaborative decision making in Air Traffic Management: Current and Future Research Directions*. Tech. rept. NEXTOR - national Center of Excellence in Aviation Operations Research. 19
- BALL, MICHAEL O., HOFFMAN, ROBERT, ODONI, AMEDEO R., & RIFKIN, RYAN. 2003. A Stochastic Integer Program with Dual Network Structure and Its Application to the Ground-Holding Problem. *Operations research*, **51**(1), 167–171. 17
- BALL, MICHAEL O., BARNHART, CYNTHIA, NEMHAUSER, GEORGE L., & ODONI, AMEDEO R. 2007. Chapter 1 Air Transportation: Irregular Operations and Control. *Pages 1–67 of: BARNHART, CYNTHIA, & LAPORTE, GILBERT (eds), Transportation*. Handbooks in Operations Research and Management Science, vol. 14. Elsevier. 13, 14

- BALL, MICHAEL O., HOFFMAN, R., & MUKHERJEE, A. 2010a. Ground Delay Program Planning Under Uncertainty Based on the Ration-by-Distance Principle. *Transportation science*, **44**(1), 1–14. 3, 8, 19, 106, 108, 113, 128, 129
- BALL, MICHAEL O., BARNHART, CYNTHIA, DRESNER, MARTIN, NEELS, KEVIN, ODoni, AMEDEO, PETERSON, EVERETT, SHERRY, LANCE, TRANI, ANTONIO, ZOU, BO, BRITTO, RODRIGO, FEARING, DOUG, SWAROOP, PREM, UMAN, NITISH, VAZE, VIKRANT, & VOLTES, AUGUSTO. 2010b (Oct.). *Total Delay Impact Study – A comprehensive assessment of the cost and impacts of flight delay in the United States*. Tech. rept. Nextor - National Centre of Excellence for Aviation Operations Research. 3, 4, 129
- BARNHART, C., BERTSIMAS, D., CARAMANIS, C., & FEARING, D. 2012. Equitable and Efficient Coordination in Traffic Flow Management. *Transportation science*, **46**(2), 262–280. 18
- BARNHART, CYNTHIA, KNIKER, TIMOTHY S., & LOHATEPANONT, MANOJ. 2002. Itinerary-Based Airline Fleet Assignment. *Transportation science*, **36**(2), 199–217. 26
- BARNIER, NICOLAS, & ALLIGNOL, CYRIL. 2008. Deconfliction with Constraint Programming. In: *International workshop on constraint programming for air traffic control & management*. 18
- BARNIER, NICOLAS, & ALLIGNOL, CYRIL. 2009 (June). 4D-Trajectory Deconfliction Through Departure Time Adjustment. In: *8th USA/Europe air traffic management research and development seminar (ATM2009)*. 18
- BARNIER, NICOLAS, BRISSET, PASCAL, & RIVIÈRE, THOMAS. 2001 (Dec.). Slot allocation with constraint programming: models and results. In: *4th USA/Europe air traffic management research and development seminar (ATM2001)*. 18
- BARRER, JONH N., KUZMINSKI, PETER, & SWEDISH, WILLIAM J. 2005 (Nov.). *Analyzing the runway capacity of complex airports*. Tech. rept. MITRE - American Institute of Aeronautics and Astronautics. 13
- BAYEN, ALEXANDRE M, GRIEDER, PASCAL, MEYER, GEORGE, & TOMLIN, CLAIRE J. 2005. Lagrangian Delay Predictive Model for Sector-Based Air Traffic Flow. *Journal of guidance, control, and dynamics*, **28**(5), 1015–1026. 15
- BEASLEY, J E, SONANDER, J, & HAVELOCK, P. 2001. Scheduling aircraft landings at London Heathrow using a population heuristic. *Journal of the operational research society*, **52**(5), 483–493. 13
- BENJAMIN, STANLEY G., BROWN, JOHN M., BRUNDAGE, KEVIN J., DEVENYI, DEZSO, GRELL, GEORG A., KIM, DONGSOON, TATIANA, G. SMIRNOVA, SMITH TRACY, LORRAINE, SCHWARTZ, BARRY E., WEYGANDT, STEPHEN S., & MANIKIN, GEOFFREY S. 2002 (May). The 20-km Rapid Update Cycle - Overview and Implications for Aviation Applications. In: *10th conference on aviation, range, and aerospace meteorology*. 68
- BERTSIMAS, D., FARIAS, V. F., & TRICHAKIS, N. 2011. The Price of Fairness. *Operations research*, **59**(1), 17–31. 18
- BERTSIMAS, DIMITRIS, & PATTERSON, SARAH STOCK. 1998. The Air Traffic Flow Management Problem with Enroute Capacities. *Operations research*, **46**(3), 406–422. 17, 23
- BERTSIMAS, DIMITRIS, & PATTERSON, SARAH STOCK. 2000. The Traffic Flow Management Rerouting Problem in Air Traffic Control: A Dynamic Network Flow Approach. *Transportation science*, **34**(3), 239–255. 17, 23
- BERTSIMAS, DIMITRIS J, LULLI, GUGLIELMO, & ODoni, AMADEO. 2008. The air traffic flow management problem: an integer optimization approach. Pages 34–46 of: *3th international conference on integer programming and combinatorial optimization (IPCO2008)*. Berlin: Springer-Verlag. 17
- BICHOT, CHARLES-EDMOND. 2006 (June). Airspace block organization with metaheuristics and partitioning packages. In: *2nd international conference on research in air transportation (ICRAT2006)*. 13
- BICHOT, CHARLES-EDMOND, & DURAND, NICOLAS. 2007 (July). A tool to design Functional Airspace Blocks. In: *7th USA/Europe air traffic management research and development seminar (ATM2007)*. 13
- BILIMORIA, KARL D, SRIDHAR, BANAVAR, CHATTERJI, GANO B, SHETH, KAPIL S, & GRABBE, SHON. 2000. FACET: Future ATM Concepts Evaluation Tool. *Air traffic control quarterly*, **9**(1), 1–20. 48, 135
- BLUMSTEIN, A. 1959. The Landing Capacity of a Runway. *Operations research*, **7**(6), 752–763. 13

- BOEING. 2007. *Fuel conservation strategies: cost index explained*. Tech. rept. Boeing, Seattle, Washington (USA). 27, 28
- BOEING, & CANSO. 2012 (Feb.). *Accelerating Air Traffic Management Efficiency: A Call to Industry – ATM Global Environment Efficiency Goals for 2050*. Tech. rept. 23
- BRITTON, ERIK, COOPER, ADRIAN, & TINSLEY, DAVID. 2005 (Oct.). *The economic catalytic effects of air transport in Europe*. Tech. rept. Association for European Transport, Strasbourg, France. 1
- BRUNET, M, DELAHAYE, D, TOBBEN, H, HELMKE, H, & HECKER, P. 2005. New air/ground function sharing in a future air transport system concept. In: *Colloque international "aircraft and ATM automation"*. 22
- BRUNETTA, LORENZO, GUASTALLA, GUGLIELMO, & NAVAZIO, LISA. 1998. Solving the multi-airport Ground Holding Problem. *Annals of operations research*, 81(0), 271–288. 17
- BUTLER, VIGGO, & POOLE JR., ROBERT W. 2008 (Mar.). *Increasing Airport Capacity Without Increasing Airport Size*. Tech. rept. Reason Foundation, Los Angeles, California (USA). 13
- CALINSKI, T., & HARABASZ, J. 1974. A dendrite method for cluster analysis. *Communications in statistics - theory and methods*, 3(1), 1–27. 83
- CANO, MAYTE, DORADO, MANUEL M, & SÁNCHEZ-ESCALONILLA, PABLO. 2007. Complexity analysis in the next generation of air traffic management system. *Pages 3.D.4–1–3.D.4–9 of: IEEE/AIAA 26th digital avionics systems conference*. IEEE. 15
- CANSO. 2011. *Airspace No.14 – Quarter 3*. Tech. rept. CANSO – the Civil Air Navigation Services Organisation. 5, 23
- CANSO ENVIRONMENTAL WORKGROUP. 2012. *Whitepaper Speed Control in Cruise to Manage Terminal Congestion*. Unpublished. 23
- CARLIER, SANDRINE, DE LÉPINAY, IVAN, HUSATCHE, JEAN-CLAUDE, & JELINEK, FRANK. 2007 (July). Environmental impact of air traffic flow management delays. In: *7th USA/Europe air traffic management research and development seminar (ATM2007)*. 2, 16
- CASTELLI, LORENZO, PESENTI, RAFFAELE, & RANIERI, ANDREA. 2011. The design of a market mechanism to allocate Air Traffic Flow Management slots. *Transportation research part C: Emerging technologies*, 19(5), 931–943. 18, 82
- CATS CONSORTIUM. 2007 (Nov.). Alignment with the SESAR programme, Contract-Based Air Transportation System CATS. In: *2nd ATM research and development projects, co-ordination and networking meeting*. 22
- CAVCAR, AYDAN, & CAVCAR, MUSTAFA. 2004. Impact of Aircraft Performance Characteristics on Air Traffic Delays. *Aircraft engineering and aerospace technology - TBC Journal*, 28, 13 – 23. 15
- CHALOULOS, GEORGIOS, CRÜCK, EVA, & LYGEROS, JOHN. 2010. A simulation based study of subliminal control for air traffic management. *Transportation research part C: Emerging technologies*, 18(6), 963–974. 22
- CHIANG, YI-JEN, KLOSOWSKI, J.T., LEE, CHANGKIL, & MITCHELL, J.S.B. 1997. Geometric algorithms for conflict detection/resolution in air traffic management. *Pages 1835–1840 of: Proceedings of the 36th IEEE conference on decision and control*, vol. 2. San Diego, California: IEEE. 16
- CONKER, ROBERT S, MOCH-MOONEY, DEBRA A, NIEDRINGHAUS, WILLIAM P, & SIMMONS, BRIAN T. 2007 (July). New process for "clean sheet" airspace design and evaluation. In: *7th USA/Europe air traffic management research and development seminar (ATM2007)*. 13
- COOK, ANDREW, & TANNER, GRAHAM. 2009. The challenge of managing airline delay costs. In: *Proceedings of the conference on air traffic management (ATM) economics*. Belgrade (Serbia): German Aviation Research Society and University of Belgrade, Faculty of Transport and Traffic Engineering. 7
- COOK, ANDREW, TANNER, GRAHAM, WILLIAMS, VICTORIA, & MEISE, GERHARD. 2009. Dynamic cost indexing – Managing airline delay costs. *Journal of air transport management*, 15(1), 26–35. 6, 8, 18, 29, 46
- COOK, LARA S., & WOOD, BRYAN. 2010. A Model for Determining Ground Delay Program Parameters Using a Probabilistic Forecast of Stratus Clearing. *Air traffic control quarterly*, 18(1). 4, 73, 84

- DAY, WILLIAM H. E., & EDELSBRUNNER, HERBERT. 1984. Efficient algorithms for agglomerative hierarchical clustering methods. *Journal of classification*, **1**(1), 7–24. 83
- DEAR, ROGER G., & SHERIF, YOSEF S. 1991. An algorithm for computer assisted sequencing and scheduling of terminal area operations. *Transportation research part A: General*, **25**(2-3), 129–139. 13
- DELAHAYE, DANIEL, PUECHMOREL, S, HANSMAN, J, & HISTON, J. 2004. Air Traffic Complexity Map Based on Non Linear Dynamical Systems. *Air traffic control quarterly*, **12**(4), 367–388. 15
- DEVASIA, SANTOSH, IAMRATANAKUL, DHANAKORN, CHATTERJI, GANO, & MEYER, GEORGE. 2011. Decoupled Conflict-Resolution Procedures for Decentralized Air Traffic Control. *IEEE transactions on intelligent transportation systems*, **12**(2), 422–437. 16
- DONOHUE, GEORGE, & LASKA, WILLIAM D. 2000 (June). United States and European Airport Capacity Assessment using the GMU Macroscopic Capacity Model (MCM). *Pages 13–16 of: 3rd USA/Europe air traffic management research and development seminar (ATM2000)*. 15
- DRAVECKA, LENKA. 2006 (Sept.). Operational feasibility of traffic synchronisation in central europe - results. *In: 25th congress of the international council of the aeronautical sciences (ICAS2006)*. ICAS, Hamburg, Germany. 24
- DURAND, NICOLAS, & ALLIOT, JEAN-MARC. 1995 (Oct.). Automatic Air Conflict Resolution Using Genetic Algorithms. *In: 11th annual ACM conference on applied computing (ACM/SAC)*. 16
- DURAND, NICOLAS, & ALLIOT, JEAN-MARC. 2009 (June). Ant Colony for Air Traffic Conflict Resolution. *In: 8th USA/Europe air traffic management research and development seminar (ATM2009)*. 16
- EBY, M.S., & KELLY, W.E. 1999. Free flight separation assurance using distributed algorithms. *Pages 429–441 vol.2 of: IEEE aerospace conference. proceedings (Cat. No.99TH8403)*. Snowmass at Aspen, CO: IEEE. 16
- EHRGOTT, MATTHIAS, & RYAN, DAVID M. 2002. Constructing robust crew schedules with bicriteria optimization. *Journal of multi-criteria decision analysis*, **11**(3), 139–150. 26
- ELFAA - EUROPEAN LOW FARES ASSOCIATION MEMBERS. 2008. *Members' statistics*. Tech. rept. European low fares association members. 46, 49, 61
- ELHEDHLI, SAMIR, & HU, FRANK XIAOLONG. 2005. Hub-and-spoke network design with congestion. *Computers & operations research*, **32**(6), 1615–1632. 12
- ENDLICH, R. M., & MCLEAN, G. S. 1957. The Structure of the Jet Stream Core. *Journal of meteorology*, **14**(6), 543–552. 40, 63
- ERASMUS CONSORTIUM. 2007. *ERASMUS - Concept of Operations - V2*. 6 Framework Programme. 7, 22
- EUROCONTROL. 2008a (Mar.). *Network Operations Report 2008 - Indicators and analysis of the ATM Network Operations Performance*. Tech. rept. March. Eurocontrol. 3
- EUROCONTROL. 2008b. *Network Operations Report Summer 2008*. Eurocontrol. 2
- EUROCONTROL. 2009a. *CFMU ATFCM Public Report December 2008*. Eurocontrol. 3, 16, 18
- EUROCONTROL. 2009b (Jan.). *EUROCONTROL Specification for the application of the Flexible Use of Airspace (FUA)*. Tech. rept. Eurocontrol. 13
- EUROCONTROL. 2012 (Sept.). *Central Flow Management Unit (CFMU)*. <http://www.cfmueurocontrol.int>. 2
- EUROCONTROL - STATFOR. 2008 (Nov.). *Challenges of Growth 2008 - Summary Report*. Tech. rept. Eurocontrol, Brussels (Belgium). 12
- EUROCONTROL - STATFOR. 2010 (Dec.). *Long-Term Forecast – Flight Movements 2010 - 2030*. Tech. rept. Eurocontrol, Brussels (Belgium). 1, 2
- EUROCONTROL - STATFOR. 2012 (Feb.). *Medium-Term Forecast – Flight Movements 2012-2018*. Tech. rept. February. Eurocontrol, Brussels (Belgium). 1
- EUROCONTROL CENTRAL FLOW MANAGEMENT UNIT. 2011. *Basic CFMU Handbook - General & CFMU Systems*. 15 edn. Eurocontrol. 18
- EUROCONTROL EXPERIMENTAL CENTRE. 2011a (June). *Coverage of 2010 European air traffic for the base of aircraft data (BADA) - Revision 3.9*. Tech. rept. Eurocontrol, Bretigny sur Orge (France). 131

- EUROCONTROL EXPERIMENTAL CENTRE. 2011b (Apr.). *User manual for the Base of Aircraft Data (BADA) revision 3.9*. Tech. rept. Eurocontrol, Bretigny sur Orge (France). 9, 50, 131
- EUROPEAN AVIATION SAFETY AGENCY. 2011. *Certification Specifications and Acceptable Means of Compliance for Large Aeroplanes CS-25*. 11 edn. European Aviation Safety Agency. 9
- EUROPEAN COUNCIL. 1991. *Council Regulation (EEC) No 3922/91 on the harmonisation of technical requirements and administrative procedures in the field of civil aviation, EU-OPS*. European Council. 46, 49
- EUROPEAN COUNCIL. 2009. *Council Regulation (EEC) No 95/93 of 18 January 1993 on common rules for the allocation of slots at Community airports*. 2
- FABEC. 2012 (Dec.). *FABEC - newsletter N°17*. Tech. rept. 22
- FAN, HENRY S. L. 1992. Effect of local operational constraints on runway capacity - A case study. *Journal of advanced transportation*, 26(2), 169–184. 13
- FEDERAL AVIATION ADMINISTRATION. 1983 (Sept.). *Airport Capacity and Delay*. Tech. rept. Federal Aviation Administration. 13
- FEDERAL AVIATION ADMINISTRATION. 2012a. *Aeronautical Information Manual – Official Guide to Basic Flight Information and ATC Procedures*. Page 726 of: AIM 4-3-11. Washington, DC. USA: Federal Aviation Administration. 15
- FEDERAL AVIATION ADMINISTRATION. 2012b (Oct.). *Air Traffic Control System Command Center*. <http://www.fly.faa.gov/>. 123
- FEDERAL AVIATION ADMINISTRATION. 2012c (Oct.). *Air Traffic Control System Command Center - Airport Arrival Demand Chart*. <http://www.fly.faa.gov/products/aadc/aadc.html>. 128
- FEDERAL AVIATION ADMINISTRATION. 2012d (Sept.). *Chicago O'Hare International Airport (ORD) Acceptance Rate*. http://www.fly.faa.gov/information/west/zau/ord/ord_aar1.htm. 86
- FEDERAL AVIATION ADMINISTRATION. 2012e (Sept.). *Newark Liberty International Airport (EWR) Acceptance Rate*. http://www.fly.faa.gov/information/east/zny/ewr/ewr_aar.htm. 86
- FEDERAL AVIATION ADMINISTRATION. 2012f (Sept.). *NextGen*. <http://www.faa.gov/about/initiatives/nextgen>. 4
- FEDERAL AVIATION ADMINISTRATION. 2012g (Sept.). *San Francisco International Airport (SFO) Acceptance Rate*. http://www.fly.faa.gov/information/west/zoa/sfo/sfo_aar.htm. 14, 85
- FERNANDES, ELTON, & PACHECO, R.R. 2002. Efficient use of airport capacity. *Transportation research part A: Policy and practice*, 36(3), 225–238. 13
- FILAR, JERZY A., MANYEM, PRABHU, & WHITE, KEVIN. 2002. How Airlines and Airports Recover from Schedule Perturbations: A Survey *. *Annals of operations research*, 108(1-4), 315–333. 17
- GALLO, EDUARDO, NAVARRO, FRANCISCO, NUIC, ANGELA, & IAGARU, MIHAI. 2006. Advanced Aircraft Performance Modeling for ATM: BADA 4.0 Results. *Pages 1–12 of: IEEE/AIAA 25th digital avionics systems conference*. Portland, OR: IEEE. 50, 133
- GARCIA, J L, & GAWINOWSKI, G. 2006. ERASMUS - The Concept of Operation and Initial Modelling Results. *In: 5th Eurocontrol innovative research workshop & exivition*. 22
- GIANAZZA, DAVID. 2007 (July). Airspace configuration using air traffic complexity metrics. *In: 7th USA/Europe air traffic management research and development seminar (ATM2007)*. DSN, Barcelona (Spain). 13
- GIANAZZA, DAVID. 2010. Forecasting workload and airspace configuration with neural networks and tree search methods. *Artificial intelligence*, 174(7-8), 530–549. 15
- GIANAZZA, DAVID, & DURAND, NICOLAS. 2005 (June). Assessment of the 3D-separation of Air Traffic Flows. *In: 6th USA/Europe air traffic management research and development seminar (ATM2005)*. 13
- GIANAZZA, DAVID, & GUITTET, KEVIN. 2006. Selection and Evaluation of Air Traffic Complexity Metrics. *Pages 1–12 of: IEEE/AIAA 25th digital avionics systems conference*. Portland, OR: IEEE. 15

- GIANAZZA, DAVID, ALLIGNOL, CYRIL, & SAPORITO, NICOLAS. 2009 (June). An efficient airspace configuration forecast. *In: 8th USA/Europe air traffic management research and development seminar (ATM2009)*. 15
- GILBO, E.P. 1993. Airport capacity: representation, estimation, optimization. *IEEE transactions on control systems technology*, **1**(3), 144–154. 13
- GILBO, E.P. 1997. Optimizing airport capacity utilization in air traffic flow management subject to constraints at arrival and departure fixes. *IEEE transactions on control systems technology*, **5**(5), 490–503. 13
- GLOVER, CHARLES N., & BALL, MICHAEL O. 2012. Stochastic optimization models for ground delay program planning with equity-efficiency tradeoffs. *Transportation research part C: Emerging technologies, In Press*(Feb.). 17
- GOPALAKRISHNAN, BALAJI, & JOHNSON, ELLIS. L. 2005. Airline Crew Scheduling: State-of-the-Art. *Annals of operations research*, **140**(1), 305–337. 26
- GRANGER, GÉRAUD, DURAND, NICOLAS, & ALLIOT, JEAN-MARC. 2001 (Dec.). Optimal resolution of en route conflicts. *Page 11 of: 4th USA/Europe air traffic management research and development seminar (ATM2001)*. 16
- GROVE, PETER G., & O'KELLY, MORTON E. 2005. Hub Networks and Simulated Schedule Delay. *Papers in regional science*, **59**(1), 103–119. 12
- GUIBERT, SANDRINE, GUICHARD, LAURENT, RIHACEK, CHRISTOPH, CASTELLI, LORENZO, & RANIERI, ANDREA. 2008. Contract-based air transportation system to fulfil the arriving-on-time objective. *In: 6th international congress of the aeronautical sciences*. 22
- GÜNTHER, THOMAS, & FRICKE, HARTMUT. 2006 (June). Potential of Speed Control on Flight Efficiency. *Pages 197–201 of: 2nd international conference on research in air transportation (icrat)*, vol. 1. 22
- GWIGGNER, C, KAGEYAMA, K, & NAGAOKA, S. 2008 (June). Propagation of airspace congestion. An exploratory correlation analysis. *In: 3rd international conference on research in air transportation (ICRAT2008)*. 16
- HARVEY, A., & COSTELLO, C. 2000 (Dec.). *EATCHIP III Evaluation and Demonstration PHASE 3 Project Experiment 3ABis: MTCD – Final Report*. Tech. rept. Eurocontrol Experimentnal Centre, Bretigny sur Orge (France). 15
- HINTON, D.A., & O'CONNOR, C.J. 2000. Development of a wake vortex spacing system for airport capacity enhancement and delay reduction. *Pages 3E6/1 – 3E610 vol.1 of: 19th digital avionics systems conference*. Hinton, D.A.: IEEE. 13
- HOFFMAN, ROBERT, & BALL, MICHAEL O. 2000. A Comparison of Formulations for the Single-Airport Ground-Holding Problem with Banking Constraints. *Operations research*, **48**(4), 578–590. 17
- HOFFMAN, ROBERT, BALL, MICHAEL O., & MUKHERJEE, AVIJIT. 2007 (July). Ration-by-distance with equity guarantees: a new approach to ground delay program planning and control. *In: 7th USA/Europe air traffic management research and development seminar (ATM2007)*. 19, 108, 128
- HUANG, H., & TOMLIN, C. 2009 (Aug.). A Network-Based Approach to En-Route Sector Aircraft Trajectory Planning. *In: AIAA guidance, navigation and control conference*. 22
- INNISS, TASHA R., & BALL, MICHAEL O. 2002. *Estimating One-Parameter Airport Arrival Capacity Distributions for Air Traffic Flow Management*. Tech. rept. The National Center of Excellence for Aviation Operations Research (NEXTOR). 4, 14
- INTERGOVERNMENTAL PANEL ON CLIMATE CHANGE. 1999. *Aviation and the global atmosphere*. Tech. rept. Intergovernmental Panel on Climate Change. 1
- JAIN, ANIL K. 2010. Data clustering: 50 years beyond K-means. *Pattern recognition letters*, **31**(8), 651–666. 83
- JANIĆ, MILAN. 1997. A model of air traffic control sector capacity based on air traffic controller workload. *Transportation planning and technology*, **20**(4), 311–335. 15
- JANIĆ, MILAN. 2008. Modelling the capacity of closely-spaced parallel runways using innovative approach procedures. *Transportation research part C: Emerging technologies*, **16**(6), 704–730. 4, 14, 85

- JARDIN, MATT R. 2004. Air Traffic Conflict Models. *Page 13 of: AIAA 4th aviation technology, integration and operations (ATIO) forum*. Chicago, IL: AIAA. 16
- KAISER, MICHAEL, SHULTZ, MICHAEL, & FRICKE, HARTMUT. 2011 (May). Enhanced Jet Performance Model for High Precision 4D Flight Path Prediction. *Pages 33–40 of: ATACCS*. 35
- KLABJAN, DIEGO, JOHNSON, ELLIS L., NEMHAUSER, GEORGE L., GELMAN, ERIC, & RAMASWAMY, SRINI. 2001. Airline Crew Scheduling with Regularity. *Transportation science*, **35**(4), 359–374. 26
- KLABJAN, DIEGO, JOHNSON, ELLIS L., NEMHAUSER, GEORGE L., GELMAN, ERIC, & RAMASWAMY, SRINI. 2002. Airline Crew Scheduling with Time Windows and Plane-Count Constraints. *Transportation science*, **36**(3), 337–348. 26
- KNORR, DAVE, CHEN, XING, ROSE, MARC, GULDING, JOHN, ENAUD, PHILIPPE, & HEGENDOERFER, HOLGER. 2011 (June). Estimating ATM Efficiency Pools in the Descent Phase of Flight. *In: 9th USA/Europe air traffic management research and development seminar (ATM2011)*. 5, 16, 23
- KOOSTER, JOEL K., DEL AMO, ANA, & MANZI, PATRICK. 2009 (June). Controlled Time-of-Arrival Flight Trials. *In: 8th USA/Europe air traffic management research and development seminar (ATM2009)*. 22
- KOPARDEKAR, PARIMAL, RHODES, JESSICA, SCHWARTZ, ALBERT, MAGYARITS, SHERRI, & WILLEMS, BEN. 2008. Relationship of maximum manageable air traffic control complexity and sector capacity. *In: 26th international congress of the aeronautical sciences*. 15
- KORN, BERND, & KUENZ, ALEXANDER. 2006. 4D FMS for Increasing Efficiency of TMA Operations. *In: IEEE/AIAA 25th digital avionics systems conference*. Portland, OR: IEEE. 21
- KOŠECKÁ, J., TOMLIN, C., PAPPAS, G., & SASTRY, S. 1997. Generation of conflict resolution manoeuvres for air traffic management. *Pages 1598–1603 of: Proceedings of the 1997 IEEE/RSJ international conference on intelligent robot and systems. innovative robotics for real-world applications. (IROS1997)*, vol. 3. Grenoble: IEEE. 16
- KUCHAR, J.K., & YANG, L.C. 2000. A review of conflict detection and resolution modeling methods. *IEEE transactions on intelligent transportation systems*, **1**(4), 179–189. 16
- LE TALLEC, CLAUDE, & JOULIA, ANTOINE. 2007 (May). IFATS: 4D contracts in 4D airspace. *In: Proceedings of the infotech and aerospace conference and exhibit*. 22
- LECCHINI VISINTINI, ANDREA, GLOVER, WILLIAM, LYGEROS, JOHN, & MACIEJOWSKI, JAN. 2006. Monte Carlo Optimization for Conflict Resolution in Air Traffic Control. *IEEE transactions on intelligent transportation systems*, **7**(4), 470–482. 16
- LEE, KEUMJIN, FERON, ERIC, & PRITCHETT, AMY. 2007 (July). Air traffic complexity: an input-output approach. *In: 7th USA/Europe air traffic management research and development seminar (ATM2007)*. 15
- LEE, KEUMJIN, FERON, ERIC, & PRITCHETT, AMY. 2008 (Jan.). *Describing Airspace Complexity: Airspace Response to Disturbances*. Ph.D. thesis, Georgia Institute of Technology. 15
- LEE, KEUMJIN, FERON, ERIC, & PRITCHETT, AMY. 2009. Describing Airspace Complexity: Airspace Response to Disturbances. *Journal of guidance, control, and dynamics*, **32**(1), 210–222. 15
- LIU, PEI-CHEN BARRY, HANSEN, MARK, & MUKHERJEE, AVIJIT. 2008. Scenario-based air traffic flow management: From theory to practice. *Transportation research – part B: Methodological*, **42**(7-8), 685–702. 14, 83, 84
- LOPEZ-DELGADO, P, & BARBAS-GONZALEZ, C. 2008. Aplicacion de la teoría de la complejidad al estudio integrado de parámetros en el entorno ATC. *In: Proceedings of the 8th congreso de ingeniería del transporte*. 15
- LOSCOS, J M. 2008. SESAR: the new separation modes for increased capacity. *In: ENRI/DSNA workshop on efficient ATM, next generation*. 22
- LOWTHER, MARCUS B, CLARKE, JOHN-PAUL B, & REN, LILING. 2008. En Route Speed Optimization for Continuous Descent Arrival. *In: Aiaa guidance, navigation and control conference*. Georgia Institute of Technology. 24
- MACQUEEN, J. 1967. Some methods for classification and analysis. *Pages 281–297 of: UNIVERSITY OF CALIFORNIA PRESS (ed), 5th Berkeley symposium on mathematical statistics and probability*. 83

- MANLEY, BENGI, & SHERRY, LANCE. 2010. Analysis of performance and equity in ground delay programs. *Transportation research part C: Emerging technologies*, **18**(6), 910–920. 3, 19, 124, 129, 130
- MARTÍN, P AYLON, USERO, M M DORADO, & JULVE, J B RAJA. 2008. Simulación de un modelo virtual de control de tráfico aéreo basado en arquitectura software de agentes interactivos. In: *Proceedings of the 8th congreso de ingeniería del transporte*. 15
- MELGOSA, MARC. 2012. *Estudio de Ground Delay Programs y de estrategias de reducción de velocidad (Ground delay program and speed reduction strategy study)*. Bachelor thesis, Telecommunications and Aeronautical School of Castelldefels - Technical University of Catalonia. 83, 84
- METRON AVIATION. 2012 (Sept.). *Airspace Flow Programs*. <http://www.metronaviation.com/solutions/traffic-flow-management/concepts/afp.html>. 2
- MUKHERJEE, A., & HANSEN, M. 2007. A Dynamic Stochastic Model for the Single Airport Ground Holding Problem. *Transportation science*, **41**(4), 444–456. 17
- MUKHERJEE, AVIJIT, HANSEN, MARK, & GRABBE, SHON. 2012. Ground delay program planning under uncertainty in airport capacity. *Transportation planning and technology*, **35**(6), 611–628. 4, 73
- MURTAGH, F. 1983. A Survey of Recent Advances in Hierarchical Clustering Algorithms. *The computer journal*, **26**(4), 354–359. 83
- NAGLE, JIM. 2009. Global Air Navigation System ATM Operational Concept. In: *ICAO workshop on the development of national performance framework*. 11, 12
- NATIONAL OCEANIC & ATMOSPHERIC ADMINISTRATION (NOAA). 2012. *Rapid Update Cycle (RUC)*. <http://ruc.noaa.gov>. 63
- NAVAZIO, L., & ROMANIN-JACUR, G. 1998. The Multiple Connections Multi-Airport Ground Holding Problem: Models and Algorithms. *Transportation science*, **32**(3), 268–276. 17
- NEWELL, G. F. 1979. Airport Capacity and Delays. *Transportation science*, **13**(3), 201–241. 13
- NUIC, A., POINSOT, C., IAGARU, M., GALLO, E., NAVARRO, F.A., & QUEREJETA, C. 2005. Advanced Aircraft Performance Modeling for ATM: Enhancements to the BADA Model. *Pages 2.B.4-1-2.B.4-1 of: 24th digital avionics systems conference, vol. 1*. Washington, DC (USA): IEEE. 50, 133
- ODONI, AMADEO R. 1987. The flow management problem in air traffic control. *Chap. pp. 269-28, pages 269-288 of: ODONI, AMADEO R., BIANCO, L., & SZEGÖ, G. (eds), Flow control of congested networks*. Berlin: Springer-Verlag. 17
- PALLOTTINO, L., FERON, E.M., & BICCHI, A. 2002. Conflict resolution problems for air traffic management systems solved with mixed integer programming. *IEEE transactions on intelligent transportation systems*, **3**(1), 3–11. 16
- PERFORMANCE REVIEW UNIT (PRU). 2012 (May). *ATM Cost-Effectiveness (ACE) 2010 Benchmarking Report with 2011-2015 outlook*. Tech. rept. Eurocontrol, Brussels (Belgium). 3
- PETERSON, MICHAEL D, BERTSIMAS, DIMITRIS J, & ODONI, AMADEO R. 1995. Decomposition Algorithms for Analyzing Transient Phenomena in Multiclass Queueing Networks in Air Transportation. *Operations research*, **43**(6), 995–1011. 17
- POLES, DAMIR, NUIC, ANGELA, & MOUILLET, VINCENT. 2010. Advanced aircraft performance modeling for ATM: Analysis of BADA model capabilities. *Pages 1.D.1-1-1.D.1-14 of: 29th digital avionics systems conference*. Salt Lake City, UT: IEEE. 50, 131, 133, 134
- PRADINES DE MENEZES JUNIOR, LUIZ. 2006. *Métodos para a redução de custos operacionais em empresas aéreas*. Ph.D. thesis, Instituto Tecnológico de Aeronáutica, São José dos Campos. 28
- PRANDINI, MARIA, PUTTA, VAMSI, & HU, JIANGHAI. 2010. A probabilistic measure of air traffic complexity in 3-D airspace. *International journal of adaptive control and signal processing*, **24**(10), 813–829. 15
- PRATS, XAVIER, & HANSEN, MARK. 2011 (June). Green Delay Programs. In: *9th USA/Europe air traffic management research and development seminar (ATM2011)*. 24
- RANIERI, ANDREA, & CASTELLI, LORENZO. 2009. A Market Mechanism to Assign Air Traffic Flow Management Slots. In: *8th USA/Europe air traffic management r&d seminar*. 18, 21, 82

- REY, DAVID, & RAPINE, CHRISTOPHE. 2012 (May). Assessing the impact of a speed regulation based conflict resolution algorithm on air traffic flow. *In: 5th international conference on research in air transportation (ICRAT2012)*. 22
- RICHETTA, O. 1994. Dynamic solution to the ground-holding problem in air traffic control. *Transportation research part A: Policy and practice*, **28**(3), 167–185. 19
- RICHETTA, O., & ODONI, AMADEO R. 1993. Solving Optimally the Static Ground-Holding Policy Problem in Air Traffic Control. *Transportation science*, **27**(3), 228–238. 17
- ROSENBERGER, JAY M., JOHNSON, ELLIS L., & NEMHAUSER, GEORGE L. 2004. A Robust Fleet-Assignment Model with Hub Isolation and Short Cycles. *Transportation science*, **38**(3), 357–368. 26
- ROSS, DON. 2009. Game Theory. *In: The stanford encyclopedia of philosophy*. Stanford. 7
- RUMLER, WILHELM, GÜNTHER, THOMAS, FRICKE, HARTMUT, & WEISS HAR, URBAN. 2010 (June). Flight profile variations due to the spreading practice of cost index based flight planning. *Pages 209–216 of: 4th international conference on research in air transportation (ICRAT2010)*. 28
- SCHAEFER, ANDREW J., JOHNSON, ELLIS L., KLEYWEGT, ANTON J., & NEMHAUSER, GEORGE L. 2005. Airline Crew Scheduling Under Uncertainty. *Transportation science*, **39**(3), 340–348. 26
- SESAR CONSORTIUM. 2006 (July). *SESAR Definition Phase - Deliverable 1 - Air Transport Framework The Current Situation - The Market*. Tech. rept. SESAR Consortium. 2, 3, 11, 12, 16, 21, 25
- SESAR CONSORTIUM. 2007 (Sept.). *SESAR Definition Phase - Deliverable 3 - The ATM Target Concept*. Tech. rept. September. SESAR Consortium. 20, 21
- SESAR CONSORTIUM. 2008 (Apr.). *SESAR Master Plan D5*. Tech. rept. April. SESAR Consortium, Brussels (Belgium). 22
- SESAR CONSORTIUM. 2012 (Sept.). SESAR. <http://www.sesar.eu>. 4
- SNELL, DEAN, & TAMBURRO, RALPH. 2011 (Oct.). New York City Airspace Overview. *In: 64th annual meeting & convention, national business aviation association (NBAA)*. 85
- SONG, LIXIA, WANKE, CRAIG, & GREENBAUM, DANIEL P. 2007 (July). Predicting sector capacity for TFM. *In: 7th USA/Europe air traffic management research and development seminar (ATM2007)*. 15
- SRIDHAR, B., GRABBE, S.R., & MUKHERJEE, AVIJIT. 2008. Modeling and Optimization in Traffic Flow Management. *Proceedings of the IEEE*, **96**(12), 2060–2080. 17
- SRIDHAR, BANAVAR, SHETH, KAPIL S, & GRABBE, SHON. 1998 (Dec.). Airspace complexity and its application in air traffic management. *In: 2nd USA/Europe air traffic management research and development seminar (ATM1998)*. 15
- STACK, JOHN, & VON DOENHOFF, ALBERT E. 1934 (Apr.). *Test of 16 related airfoils at high speeds*. Tech. rept. Langley memorial aeronautical laboratory, National advisory committee for aeronautics, Langley field, VA. 35
- TANG, JIANGJUN, ALAM, SAMEER, LOKAN, CHRIS, & ABBASS, HUSSEIN A. 2012. A multi-objective approach for Dynamic Airspace Sectorization using agent based and geometric models. *Transportation research part C: Emerging technologies*, **21**(1), 89–121. 13
- TERRAB, MOSTAFA, & ODONI, AMADEO R. 1993. Strategic Flow Management for Air Traffic Control. *Operations research*, **41**(1), 138–152. 17
- TOMLIN, C., PAPPAS, G.J., & SASTRY, S. 1998. Conflict resolution for air traffic management: a study in multiagent hybrid systems. *IEEE transactions on automatic control*, **43**(4), 509–521. 16
- TOŠIĆ, VOJIN, & HORONJEFF, ROBERT. 1976. Effect of multiple path approach procedures on runway landing capacity. *Transportation research*, **10**(5), 319–329. 13
- UNIVERSITY OF WESTMINSTER. 2011 (Mar.). *European airline delay cost reference values*. Tech. rept. Eurocontrol, Brussels. 3
- VELA, ADAN, SOLAK, SENAY, SINGHOSE, WILLIAM, & CLARKE, JOHN-PAUL. 2009. A mixed integer program for flight-level assignment and speed control for conflict resolution. *Pages 5219–5226 of: Proceedings of the 48th IEEE conference on decision and control (CDC) held jointly with 2009 28th chinese control conference*. Shanghai: IEEE. 16

- VENKATAKRISHNAN, C. S., BARNETT, A., & ODoni, A. R. 1993. Landings at Logan Airport: Describing and Increasing Airport Capacity. *Transportation science*, **27**(3), 211–227. 13
- VIRTANEN, KAI, EHTAMO, HARRI, RAIVIO, TUOMAS, & HAMALAINEN, R.P. 1999. VIATO-visual interactive aircraft trajectory optimization. *IEEE transactions on systems, man and cybernetics, part c (applications and reviews)*, **29**(3), 409–421. 28
- VOSSEN, THOMAS, & BALL, MICHAEL. 2006a. Optimization and mediated bartering models for ground delay programs. *Naval research logistics*, **53**(1), 75–90. 18
- VOSSEN, THOMAS W. M., & BALL, MICHAEL O. 2006b. Slot Trading Opportunities in Collaborative Ground Delay Programs. *Transportation science*, **40**(1), 29–43. 19
- VRANAS, P. B. M., BERTSIMAS, DIMITRIS, & ODoni, A. R. 1994a. Dynamic Ground-Holding Policies for a Network of Airports. *Transportation science*, **28**(4), 275–291. 17
- VRANAS, PETER B, BERTSIMAS, DIMITRIS J, & ODoni, AMADEO R. 1994b. The Multi-Airport Ground-Holding Problem in Air Traffic Control. *Operations research*, **42**(2), 249–261. 17
- WAMBSGANSS, MICHAEL. 1997. Collaborative Decision Making Through Dynamic Information Transfer. *Air traffic control quarterly*, **4**(2), 107–124. 19
- WAMBSGANSS, MICHAEL. 2001. Collaborative Decision Making in Air Traffic Management. *Chap. 1, page 224 of: BIANCO, LUCIO, DELL'OLMO, PAOLO, & ODoni, AMADEO R. (eds), New concept and methods in air traffic management. Transportation Analysis, vol. 1. Springer-Verlag.* 125
- WANG, RONG, BALL, MICHAEL O., & LOVELL, DAVID J. 2012 (May). Ration-by-Weight of Efficiency and Equity. *In: 5th international conference on research in air transportation (ICRAT2012).* 19, 113
- WELCH, JERRY D, ANDREWS, JOHN W, & MARTIN, BRAIN D. 2007 (July). Macroscopic workload model for estimating en route sector capacity. *In: 7th USA/Europe air traffic management research and development seminar (ATM2007).* 15
- WICHMAN, KEITH D., KLOOSTER, JOEL K., BLEEKER, OKKO F., & RADEMAKER, RICHARD M. 2007. Flight validation of downlinked flight management system 4D trajectory. *Pages 1.D.1–1–1.D.1–10 of: IEEE/AIAA 26th digital avionics systems conference.* Dallas, TX: IEEE. 22
- WILSON, IAN A B. 2007. 4-Dimensional Trajectories and Automation Connotations and Lessons learned from past research. *In: Proceedings of the integrated communications, navigation and surveillance conference (ICNS2007).* IEEE, Herndon, Virginia (USA). 5
- WU, CHENG-LUNG, & CAVES, ROBERT E. 2002. Towards the optimisation of the schedule reliability of aircraft rotations. *Journal of air transport management*, **8**(6), 419–426. 26